

NUREG/CR-3912

SAND83-0501


R3

Printed December 1984

MARCH-HECTR Analysis of Selected Accidents in an Ice-Condenser Containment

Allen L. Camp, Vance L. Behr, F. Eric Haskin

Prepared by
Sandia National Laboratories
Albuquerque, New Mexico 87185 and Livermore, California 94550
for the United States Department of Energy
under Contract DE-AC04-76DP00789



Prepared for
U. S. NUCLEAR REGULATORY COMMISSION

SF2900Q(8-81)

8503050511 850131
PDR NUREG
CR-3912

PDR

NOTICE

This report was prepared as an account of work sponsored by an agency of the United States Government. Neither the United States Government nor any agency thereof, or any of their employees, makes any warranty, expressed or implied, or assumes any legal liability or responsibility for any third party's use, or the results of such use, of any information, apparatus product or process disclosed in this report, or represents that its use by such third party would not infringe privately owned rights.

Available from
GPO Sales Program
Division of Technical Information and Document Control
U.S. Nuclear Regulatory Commission
Washington, D.C. 20555
and
National Technical Information Service
Springfield, Virginia 22161

NUREG/CR-3912
SAND83-0501
R3

MARCH-HECTR ANALYSIS OF SELECTED
ACCIDENTS IN AN ICE-CONDENSER CONTAINMENT

Allen L. Camp
Vance L. Behr
F. Eric Haskin

December 1984

Sandia National Laboratories
Albuquerque, NM 87185
Operated by
Sandia Corporation
for the
U.S. Department of Energy

Prepared for
Division of Accident Evaluation
Office of Nuclear Regulatory Research
U.S. Nuclear Regulatory Commission
Washington, D.C. 20555
Under Memorandum of Understanding DOE 40-550-75
NRC FIN Nos. A-1246, A-1258, A-1322

ABSTRACT

The MARCH and HECTR compute codes are used in this study to examine hydrogen production, transport, and combustion in an ice-condenser containment for a number of hypothesized severe accidents. Both degraded-core and core-meltdown accidents are treated. The sensitivity of the containment pressure-temperature response is assessed for a number of factors, including the hydrogen and steam source-term assumptions, ignition and propagation limits, combustion completeness, flame speed, spray operation, and recirculation fan operation. The highest containment pressures occur for those cases where the igniters are assumed to fail, the recirculation fans or containment sprays are assumed to fail, or very large steam and hydrogen releases accompanying vessel breach are predicted.

THIS PAGE INTENTIONALLY BLANK

CONTENTS

	<u>Page</u>
LIST OF FIGURES	viii
LIST OF TABLES	xiv
ACKNOWLEDGMENTS	xv
EXECUTIVE SUMMARY	1
1. INTRODUCTION	9
2. CONTAINMENT AND CASE DESCRIPTIONS	11
2.1 Ice-Condenser Containment Description	11
2.2 Case Descriptions	14
3. GENERATION OF WATER AND HYDROGEN SOURCE TERMS	20
3.1 MARCH	20
3.2 Degraded-Core Cases	21
3.2.1 "A" Cases - S ₂ D Degraded-Core, 75% Zirconium Oxidation	24
3.2.2 "B" Cases - S ₂ D Degraded-Core, 35% Zirconium Oxidation	28
3.2.3 "C" Cases - S ₂ D Degraded-Core, 75% Zirconium Oxidation	32
3.2.4 "F" Cases - S ₁ D Degraded-Core, 75% Zirconium Oxidation	34
3.2.5 "G" Cases - S ₁ H Degraded-Core, 37% Zirconium Oxidation	38
3.2.6 "H" Cases - S ₁ H Degraded-Core, 75% Zirconium Oxidation	42
3.2.7 "I" Cases - S ₁ HF Degraded-Core, 75% Zirconium Oxidation	42
3.2.8 "L" Cases - TMLU Degraded-Core, 75% Zirconium Oxidation	46
3.2.9 "M" Cases - TMLB Degraded-Core, 75% Zirconium Oxidation	50
3.3 Core-Melt Cases	54
3.3.1 "D" and "E" Cases - S ₂ D, Core-Meltdown	56
3.3.2 "J" and "K" Cases - S ₁ HF, Core-Meltdown	66
3.3.3 "N", "O", and "P" Cases - TMLB', Core-Meltdown	76

CONTENTS
(continued)

	<u>Page</u>
4. HECTR ANALYSES	84
4.1 Introduction	84
4.2 Ice-Condenser Containment Model	84
4.3 Results for Degraded-Core Accidents	87
4.3.1 Case A.00 - S ₂ D Degraded-Core Base Case	90
4.3.2 Cases A.01 through A.04 - Effects of Fans and Sprays	96
4.3.3 Case A.05 - Surface Heat Transfer Effects	102
4.3.4 Cases A.06 through A.09 - Sensitivity to Ignition Limits	103
4.3.5 Cases A.10 through A.12 - Sensitivity to Combustion Completeness and Flame Speed	107
4.3.6 Case A.13 - Effect of Upper Plenum Igniter Failure	109
4.3.7 Case A.14 - Effect of Partial Oxygen Depletion	110
4.3.8 Case A.15 - Effect of Ice-Condenser Door Failure	111
4.3.9 Case B.00 - S ₂ D Scenario, 35% Zirconium Oxidation	112
4.3.10 "C" Cases - CLASIX and COMPARE Comparisons	114
4.3.11 "F", "G", and "H" Cases - S ₁ D and S ₁ H Scenarios	123
4.3.12 "I" Cases - S ₁ HF Scenarios	129
4.3.13 "L" and "M" Cases - TMLU and TMLB Scenarios	138
4.4 Results for Core-Meltdown Accidents	140
4.4.1 "D" Cases - S ₂ D Core-Meltdown Scenarios, 100% Zirconium Oxidation	140
4.4.2 "E" Cases - S ₂ D Core-Meltdown Scenarios, 36% Zirconium Oxidation	144
4.4.3 "J" Cases - S ₁ HF Core-Meltdown Scenarios, 100% Zirconium Oxidation	146
4.4.4 "K" Cases - S ₁ HF Core-Meltdown Scenarios, 37% Zirconium Oxidation	149
4.4.5 "N" Cases - TMLB' Core-Meltdown Scenarios, 100% Zirconium Oxidation	150
4.4.6 "O" Cases - TMLB' Core-Meltdown Scenarios, 27% Zirconium Oxidation	152
4.4.7 "P" Cases - TMLB' Core-Meltdown Scenarios, 65% Zirconium Oxidation	153

CONTENTS
(continued)

	<u>Page</u>
5. CONCLUSIONS	155
5.1 Degraded-Core Versus Core-Meltdown Scenarios	155
5.2 Steam and Hydrogen Source Terms	155
5.3 Containment Sprays	156
5.4 Recirculation Fans	157
5.5 Combustion Parameters	157
5.6 Ice-Condenser Parameters	158
5.7 Containment Venting	158
5.8 Partial Oxygen Depletion	158
5.9 Effectiveness of Igniter System	159
5.10 Future Work	160
5.10.1 Unresolved Issues	160
5.10.2 Plans for Resolution of Issues	160
6. REFERENCES	161
APPENDIX A - HECTR MODEL DESCRIPTIONS	A-1
APPENDIX B - MARCH INPUT FOR DEGRADED-CORE CASES	B-1
APPENDIX C - MARCH INPUT FOR CORE-MELT CASES	C-1
APPENDIX D - HECTR INPUT DESCRIPTION	D-1

LIST OF FIGURES

<u>Figure</u>		<u>Page</u>
2-1	Simplified Diagram of Ice-Condenser Containment	12
3-1	Primary System Liquid Level for "A" Cases	25
3-2	Fractions of Core Melted and Zirconium Oxidized for "A" Cases	25
3-3	Water Source to Containment for "A" Cases	27
3-4	Hydrogen Source to Containment for "A" Cases	27
3-5	Primary System Liquid Level for "B" Cases	29
3-6	Fractions of Core Melted and Zirconium Oxidized for "B" Cases	29
3-7	Water Source to Containment for "B" Cases	31
3-8	Hydrogen Source to Containment for "B" Cases	31
3-9	Water Source to Containment for "C" Cases	33
3-10	Hydrogen Source to Containment for "C" Cases	33
3-11	Primary System Liquid Level for "F" Cases	35
3-12	Fractions of Core Melted and Zirconium Oxidized for "F" Cases	35
3-13	Water Source to Containment for "F" Cases	37
3-14	Hydrogen Source to Containment for "F" Cases	37
3-15	Primary System Liquid Level for "G" Cases	39
3-16	Fractions of Core Melted and Zirconium Oxidized for "G" Cases	39
3-17	Water Source to Containment for "G" Cases	41
3-18	Hydrogen Source to Containment for "G" Cases	41
3-19	Primary System Liquid Level for "H" and "I" Cases	43
3-20	Fractions of Core Melted and Zirconium Oxidized for "H" and "I" Cases	43

LIST OF FIGURES
(continued)

<u>Figure</u>		<u>Page</u>
3-21	Water Source to Containment for "H" and "I" Cases	45
3-22	Hydrogen Source to Containment for "H" and "I" Cases	45
3-23	Primary System Liquid Level for "L" Cases	47
3-24	Fractions of Core Melted and Zirconium Oxidized for "L" Cases	47
3-25	Water Source to Containment for "L" Cases	49
3-26	Hydrogen Source to Containment for "L" Cases	49
3-27	Primary System Liquid Level for "M" Cases	51
3-28	Fractions of Core Melted and Zirconium Oxidized for "M" Cases	51
3-29	Water Source to Containment for "M" Cases	53
3-30	Hydrogen Source to Containment for "M" Cases	53
3-31	Primary System Liquid Level for "D" Cases	57
3-32	Primary System Liquid Level for "E" Cases	57
3-33	Primary System Pressure for "D" Cases	59
3-34	Primary System Pressure for "E" Cases	59
3-35	Fractions of Core Melted and Zirconium Oxidized for "D" Cases	61
3-36	Fractions of Core Melted and Zirconium Oxidized for "E" Cases	61
3-37	Water Source to Containment for "D" Cases	63
3-38	Water Source to Containment for "E" Cases	63
3-39	Hydrogen Source to Containment for "D" Cases	65
3-40	Hydrogen Source to Containment for "E" Cases	65
3-41	Primary System Liquid Level for "J" Cases	67

LIST OF FIGURES
(continued)

<u>Figure</u>		<u>Page</u>
3-42	Primary System Liquid Level for "K" Cases	67
3-43	Primary System Pressure for "J" Cases	69
3-44	Primary System Pressure for "K" Cases	69
3-45	Fractions of Core Melted and Zirconium Oxidized for "J" Cases	71
3-46	Fractions of Core Melted and Zirconium Oxidized for "K" Cases	71
3-47	Water Source to Containment for "J" Cases	73
3-48	Water Source to Containment for "K" Cases	73
3-49	Hydrogen Source to Containment for "J" Cases	75
3-50	Hydrogen Source to Containment for "K" Cases	75
3-51	Primary System Liquid Level for "N" Cases	77
3-52	Primary System Pressure for "N" Cases	77
3-53	Fractions of Core Melted and Zirconium Oxidized for "N" Cases	78
3-54	Fractions of Core Melted and Zirconium Oxidized for "O" Cases	79
3-55	Fractions of Core Melted and Zirconium Oxidized for "P" Cases	79
3-56	Water Source to Containment for "N" Cases	80
3-57	Water Source to Containment for "O" Cases	80
3-58	Water Source to Containment for "P" Cases	81
3-59	Hydrogen Source to Containment for "N" Cases	82
3-60	Hydrogen Source to Containment for "O" Cases	83
3-61	Hydrogen Source to Containment for "P" Cases	83
4-1	HECTR Ice-Condenser Containment Model	85
4-2	Pressure Response in Dome for Case A.00	90

LIST OF FIGURES
(continued)

<u>Figure</u>		<u>Page</u>
4-3	Gas Composition in Dome for Case A.00	91
4-4	Gas Composition in Upper Plenum for Case A.00	93
4-5	Ice Inventory History for Case A.00	93
4-6	Gas Composition in Lower Compartment for Case A.00	95
4-7	Pressure Response in Dome for Case A.01	97
4-8	Upper-Plenum Hydrogen Concentration for Case A.00	97
4-9	Hydrogen Concentration in Top Ice Compartment for Case A.01	98
4-10	Pressure Response in Dome for Case A.02	99
4-11	Pressure Response in Dome for Case A.03	100
4-12	Pressure Response in Dome for Case A.04	101
4-13	Pressure Response in Dome for Case A.05	102
4-14	Pressure Response in Dome for Case A.06	103
4-15	Pressure Response in Dome for Case A.07	104
4-16	Pressure Response in Dome for Case A.08	105
4-17	Pressure Response in Dome for Case A.09	105
4-18	Gas Temperature Response in Upper Plenum for Case A.06	106
4-19	Pressure Response in Dome for Case A.10	107
4-20	Pressure Response in Dome for Case A.11	108
4-21	Pressure Response in Dome for Case A.12	108
4-22	Pressure Response in Dome for Case A.13	109
4-23	Pressure Response in Dome for Case A.14	110
4-24	Pressure Response in Dome for Case A.15	111
4-25	Pressure Response in Dome for Case B.00	112

LIST OF FIGURES
(continued)

<u>Figure</u>		<u>Page</u>
4-26	Ice Inventory History for Case B.00	113
4-27	Gas Composition in Upper Plenum for Case B.00	113
4-28	Pressure Response in Dome for Case C.00	115
4-29	Pressure Response in Dome for Case A.00	115
4-30	Hydrogen-to-Water Injection Ratio for Case C.00	117
4-31	Hydrogen-to-Water Injection Ratio for Case A.00	117
4-32	Pressure Response in Dome for Case C.01	121
4-33	Pressure Response in the Dome for Case C.02	122
4-34	Pressure Response in the Dome for Case F.00	123
4-35	Pressure Response in the Dome for Case F.01	124
4-36	Upper-Plenum Hydrogen Concentration for Case F.00	125
4-37	Upper-Plenum Hydrogen Concentration for Case F.01	125
4-38	Pressure Response in Dome for Case G.00	126
4-39	Pressure Response in Dome for Case H.00	127
4-40	Pressure Response in Dome for Case H.01	128
4-41	Pressure Response in Dome for Case I.00	129
4-42	Pressure Response in Dome for Case I.01	131
4-43	Pressure Response in Dome for Case I.02	131
4-44	Pressure Response in Dome for Case I.03	132
4-45	Pressure Response in Dome for Case I.04	133
4-46	Ice Inventory History for Case I.00	133
4-47	Ice Inventory History for Case I.03	134

LIST OF FIGURES
(continued)

<u>Figure</u>		<u>Page</u>
4-48	Ice Inventory History for Case I.04	134
4-49	Pressure Response in Dome for Case I.05	135
4-50	Pressure Response in Dome for Case I.06	136
4-51	Pressure Response in Dome for Case L.00	139
4-52	Pressure Response in Dome for Case M.00	139
4-53	Pressure Response in Dome for Case D.00	140
4-54	Pressure Response in Dome for Case D.01	142
4-55	Pressure Response in Dome for Case D.02	143
4-56	Dome Hydrogen Concentration for Case D.02	143
4-57	Pressure Response in Dome for Case E.00	144
4-58	Pressure Response in Dome for Case E.01	145
4-59	Pressure Response in Dome for Case J.00	146
4-60	Pressure Response in Dome for Case J.01	147
4-61	Pressure Response in Dome for Case J.02	148
4-62	Pressure Response in Dome for Case K.00	149
4-63	Pressure Response in Dome for Case N.00	151
4-64	Pressure Response in Dome for Case N.01	151
4-65	Pressure Response in Dome for Case O.00	152
4-66	Pressure Response in Dome for Case P.00	153
4-67	Pressure Response in Dome for Case P.01	154

LIST OF TABLES

<u>Table</u>		<u>Page</u>
2-1	Case Descriptions	16
2-2	Event Nomenclature	17
3-1	Times of Occurrence of Important Events for Degraded-Core Cases	23
3-2	Times of Occurrence of Important Events for Core-Meltdown Cases	55
4-1	HECTR Results	88
4-2	Code Comparison	119

ACKNOWLEDGMENTS

The authors thank the following people who assisted in this effort:

S. E. Dingman, who developed most of the ice-condenser models and provided consulting during the analysis;

L. N. Smith, who assisted in performing the MARCH runs; and

E. W. Shepherd and P. G. Prassinos, who assisted in the preparation of the report.

Also, extensive review and comments were provided by the following people:

B. Agrawal, NRC
A. S. Benjamin, SNL
M. Berman, SNL
D. R. Gallup, SNL
R. G. Gido, LANL
J. T. Larkins, NRC
J. H. Linebarger, SNL
W. Lyon, NRC
R. Palla, NRC
C. Tinkler, NRC
T. J. Walker, NRC

THIS PAGE INTENTIONALLY BLANK

EXECUTIVE SUMMARY

This report examines the predicted pressure-temperature response of an ice-condenser containment for a variety of important severe accident sequences identified by the Accident Sequence Evaluation Program (ASEP).[1] The analyses are based on both the MARCH and HECTR computer codes. MARCH (version 1.1 with certain Sandia modifications) was used to model the primary system and provide hydrogen and steam source terms to containment.[2 3] HECTR used the output from MARCH and modeled the containment pressure-temperature response.[4-6] This work is the first major application of HECTR to an ice condenser containment. HECTR is a fast-running, lumped-volume code that is very useful for parametric analyses of containment pressure temperature response during accidents involving hydrogen combustion. HECTR includes models for hydrogen burns, radiative and convective heat transfer, condensation, heat transfer to sprays, passive heat sinks, a recirculation sump, air return fans, and an ice condenser. HECTR allows a more realistic compartmentalization of containment and a more sophisticated treatment of important phenomena than does the MACE containment subroutine in MARCH. HECTR, which was developed specifically for modeling accidents involving hydrogen combustion, compares favorably with other containment code, that were used previously in similar analyses and is generally faster running. The combined use of MARCH and HECTR represents a significant advancement in the capability to model ice condenser containments.

Sequoyah is used as the reference plant for the analyses presented in this report; however, comparable containment pressure-temperature responses would be expected for similarly configured ice-condenser plants, such as Watts Bar.

Cases Considered

Sixteen base-case accident scenarios were analyzed with MARCH to provide steam and hydrogen source terms for HECTR. Fifty-three variations of the base cases were evaluated using HECTR. The accident scenarios examined do not represent all possible contributors to risk. However, many of the highest contributors to risk are examined in this report.

Both degraded-core and core-meltdown scenarios were examined. In the degraded-core scenarios it was postulated that emergency core cooling (ECC) was unavailable for a period of time long enough to allow significant zirconium oxidation but short enough so that core damage could be arrested when ECC was restored. In the core-meltdown scenarios, ECC was assumed to fail at some time and was not recovered.

For the degraded-core cases and for the core-meltdown cases through the time of vessel failure, the steam and hydrogen source terms were generated by recording the rates of steam and hydrogen release to containment as calculated by MARCH. These recorded values were then input to HECTR. After vessel breach in the core-meltdown cases, a coolable debris bed (requiring water to be present) was postulated to form in the reactor cavity, since HECTR could not treat the carbon monoxide and carbon dioxide that would be produced during concrete attack by the hot debris. The hydrogen generation rates were determined in MARCH, but the sump temperature and the steam generation rates were calculated in HECTR, based on the MARCH values for heat transfer. The assumption of a wet reactor cavity may not be valid for all accident sequences, e.g., TMLB'. Sequences involving dry cavities will be addressed in future studies.

Results

Predicted peak pressures varied from 161.7 to 905.5 kPa (23.5 to 131.3 psia), depending on the particular accident scenario. (The value of 905.5 kPa does not necessarily represent a worst-case containment loading because ignition limits greater than 12%, accelerated flames, and detonations were not considered.) For most of the cases involving failure of containment sprays, the pressure was still increasing at the end of the run. To put the peak pressures in perspective, estimated failure pressures for the type of ice-condenser containment analyzed in this report are 350 to 515 kPa (51 to 75 psia) for Sequoyah,[7] and 778 to 1067 kPa (113 to 155 psia) for Watts Bar.[8]

Prior to vessel breach, the degraded-core and core-meltdown cases show similar behavior and sensitivities. Hydrogen is released fairly slowly (a few kilograms per second [a few hundred pounds per minute] or less), and the results are governed by the common parameters discussed later in this summary. Prior to vessel breach, many of the core-meltdown cases are actually less severe than the degraded-core cases. In the core-meltdown cases (no restoration of ECC), little hydrogen is released from the primary system until vessel breach occurs. Therefore, hydrogen burns before the time of vessel breach (if they occur) are relatively benign.

Most of the significant differences between degraded-core and core-meltdown accidents occur due to the events during and subsequent to vessel breach. The single most important aspect of vessel breach addressed by this analysis is the rapid injection of steam and hydrogen into containment due to the release from the primary system and debris quenching in the reactor cavity. Peak hydrogen injection rates of several tens of kilograms per second (several thousand pounds per minute) are predicted by MARCH. The hydrogen released to containment following vessel breach is predicted to produce

high peak pressures for three major reasons. First, the large steam release rate raises the baseline or preburn pressure. Second, because of the high hydrogen release rates, the burns are fed hydrogen as they progress. Finally, enough hydrogen is usually released to result in two or more successive burns that are close enough together in time for their effects to be somewhat cumulative. Generally, these burns occur in the upper regions of containment (upper plenum and dome), because the steam released just after vessel breach rapidly makes inert the atmosphere in the lower compartment (if it is not already inert prior to vessel breach because of postulated failure of the air return fans).

The possible effects of steam explosions, noncoolable debris beds, ejection of melt from the vessel or reactor cavity, aerosol generation and dispersal, and core-concrete interactions are not considered in this study, but will be considered in future Severe Accident Sequence Analysis (SASA) work.

Much of the difference in results for different cases can be attributed to different accident scenarios and correspondingly different source terms. The source terms, which influence the location of the burns and their magnitude, can generally be characterized by two parameters: (1) the hydrogen-to-steam ratio and (2) the injection rates. Low hydrogen-to-steam ratios tend to cause burns to occur preferentially in the upper regions of containment (dome and upper plenum of the ice condenser), because the high steam content makes the atmosphere in the lower compartment less combustible. Rapid steam and hydrogen source injection tends to raise the baseline or preburn pressure and produce correspondingly higher burn pressures. Slow source injection leads to a better-mixed containment prior to burning and may lead to burns of a more global nature. In other words, either extreme of injection rate has negative aspects.

A degraded-core case with only 35% zirconium oxidation yields peak pressures slightly higher than those predicted for a similar case with 75% zirconium oxidation. Intuitively, one would expect the maximum pressure rise due to combustion to increase monotonically with the amount of hydrogen released. However our calculations indicate this is not the case for degraded-core scenarios in an ice-condenser containment. Instead there is a threshold amount of hydrogen above which the peak pressures cease to increase (assuming the ignitors are operating).

This finding raises questions as to the level of conservatism implied by the interim hydrogen rule for ice-condenser plants. Specifically, the rule states that these plants must be able to withstand the effects of degraded-core scenarios in which hydrogen from 75% zirconium oxidation is released to containment. Results from this study indicate that the

selection of 75% oxidation provides no margin of safety in the containment loads over that which would be produced by only 35% oxidation (for a degraded-core scenario). More calculations are needed to clearly define the relationship between amount of zirconium oxidized and maximum pressure rise due to combustion.

Containment sprays are essential for long-term accident control, since only a finite amount of ice is available in the ice condenser; without sprays, containment will eventually be breached either by leakage or by overpressure unless the steam release is terminated. In the short term, sprays keep the baseline pressure down prior to burns and remove heat during and after burns. The heat removed by sprays following burns makes the pressure (and temperature) rises less cumulative. The upper-bound failure pressure for Sequoyah, 515 kPa (75 psia), is not exceeded in this analysis for any scenario in which the sprays, the recirculation fans, and the igniters operate.

Operation of the recirculation fans tends to reduce the baseline pressures by increasing the effectiveness of the ice condenser (and therefore the melting rate of the ice). Also, operation of the fans generally prevents sustained periods of steam inerting in the lower compartment. This is significant because burns originating in the lower compartment generally result in lower peak pressures than burns originating in the dome or burns originating in the upper plenum and propagating into the dome. When the fans are off, very high hydrogen concentrations are predicted in the ice condenser, raising the possibility of accelerated flames or local detonations. These high hydrogen concentrations occur due to less air entering the bottom of the ice condenser with the hydrogen and lower flow rates through the ice condenser. The treatment of accelerated flames and local detonations is beyond the scope of this report. Throughout the report, however, we indicate those situations in which such phenomena may be possible.

The results of varying the ignition threshold, combustion completeness, and flame speed are fairly straightforward, with increasing values of these parameters producing higher pressures. High values for ignition limits and combustion completeness produce fewer burns with more hydrogen consumed in each burn. The specific pressure rise for a particular case depends strongly on the initial pressure. However, we can say that with the fans operating, burns that consume the equivalent of 6 to 7% hydrogen either in a single, confined compartment or on a containment-wide basis will generally not directly threaten containment. Burns initiated at higher concentrations in compartments that can vent into other compartments may also produce relatively low pressure rises, assuming that the amount of venting is significant over the

burn time. However, if the recirculation fans are not operating, burns ignited at 6 to 7% hydrogen could propagate into a region such as the ice condenser, where much higher concentrations may be present, leading to burns at a higher effective hydrogen concentration and possibly to accelerated flames or local detonations.

For scenarios such as TMLB', where the ignition system fails, we assumed arbitrary ignition limits (12% hydrogen in most cases). In fact, ignition in these cases may be a stochastic process, depending on available ignition sources, and may occur at hydrogen concentrations greater or less than 12%. A better analysis of these scenarios would consider ignition probability as a function of time during the accident.

We found the results to be relatively insensitive to the ice-condenser modeling parameters (drain temperature and heat transfer coefficient). Consistent results were observed for a wide range of parameters. However, we only examined the effects of these parameters for a limited set of accident scenarios.

For those cases where high pressures are predicted, containment venting has some positive effects. A 0.75-m² (8.1-ft²) vent was set to open in the dome at a pressure of 273.7 kPa (39.7 psia) and to close when the pressure fell below 239.2 kPa (34.7 psia). Compared to cases without venting, pressure reductions in the range of 10 to 20% are typical. These reductions depend on the assumed vent size and the flame speed (burn time).

The calculations performed here do not show large benefits from partial oxygen depletion and in some cases show negative effects. However, these results are due to the particular accident scenarios considered and to modeling limitations. Partial oxygen depletion limits the total amount of hydrogen that can be burned. Generally, the combustion of hydrogen from 100% zirconium oxidation will render the containment inert due to depletion of oxygen below the requisite minimum concentration (nominally 5%). Partial oxygen depletion will render the containment inert well before the hydrogen from 100% zirconium oxidation is consumed. During core-meltdown accidents, significant amounts of carbon monoxide may be produced before the oxygen inerting of the containment atmosphere occurs. Limiting the amount of carbon monoxide burned is important since it has a higher ignition limit and heat of reaction than hydrogen, and thus, could produce higher pressure rises. Also, note that none of the present analyses treat possible decreases in flame speed and combustion completeness due to decreased oxygen content, either as a result of an initially depleted atmosphere or of an atmosphere that becomes oxygen depleted as a result of repeated burning.

Based on our HECTR results, a glow-plug igniter system is beneficial for many degraded-core and core-meltdown accident scenarios involving the release of hydrogen. Pressure rises due to deflagrations will almost certainly be decreased from those that might be obtained from random combustion with no igniters present. The two most important considerations appear to be (1) whether the igniters are operating and (2) whether the fans are operating. A deliberate-ignition system of the type installed at Sequoyah is not available for all accident sequences (in our analyses the system is available for all of the degraded-core sequences and some of the core-meltdown sequences). For example, the igniters at Sequoyah and elsewhere are ac-powered. To reduce the risk due to accidents involving total loss of ac power, dc power to the igniters would be required. Also, for Sequoyah, no igniters are located in the ice regions or lower plenum (igniters are contained in all other major compartments). As a result, in accidents involving recirculation fan failure, high hydrogen concentrations can accumulate in the ice regions. The potential for accelerated flames or local detonations during such accidents could be reduced by installing a limited number of igniters in the ice regions. These igniters would probably not need to be activated if the recirculation fans are operating. Future development of a passive igniter system could alleviate many of the concerns regarding loss-of-power accidents.

Although ice-condenser containments are all similar in configuration, our calculations are for a specific ice-condenser containment design (Sequoyah--Watts Bar), and caution should be exercised in extending the results to other plants. Also, our calculations do not address the possibility of continuous burning due to stable diffusion flames or jets, or the possibility of equipment failures as a result of combustion events. Future considerations of these possibilities might alter the perceived benefits of deliberate ignition. For example, diffusion flames would be beneficial in that low pressure rises would be produced; however, high gas temperatures would be produced that might fail adjacent equipment.

Future Work

It is beyond the scope of this report to attempt to resolve several issues regarding hydrogen combustion in ice-condenser containments. These issues are:

- The potential for accelerated flames or local detonations in or near the ice condenser
- The effects of additional combustible (and noncondensable) gas generation from steel-steam reactions and molten-core/concrete interactions

- The likelihood and effects of stable diffusion flames either near the hydrogen release point, in the ice condenser, or near the fan exits
- The response of safety-related equipment to combustion (particularly if diffusion flames are present)
- Ignition in accidents in which the igniter systems may fail (either with or without ac power working)
- The relationship between maximum peak pressures and amount of zirconium oxidized for degraded-core scenarios

Work is in progress in various Nuclear Regulatory Commission (NRC) programs which will address most of the above issues. The potential for accelerated flames or detonations in the ice condenser will be addressed experimentally at Sandia (Hydrogen Behavior Program). HECTR is now being modified to address combustion in the presence of the carbon monoxide and carbon dioxide formed during core-concrete interactions (Hydrogen Behavior Program). Experiments are in progress to address diffusion flames, and models are being developed for future incorporation into HECTR (Hydrogen Behavior and Hydrogen Mitigation Programs). Equipment survival will be addressed in a subsequent report, using boundary conditions obtained from the analyses described in this report (Hydrogen Burn Survival Program). The feasibility of passive igniters that would function during an accident involving the total loss of ac power is also being studied at Sandia (Hydrogen Mitigation Program). A follow-on study is planned (Severe Accident Sequence Analysis Program) to more clearly define the relationship between the maximum pressure rise in containment and the amount of zirconium oxidized in degraded-core scenarios.

THIS PAGE INTENTIONALLY BLANK

1. INTRODUCTION

Since the accident at Three Mile Island Unit 2, many questions have been raised regarding the potential for and consequences of hydrogen combustion during nuclear reactor accidents. Nuclear reactors with small and intermediate-sized containments have received particular attention because of the potential for high hydrogen concentrations in containment during degraded-core or core-meltdown accidents. Also, some of these containments have lower failure pressures than the large, dry pressurized-water reactor (PWR) containments.

The smallest containments, Mark I and Mark II boiling-water reactor (BWR) containments, have been nitrogen-inerted to preclude hydrogen combustion. Therefore, most recent research has been directed toward the intermediate-size Mark III BWR and ice-condenser PWR containments. Current utility planning calls for these containments to be equipped with deliberate ignition systems in order to burn the hydrogen before dangerous concentrations are reached. The main purpose of this report is to examine the containment pressure-temperature response for a number of hypothesized severe accidents in an ice-condenser containment such as Sequoyah.

Sandia National Laboratories is participating in several NRC-sponsored programs to study severe accident phenomenology. Part of that effort involves the combined use of the computer codes MARCH and HECTR to examine hydrogen behavior during severe accidents. MARCH is used to model the primary system and provide hydrogen and water source terms to containment. HECTR is used to model the containment pressure-temperature response. The application of these codes to a plant with an ice-condenser containment is described in this report. This work is the first major application of HECTR to an ice-condenser containment. HECTR, which was designed specifically for accidents involving hydrogen combustion, compares favorably with other containment codes that were used previously in similar analyses and is considerably faster running. The combined use of MARCH and HECTR represents a significant advancement in the capability to model ice-condenser containments.

It is not the purpose of this report to examine the probability that particular accidents will occur or to determine the radiological consequences of such accidents. However, as discussed in Chapter 2, we have attempted to examine accident scenarios that have been identified by other analyses as major contributors to risk. The analyses presented in this report reflect use of the best analytical tools currently available to us, but significant uncertainties still remain in many key parameters. We will discuss these parameters and the associated uncertainties throughout the remainder of the report. Chapter 2 presents the case

descriptions as well as a description of the ice-condenser containment. Chapter 3 describes the MARCH runs made to generate hydrogen and water source terms for HECTR. Chapter 4 presents the HECTR analysis of the containment atmosphere pressure-temperature response, and Chapter 5 presents our conclusions.

2. CONTAINMENT AND CASE DESCRIPTIONS

2.1 Ice-Condenser Containment Description

Sequoyah was used as the reference plant for the analyses presented in this report; however, comparable containment pressure-temperature responses would be predicted for similar ice-condenser plants, such as Watts Bar. Sequoyah has a four-loop Westinghouse nuclear steam supply system rated at 3423 MW_t and has an ice-condenser containment with a deliberate-ignition system.

The general arrangement of an ice-condenser containment is shown in Figure 2-1. The total free volume of an ice-condenser containment is approximately 40 000 m³ (1.4 x 10⁶ ft³): 10 000 m³ (3.5 x 10⁵ ft³) in the lower compartment, 7000 m³ (2.5 x 10⁵ ft³) in the ice condenser, and 23 000 m³ (8.1 x 10⁵ ft³) in the dome or upper compartment. This is roughly half the free volume of a typical large, dry PWR containment. The reactor coolant system is located in the lower compartment. During an accident, pressurization due to blowdown from the reactor coolant system causes the ice-condenser doors to open and gases to flow from the lower compartment through the ice condenser to the dome. As the gases flow through the ice regions, they are cooled and steam is condensed, thereby limiting containment pressurization.

The ice condenser is essentially a cold storage room shaped in the form of a "C" made up of 300 degrees of arc with a 16-m (52-ft) inside radius and a 20-m (66-ft) outside radius. The ice condenser is approximately 24 m (79 ft) tall. It consists of three basic regions, the lower plenum, the ice region, and the upper plenum. The lower-plenum doors are normally closed. They open upon slight pressurization in the lower compartment, allowing gases to flow through the lower plenum and up into the ice regions. The lower-plenum doors are designed to reclose to block any downward gas flow through the ice condenser. The ice region contains perforated metal tubes or "baskets" which are filled with ice. Flow out of the ice region is to the upper plenum via the intermediate-deck doors. These doors are normally closed under the force of gravity. They open upon slight pressurization from below to permit upward flow, but, like the lower-plenum doors, the intermediate-deck doors are intended to close to block any downward gas flow through the ice condenser. There is some question as to whether these doors will reclose to their original position under all circumstances. Our analyses assume that the doors do reclose to block downward flow. Lightweight top-deck doors are located at the top of the ice-condenser upper plenum. These doors would be expected to be open early (perhaps being thrown clear) and remain open. Thus, they are not modeled in this analysis.

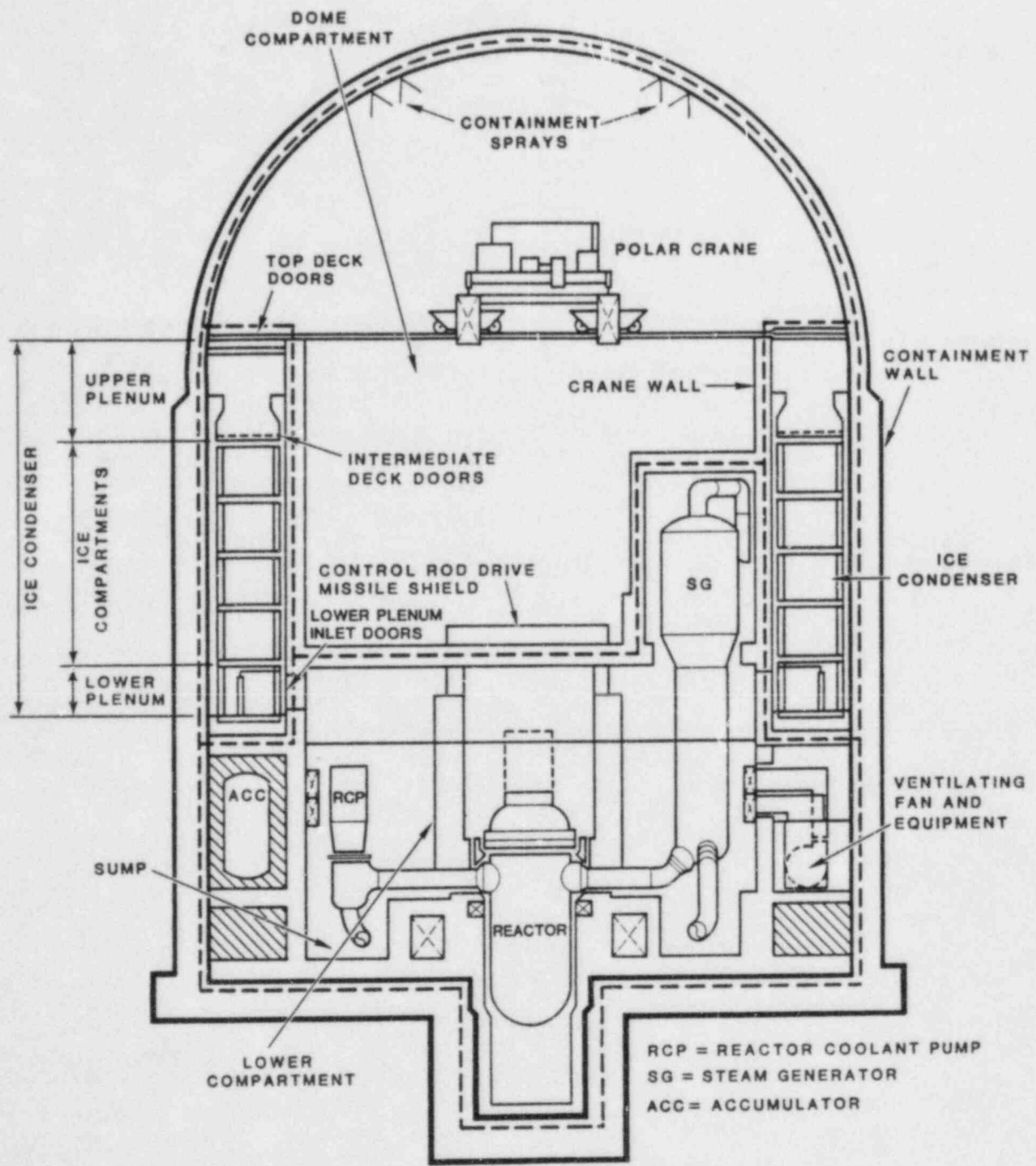


Figure 2-1. Simplified Diagram of Ice-Condenser Containment

Two recirculation fans return air from the dome to the lower compartment and reduce the postaccident concentration of hydrogen in stagnant areas. Each fan is supplied with its own separate duct system and dampers. When the air return or recirculation fans are operating, they continually draw gases from the dome and from dead-ended regions in the containment where there is potential for the accumulation of hydrogen. These spaces are the four steam-generator enclosures, the pressurizer enclosure, the four accumulator spaces, and the instrument room. The recirculation fans exhaust into the lower compartment through the annular equipment areas and ports provided for pressure equalization. The fans maintain forced circulation from the lower compartment through the ice condenser to the dome. Both fans are actuated upon a high containment-pressure signal (typically 122 kPa or 17.7 psia), but only after a delay time (typically 10 minutes).

Because there is a limited supply of ice in the ice condenser (1.11×10^6 kg or 2.45×10^6 lb), at late times in many accidents all of the ice will have melted, and steam from the lower compartment will not be condensed in the ice condenser, but rather will flow into the dome. In order to prevent this steam from building up in containment and leading to high containment atmospheric pressures, a containment spray system is provided for long-term containment heat removal. This system sprays water droplets into containment at the top of the dome. The droplets fall through the gases in the dome and condense steam. Any droplets and condensate which fall to the floor will drain to the lowest portion of the dome compartment, the refueling canal. Two drains in the bottom of the refueling canal allow the water to drain into the recirculation sump located in the lower compartment.

In Attachment 3 of Reference 9, a connection is identified between the lower and upper compartments, allowing a small amount of flow to bypass the ice condenser. It is indicated that this flow is through the drains identified above. Based on Reference 9, we assumed that flow through the drains was possible, but that flow would be precluded in certain situations. For example, when the sprays are operating, the refueling canal will fill up with water to some steady-state depth (rough calculations indicate 1.3 m or 4.3 ft) such that the flow through the drains roughly matches the flow rate of the sprays. Also, for any accident in which the inventory of the refueling water storage tank (RWST) is injected into containment, the water level in the lower compartment will rise above the level of these drains. Thus, gas flow through these drains is precluded early in most accidents.

The spray system has two modes of operation, the injection mode and the recirculation mode. In the injection mode,

the system draws the spray water from the RWST, which is located outside of the containment. This water is pumped into containment by the spray system pumps and through the spray headers. In the recirculation mode, water is drawn from the recirculation sump in the lower compartment and cooled by a recirculation heat exchanger before being reinjected into the dome via the spray headers.

Since hydrogen combustion has been identified as a concern for ice-condenser containments, deliberate-ignition systems have been proposed and in most cases (including Sequoyah) installed to mitigate the effects of hydrogen combustion. Typically, these systems consist of igniters that are located in the upper plenum of the ice condenser, the dome, and the lower compartment. The igniters are installed to cause ignition early, before hydrogen accumulates to a level which could threaten integrity. These systems are ac-powered and are activated manually by the operator.

2.2 Case Descriptions

Sixteen different basic accident scenarios were analyzed with MARCH to provide containment water and hydrogen source terms for HECTR. Fifty-three different cases were evaluated using HECTR. These cases are described in Table 2-1. Each of the cases at the top of Table 2-1 required a separate MARCH run (A.00, B.00, etc.). Variations on these cases which involved changes in the HECTR input only (cases A.01, A.02, ..., C.01, D.01, etc.) are listed in the second block of Table 2-1.

Column 2 of Table 2-1 indicates the accident scenario leading to core degradation or core meltdown for each case. These accident scenarios are denoted using the event nomenclature of the probabilistic risk assessment (PRA) which was performed for Sequoyah #1 in the Reactor Safety Study Methodology Applications Program (RSSMAP).[10] This event nomenclature is summarized in Table 2-2.

In selecting accident scenarios for analysis, we considered the accident sequences which the RSSMAP Sequoyah PRA identified as dominant contributors to the most severe release categories: $S_1D-\gamma$, $S_2D-\gamma$, $S_1H-\alpha$, $S_1H-\gamma$, $S_1HF-\gamma$, $S_1HF-\delta$, $S_2HF-\epsilon$, TML- γ , and V. For this report we investigated only containment failure due to overpressurization as a result of combustion or the accumulation of gases (containment failure modes γ and δ). In this context, the $S_1H-\alpha$, $S_2HF-\epsilon$, and V sequences are not relevant because they involve containment failure due to an in-vessel steam explosion, basemat meltthrough, and containment bypass, respectively.

Table 2-1
Case Descriptions*

Case	Accident ^a Sequence	Restore ECC	Extent Zr Oxidation	Spray Trains	Recircu- lation Fans	Contain- ment Vent	Ignition Limits	Ice Cond Drain Temp (K)
A.00	S ₂ D	yes	75%	2	2	no	8%	310
B.00	S ₂ D	yes	35%	2	2	no	8%	310
C.00	S ₂ D	yes	75%	2	2	no	8%	310
D.00	S ₂ D	no	100%	2	2	no	8%	310
E.00	S ₂ D	no	min	2	2	no	8%	310
F.00	S ₁ D	yes	75%	2	2	no	8%	310
G.00	S ₁ D	yes	37%	2	2	no	8%	310
H.00	S ₁ H	yes	75%	2	2	no	8%	310
I.00	S ₁ HF	yes	75%	2	2	no	8%	310
J.00	S ₁ HF	no	100%	2	2	no	8%	310
K.00	S ₁ HF	no	min	2	2	no	8%	310
L.00	TMLU	yes	75%	2	2	no	8%	310
M.00	TMLB	yes	75%	2	2	no	8%	310
N.00	TMLB'	no	100%	0	0	no	12%	310
O.00	TMLB'	no	min	0	0	no	12%	310
P.00	TMLB'	no	65%	0	0	no	12%	310

A.01	S ₂ D	yes	75%	2	0	no	8%	310
A.02	S ₂ D	yes	75%	1	1	no	8%	310
A.03	S ₂ D	yes	75%	0	2	no	8%	310
A.04	S ₂ D	yes	75%	0	0	no	8%	310
A.05	S ₂ D	yes	75%	0	2	no	8%	310
A.06	S ₂ D	yes	75%	2	2	no	6%	310
A.07	S ₂ D	yes	75%	2	2	no	7%	310
A.08	S ₂ D	yes	75%	2	2	no	9%	310
A.09	S ₂ D	yes	75%	2	2	no	10%	310
A.10	S ₂ D	yes	75%	2	2	no	8%	310
A.11	S ₂ D	yes	75%	2	2	no	8%	310
A.12	S ₂ D	yes	75%	2	2	no	8%	310
A.13	S ₂ D	yes	75%	2	2	no	8%	310
A.14	S ₂ D	yes	75%	2	2	no	8%	310
A.15	S ₂ D	yes	75%	2	2	no	8%	310
C.01	S ₂ D	yes	75%	2	2	no	8%	328
C.02	S ₂ D	yes	75%	2	2	no	8%	328
D.01	S ₂ D	no	100%	2	2	yes	8%	310
D.02	S ₂ D	no	100%	2	2	no	8%	310
E.01	S ₂ D	no	min	2	2	no	8%	310
F.01	S ₁ D	yes	75%	2	2	no	8%	310
H.01	S ₁ H	yes	75%	2	2	no	8%	310
I.01	S ₁ HF	yes	75%	2	2	no	8%	290
I.02	S ₁ HF	yes	75%	2	2	no	8%	310
I.03	S ₁ HF	yes	75%	2	2	no	8%	310
I.04	S ₁ HF	yes	75%	2	2	no	8%	310
I.05	S ₁ HF	yes	75%	2	2	no	8%	310
I.06	S ₁ HF	yes	75%	2	2	no	8%	310
J.01	S ₁ HF	no	100%	2	2	yes	8%	310
J.02	S ₁ HF	no	100%	2	2	no	8%	310
K.01	S ₁ HF	no	min	2	2	no	8%	310
L.01	TMLU	yes	75%	2	2	no	8%	310
M.01	TMLB	yes	75%	2	2	no	8%	310
N.01	TMLB'	no	100%	0	0	yes	12%	310
N.02	TMLB'	no	100%	0	0	no	12%	310
O.01	TMLB'	no	min	0	0	no	12%	310
P.01	TMLB'	no	65%	0	0	yes	12%	310

Notes for Table 2-1

Condenser Temperature (°F)	Notes ^b
98.6	-
98.6	-
98.6	-
98.6	-
98.6	-
98.6	-
98.6	-
98.6	c
98.6	c
98.6	c
98.6	-
98.6	d
98.6	-
98.6	-
98.6	-
98.6	-
98.6	-
98.6	-
98.6	-
98.6	e
98.6	-
98.6	-
98.6	-
98.6	-
98.6	-
98.6	f
98.6	g
98.6	h
98.6	i
98.6	j
98.6	k
131	l
131	m
98.6	-
98.6	j
98.6	j
98.6	j
98.6	j
62.6	c
134.6	c
98.6	c, n
98.6	c, o
98.6	c, e
98.6	c, j
98.6	c
98.6	c, j
98.6	c, j
98.6	j
98.6	d, j
98.6	-
98.6	j
98.6	j
98.6	-

- a = Small-break LOCAs (S_2 sequences) are 2-inch diameter breaks; intermediate-break LOCAs (S_1 sequences) are 6-inch breaks.
- b = Except as otherwise noted, default values for the ice-condenser heat-transfer coefficient, extent of combustion, and flame speed were used in all cases. See Appendix A for details.
- c = Spray trains operated in injection mode but failed in recirculation mode.
- d = Spray and fan functions were recovered when power was restored.
- e = A surface heat-transfer coefficient equal to five times the default value was used.
- f = An extent-of-combustion equal to 0.75 times that predicted by the default correlation was used.
- g = A flame speed equal to three times that predicted by the default correlation was used.
- h = A flame speed equal to one-third that predicted by the default correlation was used.
- i = Upper-plenum ignition was suppressed.
- j = Oxygen depletion to an initial mole fraction of 14% was assumed.
- k = The ice-condenser doors were removed.
- l = An extent-of-combustion of 85%, a flame speed of 1.8 m/s (6 ft/s), and no propagation into the ice condenser were used in a comparison to the CLASIX base case.
- m = An extent-of-combustion of 85% and a flame speed of 1.8 m/s (6 ft/s) were used in a comparison to COMPARE.
- n = An ice-condenser heat-transfer coefficient equal to one-fifth that predicted by the default correlation was used.
- o = An ice-condenser heat-transfer coefficient equal to five times that predicted by the default correlation was used.

Also Available On
Aperture Card

TI
APERTURE
CARD

Table 2-2

Event Nomenclature [10]

Symbol	Meaning
B	Failure of both onsite and offsite electrical power
B'	Failure to recover either onsite or offsite electrical power within about 1 to 3 hours following an initiating event
C	Failure of containment spray injection
D	Failure of emergency coolant injection
F	Failure of containment spray recirculation
H	Failure of emergency coolant recirculation
L	Failure to maintain inventory in the steam generators and transfer heat to the environment using the power conversion system and secondary steam relief
M	Failure to maintain inventory in the steam generators and transfer heat to the environment using the auxiliary feedwater system and secondary steam relief
S ₁	Small (2-inch to 6-inch diameter) break in reactor coolant system pressure boundary
S ₂	Small (1/2-inch to 2-inch diameter) break in reactor coolant system pressure boundary
T	Transient event
U	Failure of the chemical and volume control system in the high pressure injection mode (feed and bleed)
V	Failure of the check valves which isolate the low-pressure injection system in the auxiliary building from the reactor coolant system which operates at high pressure within containment
α	Containment rupture due to an in-vessel steam explosion
γ	Containment failure due to hydrogen burning
δ	Containment failure due to overpressure
ε	Containment failure due to basemat meltthrough

Recent results from the generic ASEP indicate that primary system "feed and bleed" cooling could prevent the total loss-of-feedwater (TML) scenarios from leading to core meltdown.[1] Consequently, we only considered loss-of-feedwater scenarios which also involved loss of "feed and bleed" capability, namely, the TMLU, TMLB', and TMLB scenarios. ASEP results also suggest that, for loss-of-coolant accidents (LOCAs) initiated by sufficiently small breaks, if ECC systems function in the injection mode, the operators would probably have sufficient time to depressurize the primary system, thereby precluding the need to switch over to ECC recirculation from the containment sump. For this reason, we analyzed S₁H and S₁HF scenarios but not S₂H and S₂HF scenarios.

As will be discussed in Chapter 3, the coupling between MARCH and HECTR becomes more complicated when vessel breach occurs. Consequently, many of the results presented herein are for degraded-core scenarios. In these degraded-core scenarios, ECC was assumed to be restored in time to arrest zirconium oxidation and prevent core slumping. In most of the degraded-core scenarios, the ECC restoration time was selected to yield 75% zirconium oxidation, in accordance with the NRC's interim hydrogen rule. However, this resulted in what we feel are unrealistically high predictions of fractions of the core that are molten during core quenching. Therefore, some degraded-core cases were run with smaller amounts of zirconium oxidation. Further discussion of this topic is contained in Chapter 3.

The degraded-core scenarios are indicated by a "yes" in the "Restore ECC" column in Table 2-1. In contrast, a "no" in the "Restore ECC" column of Table 2-1 indicates a core-meltdown* scenario. The "Extent Oxid." column in Table 2-1 indicates that for some core-meltdown scenarios we specified 100% oxidation of zirconium, whereas for other cases we selected MARCH input parameters which would tend to minimize predicted zirconium oxidation.

*The term "core-meltdown" is used throughout this report to describe accident scenarios which involve complete core meltdown and vessel breach. In the "degraded-core" scenarios some core melting can occur but would be arrested before the core slumps into the lower plenum.

The cases summarized in Table 2-1 were chosen not only to include scenarios that are significant contributors to risk but also to examine the major uncertainties that could affect the containment pressure-temperature responses for these scenarios. It was felt from the outset that the HECTR results would be sensitive to:

1. Hydrogen and water source terms
2. Spray and fan operation
3. Ignition and propagation criteria
4. Combustion completeness
5. Flame speed
6. Heat transfer coefficients
7. Ice-condenser drain temperature
8. Compartmentalization

As indicated in Table 2-1, all of these factors with the exception of compartmentalization are examined in this study. In addition, we examined the potential benefits of adding a containment vent in some of the core-meltdown scenarios. Bases for the combustion and heat-transfer values indicated in Table 2-1 for items 3 through 7 above are discussed in Chapter 4 and Appendix A. Compartmentalization is not as critical here as it might be for other containments, because the flow, and therefore mixing patterns, are well established when the recirculation fans are operating. Future efforts might consider the effects of asymmetric flow through the ice condenser leading to higher steam concentrations in the dome if local regions of the ice are melted. Additionally, for cases where the fans are not operating, natural convective loops within and above the ice condenser may be of importance, requiring significant refinement of the compartmentalization used here.

3. GENERATION OF WATER AND HYDROGEN SOURCE TERMS

3.1 MARCH

MARCH (Meltdown Accident Response CHaracteristics) is a fast-running computer code that was written for analyzing the thermal-hydraulic response of a nuclear power plant during hypothetical accident situations.[2] While many shortcomings of the code have been identified,[11] MARCH is still the only publicly available code which will treat the whole accident scenario from accident initiation through containment failure. However, MARCH has some limitations when attempting to predict containment loads produced during combustion events in an ice-condenser containment. Namely, MARCH is limited to a two-compartment nodalization for an ice-condenser containment and uses an intercompartmental flow model based on pressure equilibration. Also, the effects of sprays during a combustion event are modeled poorly in MARCH, and the ice-condenser model is very nonmechanistic and user-input-specific. Therefore, MARCH was used in this analysis only to model the primary system and to calculate sources of both hydrogen and water (here water refers to both the liquid and gaseous phases) which would be released into containment during hypothetical accident scenarios. Note that the MARCH primary system model is limited to a single volume, and any hydrogen production is from the oxidation of zirconium only. No steel oxidation is taken into account; thus, the amount of hydrogen production may be underestimated in some cases. However, for cases where most of the zirconium is oxidized, the hydrogen produced is sufficient to consume most of the oxygen in containment. Therefore, additional hydrogen production is of minimal importance for those cases.

The latest publicly released version of MARCH (version 1.1) was used with certain modifications that have been implemented at Sandia National Laboratories.[3] The modifications relevant to this analysis are the addition of models for axial and radial radiative heat transfer within the core, a different model for in-vessel flashing of water, and the use of the latest standardized decay heat formulation.[12] These models have an effect upon the in-vessel steam and hydrogen generation rates and hence upon the source terms to containment. The reader should see Reference 3 for more details regarding these models.

The source terms through the time of vessel failure were generated for HECTR by recording the rates of water and hydrogen releases to containment (as calculated by MARCH) each MARCH time step. These recorded values were then input to HECTR, as discussed in Chapter 4. In the core-meltdown cases, the source rates at the time of vessel failure are somewhat arbitrary due to the way MARCH treats this aspect of the accident. When the vessel fails, MARCH calculates the

source rate of hydrogen and water such that all of the primary system inventory is released to containment uniformly over the preceding time step. Thus, some very large flow rates are predicted at vessel breach if the previous MARCH time step is small. However, the total amount of material released is independent of the time step.

After vessel breach, a coolable debris bed was postulated to form in the reactor cavity, because HECTR could not treat the carbon monoxide and carbon dioxide that would be produced during concrete attack by the hot debris. During this period of the scenario, the heat transfer from the debris to the water in the reactor cavity, along with the hydrogen generation rate, were calculated with subroutine HOTDROP in MARCH and recorded each MARCH time step. Several different debris-bed models are available to the user in HOTDROP. In the one selected for this analysis, the debris is assumed to fragment into user-specified uniform diameter spheres that quench to a quasi-steady temperature. After quenching, heat is transferred from the debris at a quasisteady rate as determined by the decay heat associated with the debris. This would continue until all of the water in the reactor cavity is vaporized. (None of the calculations in this report were run to the point of reactor cavity dryout.) A sump model in HECTR (see Appendix A) then used this data to calculate steam and hydrogen source terms that were consistent with the HECTR-predicted sump temperature and containment atmospheric pressure.

3.2 Degraded-Core Cases

In the degraded-core scenarios it is postulated that ECC is unavailable for a period of time long enough to allow significant zirconium oxidation, but short enough so that core damage can be arrested when ECC is restored. When ECC fails, the core is uncovered, and decay heat within the fuel begins to heat the core. When ECC is restored, the water quenches the hot core. Steam produced in this process reacts with zirconium to produce hydrogen. Although ECC is restored soon enough to quench the core and terminate the accident without breach of the reactor vessel, significant amounts of hydrogen are still produced and released to the containment atmosphere. Break elevations are shown on the plots of the primary system liquid level accompanying each case.

MARCH does not provide the option of specifying the amount of zirconium oxidation in this type of scenario. Therefore, the criterion for zirconium oxidation in the degraded-core scenarios was met by making multiple runs and adjusting the time for ECC restoration. The predicted extent of oxidation was found to be very sensitive to the time for ECC restoration. For the cases with high primary system pressure, the source terms are also somewhat dependent upon the ECC pump performance relationship that is built into

MARCH, since the set-point for the relief valves on the primary system is very near the shutoff head for the pumps. Also, as shown later, it was necessary to allow very large fractions of the core to be molten without core slump in those cases which called for 75% zirconium oxidation. Because the fractions of core molten before slump seemed unreasonable, two additional degraded-core cases were run in which approximately 35% of the zirconium was oxidized. These cases resulted in predicted peak fractions of core molten that seemed more reasonable. This does not mean that we necessarily endorse the latter cases as being more likely than the others, because the fraction of core melted is dependent upon the MARCH models. In other words, more realistic modeling might allow more or less zirconium oxidation for the same fractions of the core melted.

The MARCH input decks for each of the degraded-core cases are listed in Appendix B. The times of occurrence of key events in each of the cases are summarized in Table 3-1. Each of the degraded-core cases is then described separately.

Table 3-1

Times of Occurrence of Important Events for Degraded-Core Cases (s)

	A	B	C	F	Cases G	H, I	L	M
ECC off	0	0	0	0	0	1350	0	0
Break uncovered (or relief valves opened)	1800	1800	*	300- 1920	300- 1920	300- 1800	(5460)	(5460)
Core uncovered	2160	2160	*	780- 2400	780- 2400	2160	8340	8280
Core melt started	3444	3894	*	3402	3246	3126	9240	9216
ECC restored	2352	2328	*	3582	3396	3228	8520	8460
Core covered	13320	10980	*	7260	4800	6720	14160	15120

*Not available from Reference 9.

3.2.1 "A" Cases - S₂D Degraded-Core, 75% Zirconium Oxidation

Case A.00 represents a 0.05-m (2-in) diameter LOCA (S₂D). In this case, ECC is assumed to fail at the beginning of the scenario but is restored in time to arrest core degradation with a total of 75% of the zirconium oxidized.

The liquid level in the primary system is plotted in Figure 3-1. The break elevation and the active core region are indicated on the figure for reference. The times at which the break and top of the core are uncovered are important in terms of the behavior of the water and hydrogen sources. Figure 3-2 shows the fractions of the core that is molten and of the zirconium that has oxidized versus time. Notice that both of these fractions are zero until after the liquid level has fallen below the top of the core. It can be seen in Figure 3-2 that later in time, after the liquid level rises back above the core, the core is quenched and the oxidation reaction has stopped.

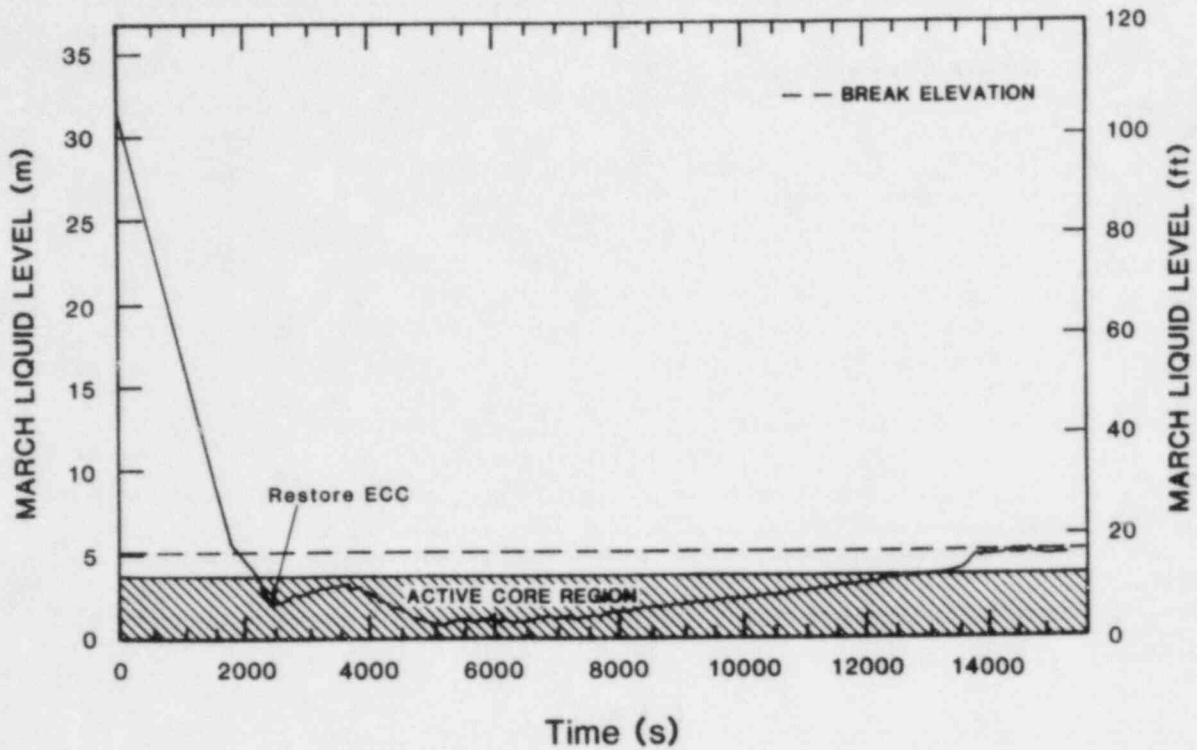


Figure 3-1. Primary System Liquid Level for "A" Cases

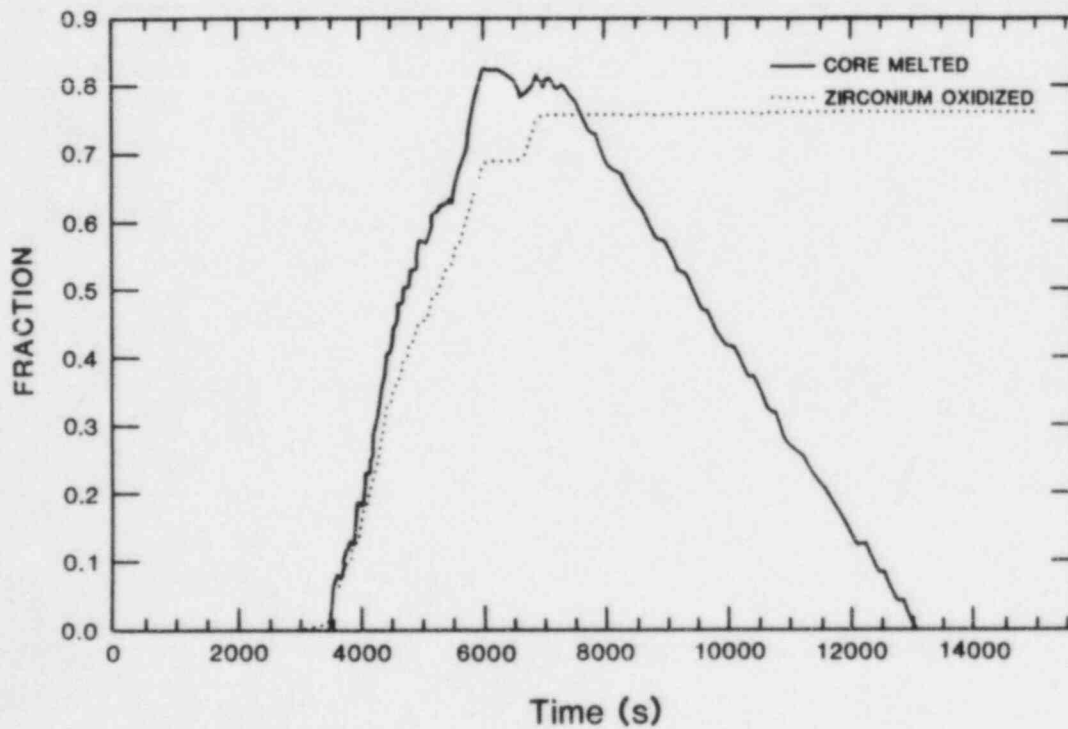


Figure 3-2. Fractions of Core Melted and Zirconium Oxidized for "A" Cases

Figures 3-3 and 3-4 show the calculated water and hydrogen source terms, respectively. The sharp drop in the water source term is due to the liquid level in the primary system falling below the pipe-break elevation. The blowdown then changes from liquid to vapor (MARCH models the break flow as a single phase and hence the sharp drop rather than a smooth transition). The time at which the core is uncovered is noted on the figures. After this time, the core starts heating up to temperatures required to initiate the oxidation reaction (1300 K or 1880°F), and the hydrogen source term starts increasing from zero.

After ECC is restored, the hydrogen production rate increases because more steam is available. This hydrogen production continues until the rising liquid level lowers the core temperature enough to quench the oxidation reaction. All of the hydrogen released for this case is produced between the time of ECC restoration and the completion of core quenching. After this time the water source term takes on quasi-steady characteristics determined by the decay heat of the core and the state of the primary system.

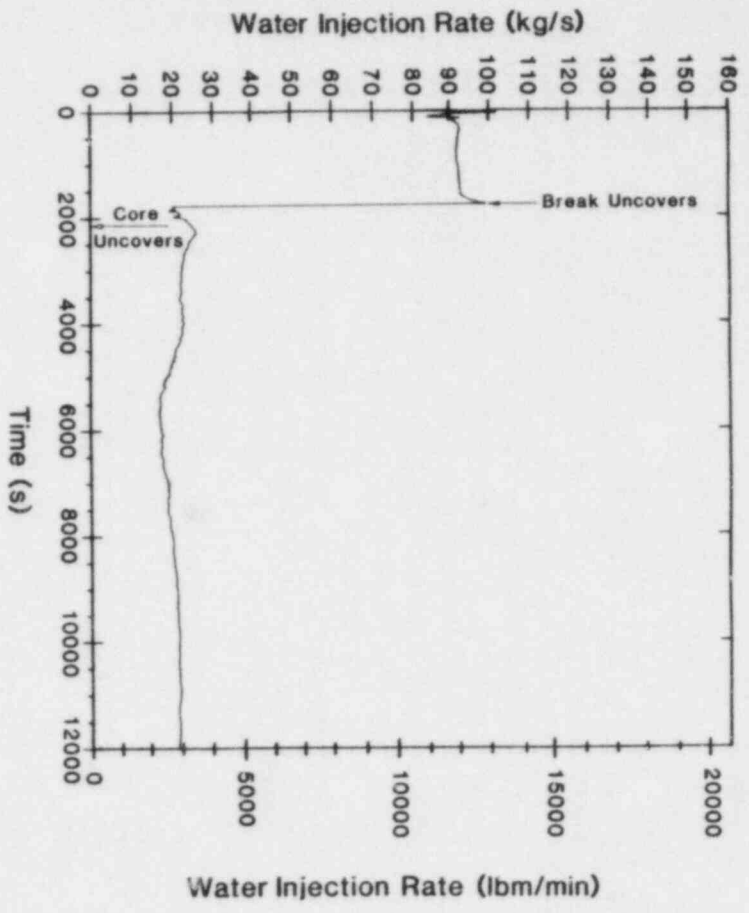


Figure 3-3. Water Source to Containment for "A" Cases

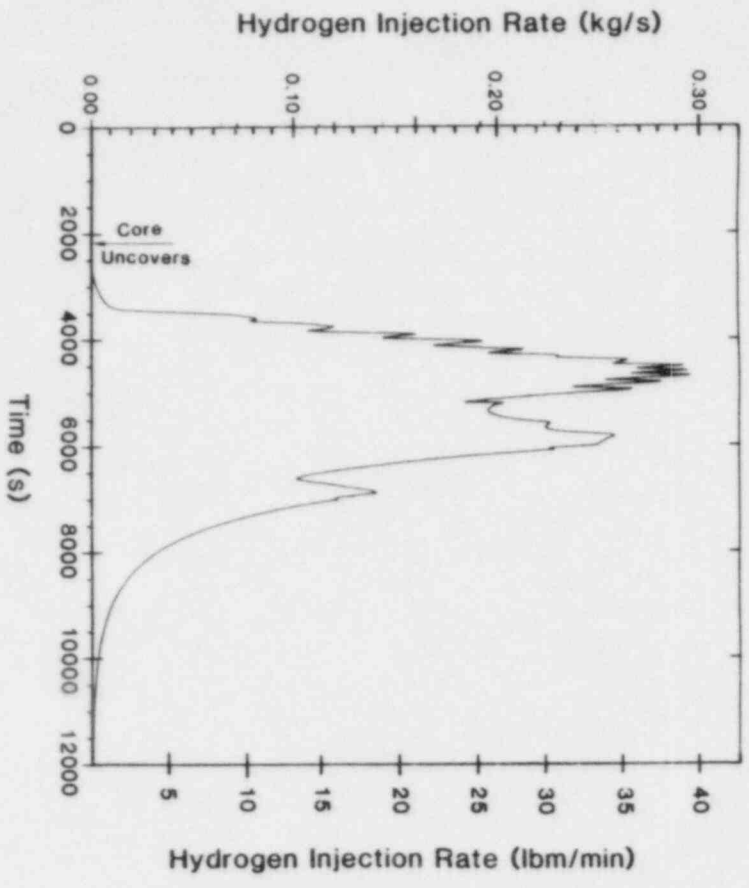


Figure 3-4. Hydrogen Source to Containment for "A" Cases

3.2.2 "B" Cases - S₂D Degraded-Core, 35% Zirconium Oxidation

Case B.00 represents the same accident scenario as case A.00 except for the extent of zirconium oxidation. In this case ECC restoration was assumed such that only 35% of the zirconium was predicted to oxidize. The MARCH-predicted primary system liquid level is shown in Figure 3-5. It is similar in nature to the predicted liquid level for case A.00. However, since ECC was restored earlier, the liquid level does not fall as low in case B.00 as in case A.00, the core remains uncovered for a shorter time, and less zirconium is oxidized. The fractions of core melted and zirconium oxidized are shown in Figure 3-6.

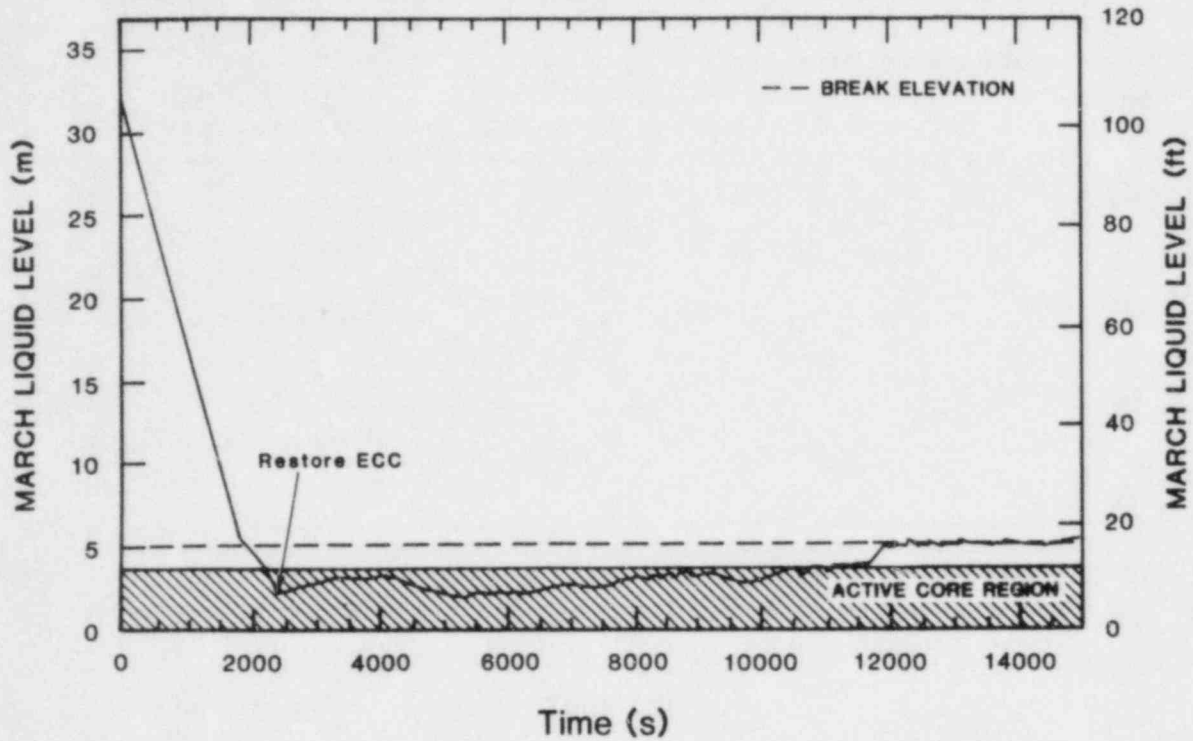


Figure 3-5. Primary System Liquid Level for "B" Cases

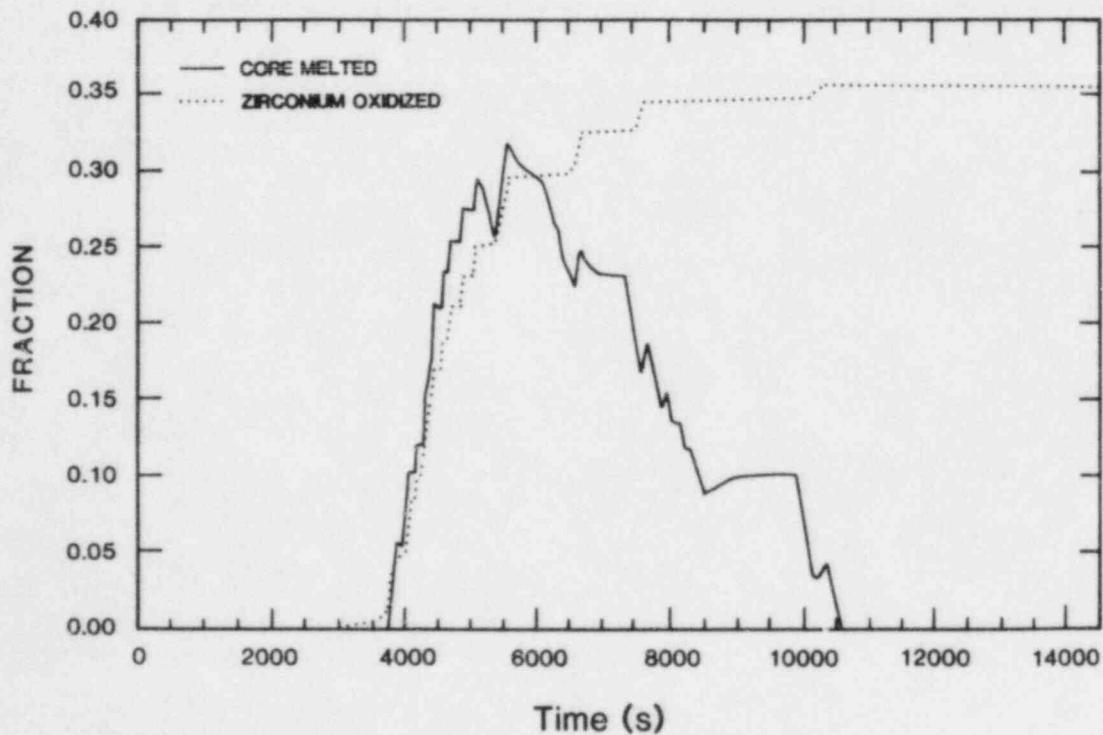


Figure 3-6. Fractions of Core Melted and Zirconium Oxidized for "B" Cases

The water and hydrogen source terms from the primary system are shown in Figures 3-7 and 3-8, respectively. The water source term is nearly identical to that for case A.00. However, a comparison between Figures 3-4 and 3-8 reveals that the peak hydrogen injection rate for case B.00 is approximately half of that for case A.00.

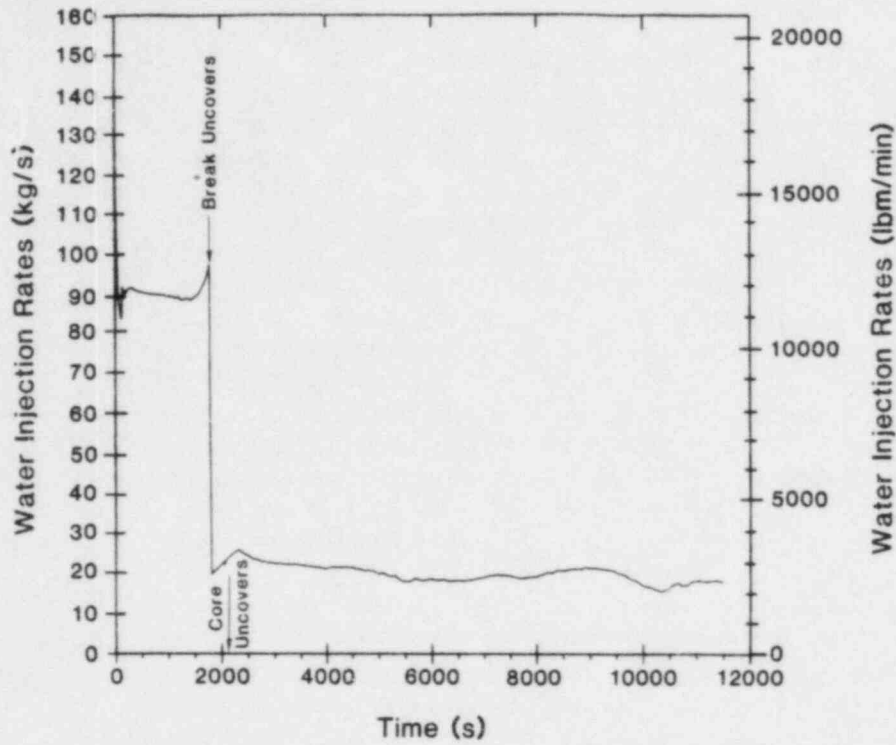


Figure 3-7. Water Source to Containment for "B" Cases

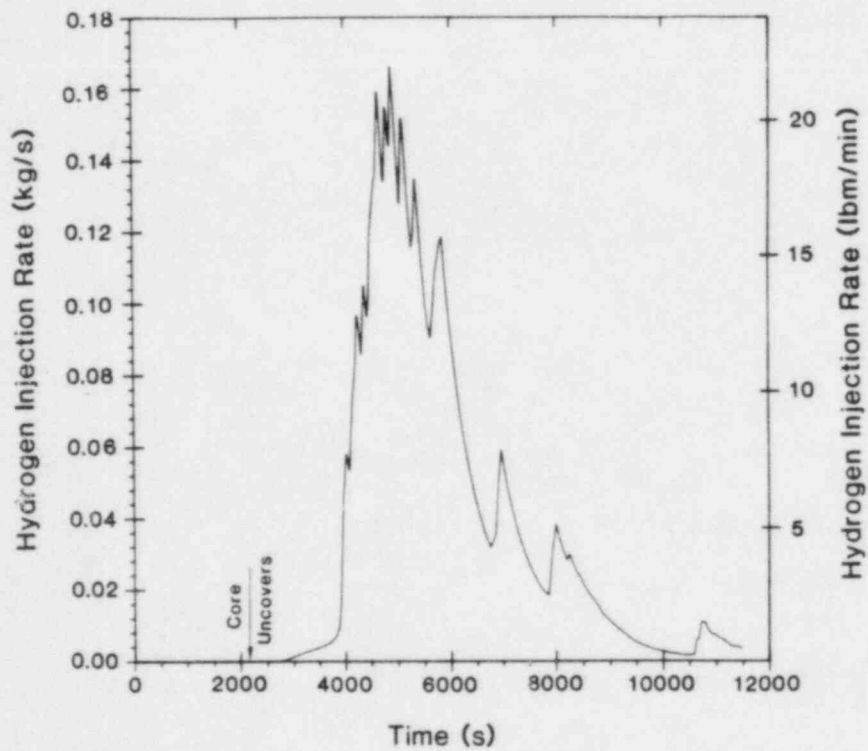


Figure 3-8. Hydrogen Source to Containment for "B" Cases

3.2.3 "C" Cases - S₂D Degraded-Core, 75% Oxidation

The source terms for case C.00 were taken from a report of a previous analysis of an ice-condenser plant.[9] The water and hydrogen source terms used in that analysis are shown in Figures 3-9 and 3-10, respectively. The report indicates that these sources were based upon MARCH analyses of a 0.05-m (2-in) diameter LOCA (S₂D) as is case A.00 of this analysis. However, a detailed look at Reference 9 reveals that these sources are actually based upon a previous MARCH analysis of an S₂D scenario which proceeds through core-meltdown rather than a degraded-core scenario.[13] Apparently no account was given in these source terms for the additional amount of steam generation that would be associated with the core quenching process in a degraded-core scenario. Comparing the two cases (A.00 and C.00) over the period when most of the hydrogen is released reveals that the ratio of hydrogen to water source rates in case A.00 is about a factor of two lower than in case C.00. Also note that the major release of hydrogen in case A.00 occurs over a time interval twice that of case C.00. The implications of these source term differences will be discussed in Chapter 4.

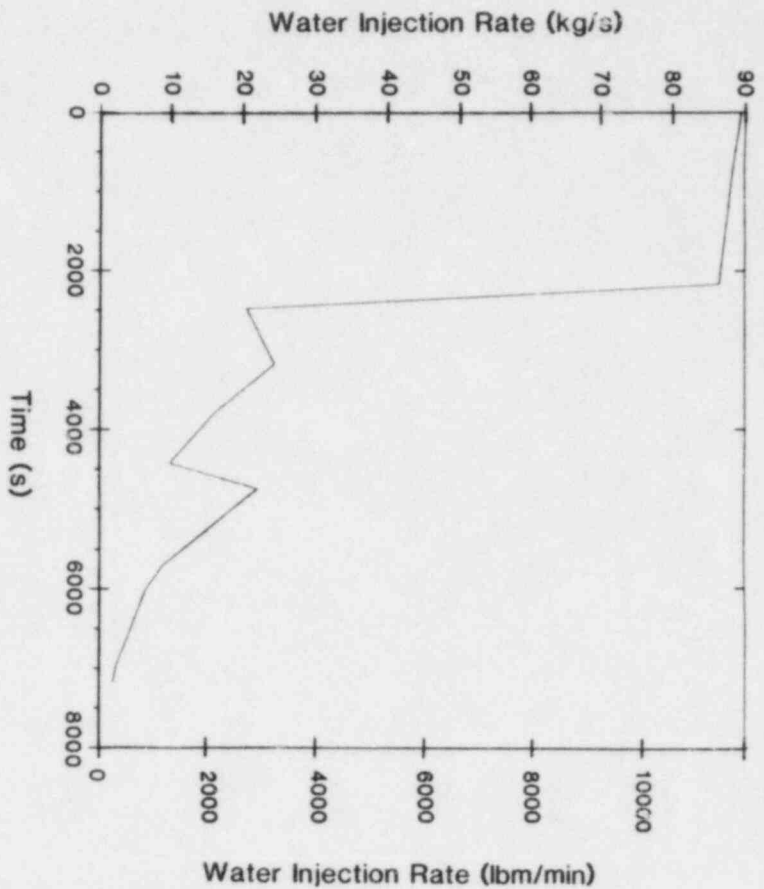


Figure 3-9. Water Source to Containment for "C" Cases

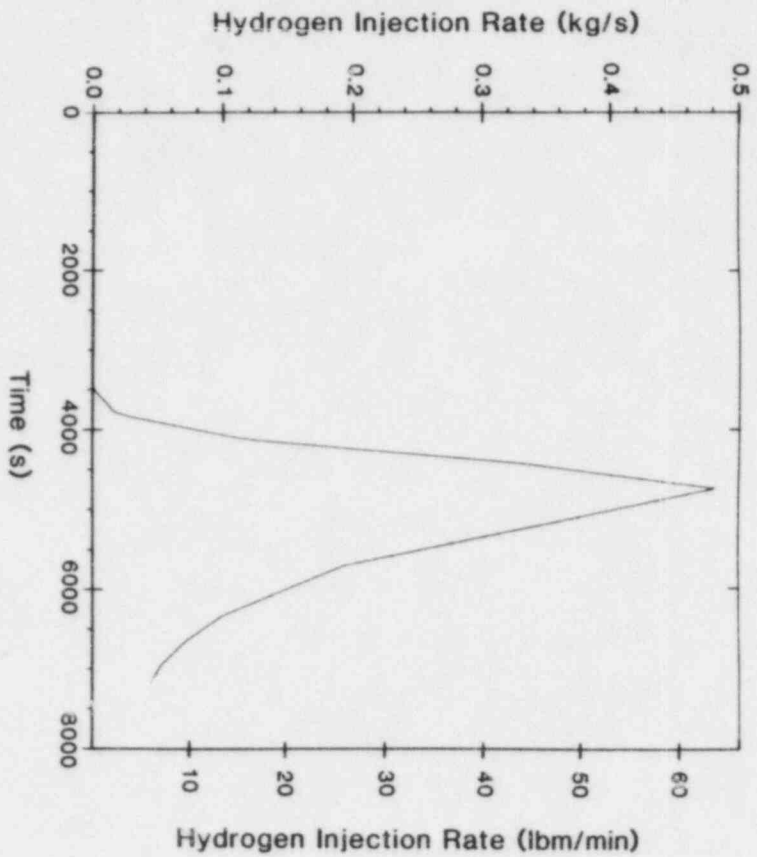


Figure 3-10. Hydrogen Source to Containment for "C" Cases

3.2.4 "F" Cases - S₁D Degraded-Core, 75% Zirconium Oxidation

Case F.00 represents a 0.15-m (6-in) diameter LOCA (S₁D) with failure of ECC in the injection mode. In early attempts to model this sequence, it was found that the 75% oxidation criterion could not be met if all the ECC pumps were turned on when ECC was restored. Upon ECC restoration (to avoid core slump and arrest the accident), the primary system pressure was low enough and correspondingly the ECC flow rate high enough so that the core was quenched with less than 75% oxidation. Thus, in this case, only the high head pumps were turned on when ECC was restored. This resulted in lower flow rates upon ECC restoration, and the oxidation criterion was achievable. Determining whether 75% oxidation is reasonable for this scenario will require more sophisticated modeling than MARCH can provide.

Similar behavior is observed in this case and in case A.00. The liquid level in the primary system is shown in Figure 3-11. The fractions of core melted and zirconium oxidized are shown in Figure 3-12. The source rates of water and hydrogen are shown in Figures 3-13 and 3-14, respectively. The important difference between this case and case A.00 is the larger source rates to containment. This is due to the larger diameter pipe break in case F.00. The erratic behavior of the liquid level after 7800 s is due to the inability of MARCH to model two-phase flow out the break. The break flow must be either all liquid or all steam in MARCH. Thus, the liquid level oscillates about the break elevation, with liquid and steam alternately flowing out the break. The plot is above the break elevation in Figure 3-11 because the swelled liquid level is shown.

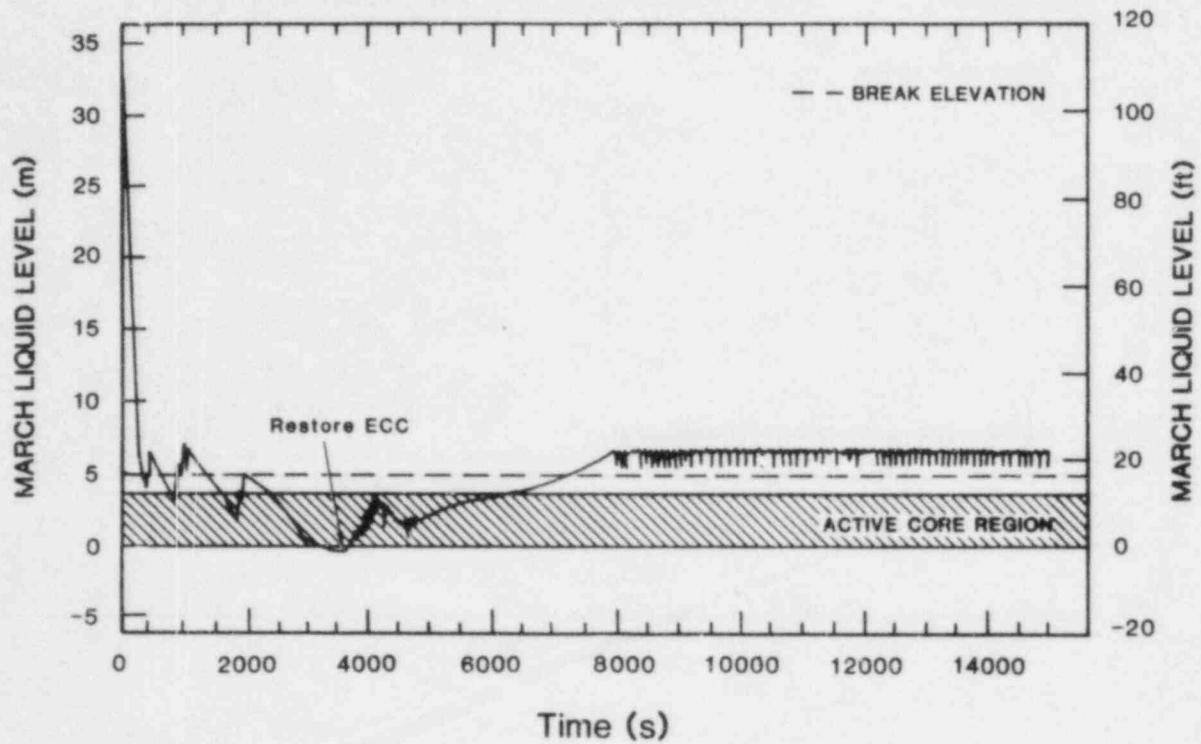


Figure 3-11. Primary System Liquid Level for "F" Cases

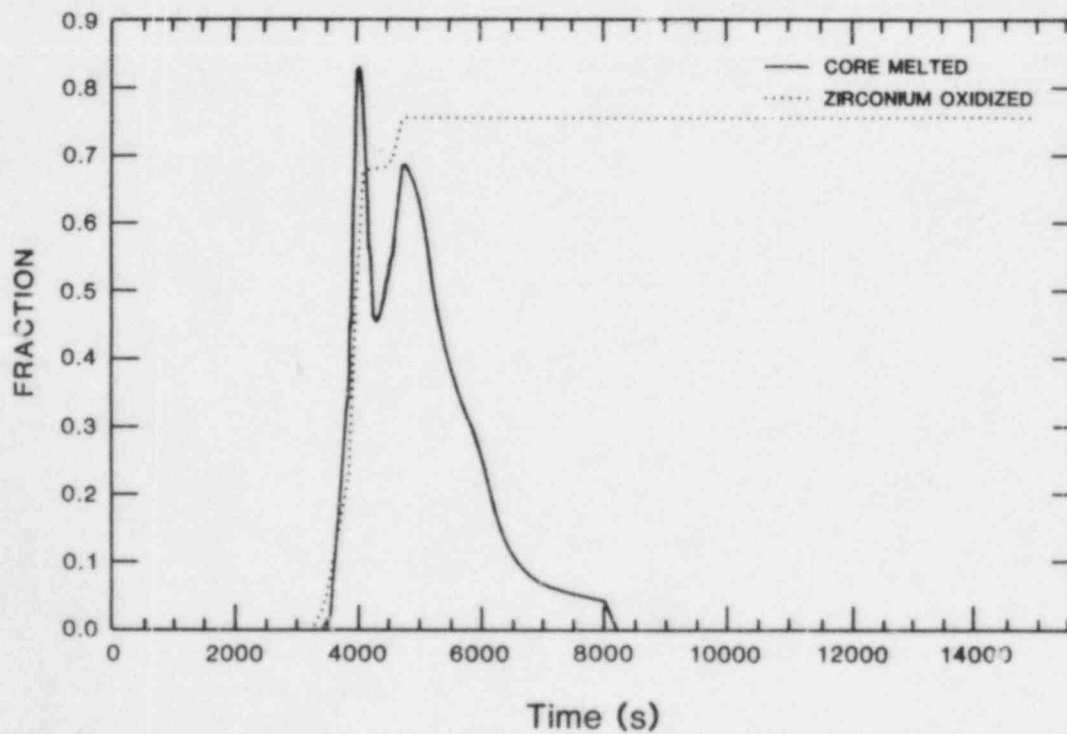


Figure 3-12. Fractions of Core Melted and Zirconium Oxidized for "F" Cases

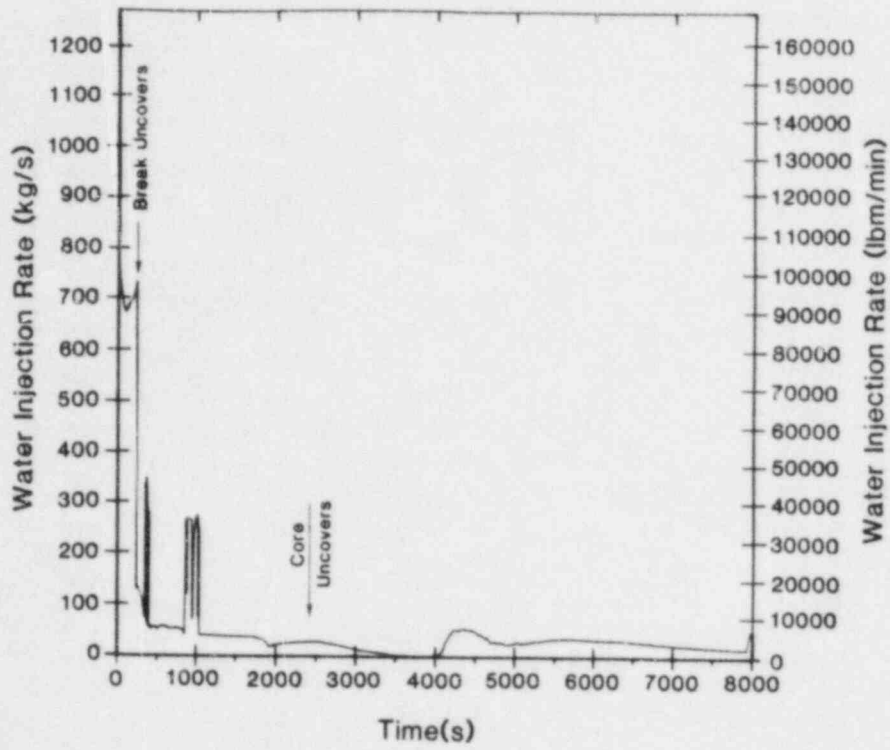


Figure 3-13. Water Source to Containment for "F" Cases

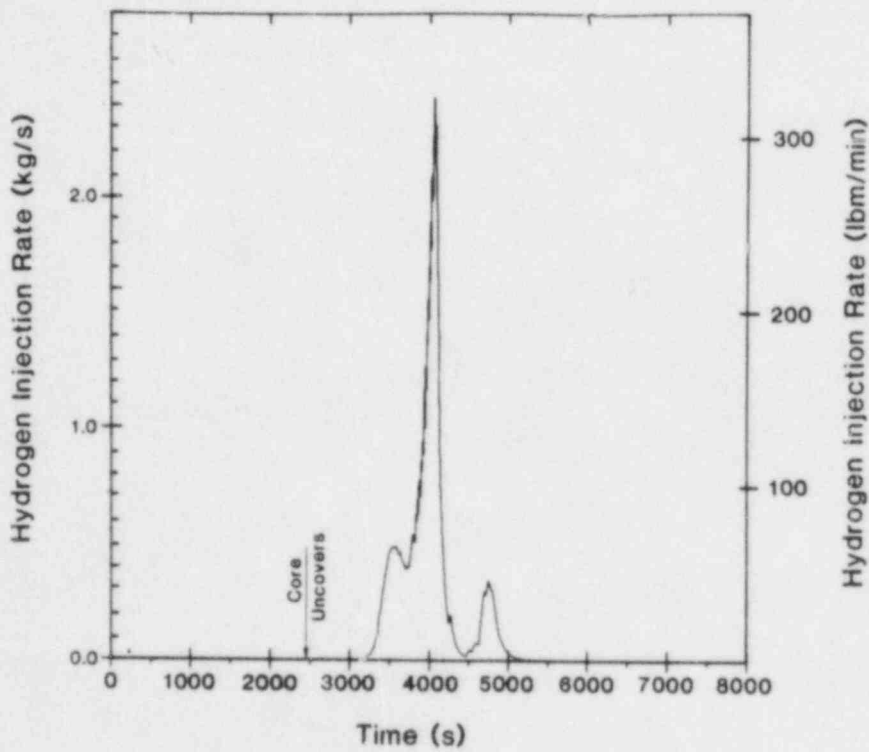


Figure 3-14. Hydrogen Source to Containment for "F" Cases

3.2.5 "G" Cases - S₁D Degraded-Core, 37% Zirconium Oxidation

Case G.00 is identical to case F.00 except for the amount of zirconium oxidation. This case was run as part of a limited parametric analysis to investigate the sensitivity of the results to the assumptions regarding zirconium oxidation. The MARCH-predicted liquid level in the primary system is shown in Figure 3-15. The liquid level behavior is nearly identical for cases F.00 and G.00, because both cases model the same initiating accident sequence. The slight differences are due to the different times for restoration of ECC, which forces the liquid level to rise sooner in case G.00. This limits the time during which the core is uncovered in case G.00 to less than that in case F.00. Thus, the fraction of zirconium is limited to 37% for case G.00, as can be seen in Figure 3-16.

The water and hydrogen source terms for case G.00 are shown in Figures 3-17 and 3-18, respectively. The water source term is nearly identical for cases G.00 and F.00, because both cases model scenarios which are initiated by the same accident sequence. However, major differences exist between the hydrogen injection rate for the two cases. This is due to the differences in the amount of zirconium oxidation.

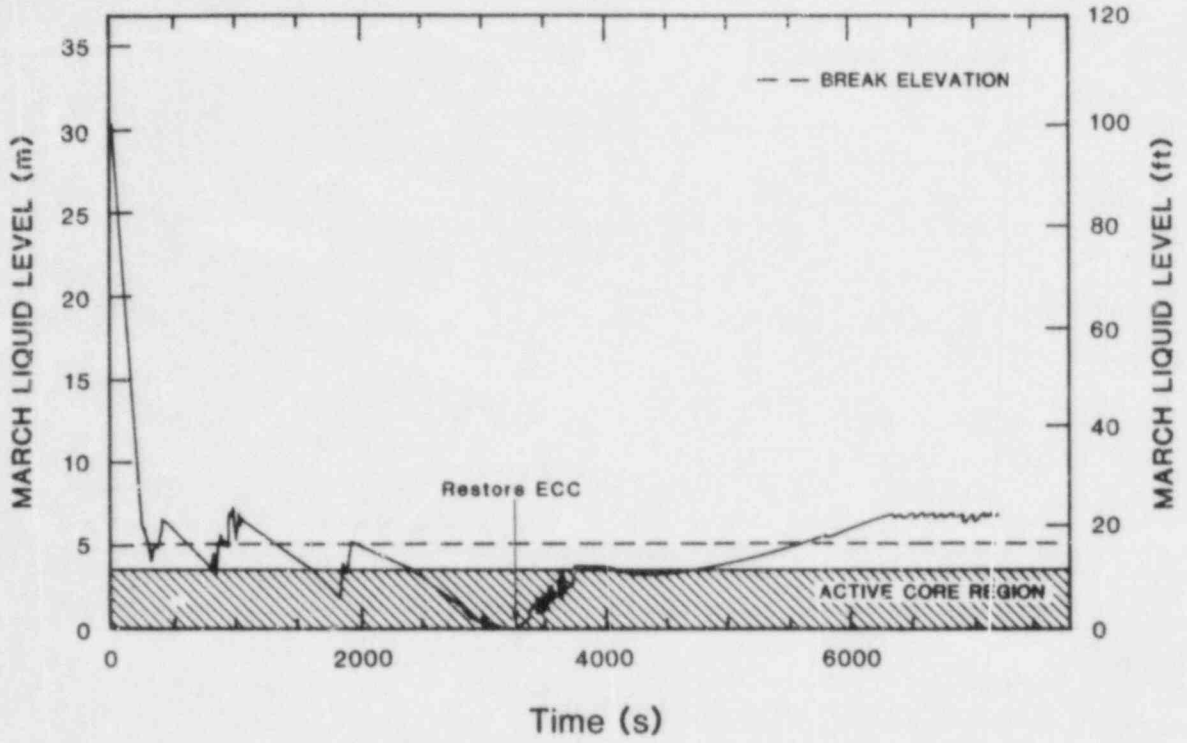


Figure 3-15. Primary System Liquid Level for "G" Cases

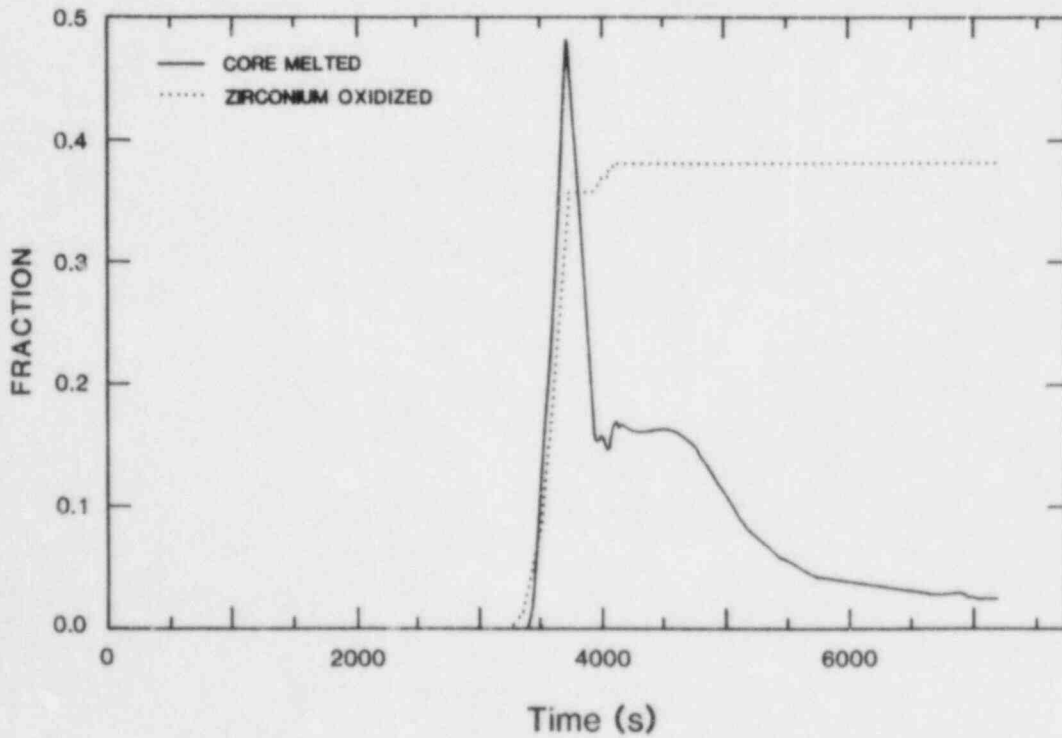


Figure 3-16. Fractions of Core Melted and Zirconium Oxidized for "G" Cases

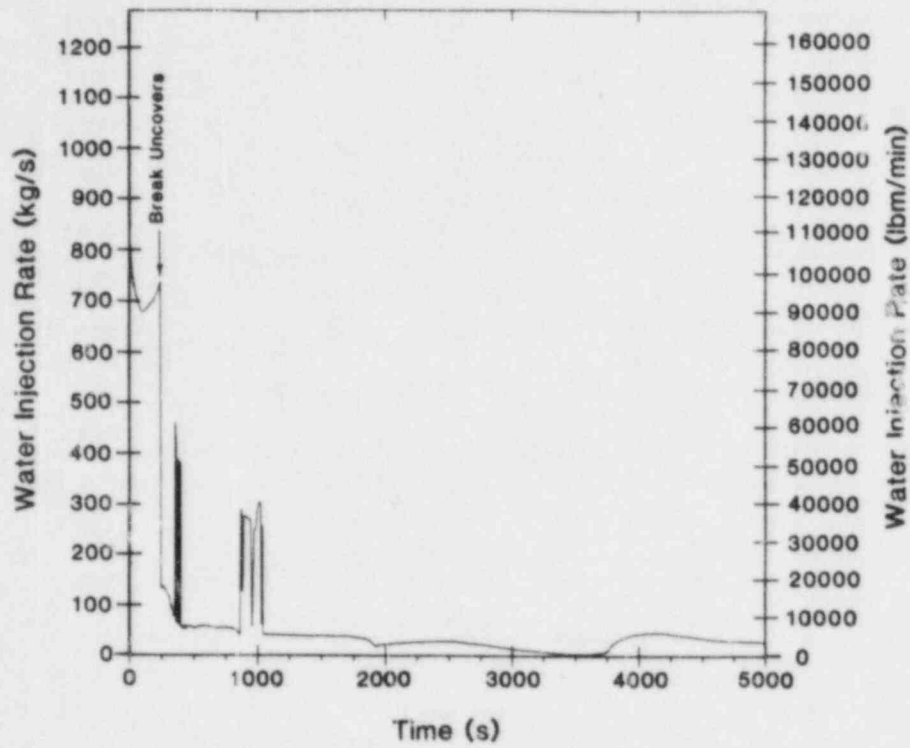


Figure 3-17. Water Source to Containment for "C" Cases

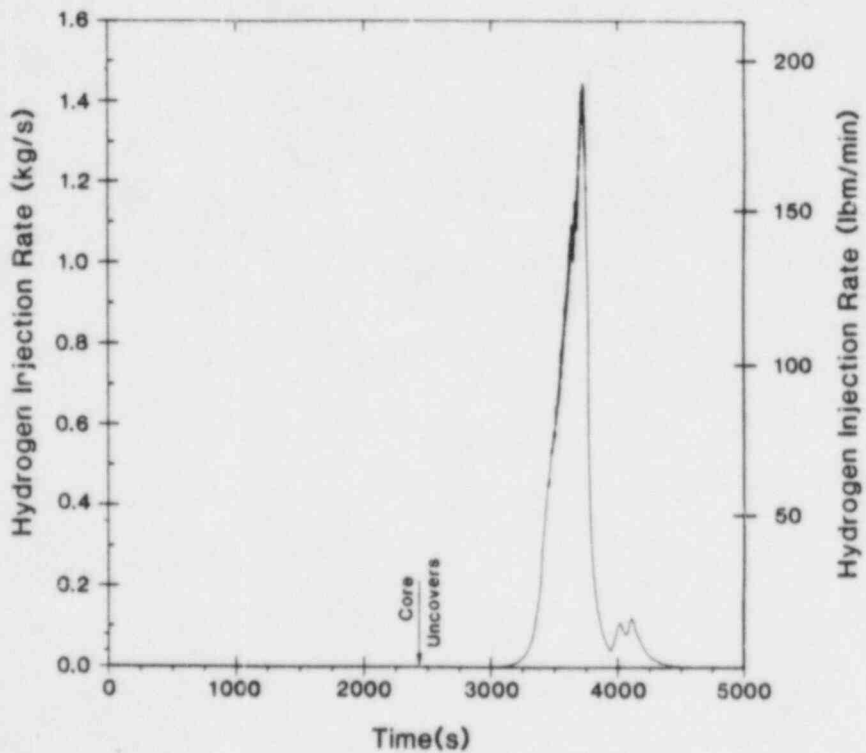


Figure 3-18. Hydrogen Source to Containment for "G" Cases

3.2.6 "H" Cases - S_1H Degraded-Core, 75% Zirconium Oxidation

Case H.00 represents a 0.15-m (6-in) diameter LOCA with failure of ECC in the recirculation mode (S_1H). The liquid level in the primary system is shown in Figure 3-19. The fractions of core melted and zirconium oxidized are shown in Figure 3-20. The source rates of water and hydrogen are shown Figures 3-21 and 3-22, respectively.

The general behavior in this case is very similar to that in case F.00. However, everything is shifted to later times since the core does not become uncovered until the switch of ECC from injection to recirculation occurs. The problem of oscillating liquid level across the break, as discussed in the case F.00 description above, occurs early in this case while ECC is functioning. This is what causes the "noisy" behavior in the liquid level and water source rate. This behavior should only minimally affect the final results because it ceases well before any hydrogen is released to containment; however, the timing of events may be affected. Pure steam is injected into containment for about 1500 s before hydrogen injection begins (see Figures 3-21 and 3-22).

3.2.7 "I" Cases - S_1HF Degraded-Core, 75% Zirconium Oxidation

This case represents a 0.15-m (6-in) diameter LOCA with failure of both ECC and containment sprays upon switch-over from injection to recirculation (S_1HF). Since the switch-over from injection to recirculation occurs earlier for ECC than for the sprays, failure of ECC occurs before failure of the sprays. Also, pressure feedback from containment has negligible impact on the primary system response. This means that the primary system response is no different for this case than for case H.00. Thus, the source terms for this scenario are no different than for case H.00, and the same source terms were used for both cases.

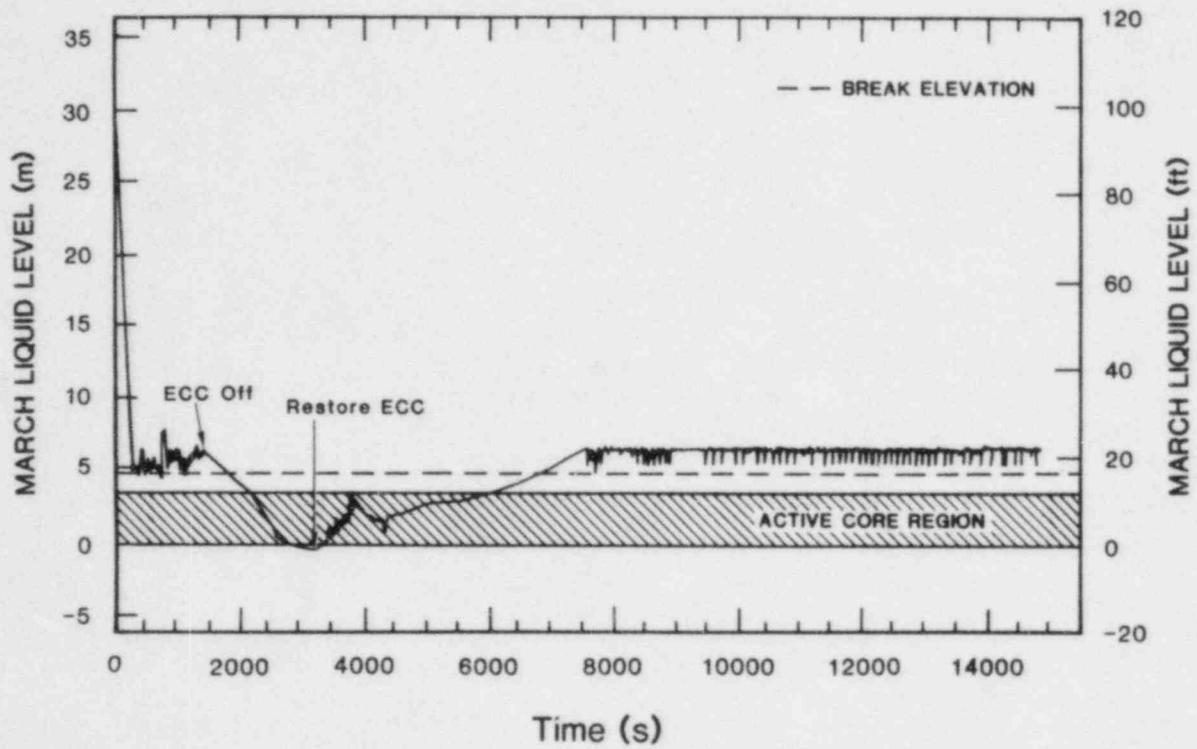


Figure 3-19. Primary System Liquid Level for "H" and "I" Cases

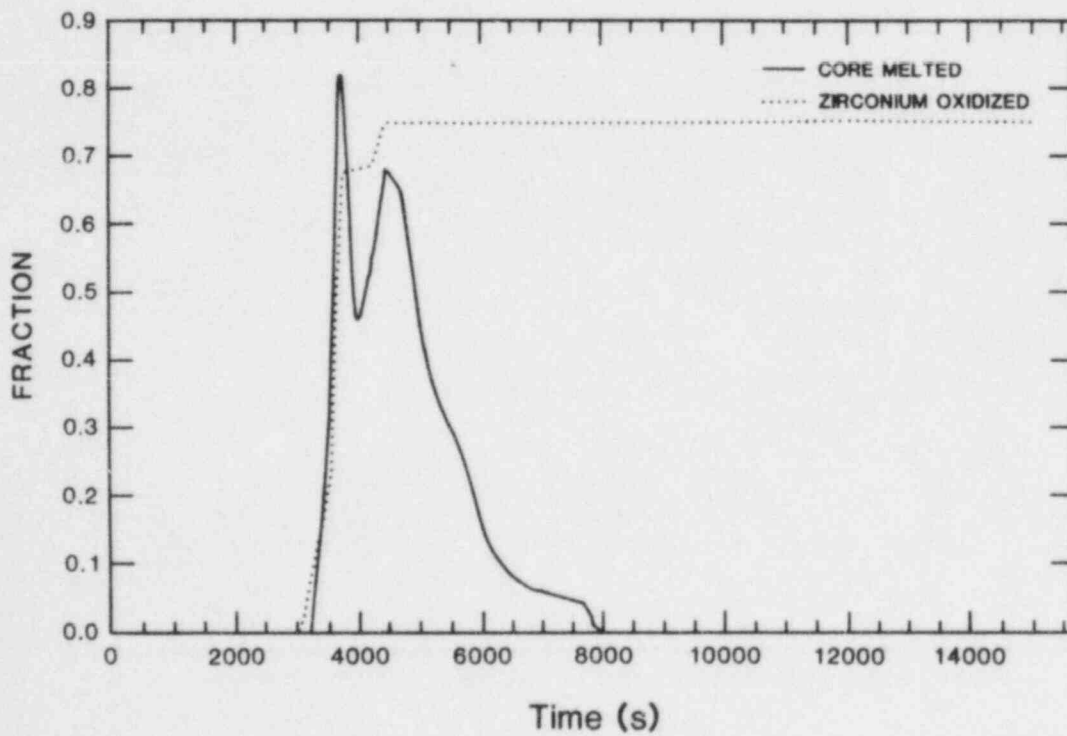


Figure 3-20. Fractions of Core Melted and Zirconium Oxidized for "H" and "I" Cases

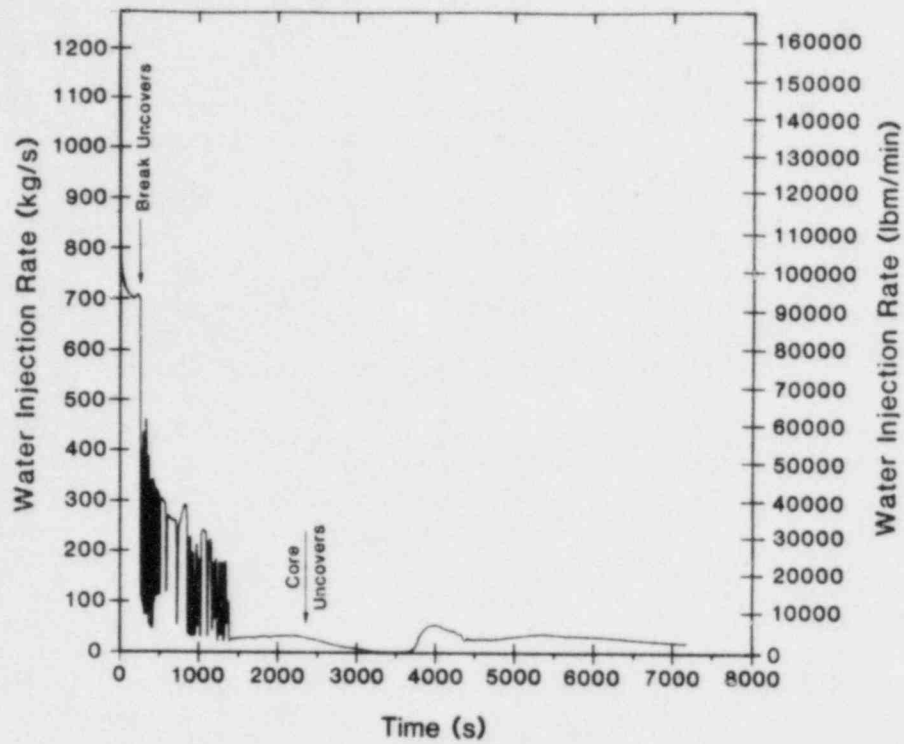


Figure 3-21. Water Source to Containment for "H" and "I" Cases

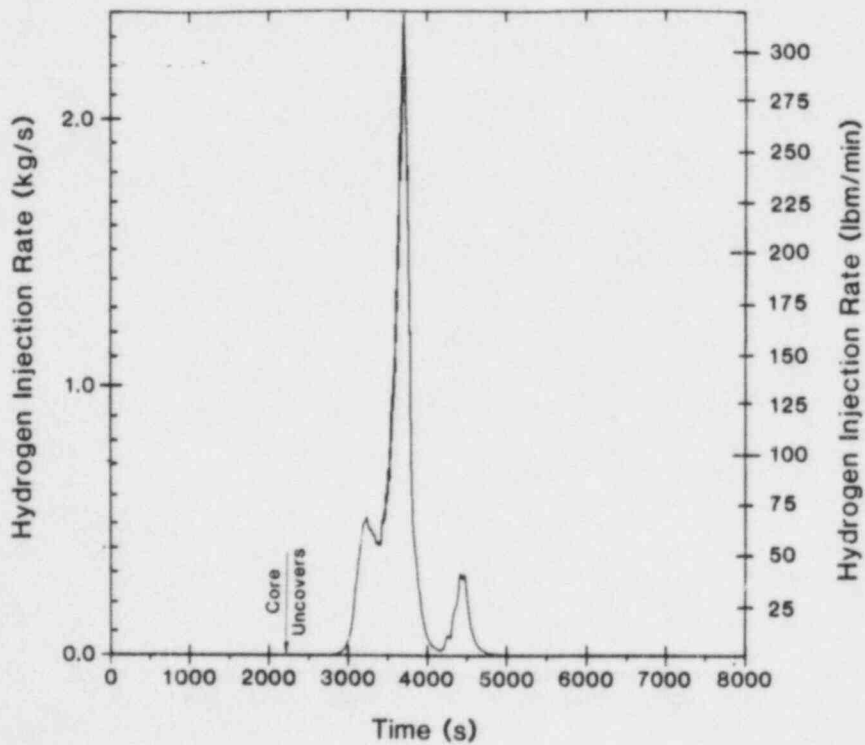


Figure 3-22. Hydrogen Source to Containment for "H" and "I" Cases

3.2.8 "L" Cases - TMLU Degraded-Core, 75% Zirconium Oxidation

This case represents a transient-initiated degraded-core scenario with loss of all feedwater capability and failure of ECC (TMLU). Power is assumed to be restored at an appropriate time to meet the 75% oxidation criterion. The plot of liquid level is shown in Figure 3-23. The fractions of core melted and zirconium oxidized are shown in Figure 3-24. Notice the slow oscillatory behavior in the liquid level between 9000 and 15000 s. For reasons that are not clear, this behavior is predicted with MARCH whenever an attempt is made to quench the core while the pressure in the primary system is near the shutoff head for the high head pumps. In this case, when ECC is restored, slow oscillations start in the primary system pressure which cause oscillations in the ECC flow rate. It is suspected that this is not physically realistic due to the time scales involved but rather is a peculiarity of the MARCH code.

The source rates of water and hydrogen are shown in Figures 3-25 and 3-26, respectively. Notice that the oscillatory behavior shows up quite clearly in the source of water to containment, but that it is masked somewhat in the case of the hydrogen source term since the oxidation rate varies over the time period as well.

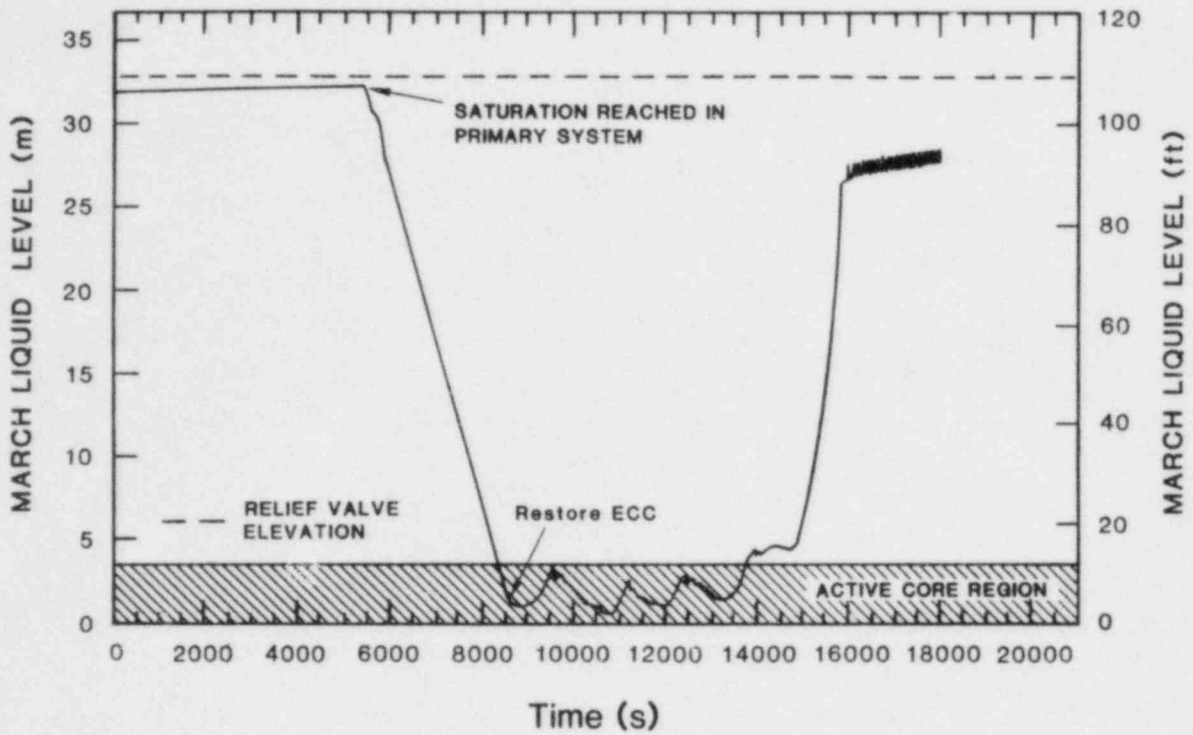


Figure 3-23. Primary System Liquid Level for "L" Cases

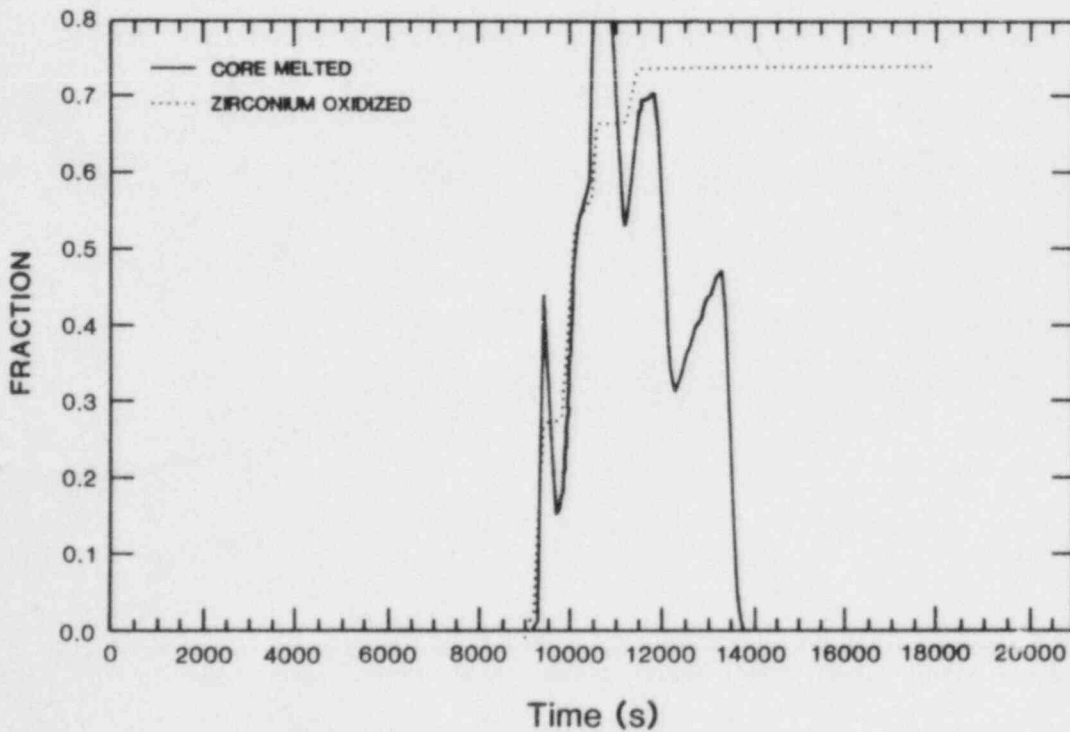


Figure 3-24. Fractions of Core Melted and Zirconium Oxidized for "L" Cases

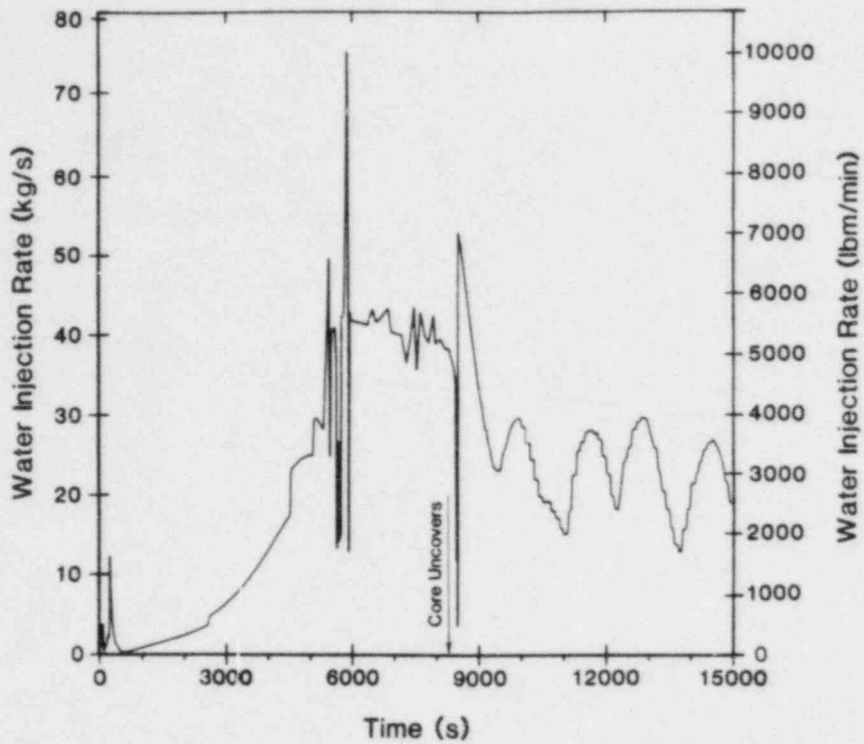


Figure 3-25. Water Source to Containment for "L" Cases

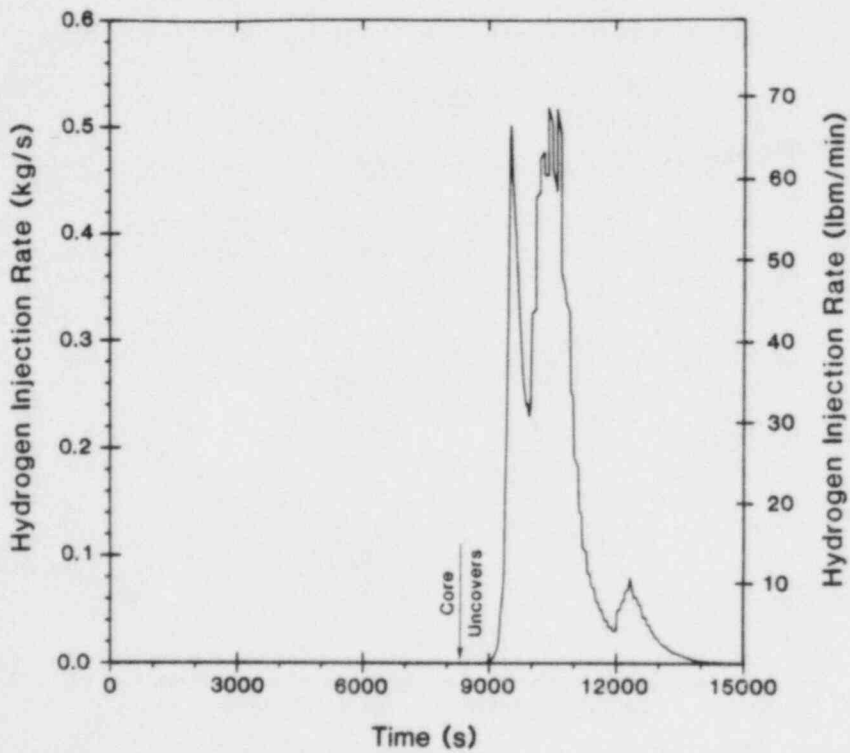


Figure 3-26. Hydrogen Source to Containment for "L" Cases

3.2.9 "M" Cases - TMLB Degraded-Core, 75% Zircorium Oxidation

Case M.00 represents a transient-initiated degraded-core scenario with loss of all feedwater capability and loss of offsite power (TMLB). With regard to the source terms, there was only a minor difference between this case and the previous one. That is, the sprays did not operate in this case until power was restored, and the RWST remained full. This means that when ECC was initially turned on, it operated in the injection mode. In case L.00 the sprays operated continually from the beginning of the accident, depleting the RWST, so that when ECC was restored, it was in the recirculation mode. This made a difference in the temperature of the ECC water that was being injected into the primary system and gave rise to the minor differences that can be observed in the source terms.

Figure 3-27 illustrates the liquid level in the primary system for this case. The fractions of core melted and zirconium oxidized are shown in Figure 3-28. The long-term oscillations in these two figures are again due to peculiarities of the MARCH code as presented in the L.00 case discussion. The source terms of water and hydrogen are found in Figures 3-29 and 3-30, respectively. The similarity between these source terms and those shown for case L.00 can be seen by comparing to Figures 3-25 and 3-26.

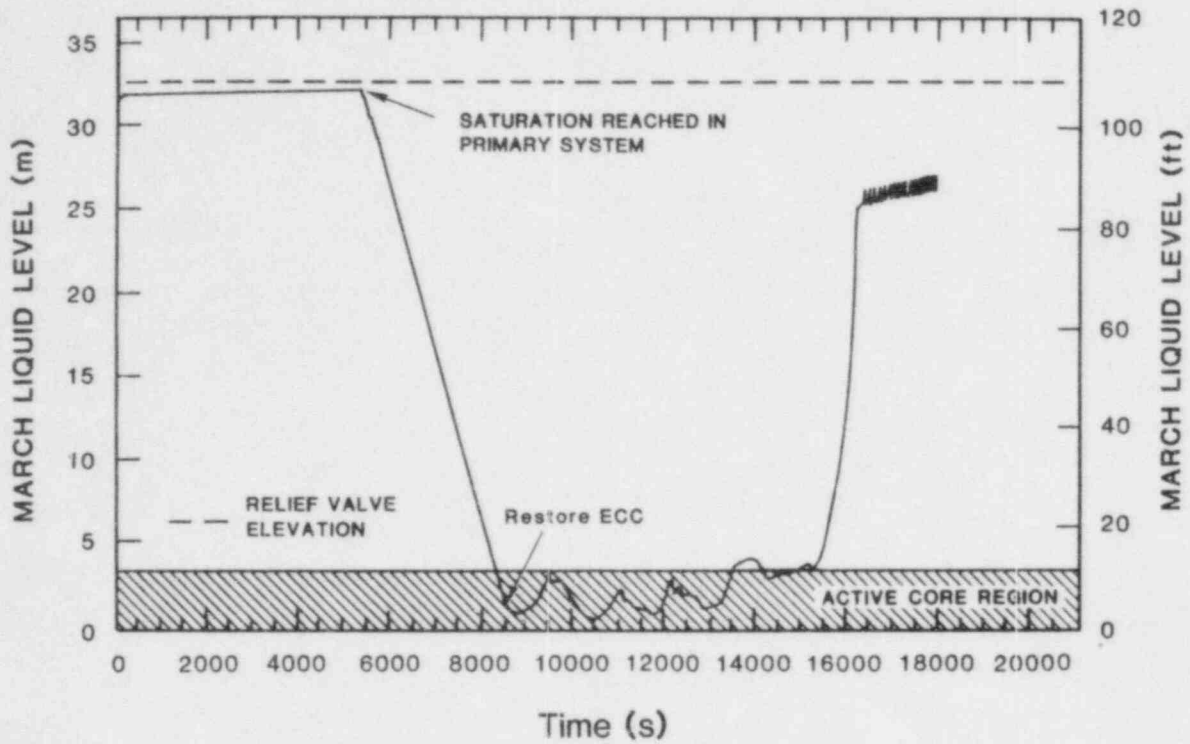


Figure 3-27. Primary System Liquid Level for "M" Cases

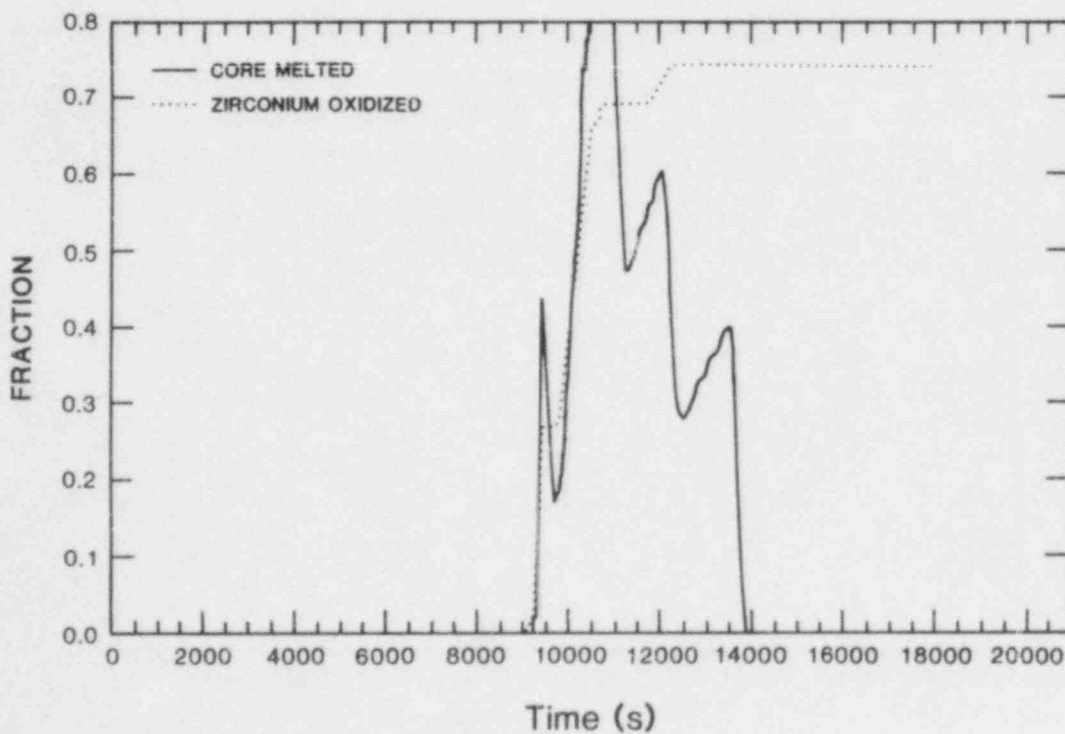


Figure 3-28. Fractions of Core Melted and Zirconium Oxidized for "M" Cases

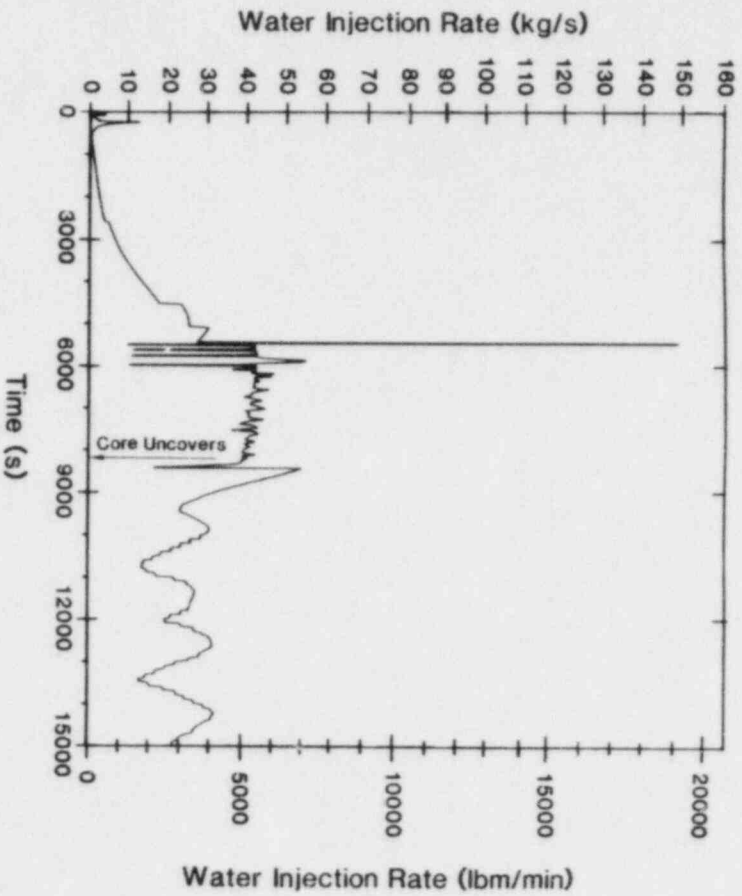


Figure 3-29. Water Source to Containment for "M" Cases

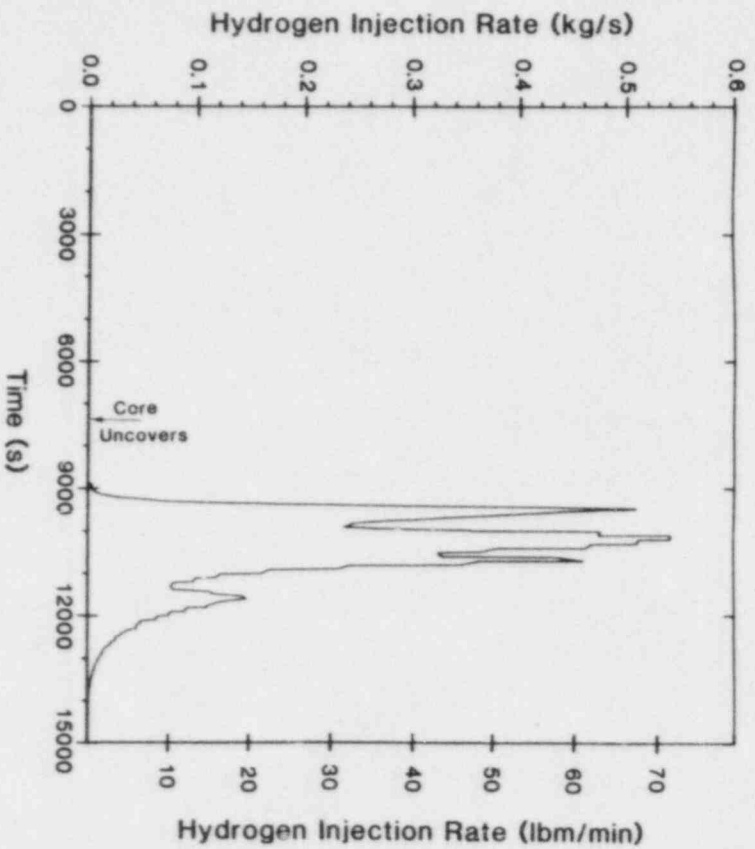


Figure 3-30. Hydrogen Source to Containment for "M" Cases

3.3 Core-Melt Cases

In the core-meltdown cases, as opposed to the degraded-core cases, ECC failure was assumed to be permanent. This results in the core becoming uncovered, heating up, and slumping into the lower plenum. Subsequently, the debris heats up the lower head of the pressure vessel, leading to its failure and the deposition of the debris in the reactor cavity. As explained earlier, a coolable debris-bed configuration is postulated to form in the reactor cavity since carbon-monoxide and carbon-dioxide could not be treated with HECTR. Thus, the major release of hydrogen to containment occurs during the time period beginning with in-vessel meltdown of the core through the time of vessel failure. Future analyses will consider the effects of a dry cavity or a non-coolable debris bed.

In most of the core-meltdown scenarios analyzed, one of the following two sets of MARCH input assumptions was made: One set was selected to yield minimal production of hydrogen, and the other forced all of the zirconium to oxidize in-vessel. This approach was taken in an attempt to bound the expected source terms of hydrogen to containment during a given scenario. Examples of MARCH modeling assumptions which were varied include whether zirconium oxidation was allowed in a computational node where melting had occurred, and whether steam flow in the core was simply blocked or diverted around the melted nodes. For the minimum oxidation cases, zirconium oxidation upon core slump into the lower plenum was calculated internally in the code using subroutine MWDRP and a large (0.046-m [1.8-in] diameter) debris particle size. In the 100% cases the oxidation was forced to 100% at the point of core slump. All other input parameters were held constant for a given accident scenario.

The times of occurrence of various key events are summarized in Table 3-2. The MARCH input decks for all of the core-meltdown cases are listed in Appendix C. Each of the core-meltdown cases is described below.

Table 3-2

Times of Occurrence of Important Events for Core-Melt Cases (s)

	D	E	J	Cases K	N	O	P
ECC off	0	0	1356	1356	0	0	0
Break uncovered (5400) (or relief valves opened)	1800	1800	240- 1380	240- 1380	(5400)	(5400)	
Core uncovered	2160	2160	2160	2160	6180	6180	6180
Core melt started	3000	3000	3120	3120	7320	7320	7320
Core slump started	3960	3738	4236	3846	9030	8838	9012
Head attack started	4080	3798	4458	3894	9228	9000	9210
Head fails	4110	3840	5274	6480	9348	9480	9330
Debris quenched	4440	3900	5400	6600	9480	9600	9420

3.3.1 "D" and "E" Cases - S₂D, Core-Melt

Cases D.00 and E.00 both represent 0.05-m (2-in) diameter LOCAs with failure of ECC in the injection mode (S₂D). However, in case D.00 all of the zirconium was oxidized in-vessel, while in case E.00 the input assumptions for minimal hydrogen generation were used, resulting in 36% zirconium oxidation. The liquid levels in the primary system are shown in Figures 3-31 and 3-32 for cases D.00 and E.00, respectively, and the primary system pressures are shown in Figures 3-33 and 3-34. Notice that the liquid level plots are nearly identical for both cases. This would be expected since the cases represent the same accident sequence. The break in the slope at approximately 1800 s occurs because the liquid level in the primary system falls below the break elevation, causing a transition in break flow from liquid to steam.

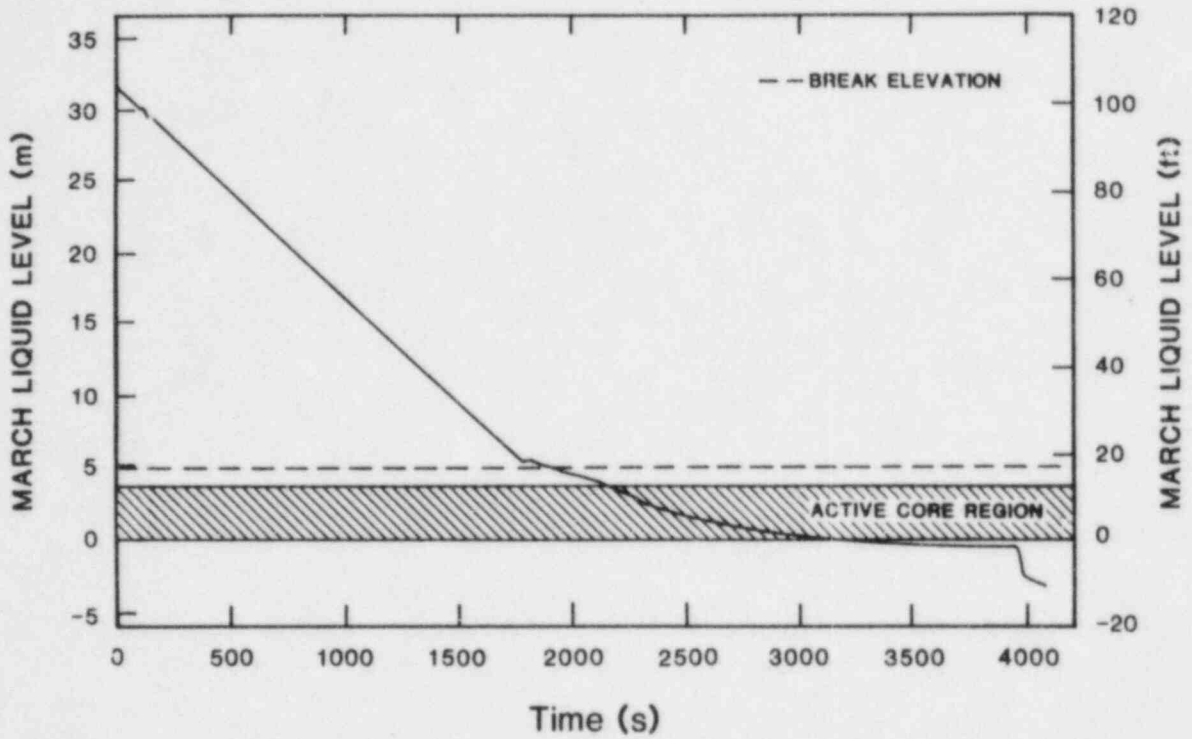


Figure 3-31. Primary System Liquid Level for "D" Cases

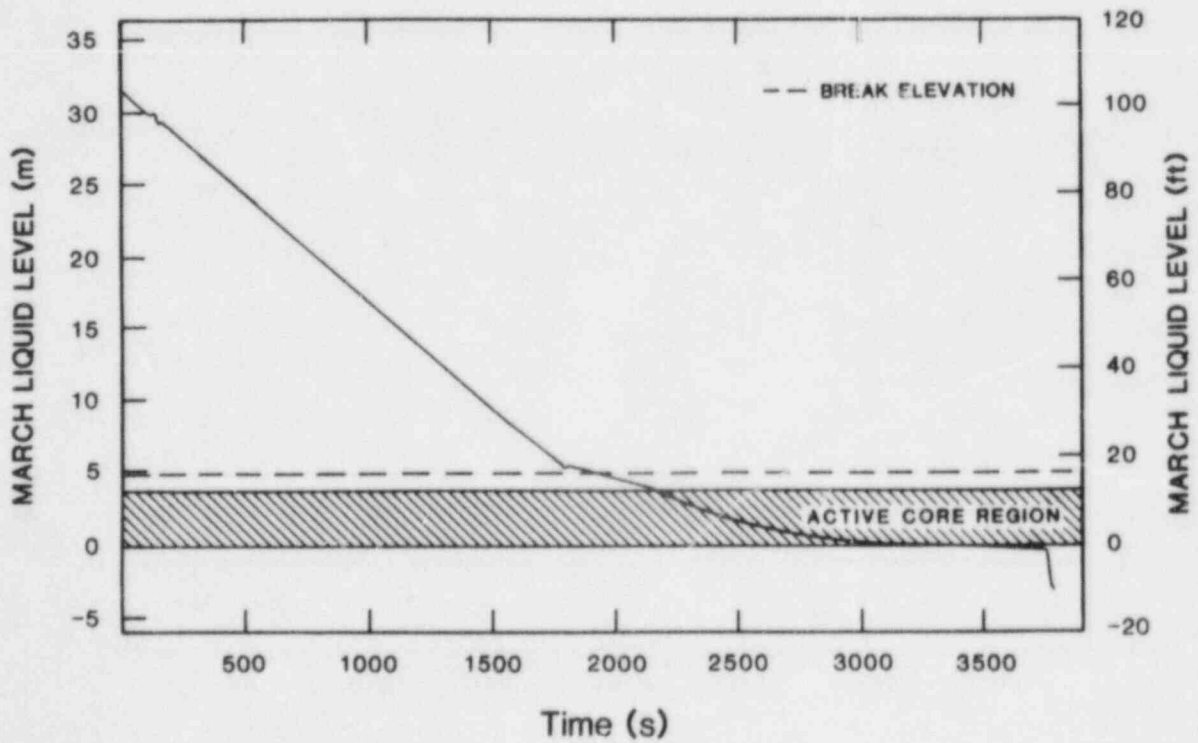


Figure 3-32. Primary System Liquid Level for "E" Cases

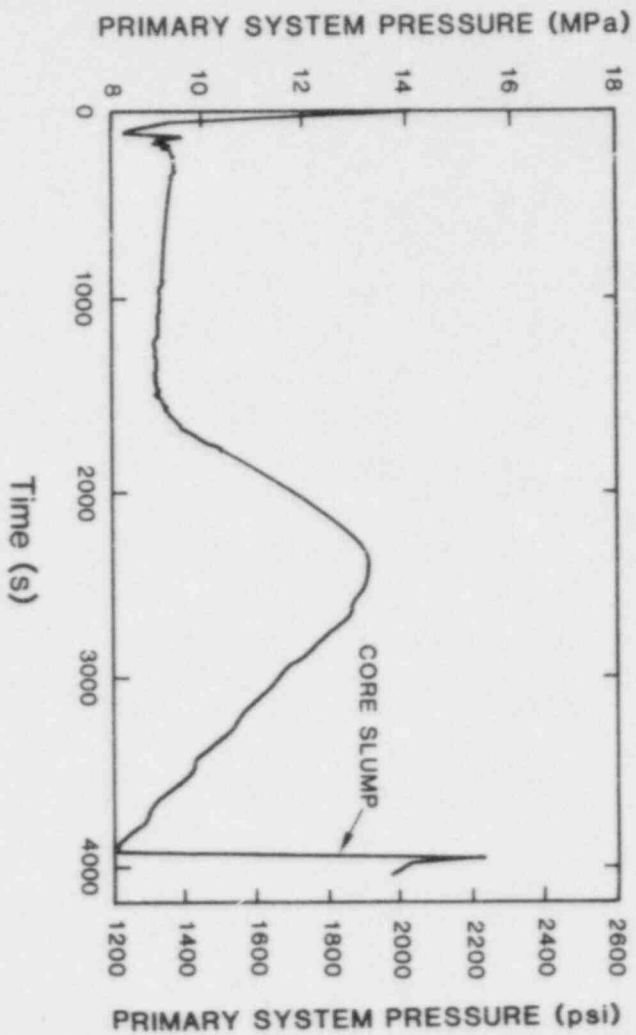


Figure 3-33. Primary System Pressure for "D" Cases

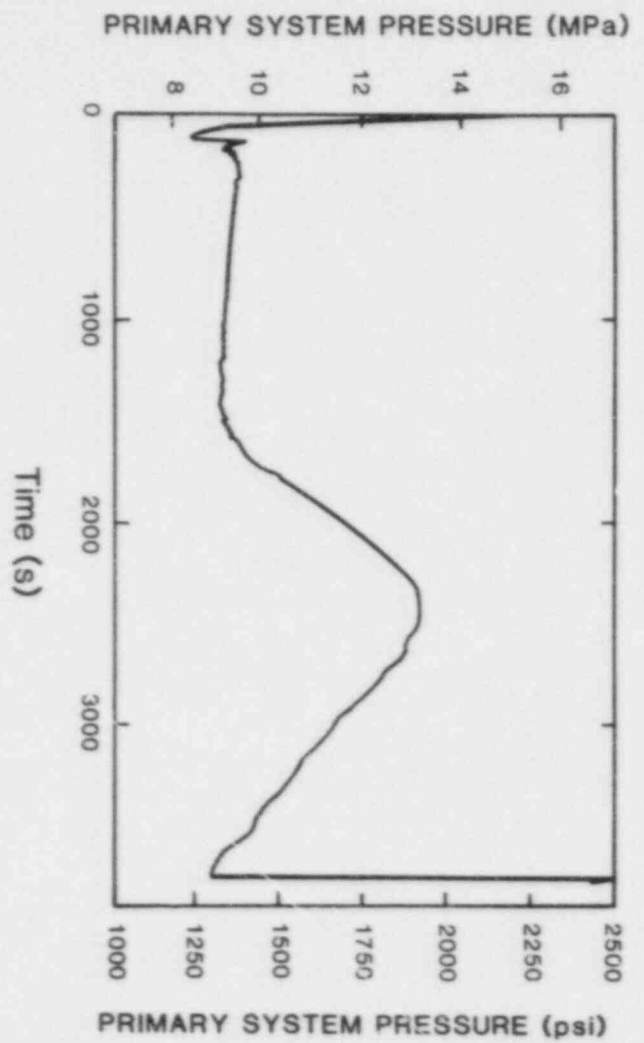


Figure 3-34. Primary System Pressure for "E" Cases

The fractions of core melted and zirconium oxidized are shown in Figures 3-35 and 3-36 for cases D.00 and E.00, respectively. These plots show similar trends but differ quantitatively due to the different assumptions regarding the rate and amount zirconium oxidation. Notice the large amount of zirconium oxidized at the time of core slump in case D.00, which was forced to 100% oxidation.

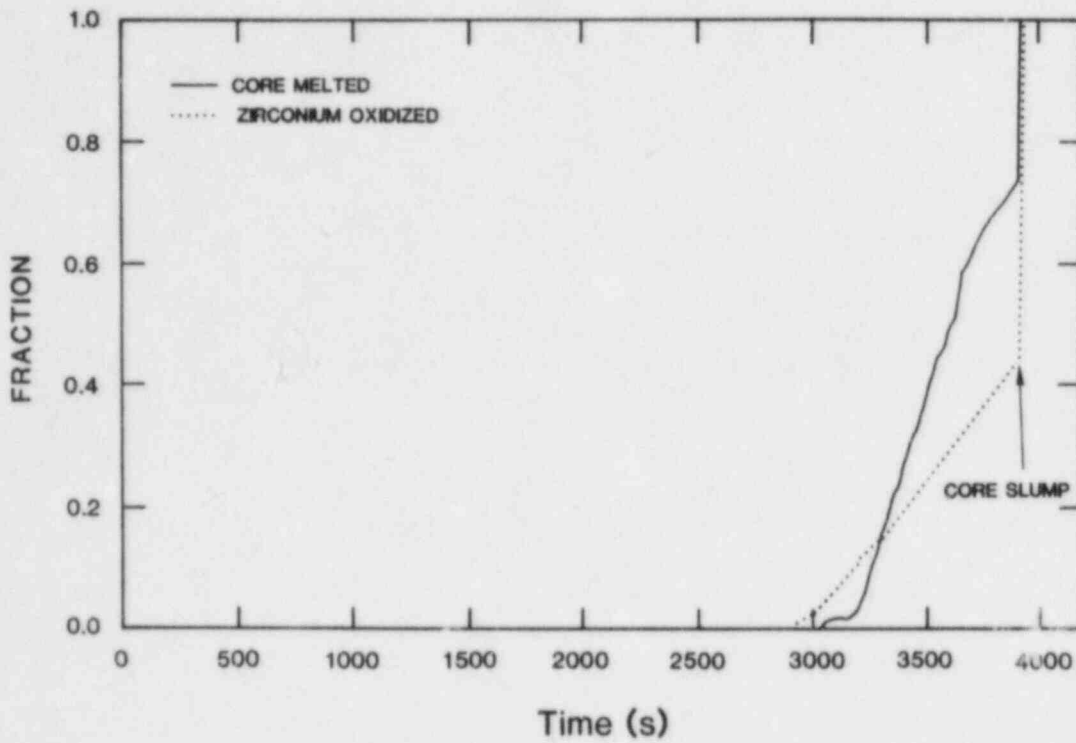


Figure 3-35. Fractions of Core Melted and Zirconium Oxidized for "D" Cases

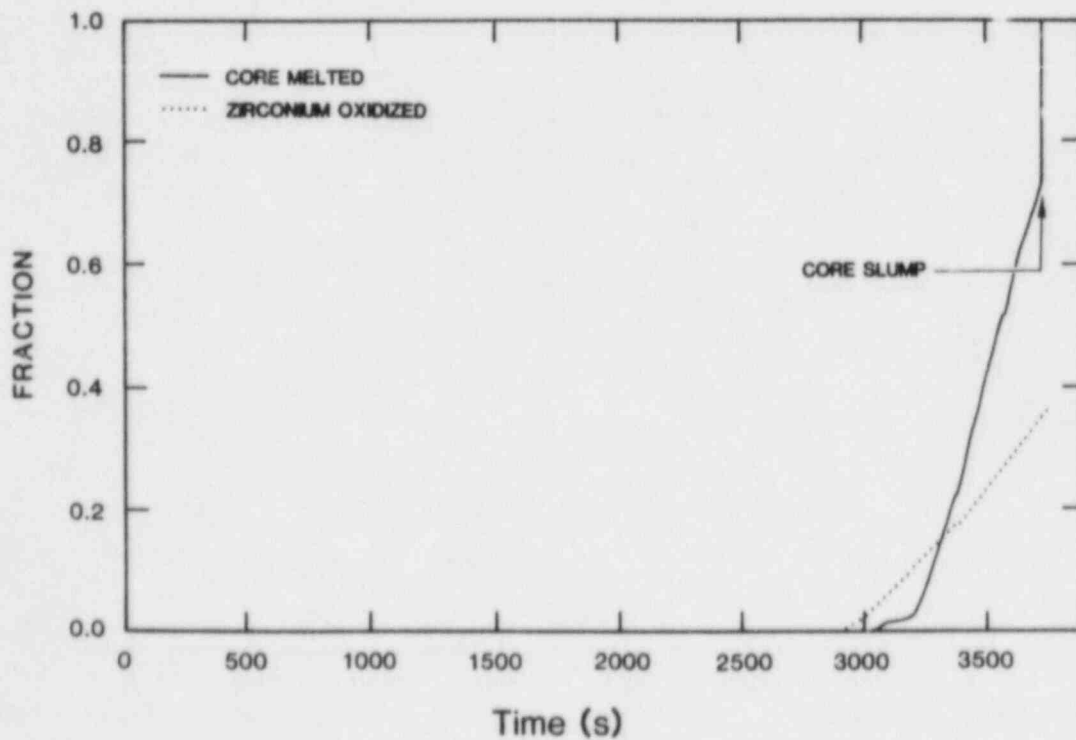


Figure 3-36. Fractions of Core Melted and Zirconium Oxidized for "E" Cases

The water source rates are shown in Figures 3-37 and 3-38 for cases D.00 and E.00, respectively. They are similar in nature with a peak water source rate that is slightly higher for case D.00. There are two reasons why the rate is slightly higher for case D.00, one physical and one nonmechanistic. The physical reason is since more zirconium was oxidized in case D.00, more heat was released in the chemical reaction, the core debris was hotter, and hence, greater quantities of steam were produced at core slump. The non-mechanistic reason is the dependency of the release rate at the time of vessel failure upon the MARCH time step just before vessel failure (i.e., all steam and hydrogen released in one time step). In any case, the very sharp peak in the source rate does have a qualitatively physical basis due to the large release that would be observed at the time of vessel failure and subsequent depressurization.

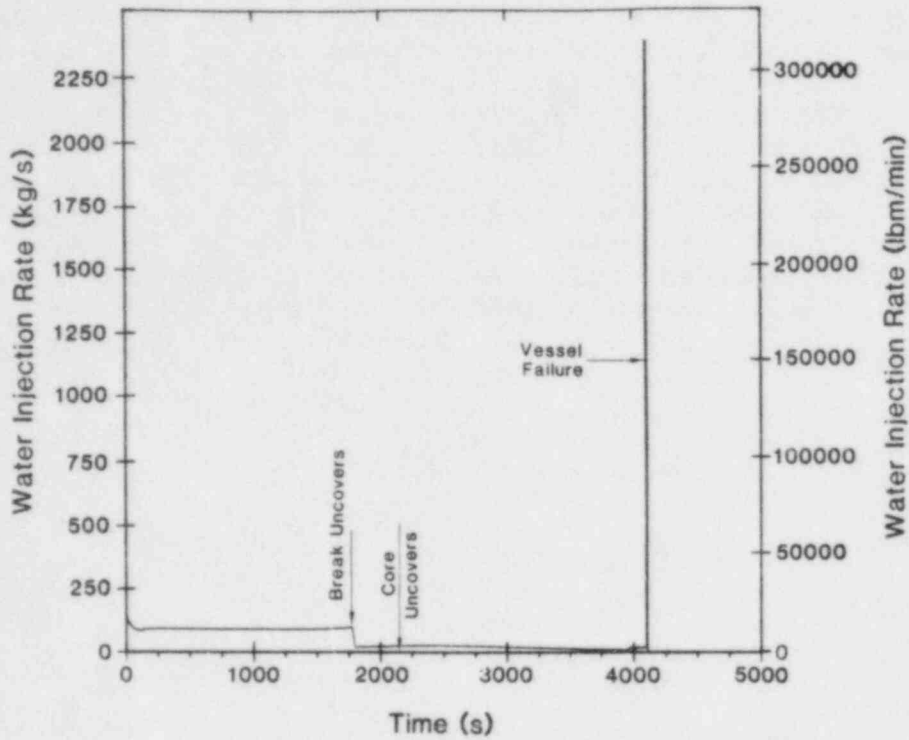


Figure 3-37. Water Source to Containment for "D" Cases

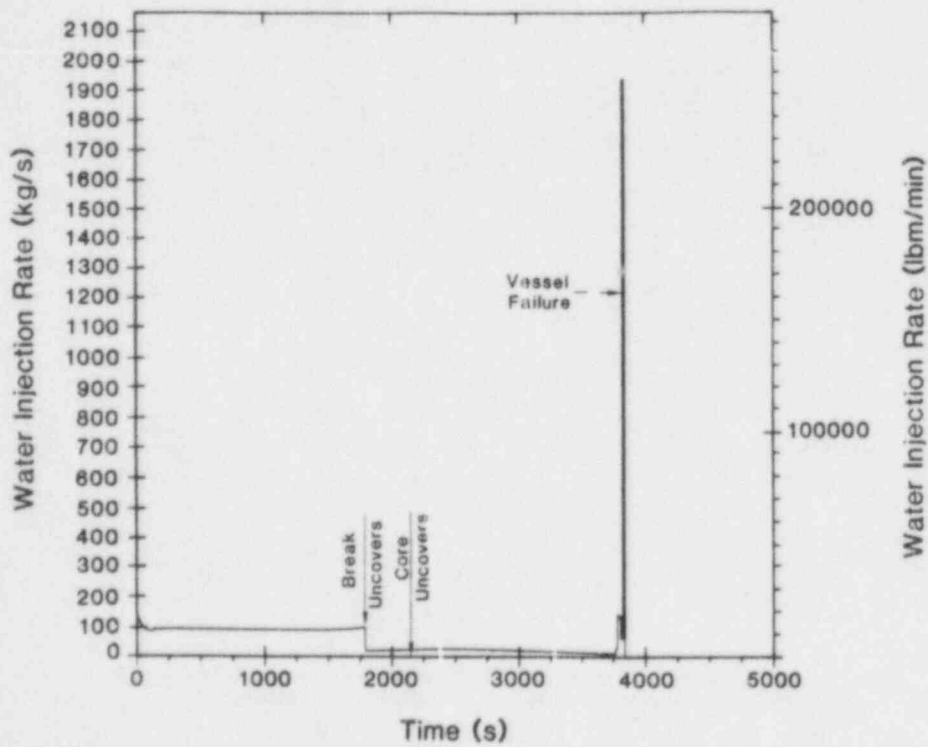


Figure 3-38. Water Source to Containment for "E" Cases

The hydrogen source terms are found in Figures 3-39 and 3-40 for cases D.00 and E.00, respectively. It can be seen from these figures that the hydrogen source terms are also qualitatively similar (as would be expected) since the same sequence is being modeled in both cases. Much of the hydrogen is released at the time of vessel breach. The large differences in the peak release rate are at least partially due to the differences in the extent of zirconium oxidation. The reader is again cautioned that this peak in the hydrogen source rate depends upon the MARCH time step before vessel failure.

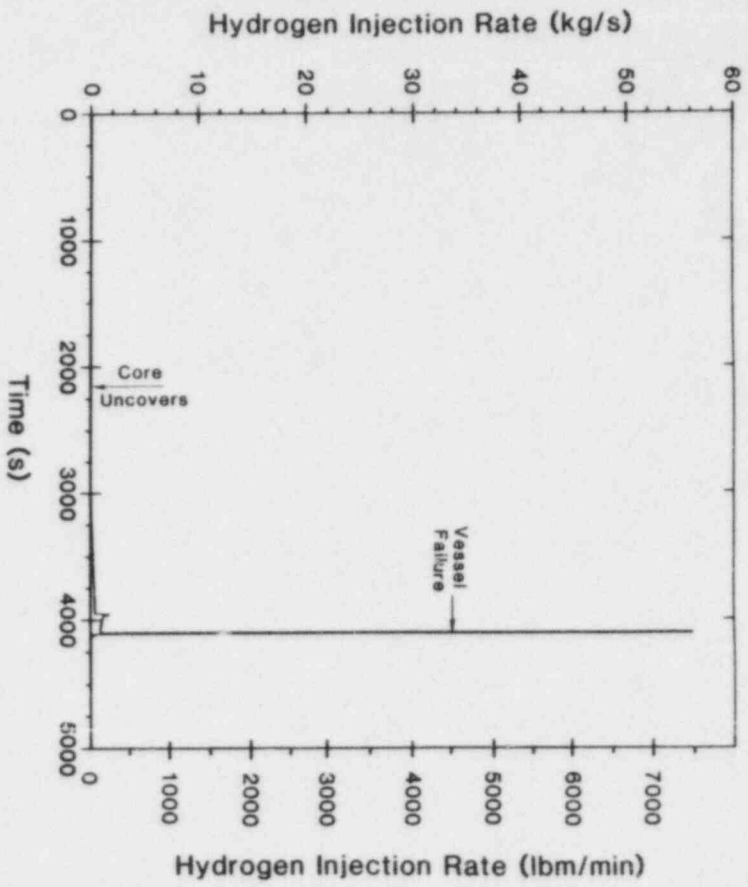


Figure 3-39. Hydrogen Source to Containment for "D" Cases

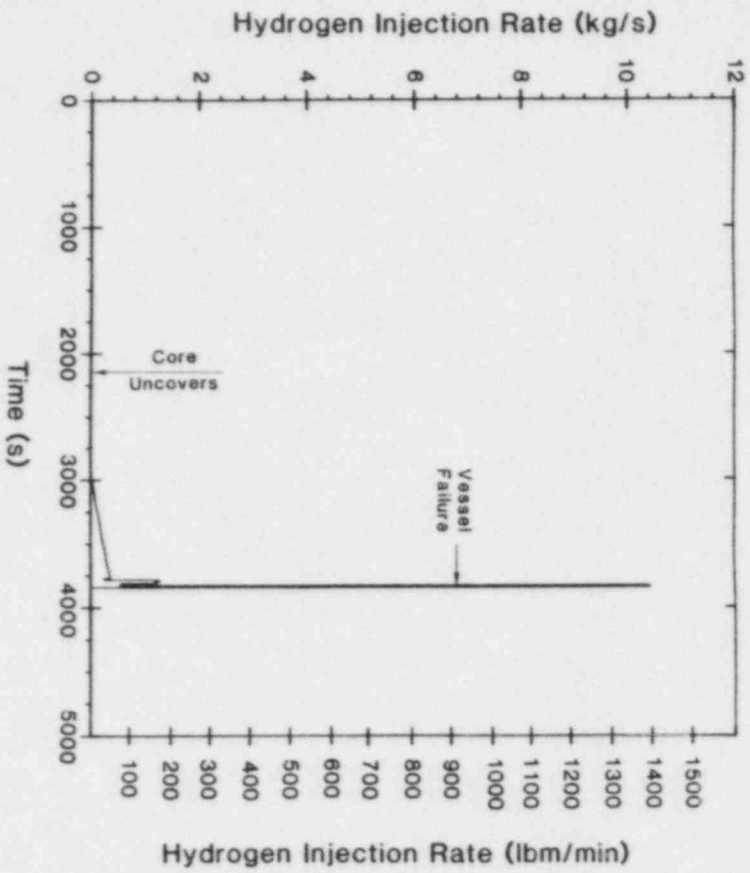


Figure 3-40. Hydrogen Source to Containment for "E" Cases

3.3.2 "J" and "K" Cases - S₁HF, Core-Melt

Cases J.00 and K.00 both represent 0.15-m (6-in) diameter LOCAs with failure of ECC and containment sprays in the recirculation mode (S₁HF). However, case J.00 considered 100% zirconium oxidation, and case K.00 used the MARCH input assumption set for minimal hydrogen generation. The liquid levels in the primary system are plotted in Figures 3-41 and 3-42 for cases J.00 and K.00, respectively, and the primary system pressures are shown in Figures 3-43 and 3-44. Comparing these figures and the times listed in Table 3-2, one sees how similarly the two cases progressed. The erratic behavior in the liquid level between 300 and 1500 s is due to the MARCH characteristic of treating the break flow as a single-phase fluid only, which has already been discussed. In these cases after approximately 1380 s, ECC fails upon switching to recirculation, the break is uncovered for the rest of the accident, and the oscillations cease.

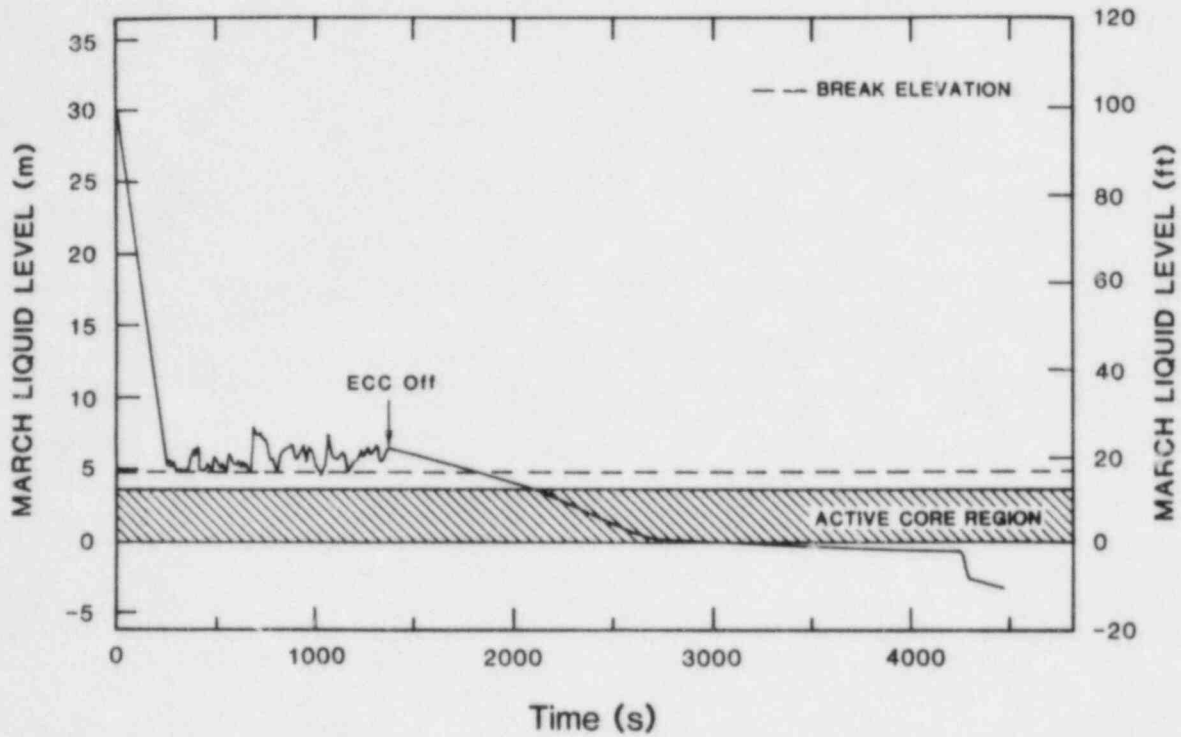


Figure 3-41. Primary System Liquid Level for "J" Cases

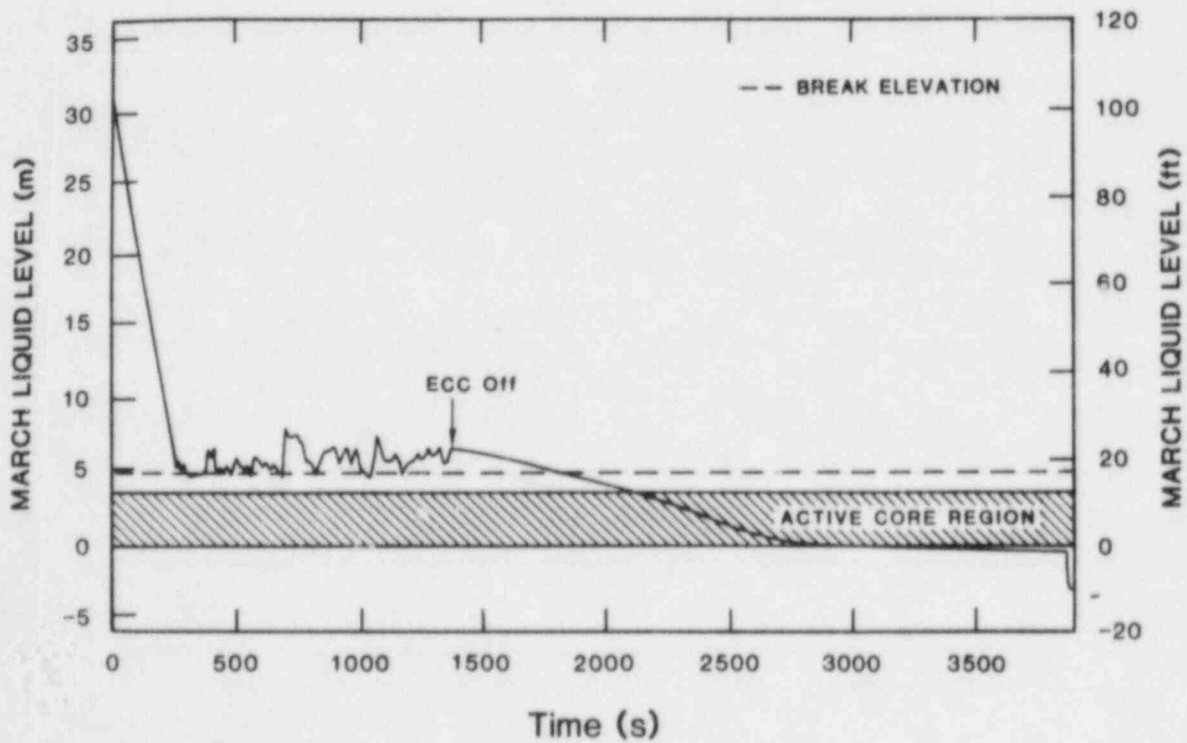


Figure 3-42. Primary System Liquid Level for "K" Cases

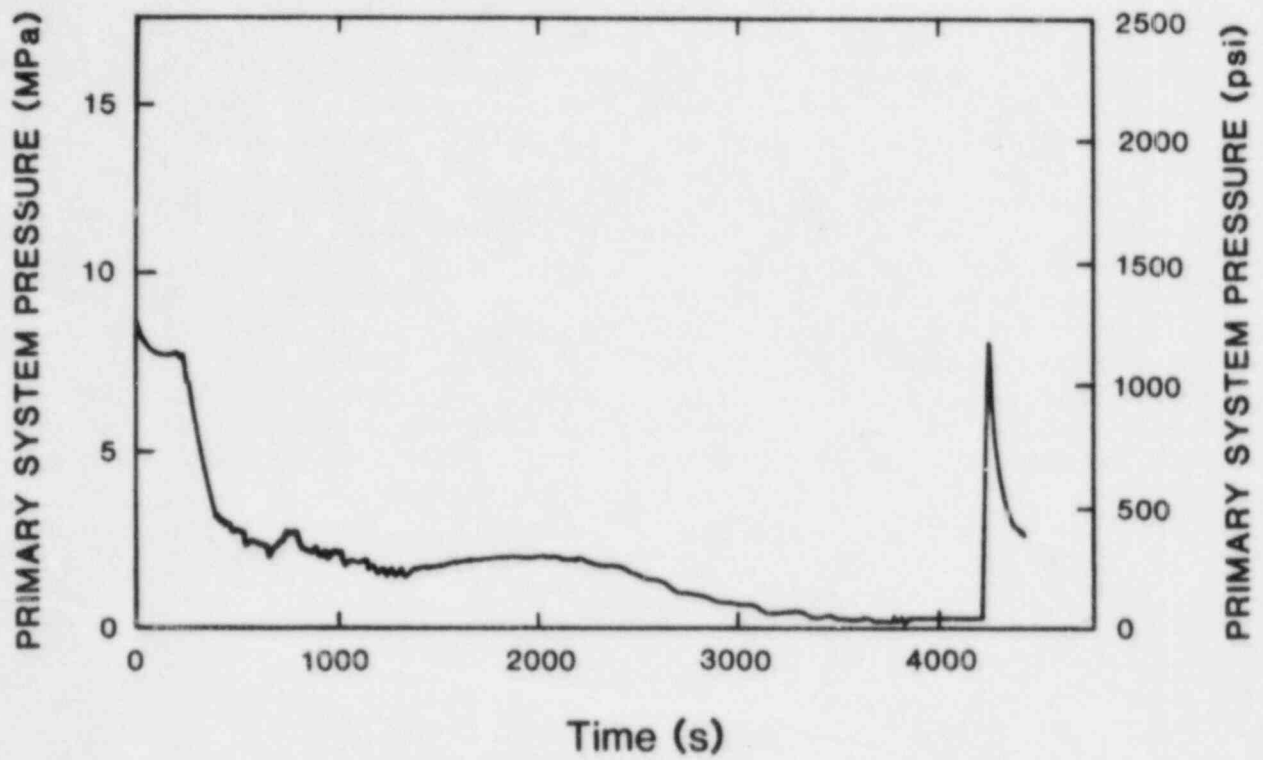


Figure 3-43. Primary System Pressure for "J" Cases

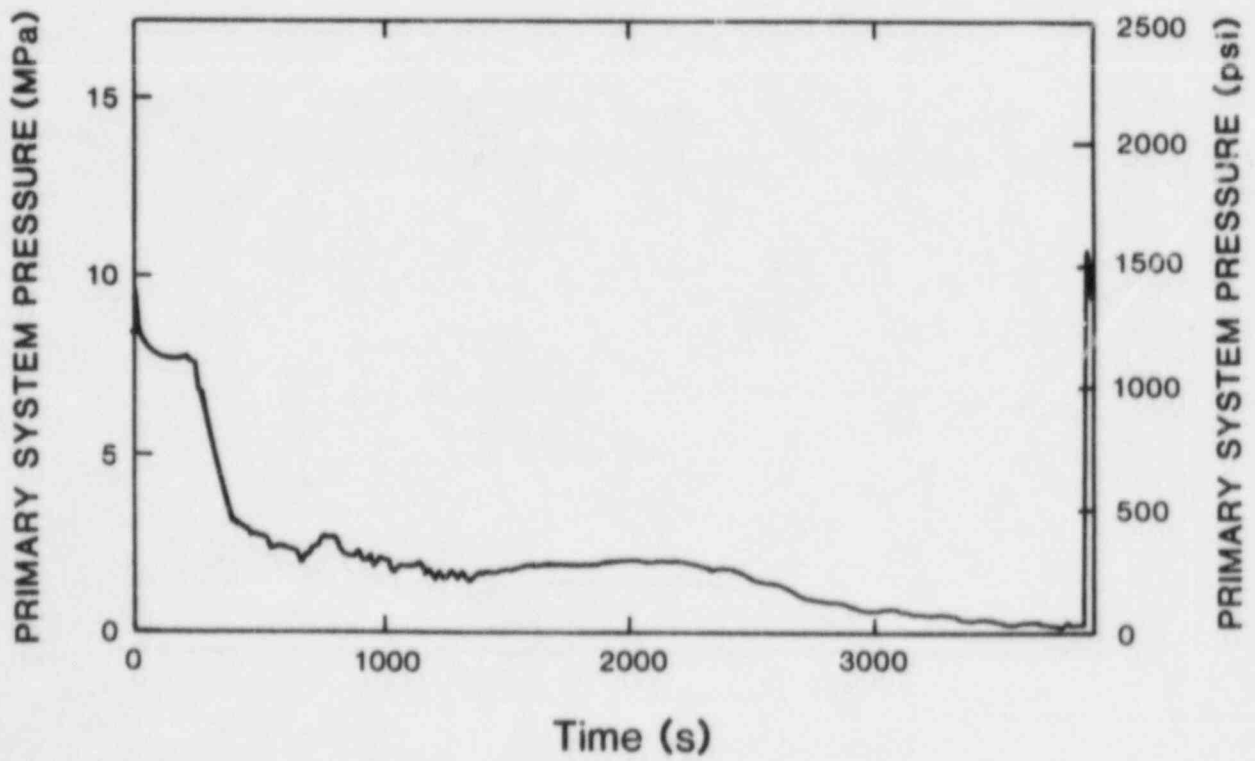


Figure 3-44. Primary System Pressure for "K" Cases

Figures 3-45 and 3-46 illustrate the fractions of core melted and zirconium oxidized over the course of the scenario for cases J.00 and K.00, respectively. The figures for the two cases show the same general trends. Once again notice the large fraction of zirconium which is forced to oxidize upon core slump in the 100% oxidation case. Also note in Figure 3-45 that during the MARCH-predicted core slumping process (from approximately 3780 to 4200 s), no zirconium oxidation takes place. Then, at the end of the core slumping process the remainder of the zirconium is forced to oxidize. This behavior is not physically realistic, but rather is a peculiarity of the MARCH code. The time from core slump to vessel breach is longer than in most of the other cases considered because of the lower primary system pressure.

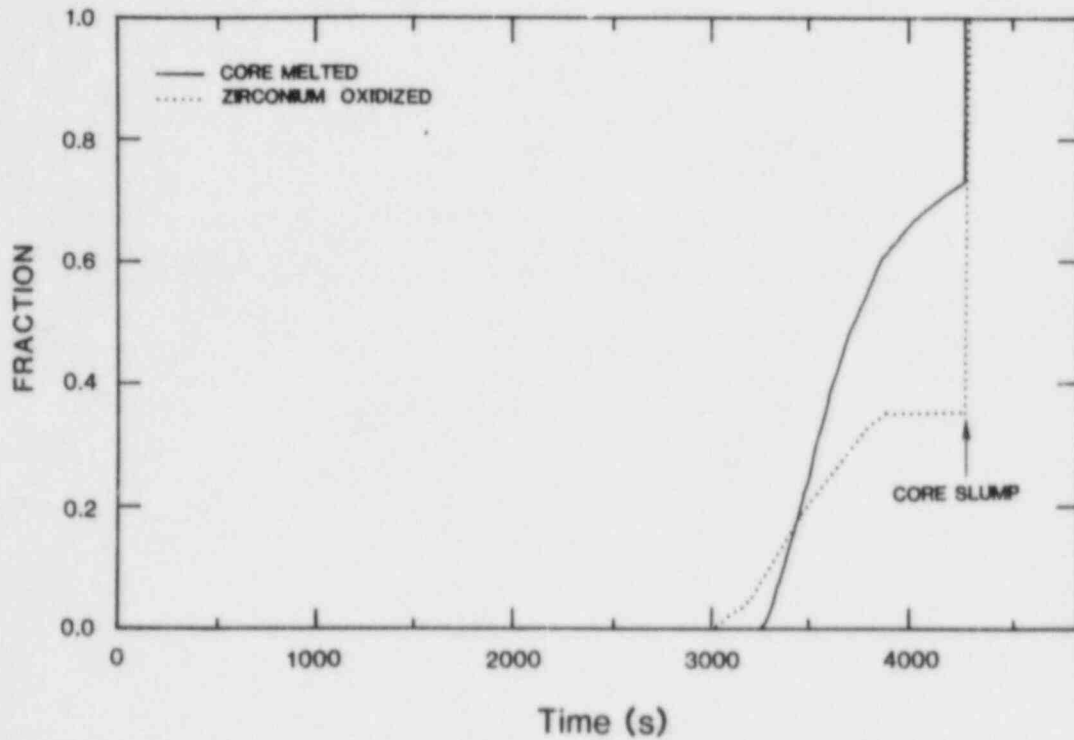


Figure 3-45. Fractions of Core Melted and Zirconium Oxidized for "J" Cases

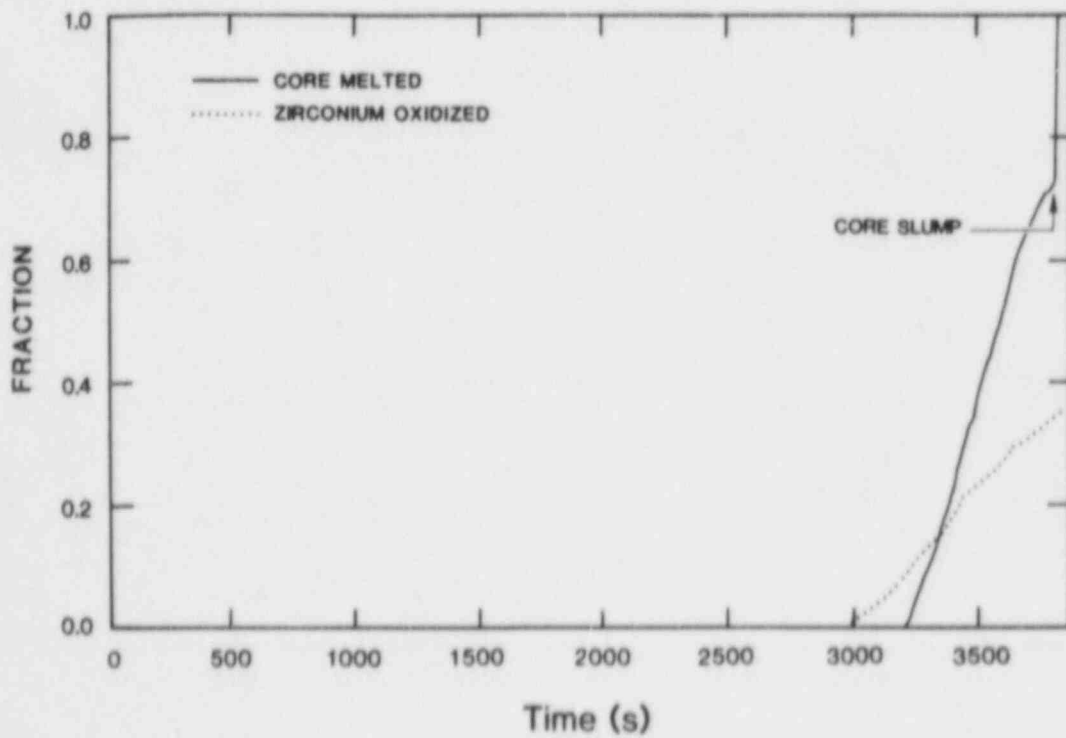


Figure 3-46. Fractions of Core Melted and Zirconium Oxidized for "K" Cases

The water source terms for cases J.00 and K.00 are shown in Figures 3-47 and 3-48, respectively. The erratic behavior in the water source term early in time is due to the liquid level oscillation problem discussed earlier. Because no hydrogen is released until after this erratic behavior has ceased, we believe that the effect of this artifact of MARCH on the results is negligible. There may be some residual effects from this behavior on the containment pressure-temperature response and steam concentrations. The water source term late in the accident is seen to be comparable for the two cases.

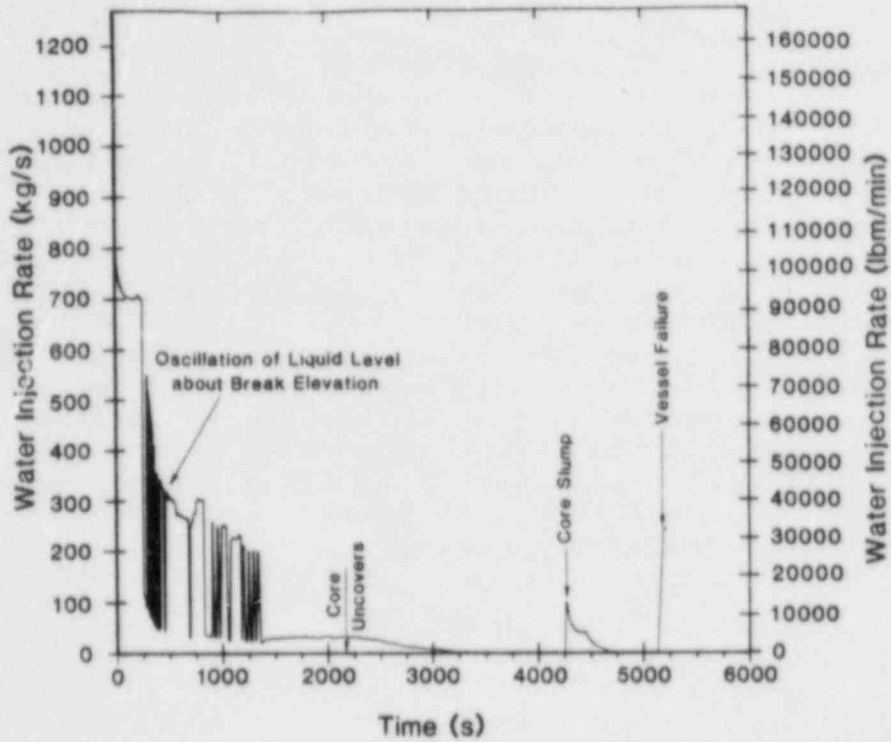


Figure 3-47. Water Source to Containment for "J" Cases

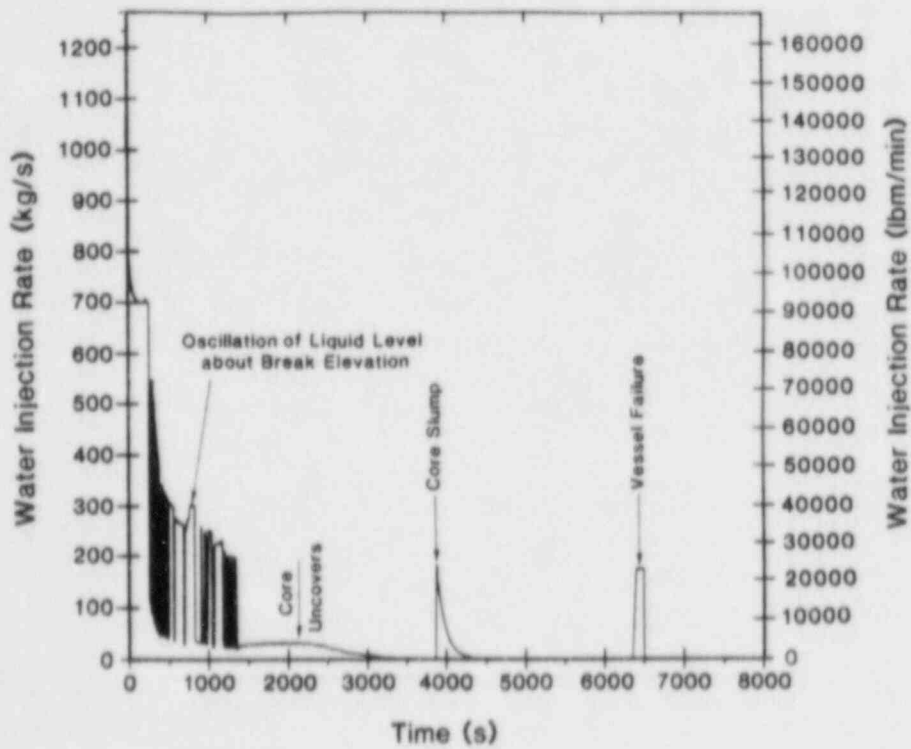


Figure 3-48. Water Source to Containment for "K" Cases

The hydrogen source terms for cases J.00 and K.00 are found in Figures 3-49 and 3-50, respectively. A comparison between the two cases shows the hydrogen sources to be similar qualitatively. However, the peak source rate in case J.00 (100% zirconium oxidation) is nearly an order of magnitude higher than in case K.00 (minimal hydrogen production assumptions). These two cases clearly demonstrate the arbitrary nature of the source rate at the time of vessel failure as calculated by MARCH. Notice that the last spike in the source rate in both cases is associated with vessel failure. Also note that this spike (representing the release of the hydrogen remaining in the primary system at the time of vessel failure) is spread over approximately 120 s in case J.00 but over a very short time in case K.00. Thus, the release at vessel failure in case J.00 appears to be gradual and nearly uniform, while the release in case K.00 appears to be very rapid and impulsive in nature.

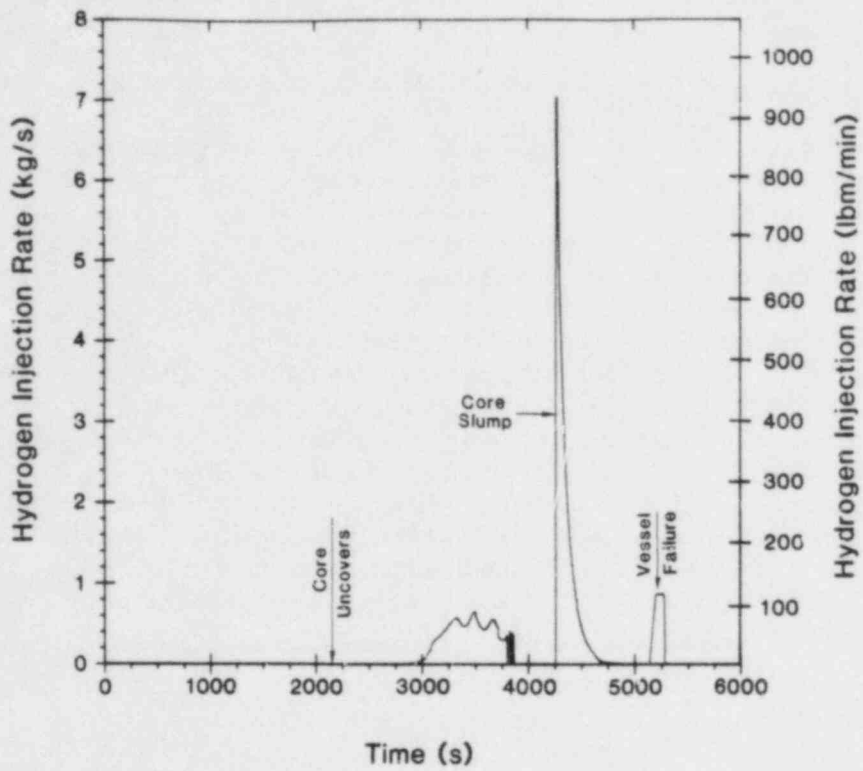


Figure 3-49. Hydrogen Source to Containment for "J" Cases

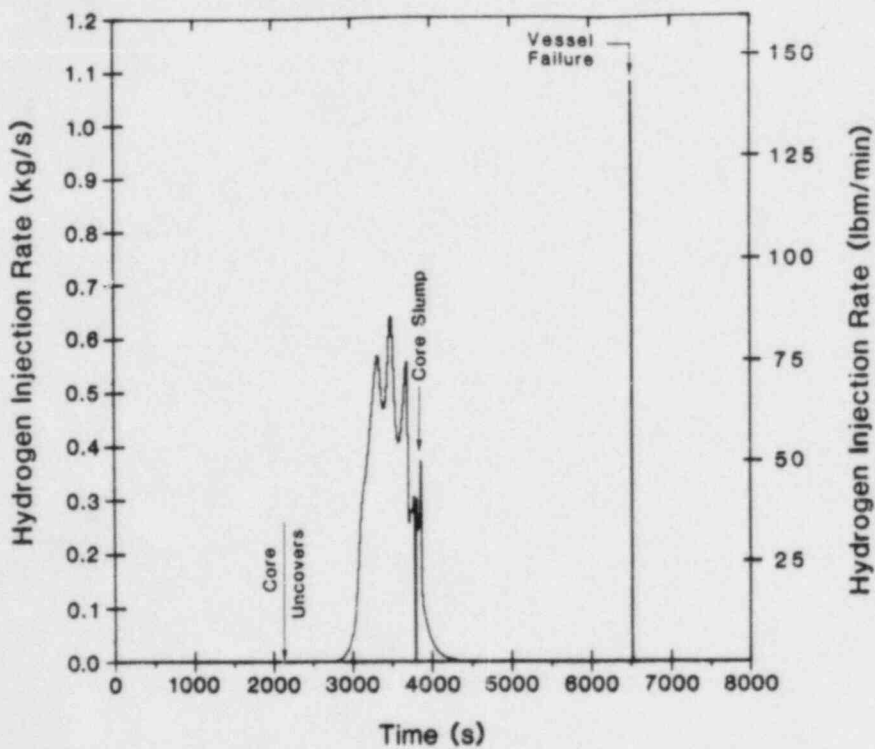


Figure 3-50. Hydrogen Source to Containment for "K" Cases

3.3.3 "N", "O", and "P" Cases - TMLB', Core-Meltdown

Cases N.00, O.00 and P.00 all represent transient-initiated scenarios with loss of all feedwater capability and loss of all ac power (TMLB'). However, in case N.00 all of the zirconium was forced to oxidize in-vessel, in case O.00 the MARCH input set for minimal zirconium oxidation was used, and in case P.00 MARCH input parameters were selected which yielded a total fraction of zirconium oxidized (65%) between the values for cases N.00 and O.00. Thus, taken together, these three cases represent a parametric treatment of the amount of oxidation during a TMLB' scenario. The liquid level and pressure in the primary system for case N.00 are shown in Figures 3-51 and 3-52. The liquid level and primary system pressure are similar for all three cases because all three cases are focused upon the same accident scenario, namely TMLB', and most of the differences in oxidation occur after core slump.

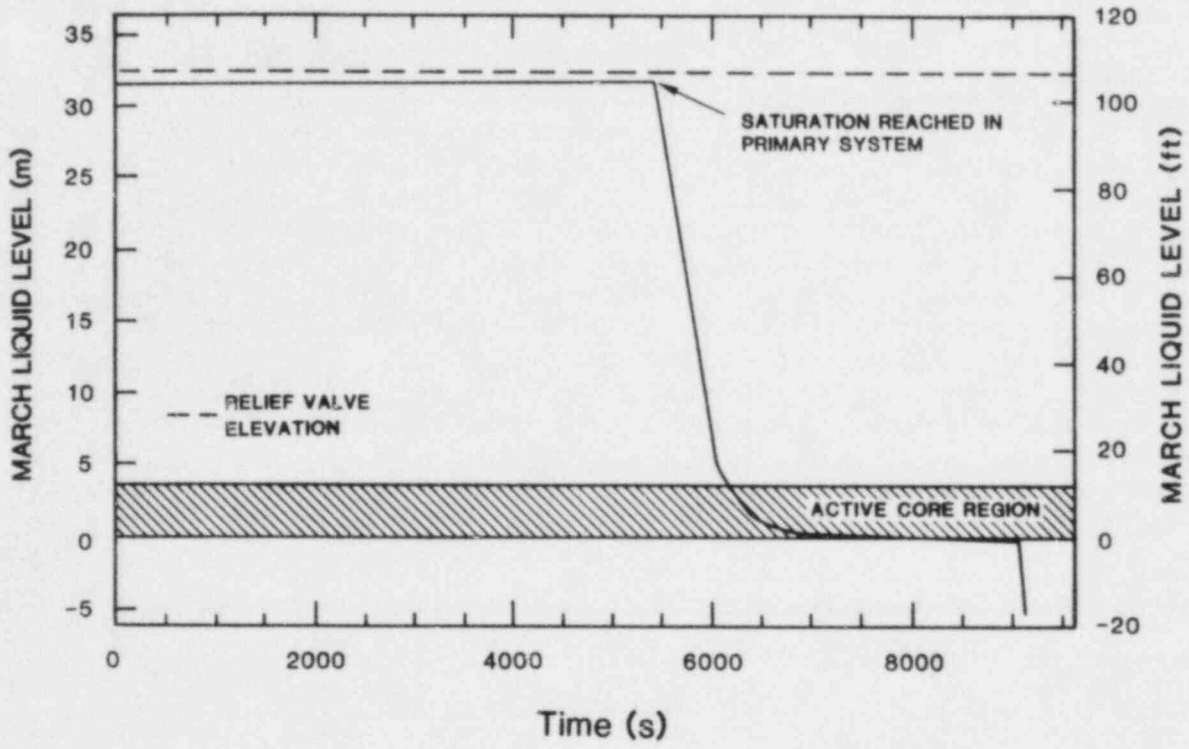


Figure 3-51. Primary System Liquid Level for "N" Cases

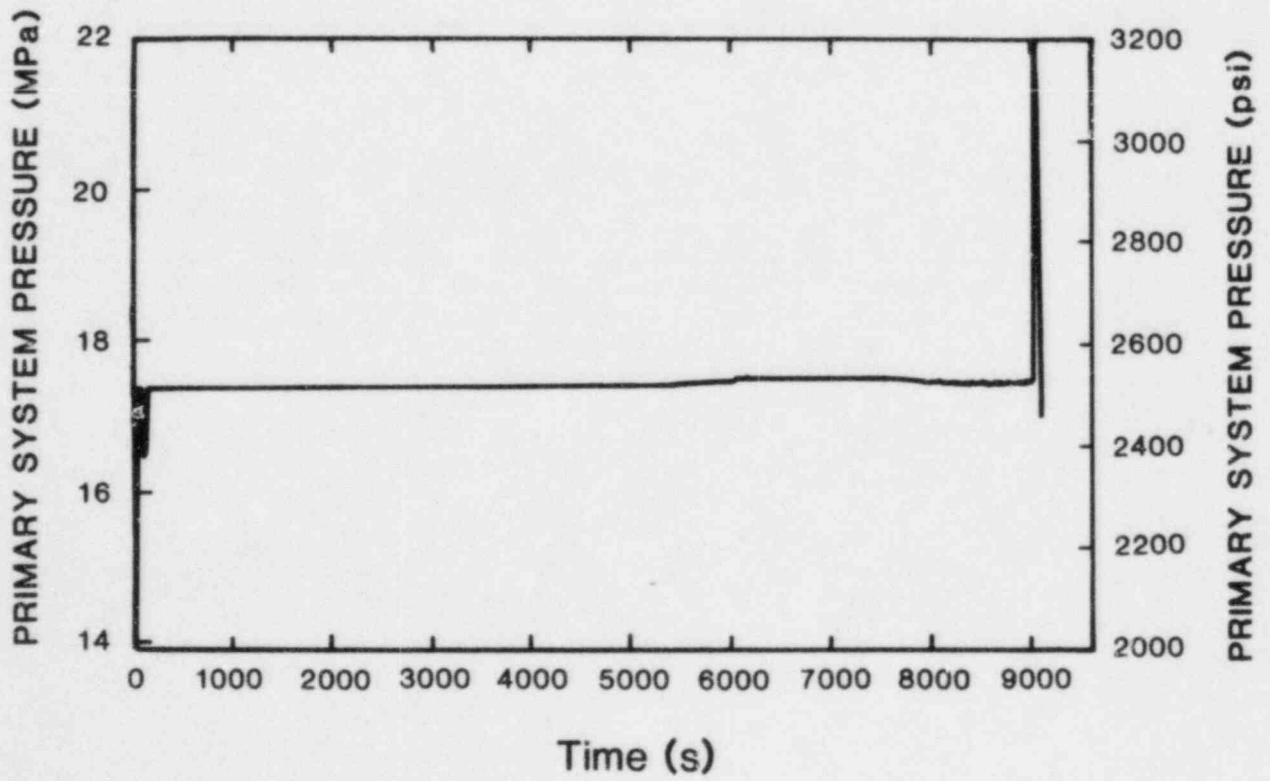


Figure 3-52. Primary System Pressure for "N" Cases

The fractions of core melted and zirconium oxidized are found in Figures 3-53, 3-54, and 3-55 for cases N.00, O.00, and P.00, respectively. All three plots are very similar until the time of core slump. Just prior to this time the fraction of zirconium oxidized is comparable in all three cases. Notice that in case N.00 80% of the zirconium is forced to oxidize instantaneously at the time of core slump to achieve the desired level of 100%. This gives rise to what may be unrealistically high source rates of hydrogen. Case O.00 provides what are probably unrealistically low source rates of hydrogen, and case P.00 provides intermediate values. None of these cases should be considered "best estimate" cases. Defining such a case is beyond our current capability.

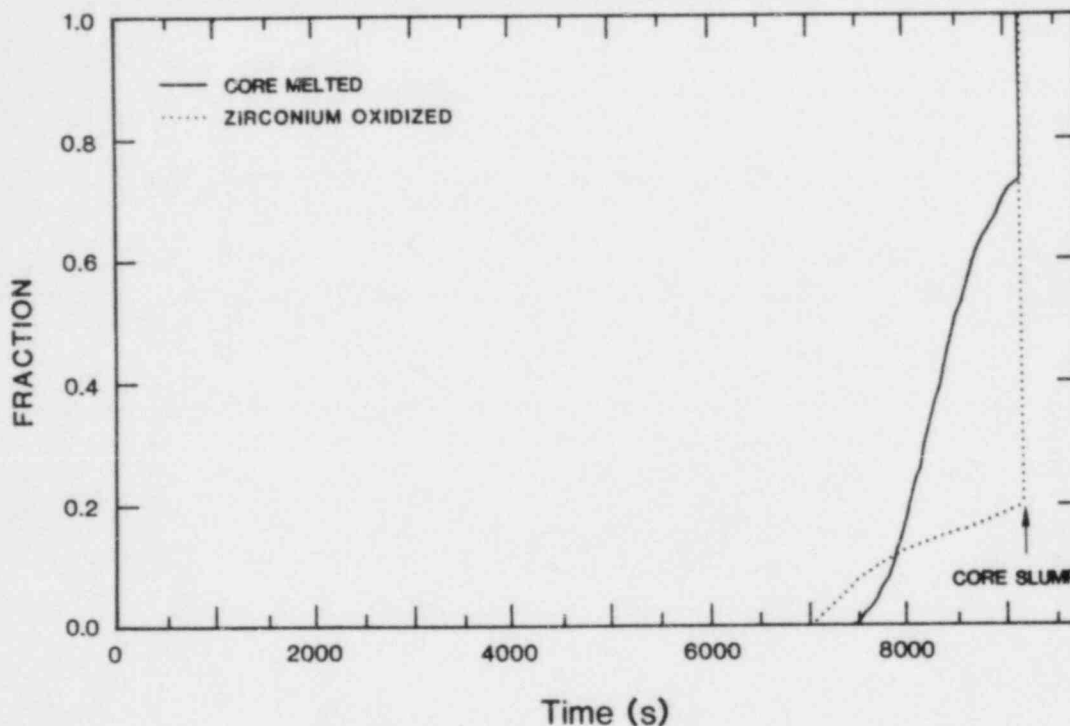


Figure 3-53. Fractions of Core Melted and Zirconium Oxidized for "N" Cases

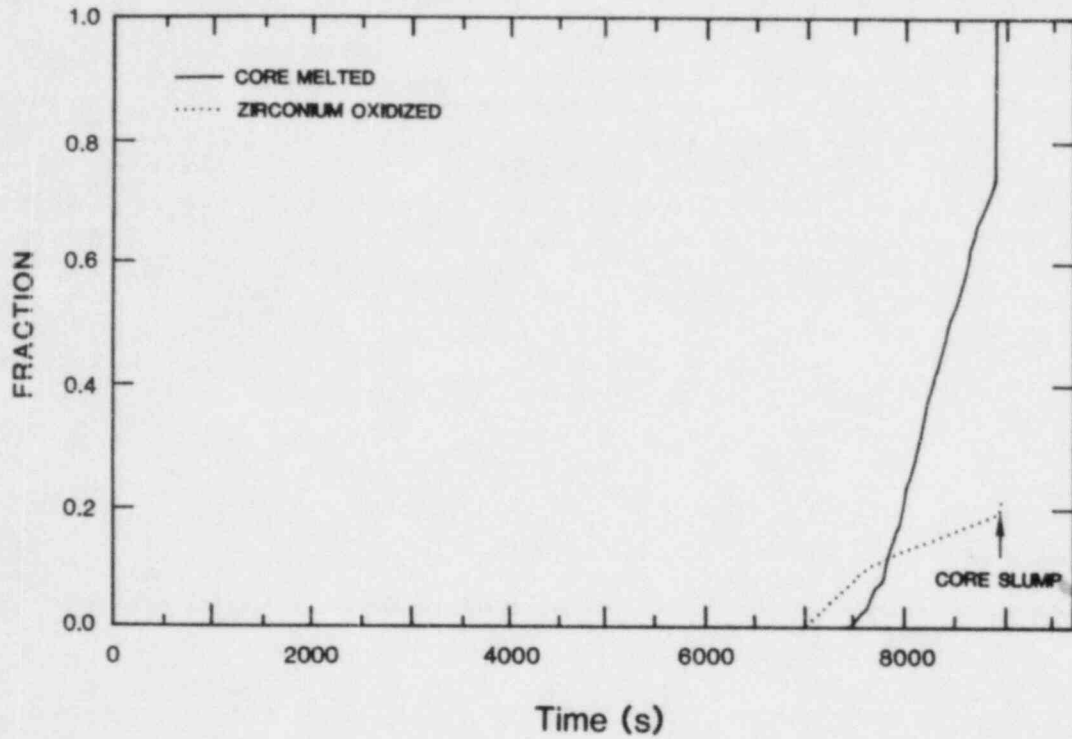


Figure 3-54. Fractions of Core Melted and Zirconium Oxidized for "O" Cases

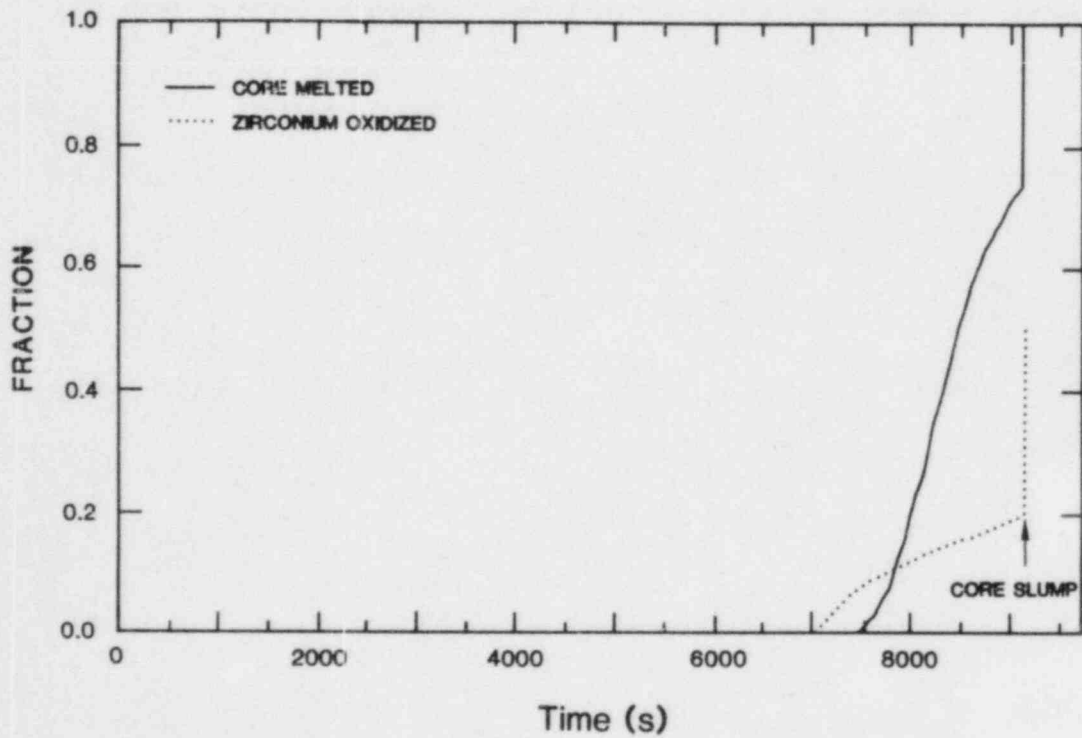


Figure 3-55. Fractions of Core Melted and Zirconium Oxidized for "P" Cases

The source of water to containment is shown in Figures 3-56, 3-57, and 3-58 for cases N.00, O.00, and P.00, respectively. These figures are qualitatively similar for all three cases. As was mentioned in earlier case descriptions, the source rate at the time of vessel failure increases slightly with fraction of zirconium oxidized due to the increase in total amount of heat released during the reaction.

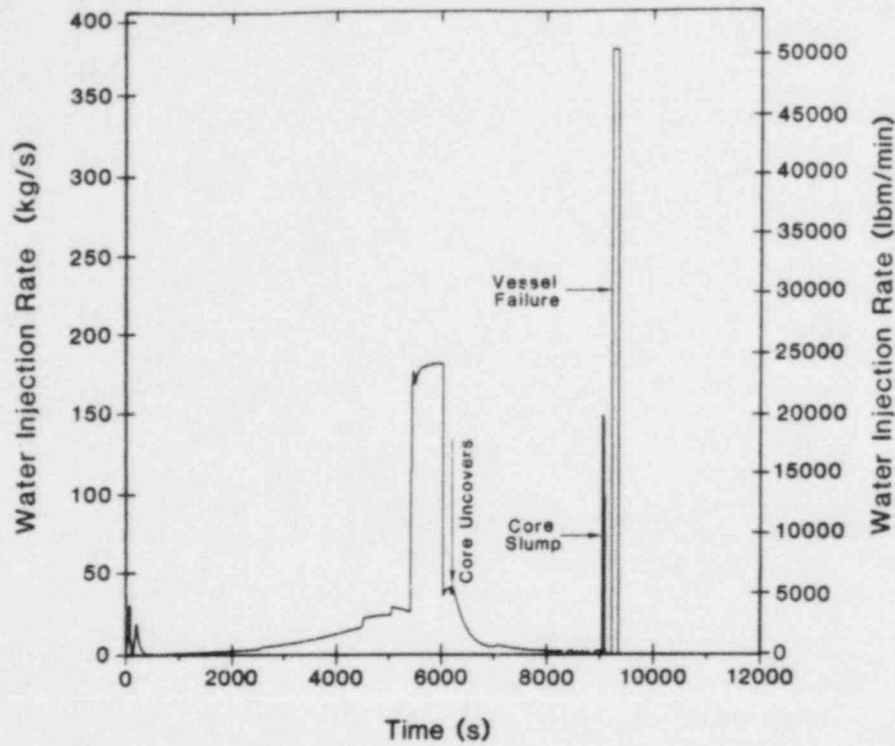


Figure 3-56. Water Source to Containment for "N" Cases

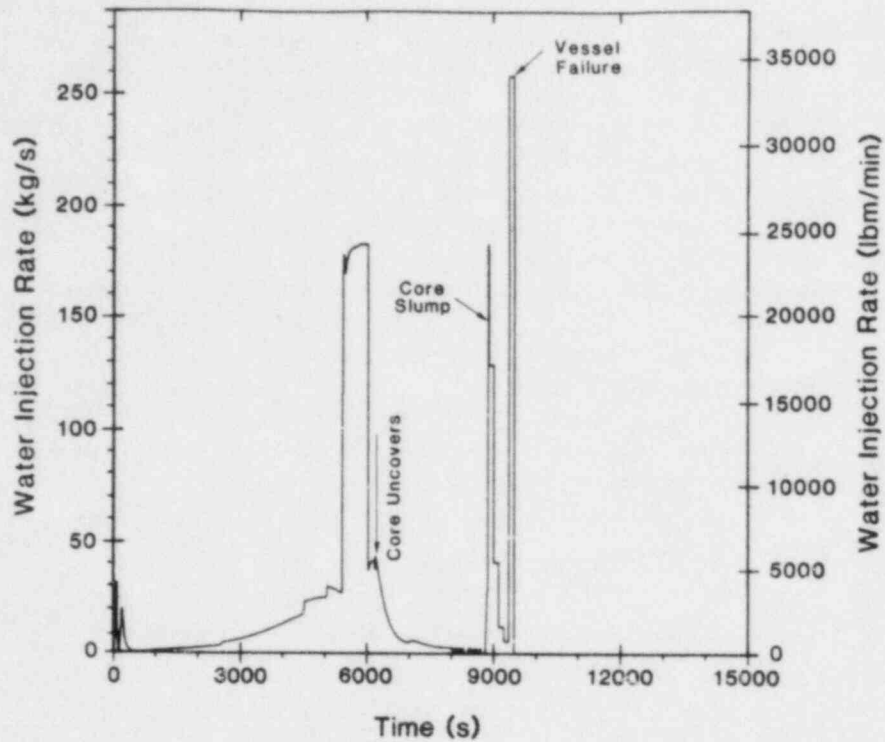


Figure 3-57. Water Source to Containment for "O" Cases

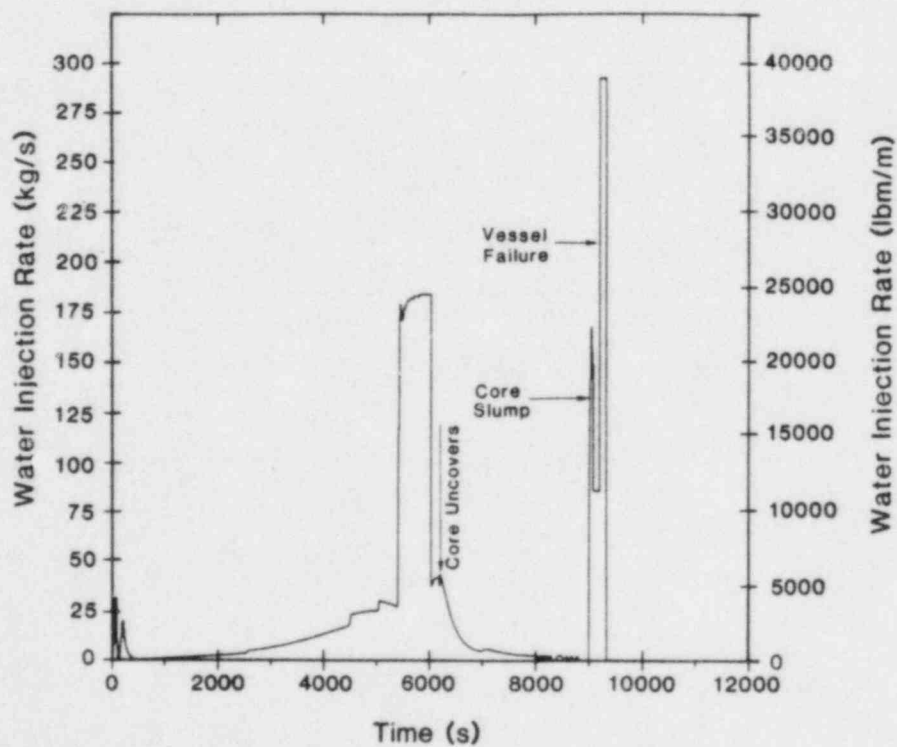


Figure 3-58. Water Source to Containment for "P" Cases

The source of hydrogen is shown in Figures 3-59, 3-60, and 3-61 for cases N.00, O.00, and P.00, respectively. Again the arbitrary nature of these source terms at the time of vessel failure is obvious when comparing the source rate at vessel failure for case N.00 to that for either case O.00 or P.00. Notice that the release rate during core slump is larger for those cases with larger fractions of zirconium oxidized (as would be expected), but that this release is smaller than the release of hydrogen at the time of vessel failure. While some of this is an artifact of the calculational scheme in MARCH, something similar to this could be expected for this sequence under real accident situations, since vessel failure may result in a much larger relief path for the fluids in the primary system than had been previously provided by the relief valves.

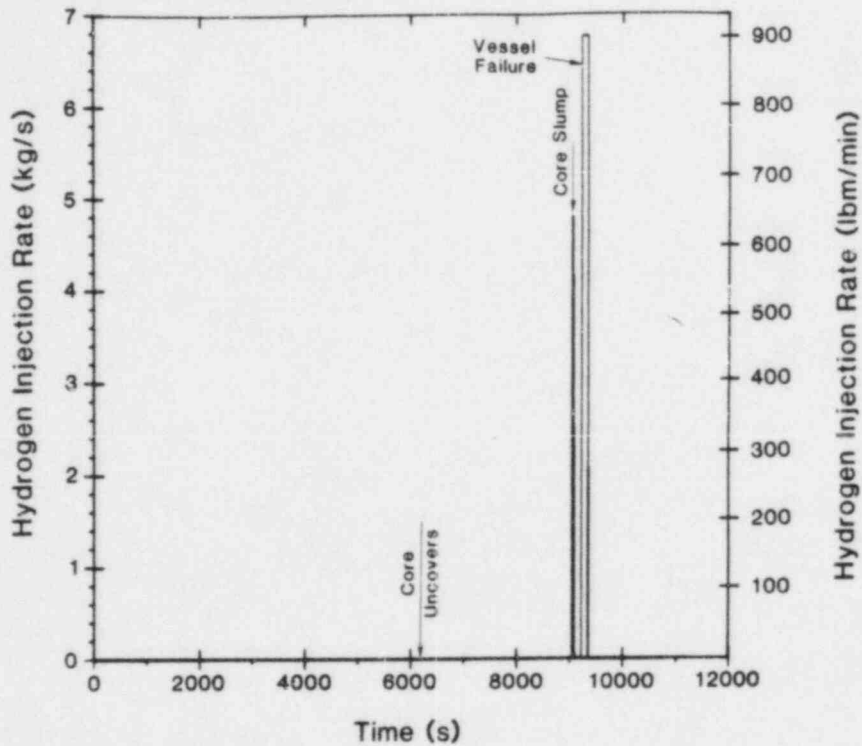


Figure 3-59. Hydrogen Source to Containment for "N" Cases

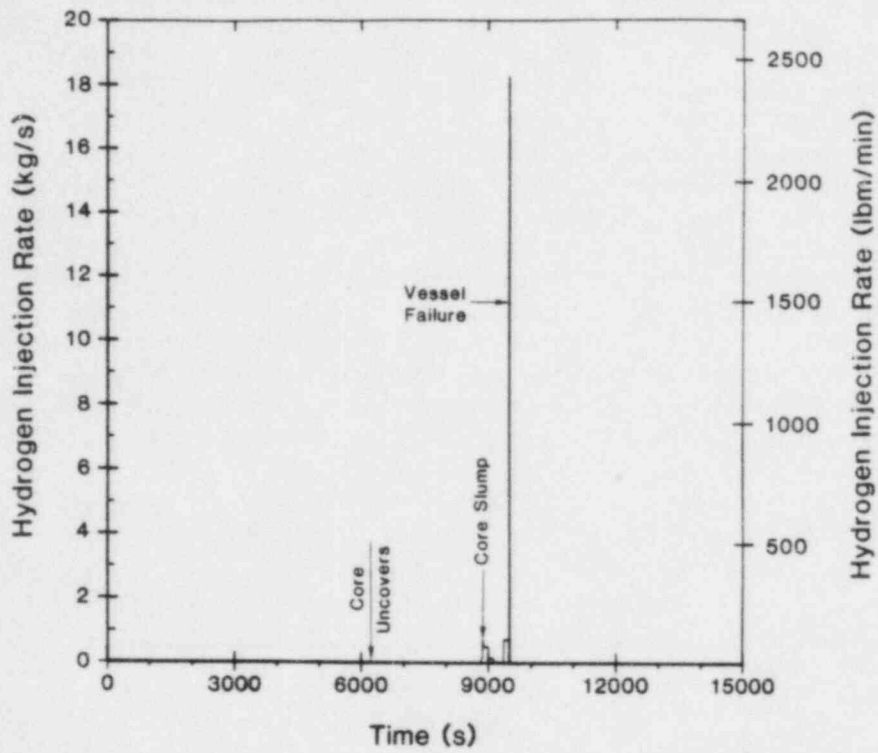


Figure 3-60. Hydrogen Source to Containment for "O" Cases

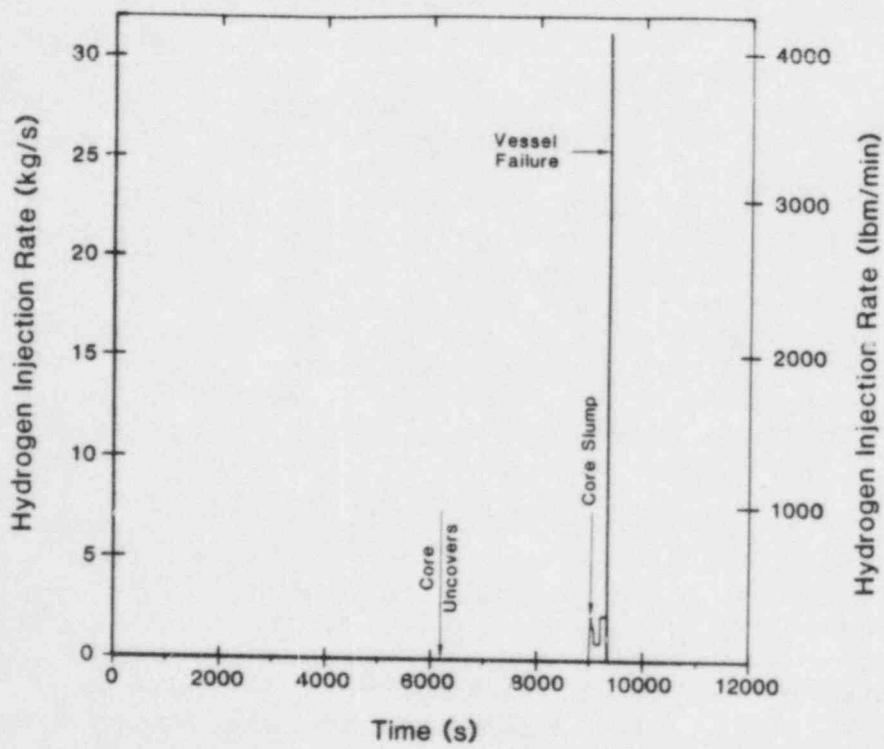


Figure 3-61. Hydrogen Source to Containment for "P" Cases

4. HECTR CONTAINMENT ANALYSES

4.1 Introduction

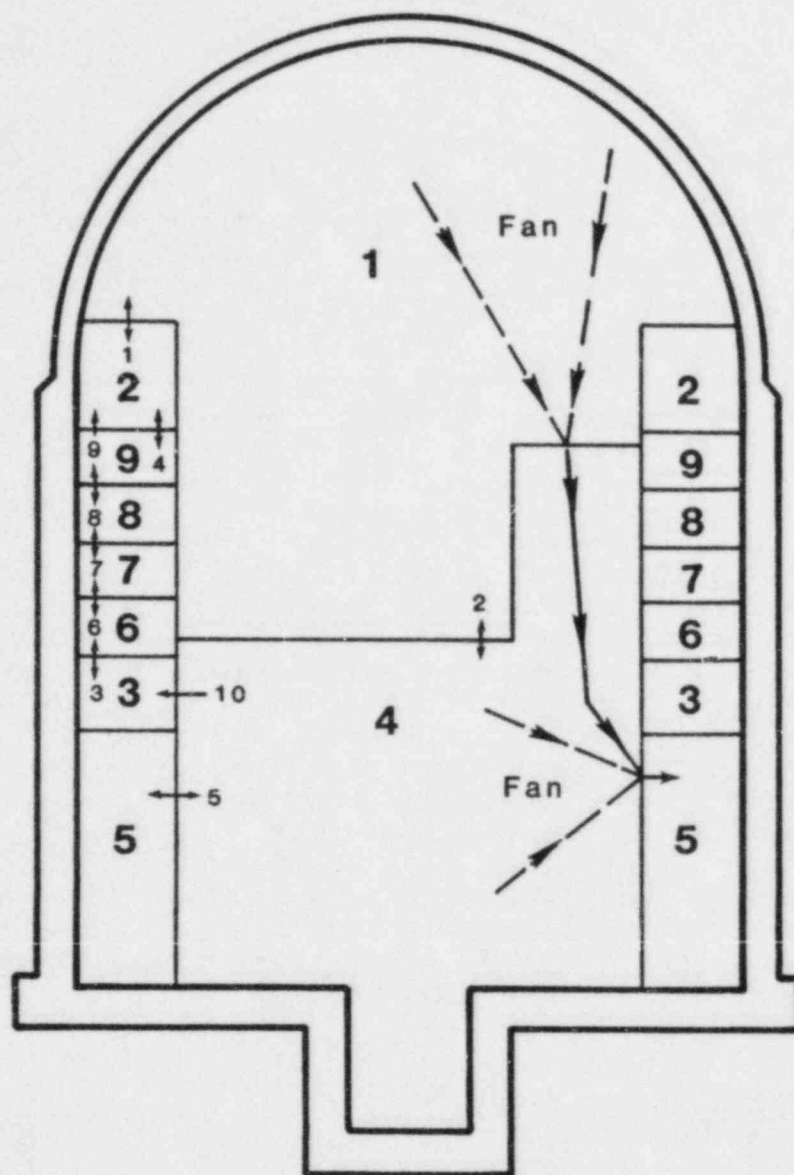
The containment pressure-temperature response has been examined using the HECTR (Hydrogen Event: Containment Transient Response) code.[4-6] HECTR has been developed at Sandia specifically for the purpose of evaluating the containment atmosphere pressure-temperature response to reactor accidents involving the release of significant amounts of hydrogen. HECTR is a fast-running, lumped-volume code that is very useful for parametric analyses. It includes models for hydrogen burns, radiative and convective heat transfer, condensation, heat transfer to sprays, passive heat sinks, a sump, a heat exchanger, air return fans, and an ice condenser. Inertial and buoyancy terms are included in the inter-compartment flow equations. Steam is treated as a real gas, while all other gases (oxygen, nitrogen, and hydrogen) are treated as ideal. Descriptions of some of the models in HECTR are presented in Appendix A.

4.2 Ice-Condenser Containment Model

The ice-condenser containment model is discussed here only in general terms. A detailed description of the HECTR input is presented in Appendix D. The containment model used for these calculations is shown in Figure 4-1. A nine-compartment model is employed, including the dome (1), the upper plenum (2) and lower plenum (3) of the ice condenser, the lower compartment (4), a dead-ended region (5), and four ice compartments (6, 7, 8, 9). The compartments will be identified by these names throughout the rest of the report.

The ice condenser is represented by six compartments. Compartment 2 represents the upper plenum of the ice condenser, compartment 3 represents the lower plenum of the ice condenser, and compartments 6 through 9 are four equal volumes containing ice. Volume changes due to ice melting and heatup of the water falling through the lower plenum are included. In existing ice-condenser containments, the only igniters in the ice condenser are in the upper plenum. No igniters are present in the lower plenum or the ice compartments, so the only burns that occur in these compartments are those which begin elsewhere (compartments 1, 2, 4, or 5) and propagate in.

For accidents in which ac power is available, it is anticipated that the igniters will be actuated well before the beginning of hydrogen production. Thus, we assume igniter operation from the beginning of the calculations. In compartments with igniters, HECTR assumes that ignition will occur at 8% hydrogen unless otherwise specified. Propagation into adjacent compartments, either with or without igniters, can occur if the hydrogen concentrations are above 4.1% for



KEY

- 1 - Compartment Number
- 1 - Flow Junction Number
- - One-way Flow Junction
- ↔ - Two-way Flow Junction

Note: Igniters Present in
Compartments 1, 2, 4, and 5.

Compartment Descriptors

- 1. Dome
- 2. Upper Plenum
- 3. Lower Plenum
- 4. Lower Compartment
- 5. Dead-Ended Region
- 6-9. Ice Compartments

Figure 4-1. HECTR Ice-Condenser Containment Model

upward propagation, 6% for horizontal propagation, or 9% for downward propagation. Combustion cannot occur in any compartment in which the oxygen concentration is below 5% or the steam concentration is above 55%.

Flow junctions are also indicated in Figure 4-1. Of particular importance are junctions 2, 4, 9, and 10. Junction 2 represents floor drains connecting the dome and the lower compartment. We assume that gas flow through the drains is possible, but that gas flow through this junction is precluded in either of two situations. First, when the sprays are operating, drainage from the dome to the lower compartment through this junction is assumed to preclude simultaneous gas flow through this junction. Second, when sufficient water (750 m³ or 26 500 ft³) accumulates in the recirculation sump, the liquid level is high enough to block gas flow through this junction. Junction 4 represents bypass flow around the ice-condenser intermediate deck doors, and junctions 9 and 10 represent the intermediate deck doors and the lower plenum inlet doors, respectively. As noted in Chapter 2, we assume that these doors will close to block reverse gas flow. However, some situations may arise where the doors will be thrown open so as not to reclose or will be damaged such that substantial leakage could occur. As discussed later in this chapter, we examined one case in which the doors were removed entirely, thus bounding the possible effects. Fans are assumed to transfer gas from compartments 1 and 4 into compartment 5, with the flow from compartment 1 to compartment 5 being dominant (see Appendix D). A head curve is included in the model. Dampers are installed in the distribution system for the fans to assure one-way flow; thus, in our model reverse flow through the fans is not allowed.

The water and hydrogen sources are introduced in the lower compartment. The containment recirculation sump is located in the lower compartment. Liquid which drains from the dome, condensate on surfaces, melted ice, and liquid from the primary system are all added to the inventory of the sump. Water drawn by the ECC system and containment spray system when in the recirculation mode is subtracted from the sump inventory. The volume of the lower compartment is adjusted to account for changes in the free gas volume due to the accumulation of liquid.

Both the sprays and the fans are activated based on the pressure setpoint of 122 kPa (17.7 psia). Once this containment pressure is reached, the sprays are activated after a 30-s delay, and the fans are activated after a 600 s delay. When in the recirculation mode, spray water is drawn from the sump and passed through a heat exchanger before being injected into containment.

Twenty-nine heat transfer surfaces were treated in this analysis. Nine of these surfaces (three each in the dome, the upper plenum, and the lower compartment), were included to simulate the presence of equipment. The response of these surfaces will be the subject of a subsequent report.

The analyses in this report do not address the possible effects of stable diffusion flames or jets. Such burning might occur at the hydrogen release point if the local area is not steam-inerted. It may also be possible to establish stable flames in or just above the ice condenser, although nonsteady gas flow due to movement of the ice-condenser doors makes this unlikely. In general, diffusion flames or jets will not cause significant overpressures, but may threaten safety-related equipment due to the high local heat fluxes involved. Future versions of HECTR will be modified to treat diffusion flames.

4.3 Results for Degraded-Core Accidents

The degraded-core accident scenarios are designated in Table 2-1 by the letters A, B, C, F, G, H, I, L, and M. Results for these cases are shown in Table 4-1, which includes the number of burns predicted to occur in each compartment, the peak pressure and temperature, and the compartment(s) that the peak values were predicted to occur in. All pressures given are absolute. To put the peak pressures in perspective, estimated failure pressures for ice-condenser containments are 350 to 515 kPa (51 to 75 psia) for Sequoyah,[7] and 778 to 1067 kPa (113 to 155 psia) for Watts Bar.[8] Each of the cases is discussed in more detail below.

Table 4-1

HECTR Results

Case	Sequence Time (10 ³ s)	Number of Burns by Compartment									Ice Remaining ^a (%)	Maximum Pressure ^b			Maximum Temperature		
		1	2	3	4	5	6	7	8	9		(kPa)	(psia)	Comp.	(K)	(°F)	Comp.
A.00	12.0	5	6	0	0	0	0	0	0	0	0	343	50	1,2	960	1268	2
B.00	11.5	1	0	0	0	0	0	0	0	0	1	369	54	1,2	873	1111	1
C.00	7.2	5	19	1	1	0	1	2	5	8	24	233	34	1,2	994	1329	2
D.00	4.5	4	6	5	6	1	5	1	2	3	31	429	62	1,2	1226	1747	2
E.00	4.5	2	6	0	0	0	1	2	1	3	36	250	36	ALL	1110	1538	2
F.00	8.0	2	5	10	16	0	9	2	2	2	0	348	50	1,2	1242	1776	4
G.00	5.0	0	1	8	8	0	8	2	2	1	5	162	23	ALL	1132	1578	4
H.00	7.2	1	4	10	16	0	9	2	2	3	0	183	27	1-3, 6-9	1242	1776	4
I.00	7.2	0	4	8	13	0	7	3	3	3	0	473	69	ALL	1210	1718	4
J.00	6	3	8	6	8	0	6	6	6	8	6	520	75	1,2	1354	1977	2
K.00	7.2	0	3	5	5	0	5	5	5	5	7	189	27	ALL	1071	1468	4
L.00	15.0	5	12	2	2	0	2	2	0	0	1	361	52	1,2	981	1306	2
M.00	15.0	4	9	2	2	0	2	1	1	6	0	355	52	1,2	1019	1374	4
N.00	10.8	1	4	0	0	2	0	1	1	1	46	887	129	1,2	2025	3185	2
O.00	15.0	0	2	0	0	0	0	1	2	2	45	201	29	ALL	1246	1783	2
P.00	10.8	1	4	0	0	0	0	1	1	2	46	452	66	1,2	1410	2078	2
A.01	12.0	2	24	0	0	2	0	0	2	6	0	521	76	1,2	1756	2701	2
A.02	12.0	6	22	0	0	0	0	0	2	11	0	380	55	1,2	970	1286	2
A.03	12.0	4	7	0	0	0	0	0	0	0	0	440 ^c	64 ^c	ALL	957	1263	2
A.04	12.0	1	25	0	0	2	0	2	4	7	0	631 ^c	91 ^c	1,2	1363	1993	2
A.05	12.0	5	10	0	0	0	0	0	0	0	0	381 ^c	55 ^c	ALL	946	1243	2
A.06	12.0	8	43	1	1	0	1	0	0	0	0	218	32	1,2	760	962	2
A.07	12.0	7	16	0	0	0	0	0	0	0	1	279	40	1,2	832	1038	2
A.08	12.0	4	3	0	0	0	0	0	0	0	1	384	56	1,2	1062	1452	2
A.09	12.0	3	2	0	0	0	0	0	0	2	1	419	61	1,2	1144	1599	2
A.10	12.0	8	9	0	0	0	0	0	0	0	0	286	41	1,2	831	1036	2
A.11	12.0	5	5	0	0	0	0	0	0	0	0	405	59	1,2	1023	1381	1,2
A.12	12.0	5	7	0	0	0	0	0	0	0	1	241	35	1-3, 6-9	924	1203	2
A.13	12.0	3	2	2	2	2	2	2	2	2	0	415	60	1,2	1059	1446	2
A.14	12.0	5	5	0	0	0	0	0	0	0	1	342	50	1,2	964	1275	2
A.15	12.0	5	5	0	0	0	0	0	0	0	0	252	36	ALL	940	1232	2

Notes: ^aPercentage of ice remaining at end of sequence.

^bAll pressures are absolute.

^cThe pressure is still increasing at the end of cases A.03, A.04, A.05, and the "I" cases due to steam overpressure, although in case A.04 the peak pressure occurs earlier due to burns.

Table 4-1

HECTR Results
(continued)

Case	Sequence Time (10 ³ s)	Number of Burns by Compartment									Ice Remaining ^a (%)	Maximum Pressure ^b			Maximum Temperature		
		1	2	3	4	5	6	7	8	9		(kPa)	(psia)	Comp.	(K)	(°F)	Comp.
C.01	7.2	0	30	0	10	0	0	0	0	0	24	188	27	ALL	1006	1351	2
C.02	7.5	0	19	0	6	0	2	7	12	17	25	175	25	ALL	881	1126	2
D.01	4.5	4	7	5	6	2	5	1	2	2	32	385	56	ALL	1074	1473	4
D.02	4.5	3	3	3	5	1	3	1	1	1	35	425	62	1,2	1075	1475	4
E.01	4.5	2	5	0	0	0	1	1	1	2	36	309	45	1,2	1104	1527	2
F.01	8.0	2	7	6	10	0	6	3	3	3	0	399	58	1,2	1303	1885	4
H.01	7.2	2	6	6	10	0	6	2	2	3	0	361	52	1,2	1295	1891	4
I.01	7.2	0	3	7	12	0	7	3	3	2	0	500 ^c	72 ^c	ALL	1187	1677	4
I.02	7.2	1	6	8	13	0	8	3	3	3	0	459 ^c	66 ^c	ALL	1206	1711	4
I.03	7.2	0	3	5	8	0	5	2	2	2	7	419 ^c	61 ^c	ALL	1142	1596	4
I.04	7.2	0	5	9	16	0	8	3	3	4	0	498 ^c	72 ^c	ALL	1248	1786	4
I.05	7.2	1	5	8	12	0	7	3	3	4	0	424 ^c	62 ^c	ALL	1142	1596	4
I.06	7.2	2	5	5	8	0	5	3	3	3	0	475 ^c	69 ^c	ALL	1287	1857	4
J.01	6.0	2	14	6	8	0	6	6	6	9	7	401	58	1,2	1312	1902	4
J.02	6.0	2	5	6	6	0	6	5	5	5	9	460	67	1,2	1176	1657	4
K.01	7.2	0	3	5	5	0	5	5	5	5	7	189	27	ALL	1074	1473	4
L.01	15.0	5	12	1	2	0	1	0	0	0	1	357	52	1,2	976	1297	2
M.01	15.0	4	10	1	1	0	0	1	7	10	0	354	51	1,2	977	1299	4
N.01	10.8	2	5	0	0	2	0	1	3	3	41	699	101	1,2	1512	2262	2
N.02	10.8	1	2	0	0	1	0	0	1	1	47	906	131	1,2	1508	2254	1
O.01	15.0	0	3	0	0	0	0	0	1	2	47	210	30	ALL	1246	1783	2
P.01	10.8	1	9	0	0	0	0	1	2	3	44	407	59	1,2	1532	2298	2

Notes: ^aPercentage of ice remaining at end of sequence.^bAll pressures are absolute.^cThe pressure is still increasing at the end of cases A.03, A.04, A.05, and the "I" cases due to steam overpressure, although in case A.04 the peak pressure occurs earlier due to burns.

4.3.1 Case A.00 - S₂D Degraded-Core Base Case

The "A" cases represent S₂D degraded-core accident scenarios with 75% zirconium oxidation. The reference case, A.00, assumes that the fans and sprays are operational and uses the default combustion parameters (see Appendix A). The pressure response for the dome is shown in Figure 4-2. The drop in pressure that is predicted to occur 600 s into the accident is due to activation of the fans, which force more steam into the ice condenser, thereby condensing steam from and cooling the containment atmosphere. The minor variations that are predicted to occur at about 2000 s are due to changes in the water source term and switch-over of the sprays to the recirculation mode.

The first burn occurs at about 4600 s. Ignition occurs in the upper plenum when the hydrogen concentration reaches 8%. The burn then propagates upward into a mixture of 5.6% hydrogen in the dome. Three other burns are predicted that are similar in nature. Also, two burns occur that are restricted to the upper plenum. These burns are represented by the two very small peaks that are present on the "tail" of the first two larger peaks. These smaller upper plenum burns result in negligible pressure rises, because the gas expands into the very large volume of the dome.

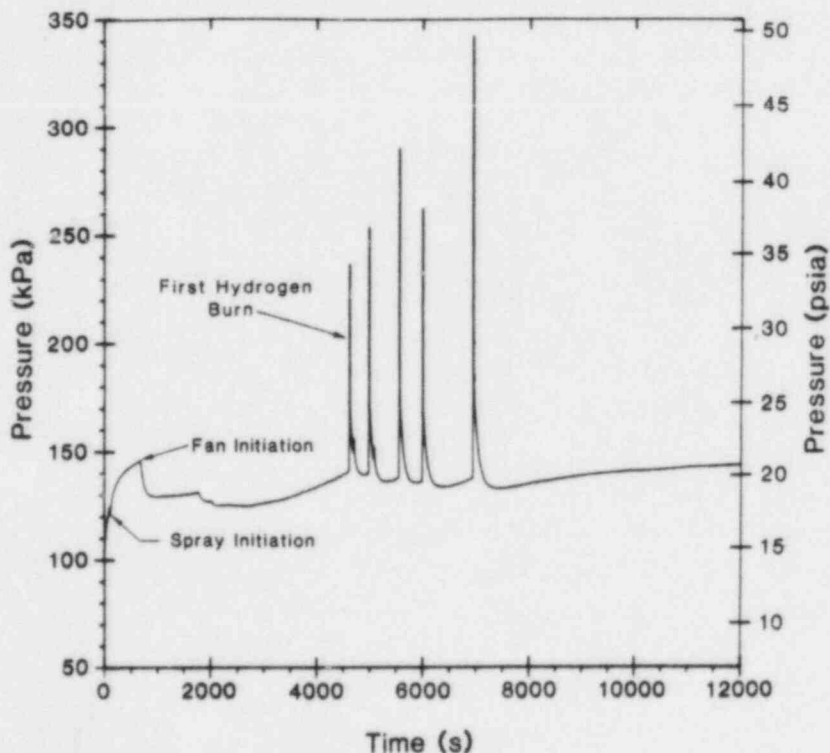


Figure 4-2. Pressure Response in Dome for Case A.00

Generally, it may be expected that combustion will begin in the upper plenum because steam is removed as the gases pass through the ice condenser, and the resultant mixture will be richer in hydrogen and air. However, the last and largest pressure spike is due to a burn that occurs in the dome only. Late in the accident much of the ice has melted, the efficiency of the ice condenser in removing steam decreases, and the mixture entering the upper plenum is progressively richer in steam. This excess steam is removed by the containment sprays in the dome, resulting in higher hydrogen concentrations in the dome than in the upper plenum. Thus, the last burn is initiated in the dome, rather than in the upper plenum. Figures 4-3 through 4-5 show the gas compositions in the dome and the upper plenum and the fraction of ice remaining in the ice condenser as a function of time.

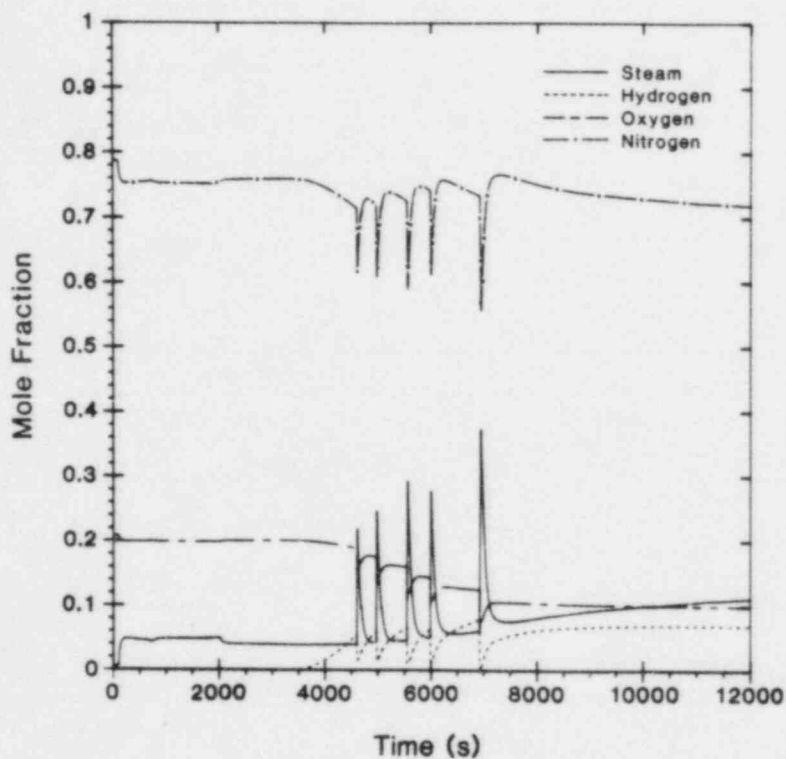


Figure 4-3. Gas Composition in Dome for Case A.00

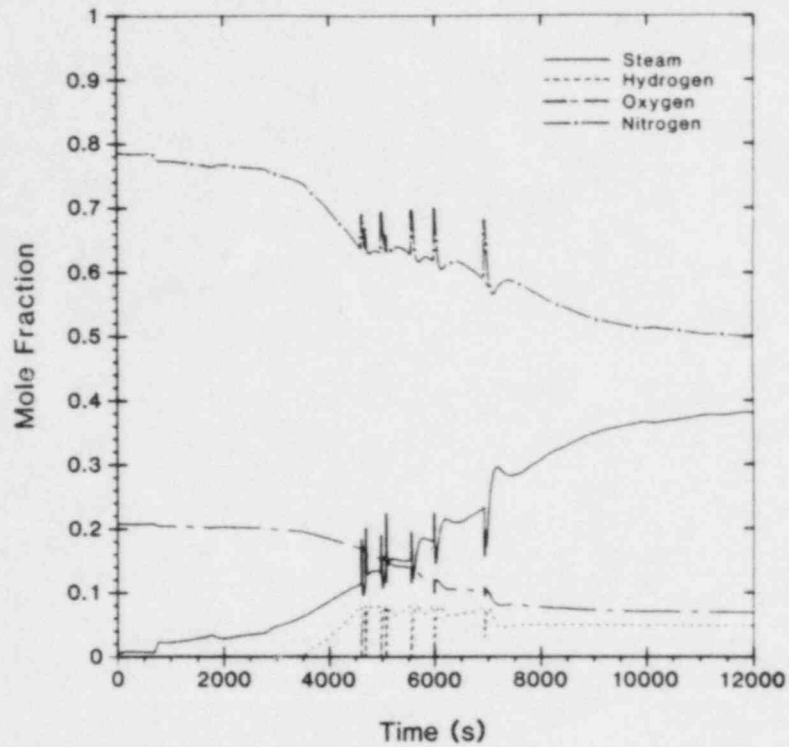


Figure 4-4. Gas Composition in Upper Plenum for Case A.00

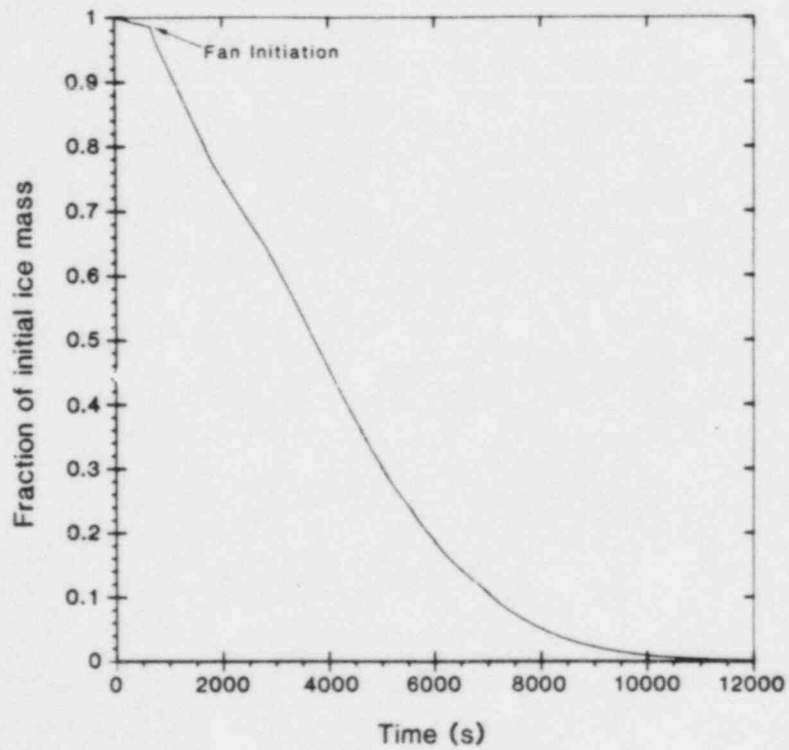


Figure 4-5. Ice Inventory History for Case A.00

No burns are predicted in the ice compartments because no igniters are located there and because the 9% downward propagation limits were not reached to allow a burn to propagate downward from the upper plenum. Also, no burns are predicted in the lower regions of the containment because of the high steam concentrations found there and the assumed ignition limits. As shown in Figure 4-6, the lower compartment is not steam inerted, but the steam concentrations are high enough so that ignition occurs preferentially in the dome and upper plenum after the steam is removed. Note that in several instances the hydrogen concentration is above 7% in the lower compartment when ignition occurs in either the dome or the upper plenum. Thus, burns in the lower compartment should not be ruled out based on these results.

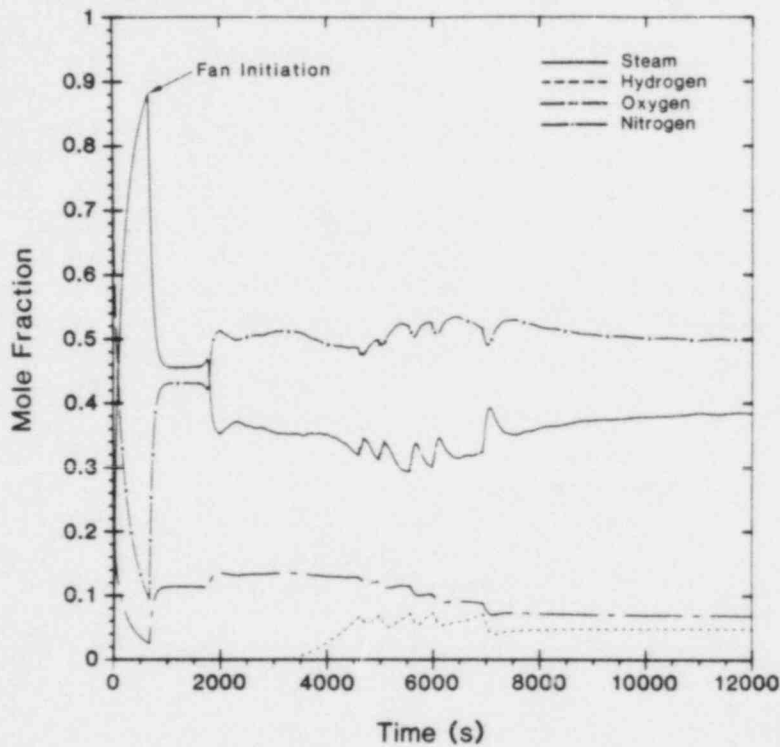


Figure 4-6. Gas Composition in Lower Compartment for Case A.00

4.3.2 Cases A.01 through A.04 - Effects of Fans and Sprays

The majority of the sensitivity analyses performed involved the "A" cases. Cases A.01 through A.04 were run to examine the importance of certain engineered safety features (fans and sprays).

Case A.01 was run to examine the effects of failure of the recirculation fans. A pressure plot for the dome is shown in Figure 4-7. One result of fan failure is that the baseline pressure before the burns is higher due to reduced ice-condenser effectiveness (i.e., less steam is removed from the lower compartment). The small spikes in Figure 4-7 are the result of burns that are initiated in the upper plenum, with no propagation into the dome. Six of these burns propagate downward into one or more of the ice compartments (6-9). The two large peaks in Figure 4-7 are due to burns that are initiated in the dome. These pressure rises are larger than those of case A.00 for two reasons. First, the baseline pressure is higher when the burn begins, because of reduced ice-condenser effectiveness in the absence of fans. Second, as shown in Figure 4-8, the upper plenum becomes temporarily inerted due to oxygen depletion before the large burns occur. Once the burns begin in the dome, oxygen is pushed back into the upper plenum, and burns occur there also, but at a higher hydrogen concentration (i.e., >8%). Thus, the burns are effectively at a hydrogen concentration above 8%.

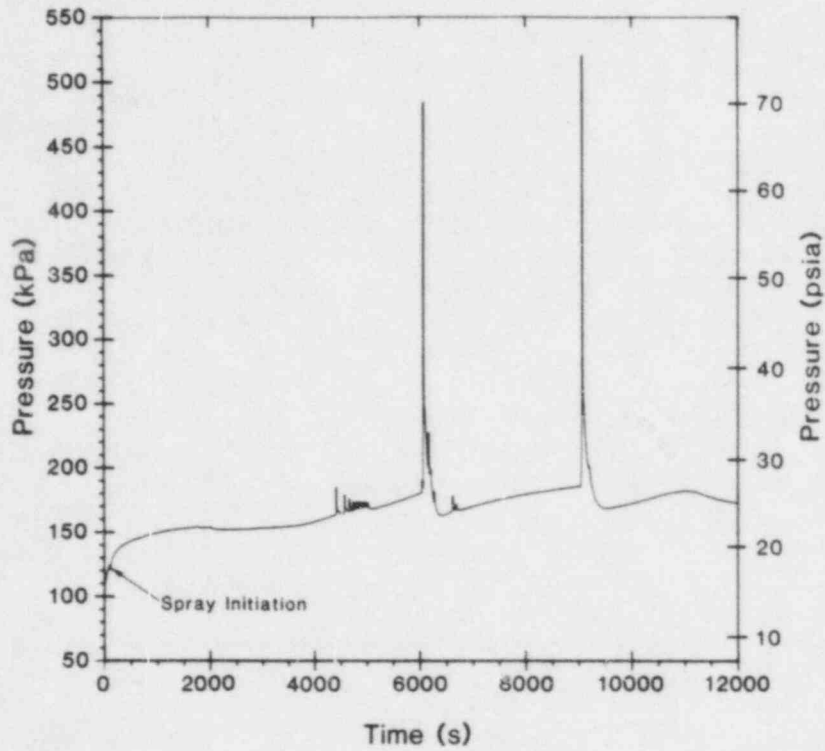


Figure 4-7. Pressure Response in Dome for Case A.01

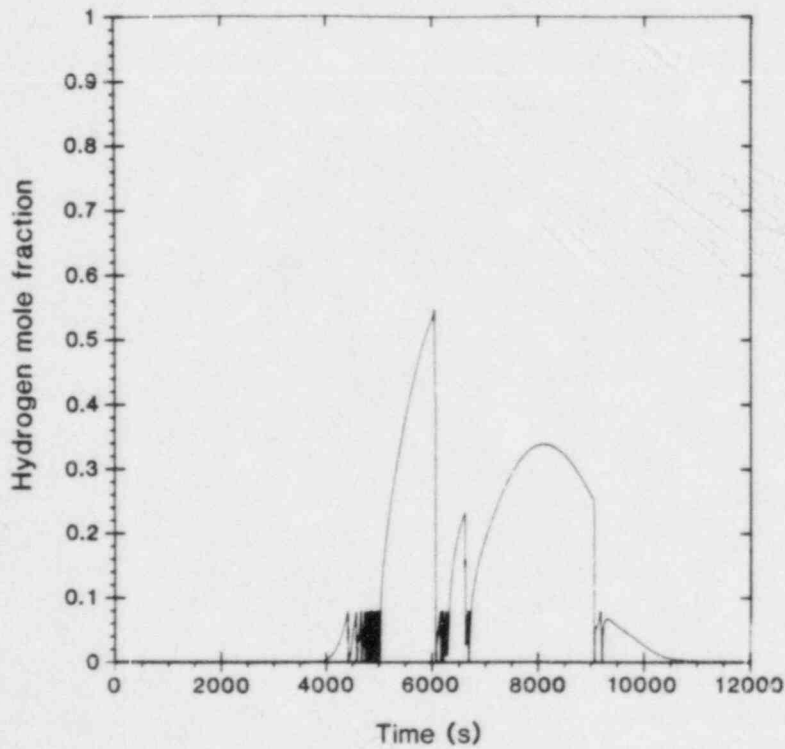


Figure 4-8. Upper-Plenum Hydrogen Concentration for Case A.00

A potentially serious situation is indicated in the results of case A.01. With the fans off, very high hydrogen concentrations are predicted in the upper ice compartments (8, 9). Figures 4-8 and 4-9 show that by the time 8% hydrogen is reached in the upper plenum at about 4400 s, the hydrogen concentration in the top ice compartment (9) is above 30%. Because HECTR cannot treat detonations or accelerated flames, this hydrogen is burned in a relatively benign manner. It is beyond our present capability to state with any certainty the probability that a detonation would occur under these circumstances. Research is underway at Sandia that may help answer that question.[14] If a detonation were possible in the ice condenser, then the consequences of damage to the ice condenser would have to be evaluated, along with the potential for direct containment failure. These high hydrogen concentrations are predicted in all computations involving failure of the fans, not just in case A.01. We should also point out that failure of the fans could be postulated to occur during other scenarios if the fans do not survive the temperature and differential pressure environments during hydrogen burns.

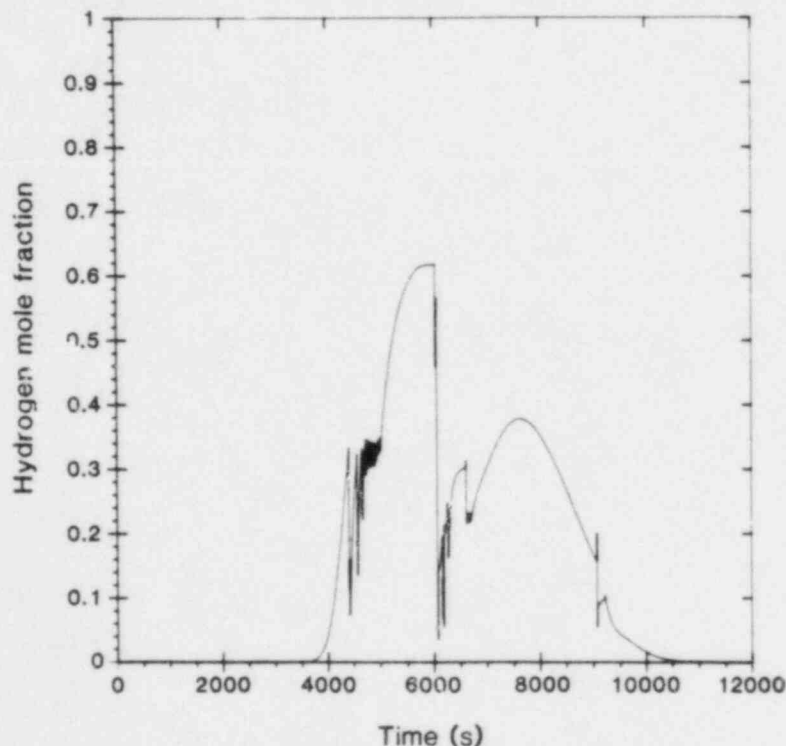


Figure 4-9. Hydrogen Concentration in Top Ice Compartment for Case A.01

The predictions of hydrogen and oxygen concentrations in the ice condenser and upper plenum by HECTR should be considered preliminary. It is possible that a finer nodalization of the problem would result in natural convective mixing loops within and above the ice condenser that would reduce the concentration gradients. However, the mixing will be influenced by the behavior of the ice-condenser doors (e.g., which doors are closed and which are open), and we do not currently have sufficient information to properly model the processes.

Case A.02 shows the effects of having only one fan and one train of sprays operational. A pressure plot for the dome is shown in Figure 4-10. More burns are predicted in the upper plenum than in case A.00, because of reduced recirculation flow through the ice condenser and less transfer of gas into the dome. Enough hydrogen is transferred into the dome, however, to allow several of the burns to propagate upward from the upper plenum and to allow for one large burn in the dome at about 7500 s. Many of the upper plenum burns propagate downward into some of the ice compartments (8-9). However, unlike case A.01, the concentrations in these ice compartments (8-9) are in the range of 9 to 10%, and it appears that 50% fan flow (i.e., one of two fans) is sufficient to preclude formation of the high concentrations predicted in case A.01.

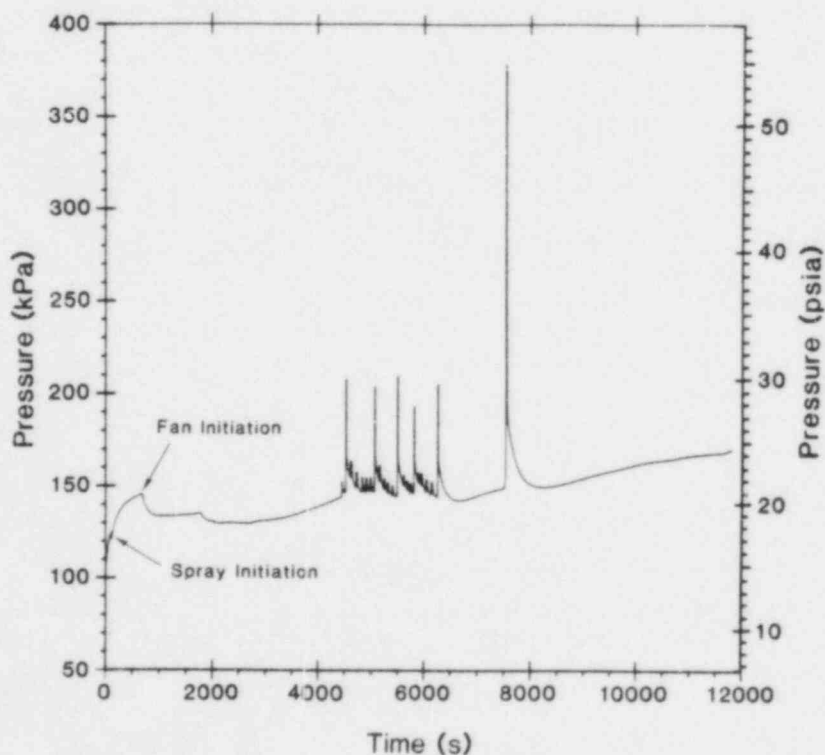


Figure 4-10. Pressure Response in Dome for Case A.02

Case A.03 was run to examine the effects of failure of the containment sprays. The pressure response for the dome is shown in Figure 4-11. During the first part of the accident, the response is similar to case A.00. During this time the ice condenser is removing most of the steam and providing containment cooling. However, as the ice melts, the containment pressure begins increasing due to steam buildup. With no remaining containment heat removal, except for heat transfer to passive heat sinks, the pressure will continue to increase until the failure pressure is reached. This case illustrates the importance of the containment sprays. Without sprays, the containment will eventually fail regardless of whether hydrogen burns occur (unless, of course, the injection of steam into containment is terminated, as is the case in many degraded-core scenarios). The ice condenser is only effective for a finite period of time, based on the mass of ice present, and cannot be used for long-term containment heat removal. Containment sprays are also an important source of heat removal during a burn. The heat removal effect is not well illustrated in this case, because the burn sequence and preburn conditions are somewhat different than in case A.00. However, for burn times of a few seconds or more, the heat transfer effects of sprays are very significant, as will become more apparent during the discussions of later cases.

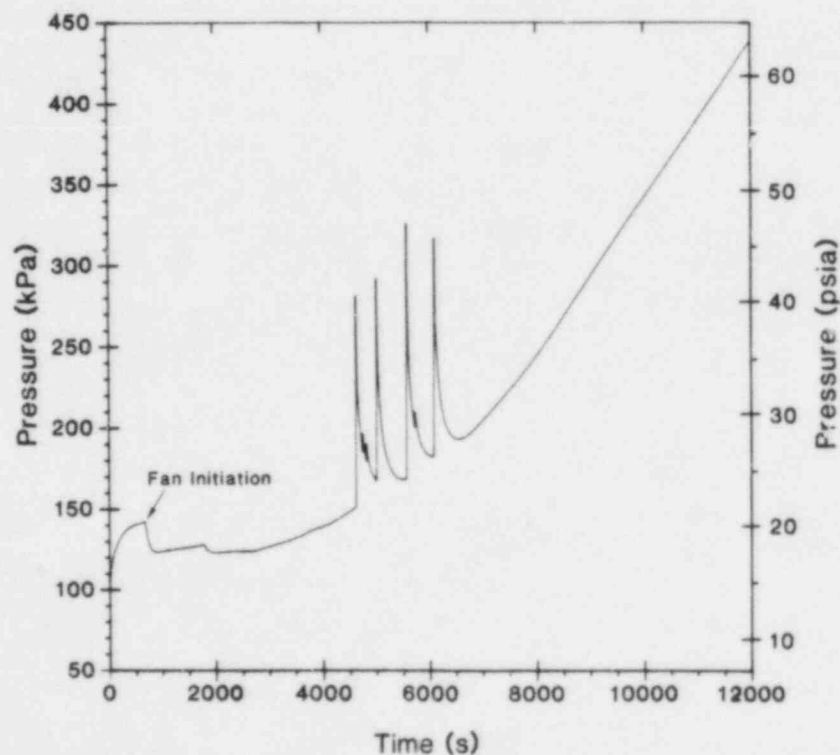


Figure 4-11. Pressure Response in Dome for Case A.03

Case A.04 was run to examine the effects of loss of both sprays and fans. The pressure response for the dome is shown in Figure 4-12. In general, the results exhibit all of the bad features of cases A.01 and A.03. High hydrogen concentrations are predicted in the upper ice compartments (8, 9), high preburn baseline pressures are calculated, and a large burn in the dome propagating into a high hydrogen concentration in the upper plenum is predicted. High hydrogen concentrations are found in the upper plenum, as well as in the upper ice compartments (8, 9), after the upper plenum atmosphere becomes inert due to oxygen depletion. Also, eventual containment failure by steam overpressure is predicted, assuming failure does not occur earlier due to hydrogen burns.

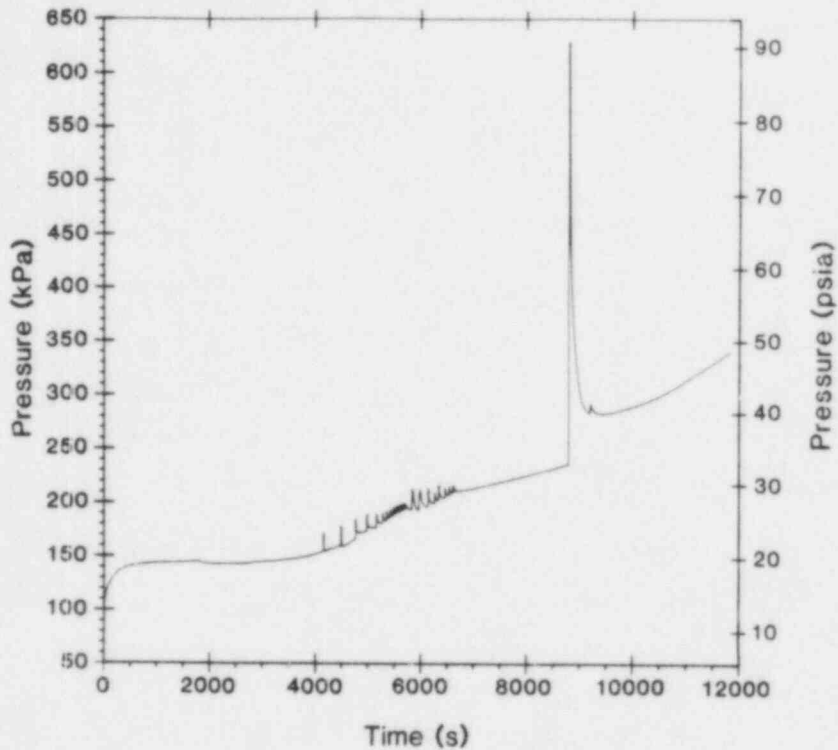


Figure 4-12. Pressure Response in Dome for Case A.04

4.3.3 Case A.05 - Surface Heat Transfer Effects

Case A.05 was run to examine the effects of arbitrarily increasing the surface convective heat transfer coefficients by a factor of 5. The pressure response in the dome is shown in Figure 4-13. The case is a direct comparison to case A.03, with the sprays inoperative in both cases. The results are fairly similar, with case A.05 indicating a slower rate of pressure rise, due to more heat transfer (and more steam condensation) to the passive heat sinks, but showing the same general trends toward long-term containment overpressure.

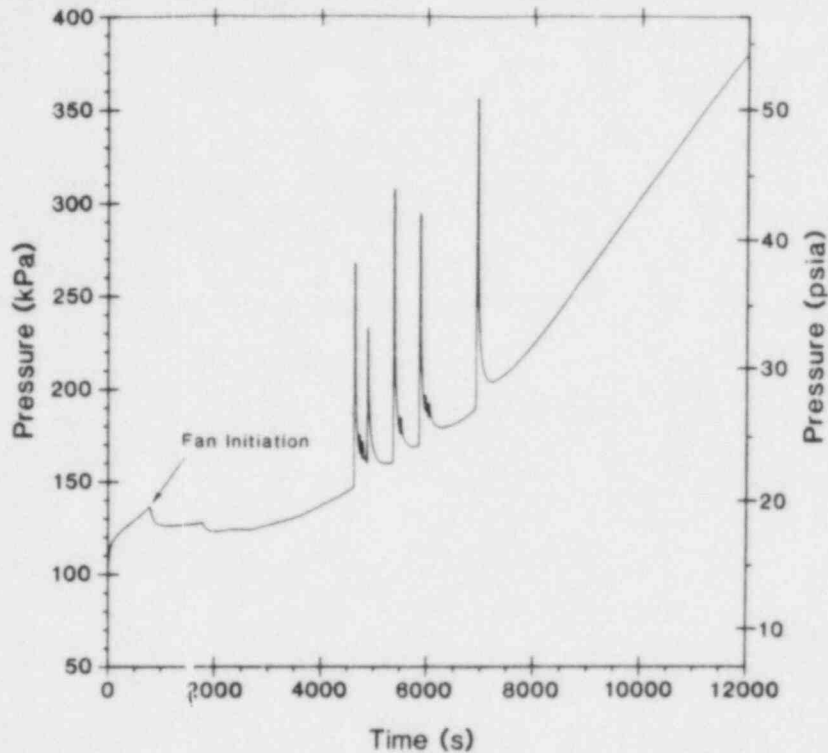


Figure 4-13. Pressure Response in Dome for Case A.05

4.3.4 Cases A.06 through A.09 - Sensitivity to Ignition Limits

Cases A.06 through A.09 show the sensitivity to the ignition limits which were varied between 6 and 10 percent. The dome pressure response for Case A.06 is shown in Figure 4-14. A large number of upper plenum burns are predicted due to the lower ignition limits of 6%. Some of these burns propagate upward into the dome, but the projected pressure rises are fairly small. Note that combustion at 6% hydrogen is only 75% complete, based on the default combustion-completeness model. Also, slightly lower flame speeds are assumed (see Appendix A). Unlike the previous cases, one burn is predicted to begin in the lower compartment.

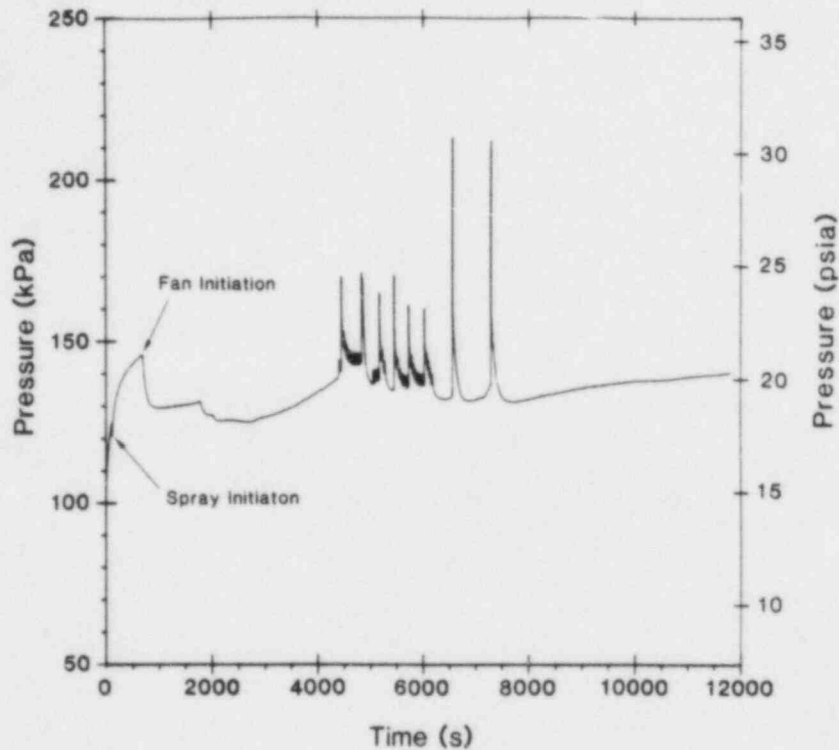


Figure 4-14. Pressure Response in Dome for Case A.06

Dome pressure responses for cases A.07 through A.09 are shown in Figures 4-15 through 4-17. In general, the higher concentrations produce fewer burns that are faster and more complete. As expected, higher ignition limits produce higher peak pressures. It is interesting to note that, as far as gas pressure response is concerned, the burns do not tend to be very cumulative in nature. Even in case A.06 with a very large number of burns, there is sufficient cooling between burns to prevent much addition of the pressure rises. It appears that this will be the case any time that the burns are more than a few tens of seconds apart. Note, however, that some cumulative effects are predicted in the gas temperature response, with even more cumulative effects predicted in the equipment temperature response. The upper plenum temperature response for case A.06 is shown in Figure 4-18. As mentioned previously, equipment response will be the topic of a future report.

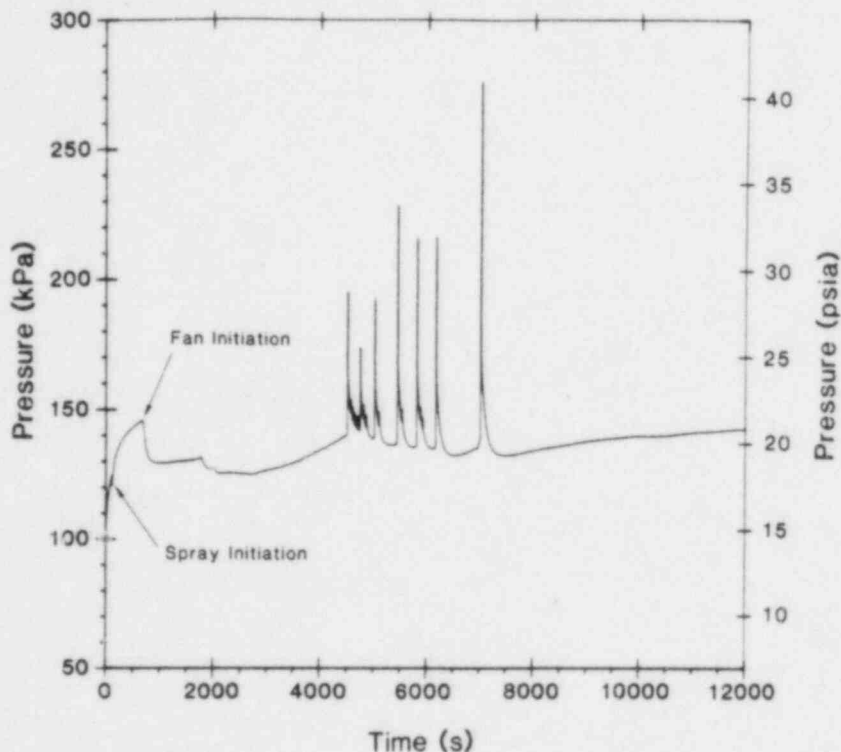


Figure 4-15. Pressure Response in Dome for Case A.07

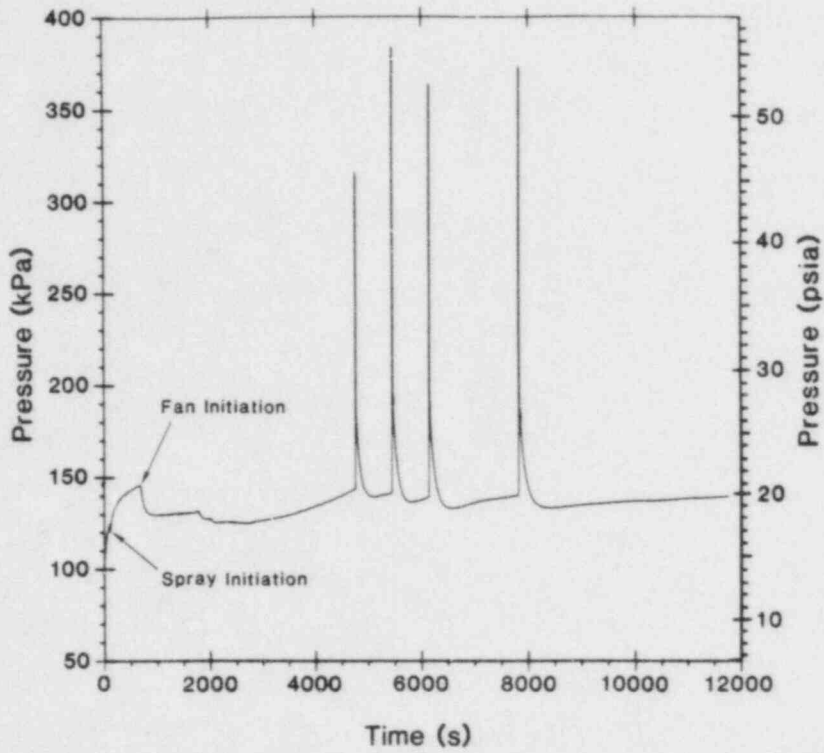


Figure 4-16. Pressure Response in Dome for Case A.08

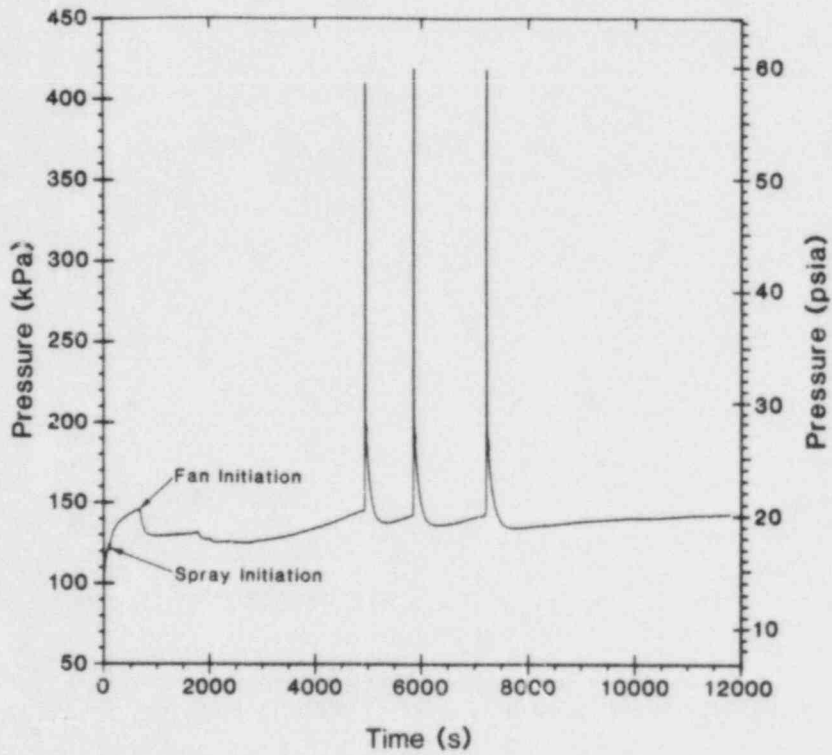


Figure 4-17. Pressure Response in Dome for Case A.09

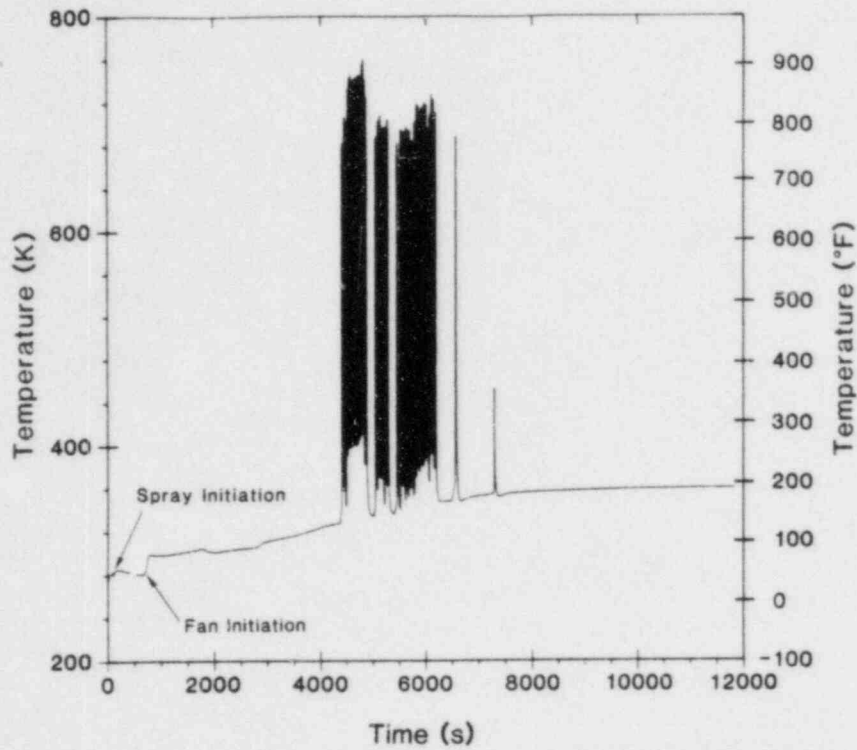


Figure 4-18. Gas Temperature Response in Upper Plenum for Case A.06

4.3.5 Cases A.10 through A.12 - Sensitivity to Combustion Completeness and Flame Speed

Cases A.10 through A.12 were run to examine the effects of altering certain combustion parameters. Case A.10 assumes that the burns are only 75% as complete as the burns in case A.00 (see Appendix A). This assumption results in lower pressure rises and more burns, because less hydrogen is consumed in each burn (see Figure 4-19). In actuality, burn completeness would be very geometry- and composition-dependent, so that there is substantial uncertainty in these values. However, it is clear that incomplete combustion is beneficial from a pressure-suppression point of view.

Cases A.11 and A.12, respectively, examine the effects of increasing and decreasing the flame speed by a factor of three. The dome pressure responses for these cases are shown in Figures 4-20 and 4-21. While the burn sequences are similar, the differences in peak pressure are quite large. These differences in peak pressure are due to the differences in burn time that allow more or less time for heat transfer to occur. The dominant heat removal mechanism in the dome is the containment sprays. These cases, along with cases A.03 to A.05, demonstrate the importance of containment sprays.

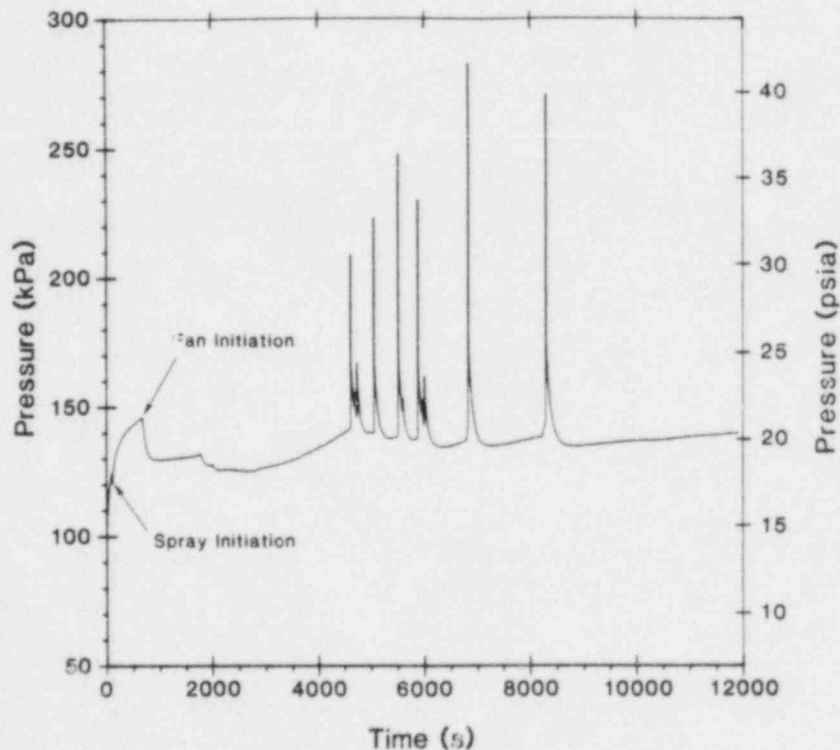


Figure 4-19. Pressure Response in Dome for Case A.10

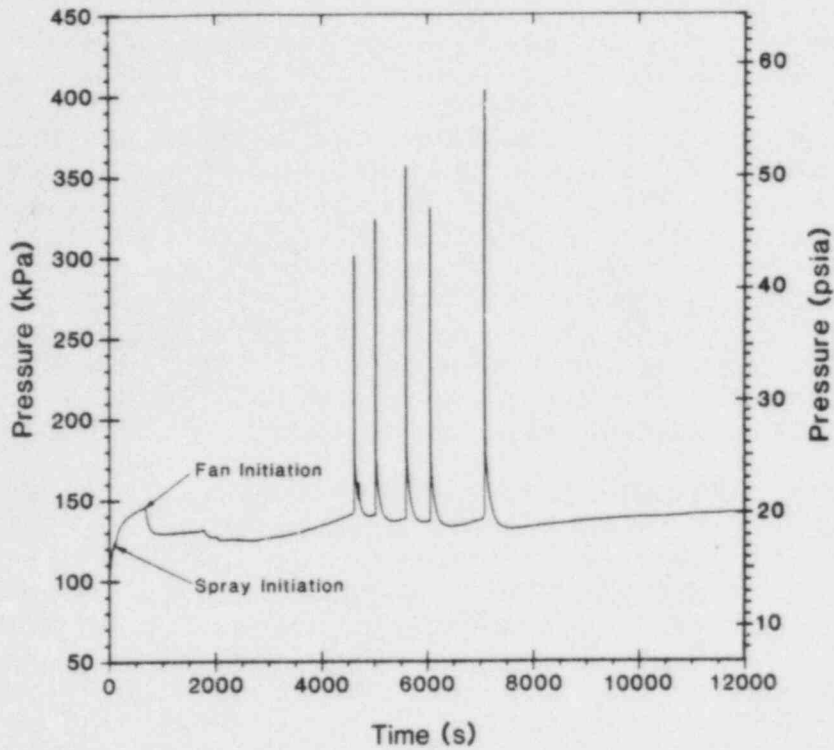


Figure 4-20. Pressure Response in Dome for Case A.11

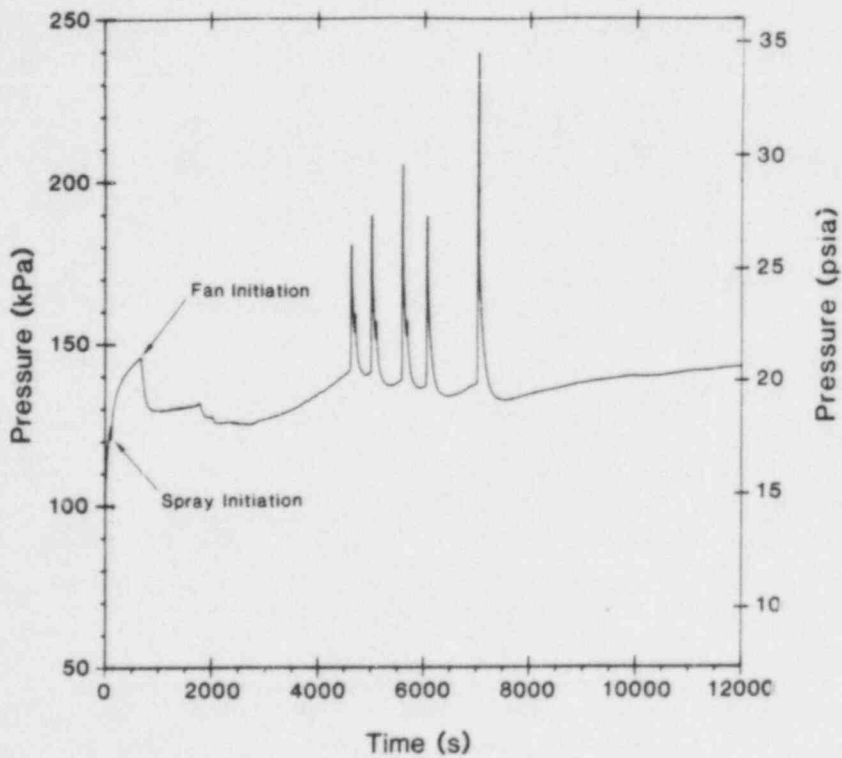


Figure 4-21. Pressure Response in Dome for Case A.12

4.3.6 Case A.13 - Effect of Upper Plenum Igniter Failure

Case A.13 assumes that the upper plenum igniters do not function properly but still allows propagation into the upper plenum. This might occur if suspended water droplets or fogs traveling upward out of the ice compartments prevent the igniters from igniting the mixture, or if a limited electrical failure occurs. It could also occur if the igniters function only to a limited extent, such that substantial amounts of hydrogen reach the dome. The dome pressure response for this case is shown in Figure 4-22. The first two large pressure spikes of Figure 4-22 are the result of burns that begin in the lower compartment and propagate up through the ice condenser into the dome. With ignition precluded in the upper plenum, the lower compartment is the first compartment in which the ignition limits (8% hydrogen) are achieved. Because the hydrogen concentrations in the other compartments are in the vicinity of 8%, large pressure rises are predicted from these "global burns." The last pressure spike is due to a burn that is confined to the dome. A significant result of failure of the upper plenum igniters seems to be that more time is available to transport hydrogen throughout the containment before burns occur, thus resulting in a more uniformly mixed containment atmosphere and making global burns with large pressure spikes more likely.

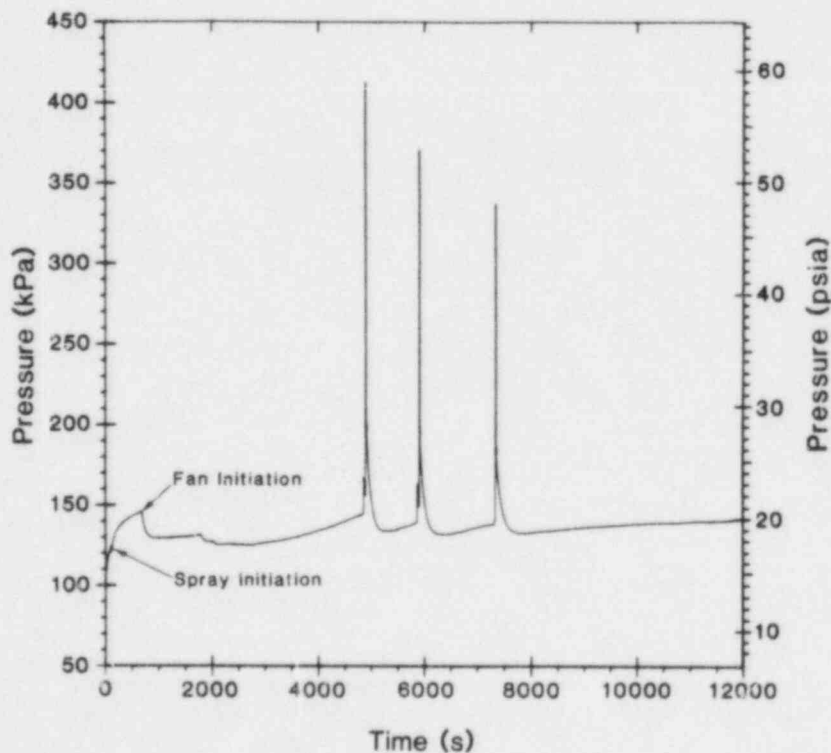


Figure 4-22. Pressure Response in Dome for Case A.13

4.3.7 Case A.14 - Effect of Partial Oxygen Depletion

Case A.14 examines the effects of an atmosphere that has been partially depleted in oxygen before the accident (14% oxygen and 86% nitrogen, as opposed to 21% oxygen and 79% nitrogen). Such partial oxygen depletion would allow containment entry without special equipment. If the amount of oxygen is reduced, the total amount of hydrogen that can be burned will be reduced (similar to the way in which limiting the amount of zirconium oxidation reduces the amount of hydrogen that is available to burn). For this case HECTR does not predict substantial benefits from such a strategy (see Figure 4-23). The burn sequence is similar to that for case A.00, and the pressure rises are comparable. However, at the end of the calculation for case A.14 the containment is inert due to low oxygen concentration, whereas in case A.00 further combustion is possible. HECTR does not properly account for changes in key combustion parameters (such as flame speed and combustion completeness), as a function of oxygen concentration. These changes would be expected to result in lower pressures and temperatures from combustion. Further analyses would be required to quantify the effects of partial oxygen depletion.

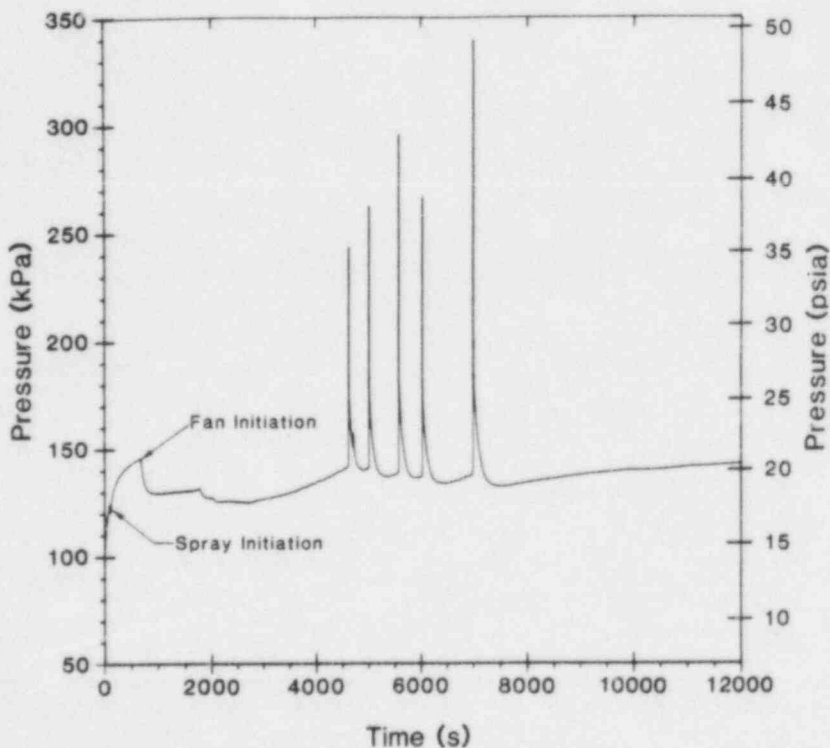


Figure 4-23. Pressure Response in Dome for Case A.14

4.3.8 Case A.15 - Effect of Ice-Condenser Door Failure

Case A.15 was run to examine the effects of failure of the ice-condenser doors. In this case failure is defined as the inability of the doors to block reverse flow. For case A.15 we assumed that all ice-condenser doors were removed at the start of the run, thus allowing gas flow to occur freely in both directions. The dome pressure response for this case is shown in Figure 4-24. In this case it appears that such a failure would be beneficial. The burn sequences are similar to those for case A.00, but the pressure rises are smaller for two reasons. First, in case A.15 there is volumetric expansion of the gases in the upper regions of containment into the lower compartments, reducing the pressure rises. Second, as the gas flows at high velocity down through the ice condenser, a significant amount of cooling and steam removal occurs, further lowering the pressure. We did not consider the possibility of partial failure of the doors, resulting in more restricted and possibly asymmetric flow.

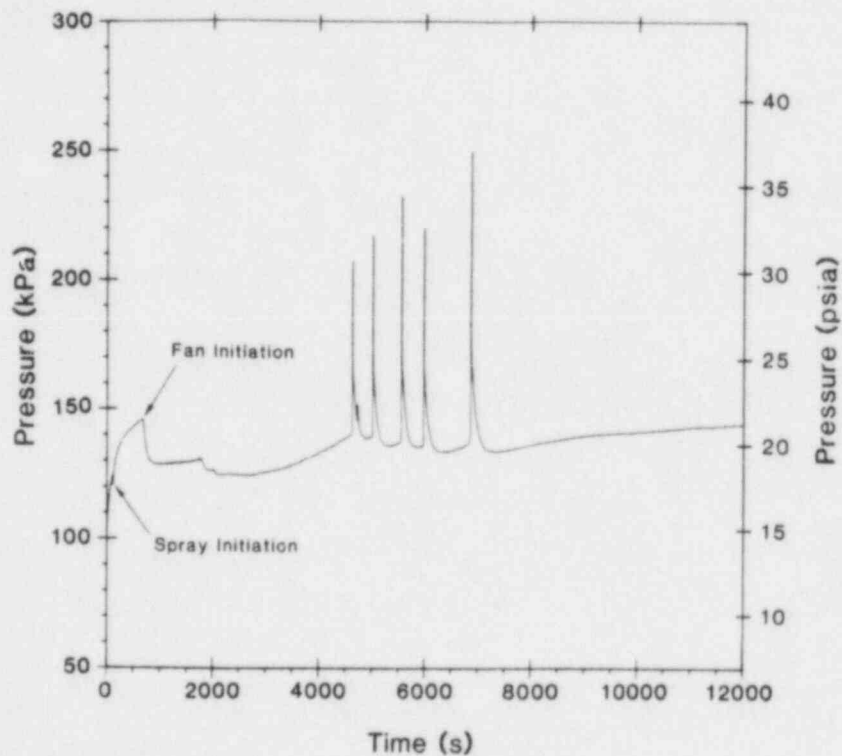


Figure 4-24. Pressure Response in Dome for Case A.15

4.3.9 Case B.00 - S₂D Scenario, 35% Zirconium Oxidation

While most of the degraded-core scenarios we consider assume 75% zirconium oxidation, case B.00 assumes 35% zirconium oxidation. Thus, cases A.00 and B.00 represent a limited parametric treatment of the effect of the amount of oxidation on the containment pressure-temperature response. The dome pressure response for case B.00 is shown in Figure 4-25. The early response is similar to that for case A.00, as the blowdown phase is the same. The large spike in Figure 4-25 at about 6300 s represents a burn that is predicted to occur in the dome. Unlike all of the other cases to be presented, no burns are predicted to occur in the upper plenum because the hydrogen is coming into containment more slowly in this case, and by the time combustion begins, much of the ice has melted (see Figure 4-26). This results in higher steam concentrations and lower hydrogen concentrations in the upper plenum, which prevent ignition there (see Figure 4-27). The excess steam is removed by the sprays, so that the hydrogen concentration is higher in the dome, and combustion begins there rather than in the upper plenum.

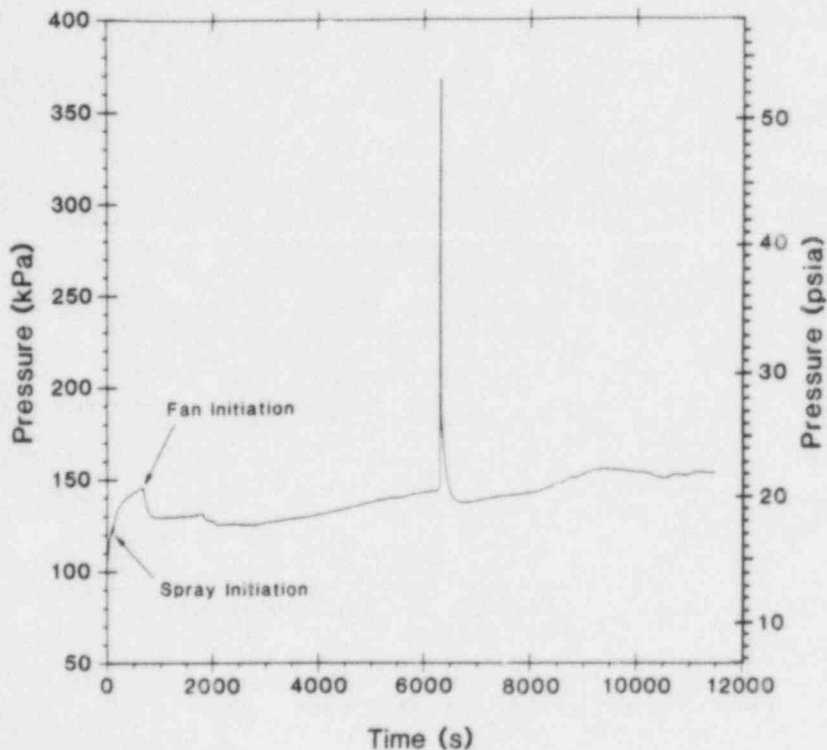


Figure 4-25. Pressure Response in Dome for Case B.00

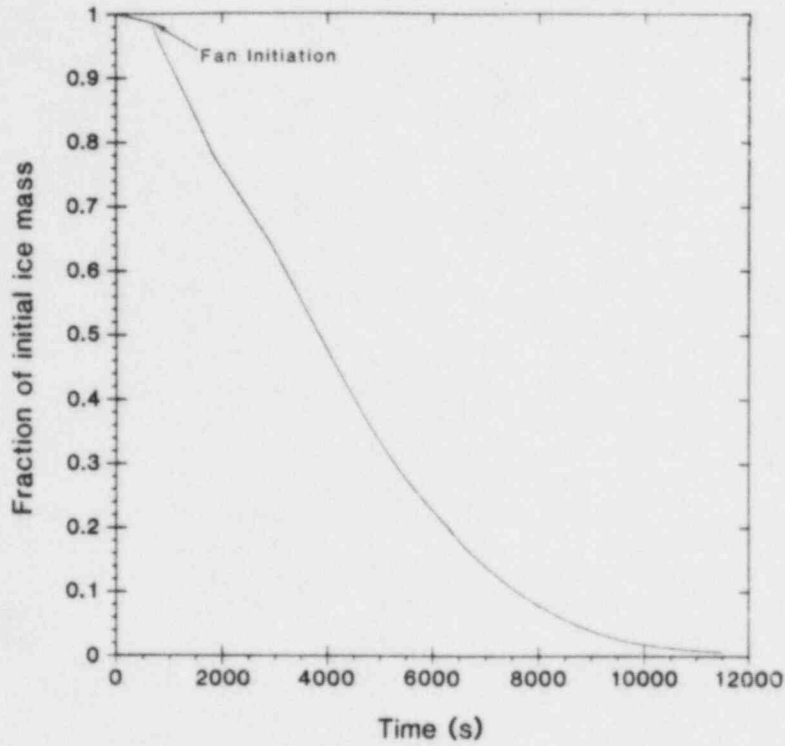


Figure 4-26. Ice Inventory History for Case B.00

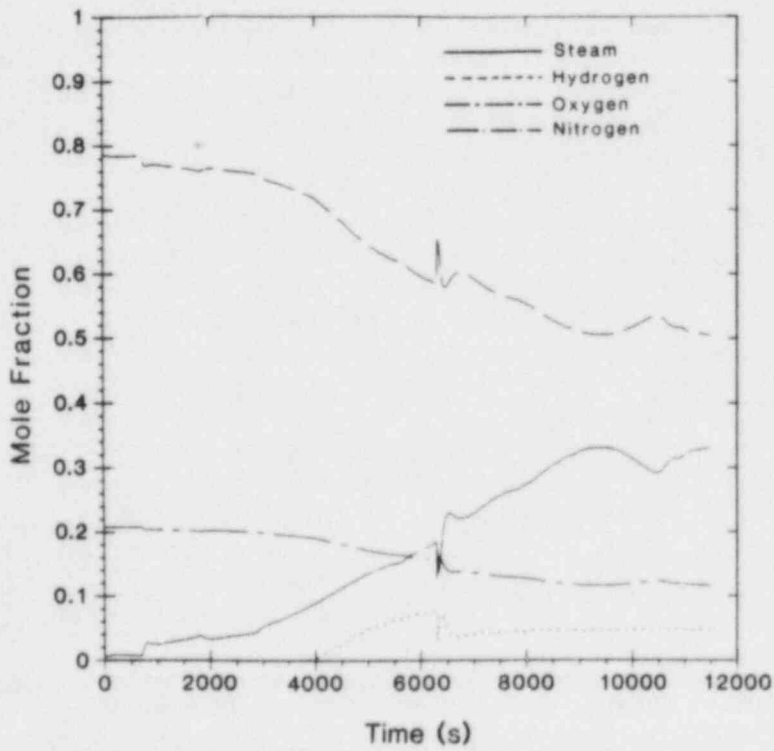


Figure 4-27. Gas Composition in Upper Plenum for Case B.00

There is an important point to be made from this case. Surprisingly, the peak pressure is not significantly reduced from Case A.00, as might be expected. This raises questions regarding the conservatism in the assumption of 75% zirconium oxidation for degraded core scenarios. Closer examination of the cases reveals that the controlling factor is whether or not large dome burns occur. If large dome burns occur, high pressure rises result, and it doesn't matter much whether one or several burns occur, as the pressure rises are not cumulative. There is threshold quantity of hydrogen above which large dome burns will occur. Hydrogen releases below this threshold would preclude dome burns and thus, produce proportionately reduced pressure-temperature containment loads. However, large dome burns are possible for all cases where the threshold quantity of hydrogen is exceeded, and none of these cases is a priori more conservative than any other case. The above arguments are based on the assumption that the igniters are operating and that ignition is guaranteed at some hydrogen concentration. If the igniters are not operating, then the pressure rise will be directly proportional to the amount of hydrogen released, assuming that ignition occurs after the release.

4.3.10 "C" Cases - CLASIX and COMPARE Comparisons

Previous analyses of the Sequoyah plant have been performed by TVA using the CLASIX code,[9] and by Los Alamos National Laboratory (LANL) using the COMPARE code.[7] These codes are lumped-volume containment codes similar in concept to HECTR. Cases C.00 to C.02 were run to examine the behavior of the codes given similar input assumptions. The "C" cases represent S₂D accident scenarios, with source terms that were taken from Reference 9.

Case C.00 uses these source terms from Reference 9 and the same input assumptions as case A.00. The pressure response in the dome for case C.00 is shown in Figure 4-28. The pressure response for case A.00 is reproduced here as Figure 4-29 for comparison. As can be seen by comparing the two figures, the results are quite different for the two cases. In case C.00 most of the burns occur in the upper plenum, with several of the burns propagating downward into the ice compartments (6-9) and some of the burns propagating upward into lean hydrogen mixtures in the dome. Also, one burn is initiated in the lower compartment.

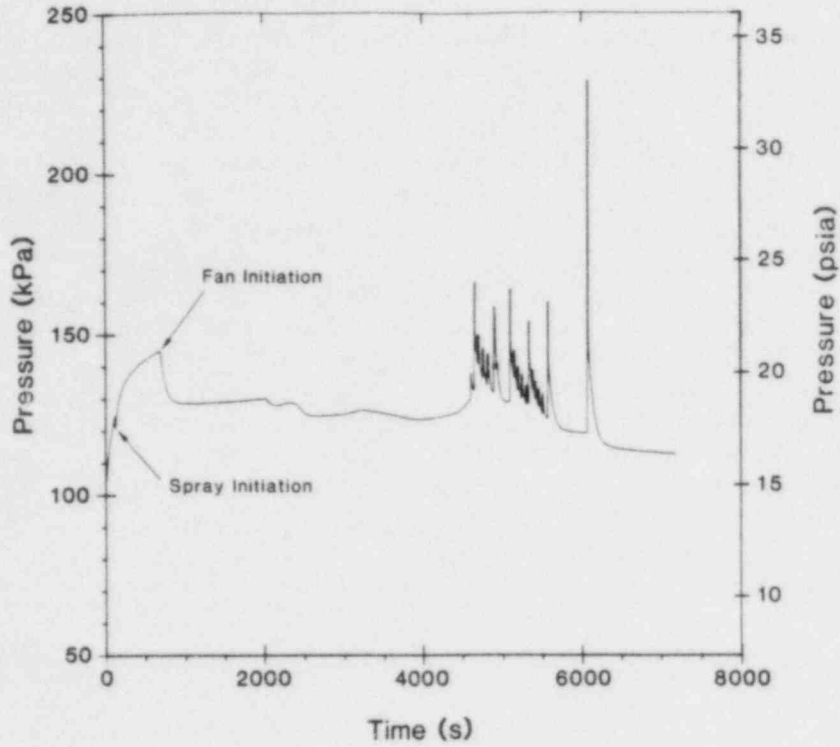


Figure 4-28. Pressure Response in Dome for Case C.00

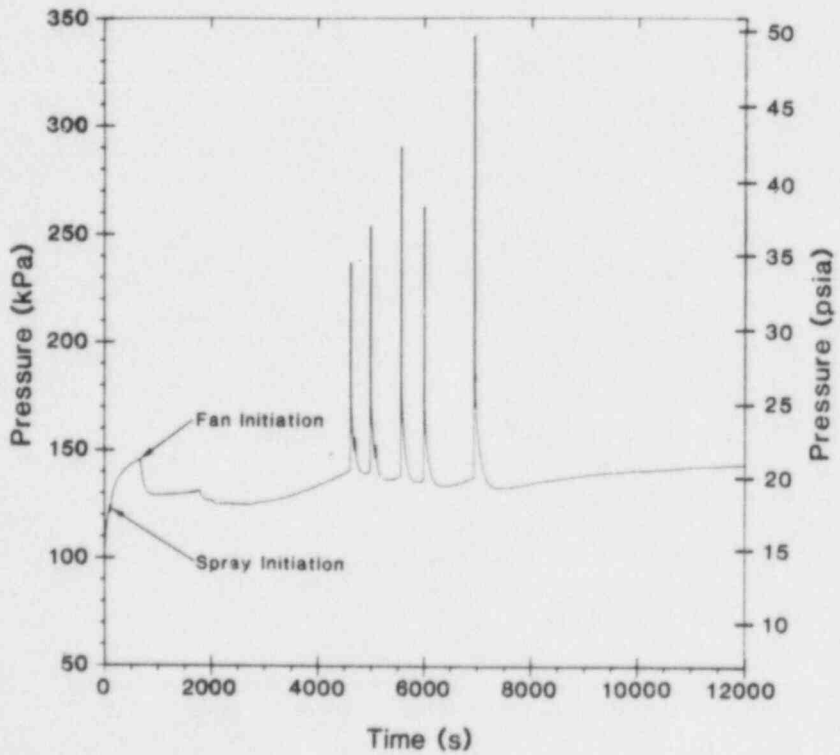


Figure 4-29. Pressure Response in Dome for Case A.00

From source-term information presented in Chapter 3, we can make some observations. First, the total amount of hydrogen injected is virtually the same for the two cases, with some differences in the timing of the release (it is released more quickly in case C.00). Second, much more water is released in case A.00 than in case C.00. The ratio of hydrogen to water injection rates has been plotted in Figures 4-30 and 4-31 for cases C.00 and A.00, respectively. A comparison of the two figures reveals that the ratio of hydrogen to water injection rates in case C.00 is approximately twice that of case A.00. The greater amounts of steam present in case A.00 tend to impede combustion in the lower compartments and also allow more hydrogen to be transported into the dome before combustion begins in the upper plenum. These results illustrate the sensitivity of the results to differences in the source terms.

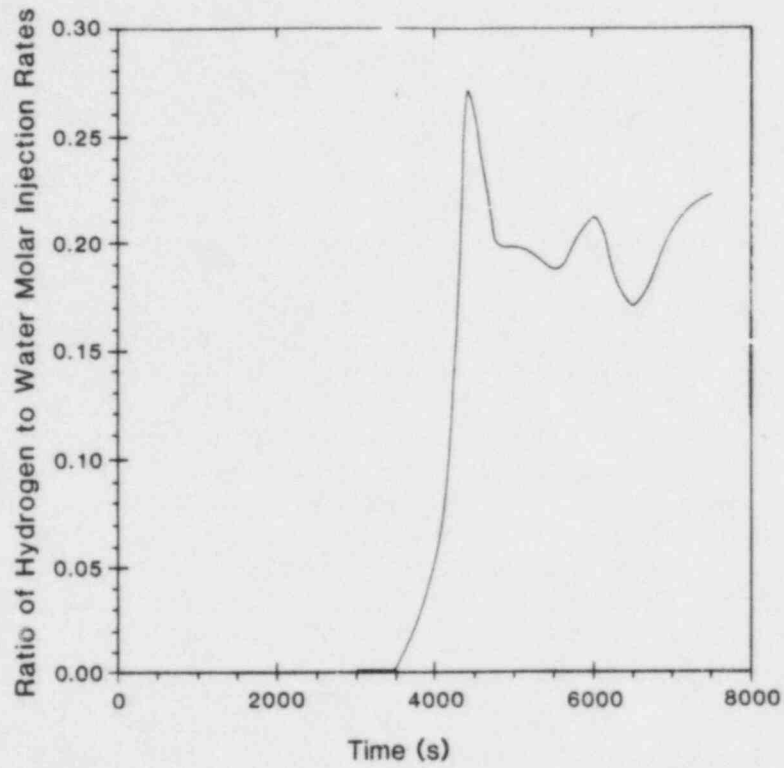


Figure 4-30. Hydrogen-to-Water Injection Ratio for Case C.00

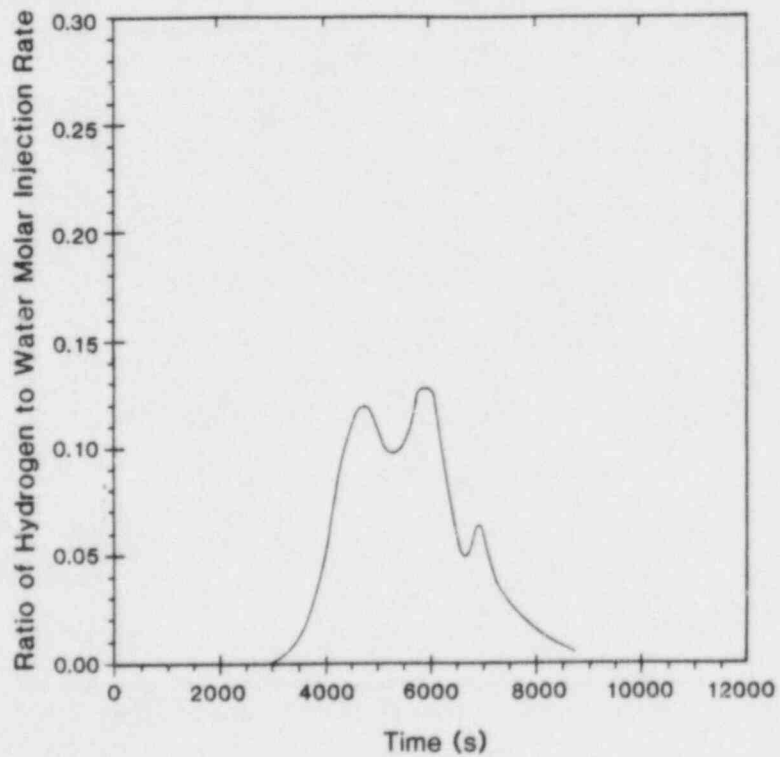


Figure 4-31. Hydrogen-to-Water Injection Ratio for Case A.00

Case C.01 was performed as a direct comparison to the CLASIX base case from Reference 9. All possible input values such as spray temperature, flame speed, and combustion completeness were set to the CLASIX values. Ignition and propagation limits were set to 8%, and burning in the ice compartments (6-9) was precluded. Results of the HECTR and CLASIX code comparison are shown in Table 4-2. The dome pressure response is shown in Figure 4-32. The burn sequences are similar, with HECTR predicting three more burns in the lower compartment than CLASIX. This difference may be due to the fact that HECTR accounts for changes in the lower compartment gas volume as the sump fills up. As the lower compartment gas volume decreases, it takes less hydrogen to reach a concentration of 8%; hence, more burns occur. The peak gas temperatures predicted are comparable in magnitude, with differences due to different surface areas and different heat transfer models. Some differences are predicted in the peak pressures, with CLASIX producing the higher values. During burns, CLASIX predicts fairly large pressure differentials between the compartments (with the higher pressure in the lower compartment), which we would not expect to occur for this case, given the large flow areas connecting the compartments. HECTR predicts rapid pressure equilibration, and only small pressure differences between compartments. As shown later, COMPARE also predicts rapid pressure equilibration. If pressure equilibration had occurred in the CLASIX case, one can see by volume-averaging the pressures that the results would have been very similar to the HECTR results.

In addition to the results presented in Table 4-2, the pressure response during the blowdown (preburn) phase of the accident was examined. The CLASIX and HECTR results agreed very well, generally to within 7 kPa (1 psi). Thus, we conclude that the agreement between the codes is reasonable for this accident scenario, and that the differences between the results presented in this report and those presented in Reference 6 are due largely to differences in input assumptions and not to differences in the codes. (Note that other scenarios may produce large pressure differentials between the dome and lower compartment if large burns occur in the dome and the ice-condenser doors block downward flow.)

Table 4-2
Code Comparison

Case	Code	Compartment Number	Number of Burns	Peak Temperature (K)	Peak Temperature (°F)	Peak Pressure (kPa)	Peak Pressure (psia)	Ice Remaining* (%)
C.01 [6]	CLASIX	1	0	346	163	173	25.1	
		2	30	933	1219	192	27.8	
		4	7	947	1245	230	33.4	
	HECTR	1	0	355	179	186	27.0	
		2	30	1006	1351	186	27.0	
		4	10	898	1156	188	27.3	
C.02 [14]	COMPARE	1	0	361	190	184	26.7	13
		2	35	1008	1354	185	26.8	
		3	0	772	930	184	26.7	
		4	6	951	1252	183	26.5	
		5	0	374	213	182	26.4	
		6	0	648	705	184	26.7	
		7	0	555	539	183	26.5	
		8	10	975	1295	183	26.5	
		9	14	949	1248	186	27.0	
	HECTR	1	0	345	161	174	25.2	
		2	19	881	1126	174	25.2	
		3	0	695	791	175	25.4	
		4	6	848	1060	175	25.4	
		5	0	353	175	175	25.4	
6		2	752	894	175	25.4		
7		7	807	993	175	25.4		
8		12	796	973	175	25.4		
9		17	732	858	175	25.4		

*At end of sequence calculation (see Table 4-2).

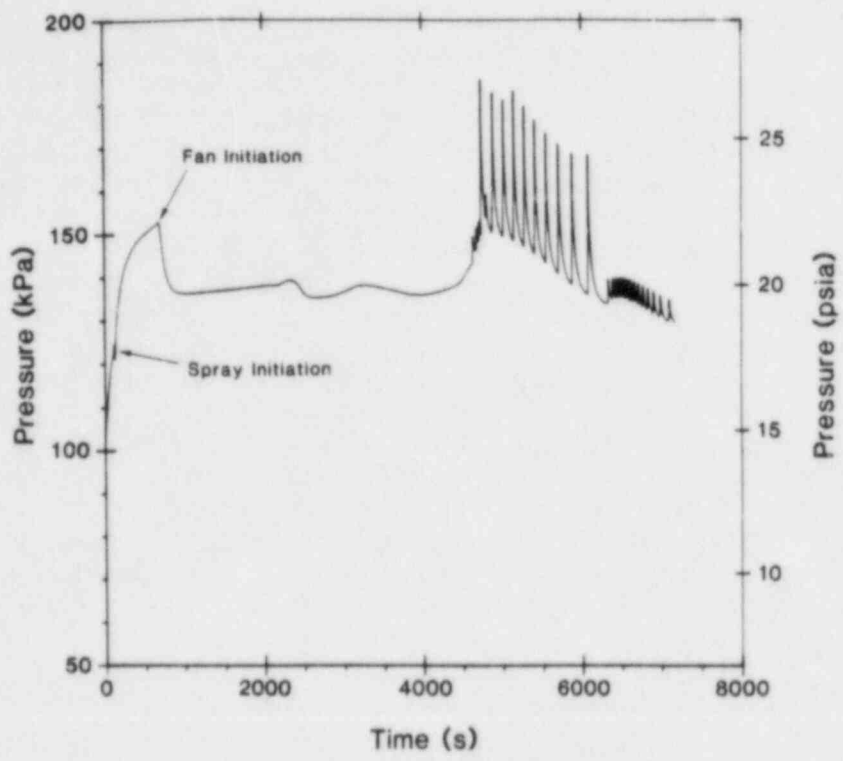


Figure 4-32. Pressure Response in Dome for Case C.01

Case C.02 was performed as a direct comparison to the COMPARE base case from Reference 15. All input values were set to the COMPARE values where possible. In this case propagation of burns into the ice compartments (6-9) was allowed, in order to be consistent with COMPARE. The dome pressure response is presented in Figure 4-33, and the results of the code comparison are shown in Table 4-2. Both codes predict six burns in the lower compartment and similar peak pressures. HECTR predicts more burning in the ice compartments (6-9) and less in the upper plenum than COMPARE, probably due to differences in the ice-condenser models. As shown in Table 4-3, for the two cases considered, HECTR predicts more ice melting than CLASIX and less ice melting than COMPARE. The differences are probably due to differences in the heat transfer and condensation models in the ice condenser, rather than differences in the burn sequences. Based on the results of cases C.01 and C.02, we conclude that the codes will behave similarly, given similar input and modeling assumptions (at least for the type of ice-condenser modeling addressed here). One reason that the codes behave similarly for these cases is that the gas transport is characterized by forced (fan-driven and break-flow-driven) convection through series-connected compartments. For cases where natural convection is important and parallel flow paths are present, differences in the intercompartment flow equations (e.g., CLASIX does not include buoyancy terms) will probably cause significant differences in the results.

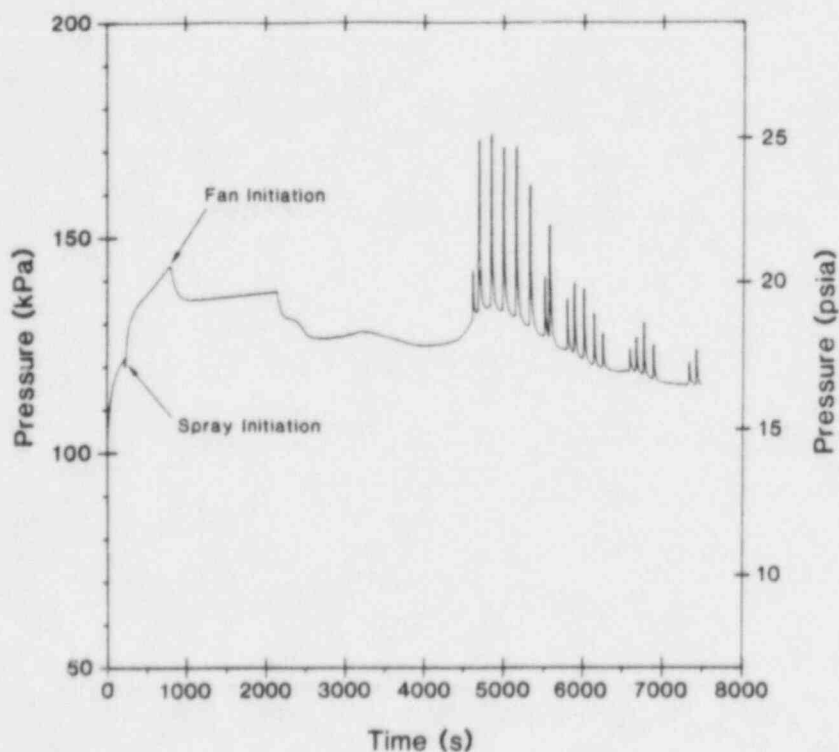


Figure 4-33. Pressure Response in the Dome for Case C.02

4.3.11 "F", "G", and "H" Cases - S₁D and S₁H Scenarios

Case F.00 represents an S₁D scenario. As shown in Figure 4-34, higher baseline pressures are predicted than in case A.00, due to the much higher break-flow rate. Once the hydrogen begins entering the containment, it does so at a very high rate (see Chapter 3) and causes combustion to occur both in the upper plenum and the lower compartment, with some propagation to other compartments. After several consecutive burns in the upper plenum, the atmosphere becomes inert because of oxygen depletion, but soon thereafter a large burn occurs in the dome which pushes oxygen back into the upper plenum and causes a burn to occur there also. Note that, even with these high hydrogen release rates and corresponding closely spaced burns, the gas pressure rises are not predicted to be very cumulative in nature.

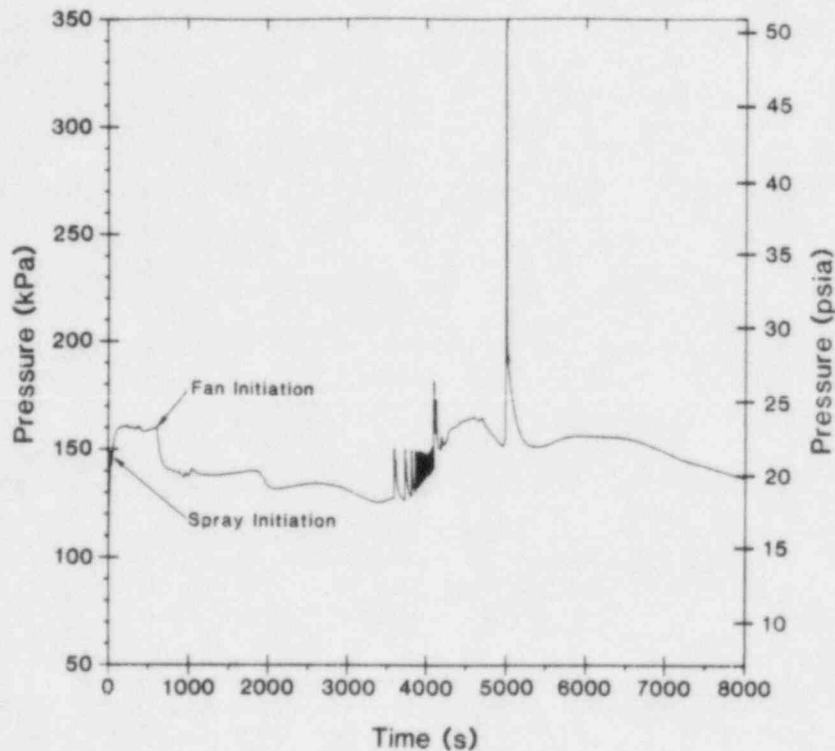


Figure 4-34. Pressure Response in the Dome for Case F.00

Case F.01 examines the effect of partial oxygen depletion. As with case A.14, the initial oxygen concentration was set to 14%. For this case, as shown in Figure 4-35, partial oxygen depletion appears to be detrimental, with higher pressures predicted than for case F.00. The reason for this result is that with less oxygen present, the tendency for the upper plenum to become inert is enhanced, leading to more hydrogen being transported to the dome and allowing more hydrogen to be present in the upper plenum when the burn begins in the dome and pushes oxygen back into the upper plenum. Figures 4-36 and 4-37 show the hydrogen concentrations in the upper plenum for cases F.00 and F.01.

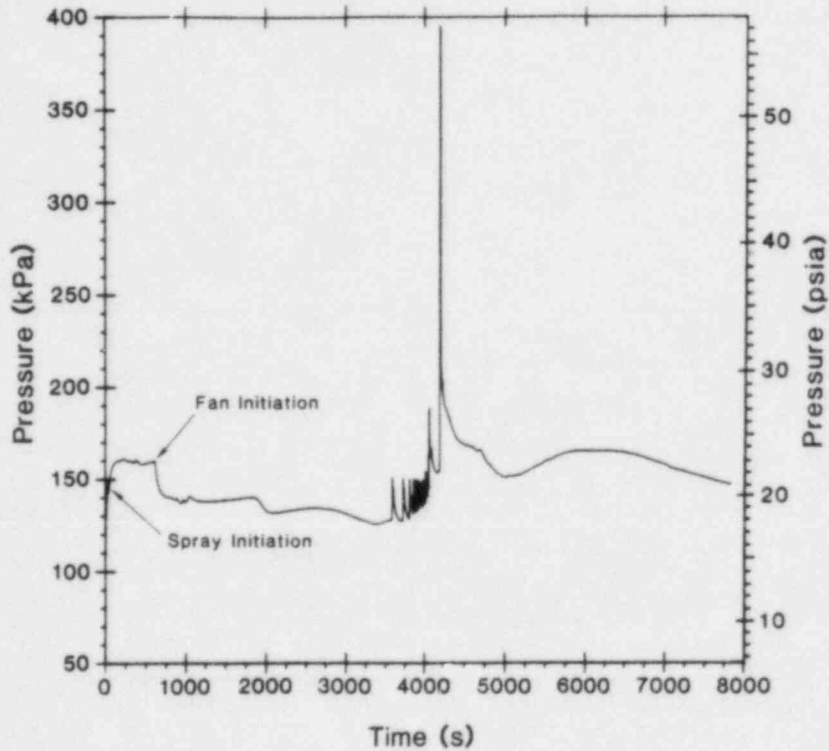


Figure 4-35. Pressure Response in the Dome for Case F.01

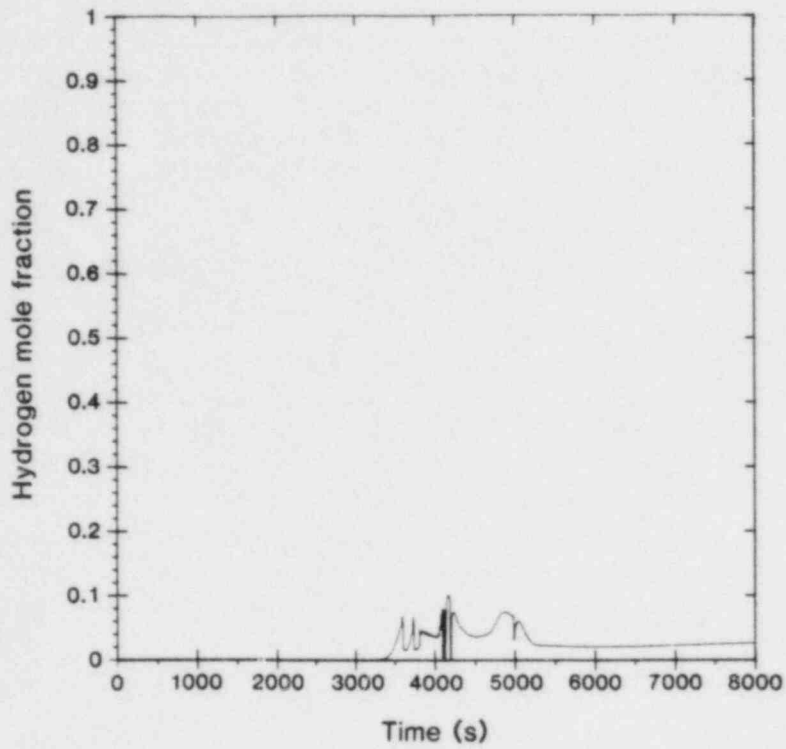


Figure 4-36. Upper-Plenum Hydrogen Concentration for Case F.00

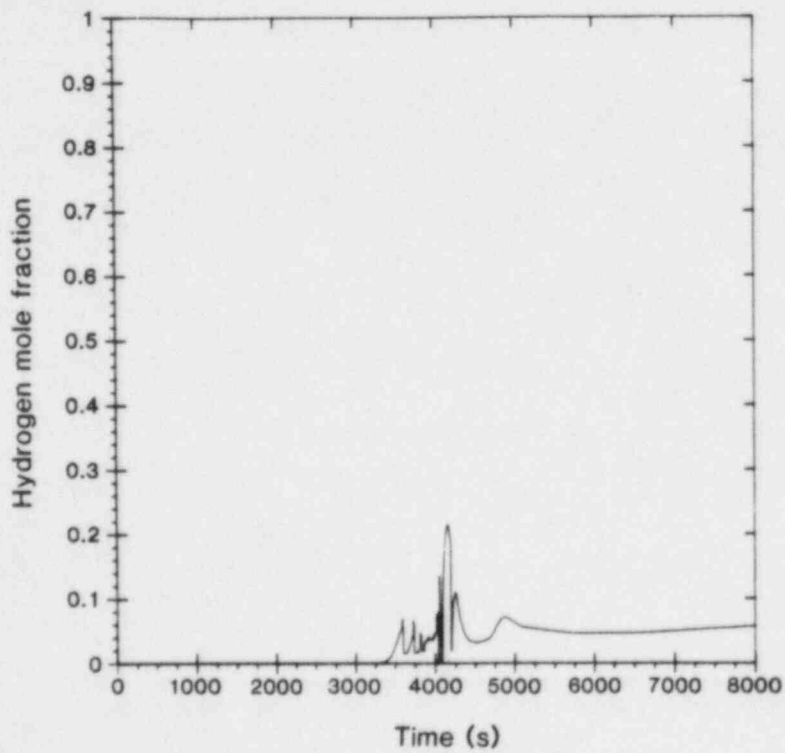


Figure 4-37. Upper-Plenum Hydrogen Concentration for Case F.01

Case G.00 represents an S₁D accident scenario with 37% zirconium oxidation, as opposed to 75% zirconium oxidation for case F.00. The dome pressure response for this case is shown in Figure 4-38. The low peak pressure for this case (161.7 kPa or 23.5 psia) occurs during the blowdown phase and not during the hydrogen combustion that takes place later. Because of the low steam-release rates at the time of hydrogen injection, most of the burns begin in the lower compartment and propagate into the lower plenum (3) and some of the ice compartments (6-9). This response is initially similar to that for case F.00. However, in case G.00 the hydrogen injection is terminated before sufficient hydrogen accumulates in the dome to allow a burn to occur there. Thus, the large pressure spike of case F.00 is not predicted in case G.00.

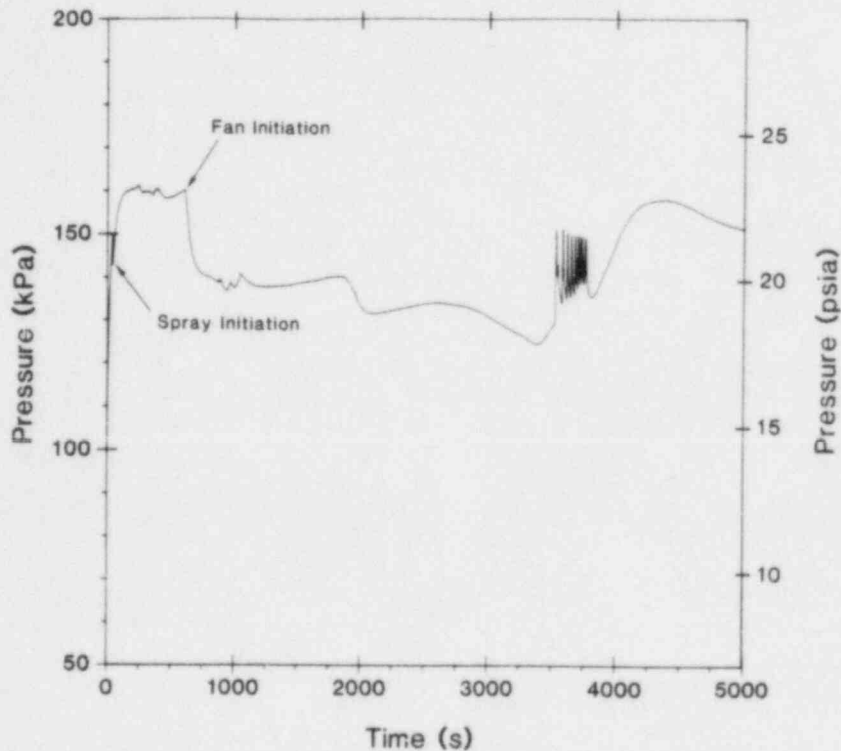


Figure 4-38. Pressure Response in Dome for Case G.00

Case H.00 represents an S₁H accident scenario. The dome pressure response for this case is shown in Figure 4-39. In this case most of the burns are initiated in the upper plenum and the lower compartment, with only one burn propagating into the dome, and then into a lean mixture. Very little tendency for inerting in the upper plenum is predicted, and thus, the pressure rises are small.

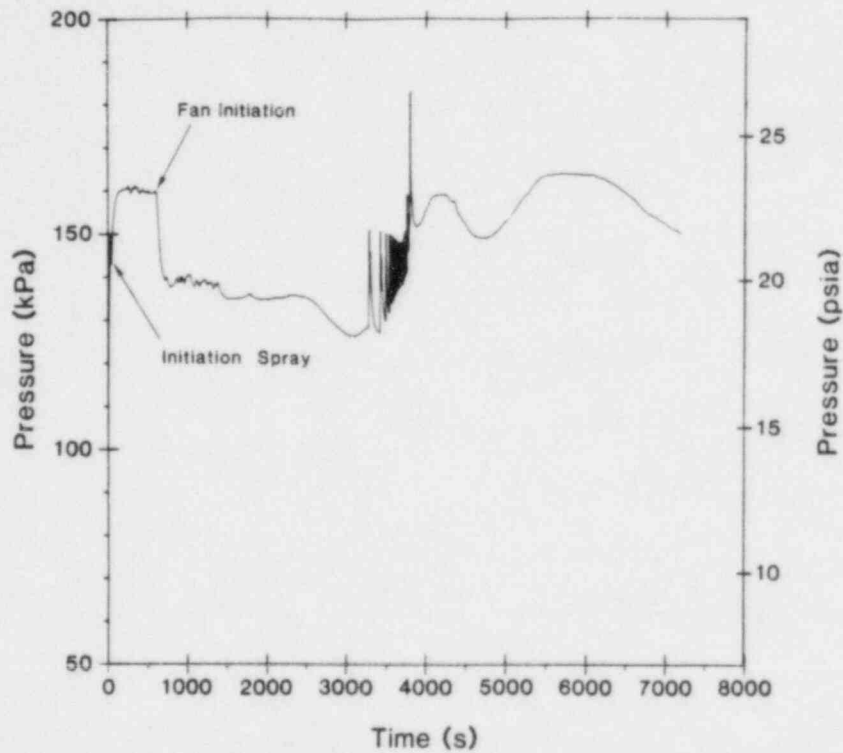


Figure 4-39. Pressure Response in Dome for Case H.00

Case H.01, with the dome pressure rise shown in Figure 4-40, is the same as case H.00, except for the assumption of partial oxygen depletion. As in cases F.00 and F.01, there is a tendency for the upper plenum to inert, thus leading to a large burn in the dome.

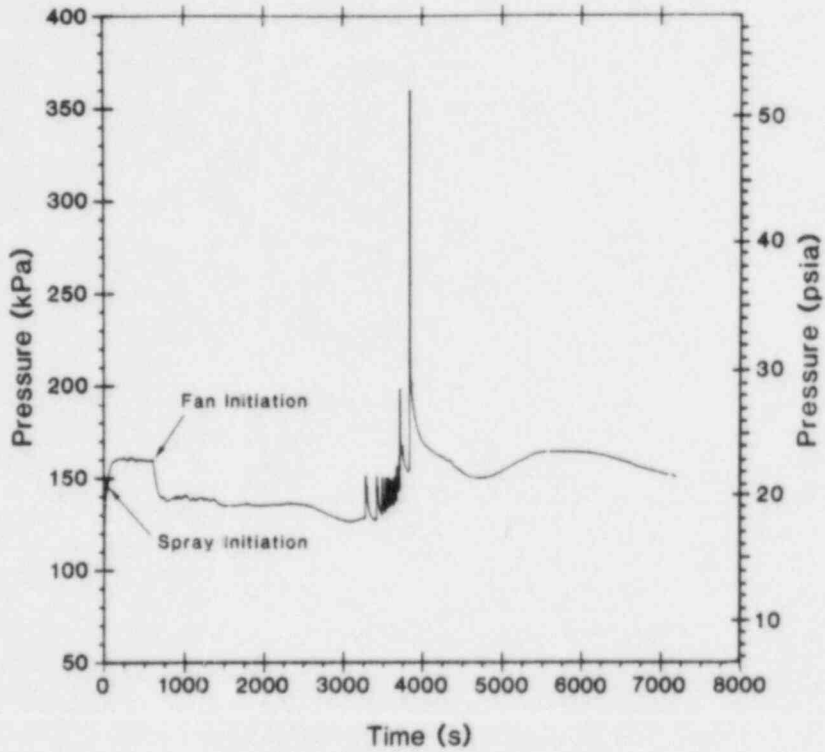


Figure 4-40. Pressure Response in Dome for Case H.01

4.3.12 "I" Cases - S₁HF Scenarios

The "I" cases represent S₁HF accidents with the sprays failing in the recirculation mode, approximately 1800 s into the accident. As shown by the dome pressure response in Figure 4-41, case I.00 initially is similar to case H.00. However, later on in the accident, with no sprays and most of the ice gone, the baseline pressure begins increasing due to steam buildup much in the same manner as in cases A.03 to A.05.

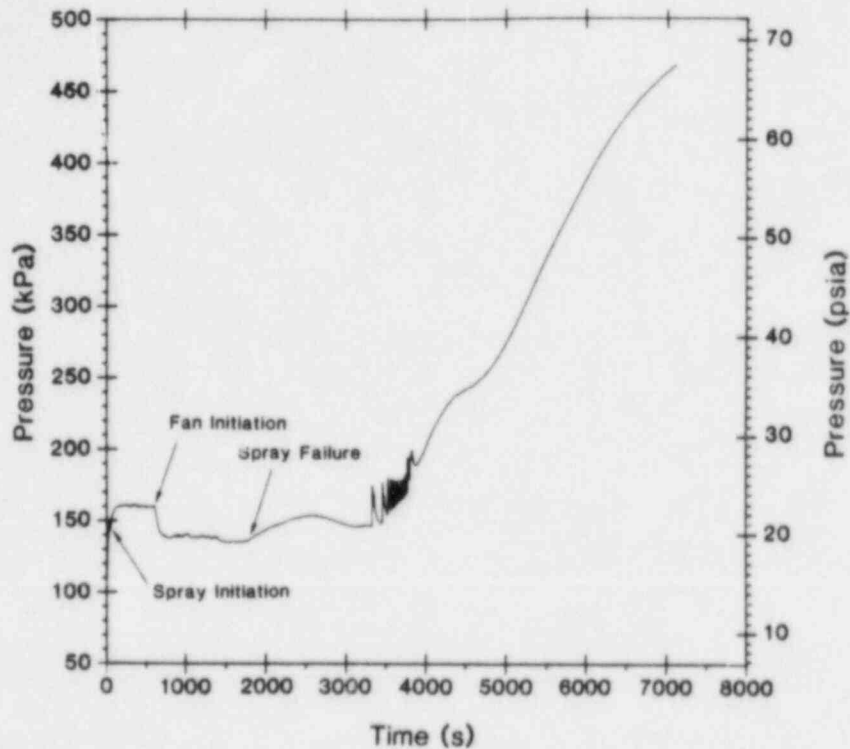


Figure 4-41. Pressure Response in Dome for Case I.00

Cases I.01 and I.02, respectively, were run to examine the effects of decreasing and increasing the ice-condenser drain temperature by 20 K (36°F). The dome pressure responses for cases I.01 and I.02 are shown in Figures 4-42 and 4-43, respectively. Case I.01 predicts a higher pressure rise than case I.02, because less heat is transferred to the water falling through the lower plenum. However, the general behavior of the results is unchanged.

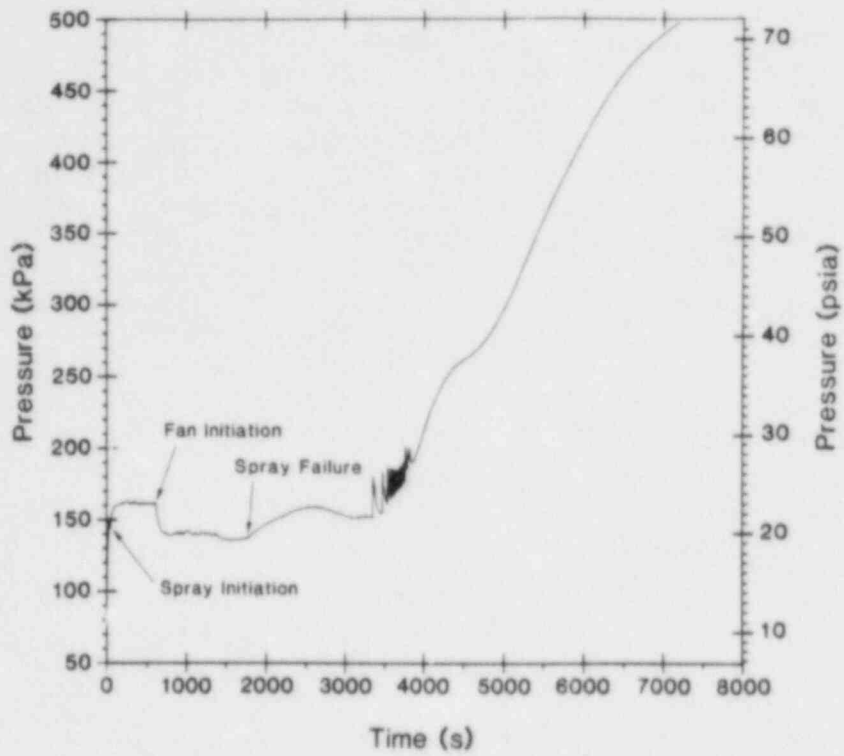


Figure 4-42. Pressure Response in Dome for Case 1.01

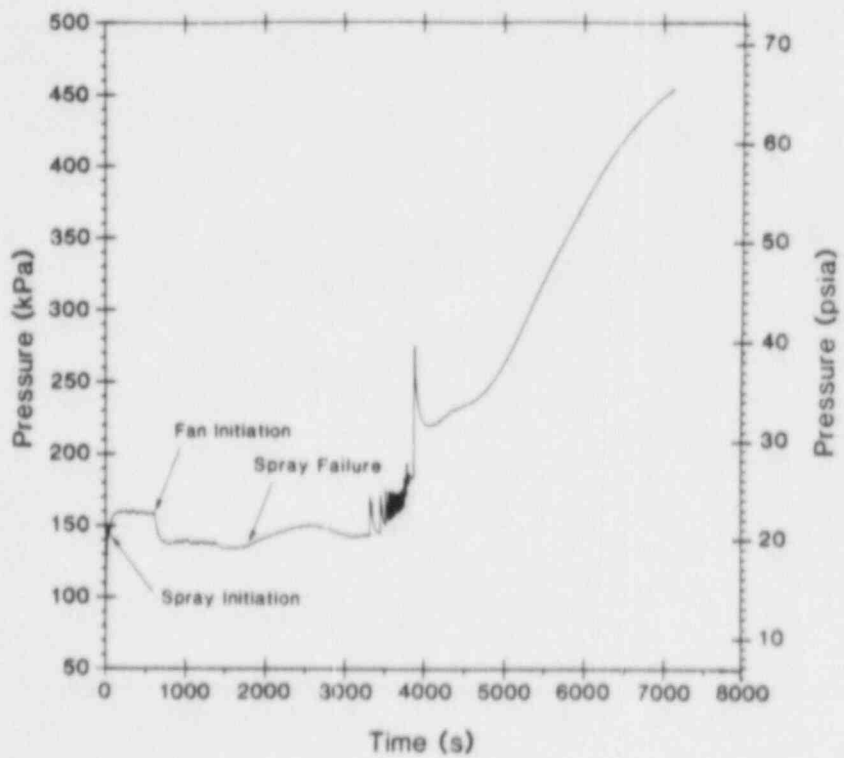


Figure 4-43. Pressure Response in Dome for Case 1.02

Cases I.03 and I.04, were run to examine the respective effects of decreasing and increasing the ice-condenser heat transfer coefficient by a factor of five. The dome pressure responses for cases I.03 and I.04 are shown in Figures 4-44 and 4-45, respectively. Case I.03 initially predicts higher pressures than case I.04, because less steam is removed by the ice condenser in case I.03. These higher baseline pressures produce substantially higher burn pressures. However, at late times the pressure is lower in case I.03, because some ice still remains, while in case I.04 the ice has all melted. The differences in the amount of ice melted are illustrated in Figures 4-46 through 4-48. With the above considerations in mind, it is not clear which of these cases would be considered to be "conservative".

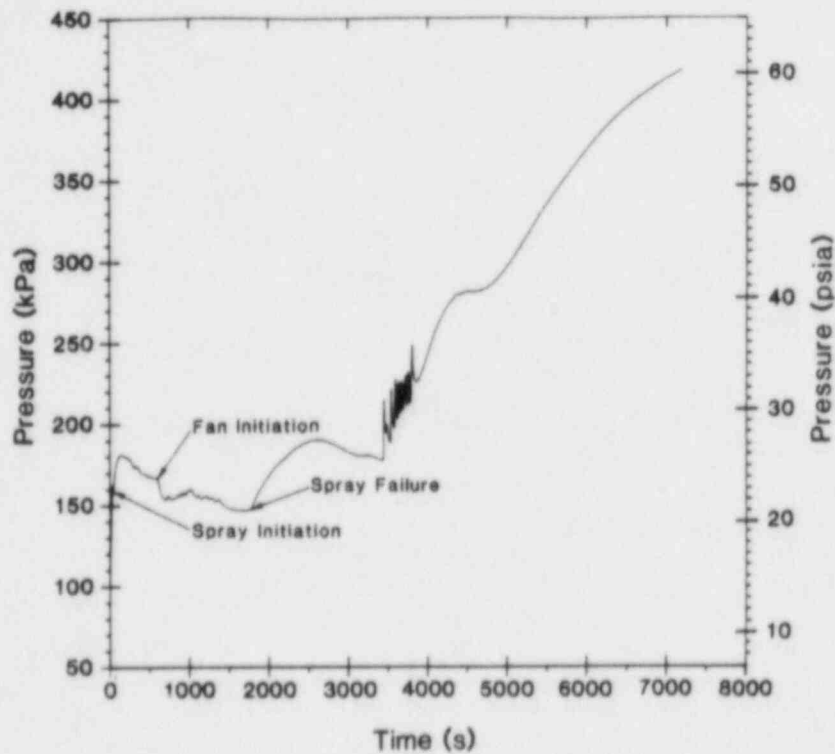


Figure 4-44. Pressure Response in Dome for Case I.03

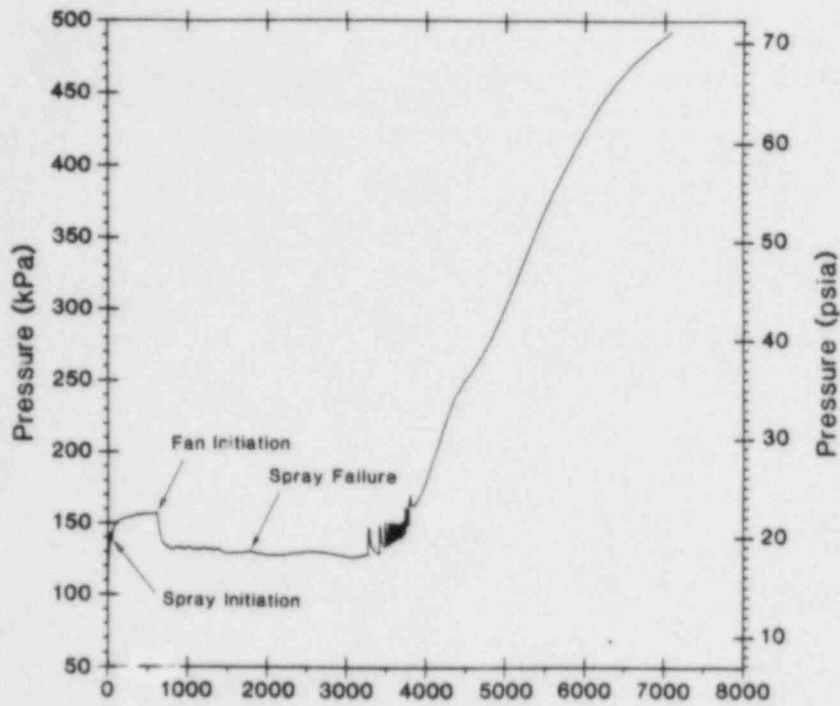


Figure 4-45. Pressure Response in Dome for Case I.04

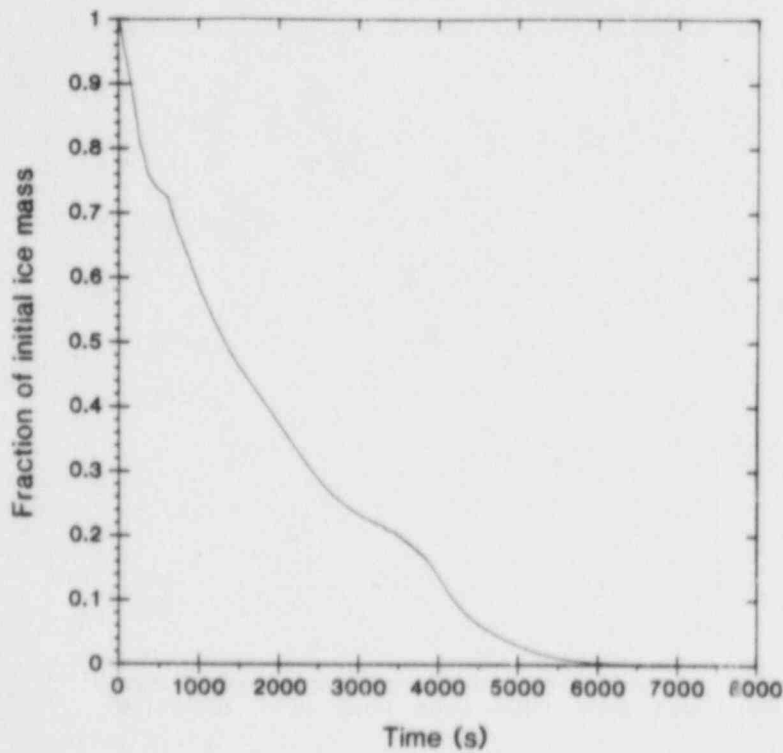


Figure 4-46. Ice Inventory History for Case I.00

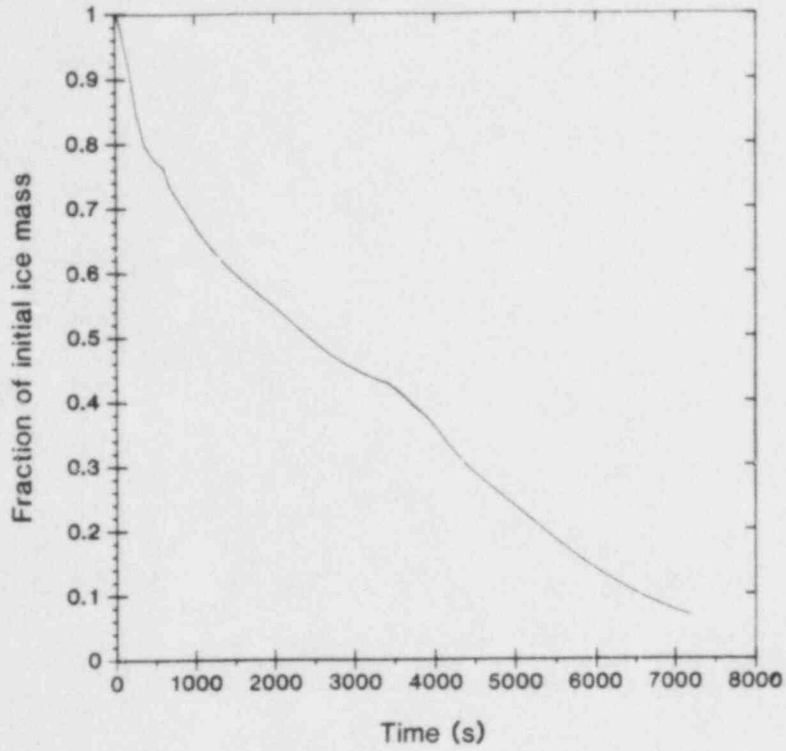


Figure 4-47. Ice Inventory History for Case I.03

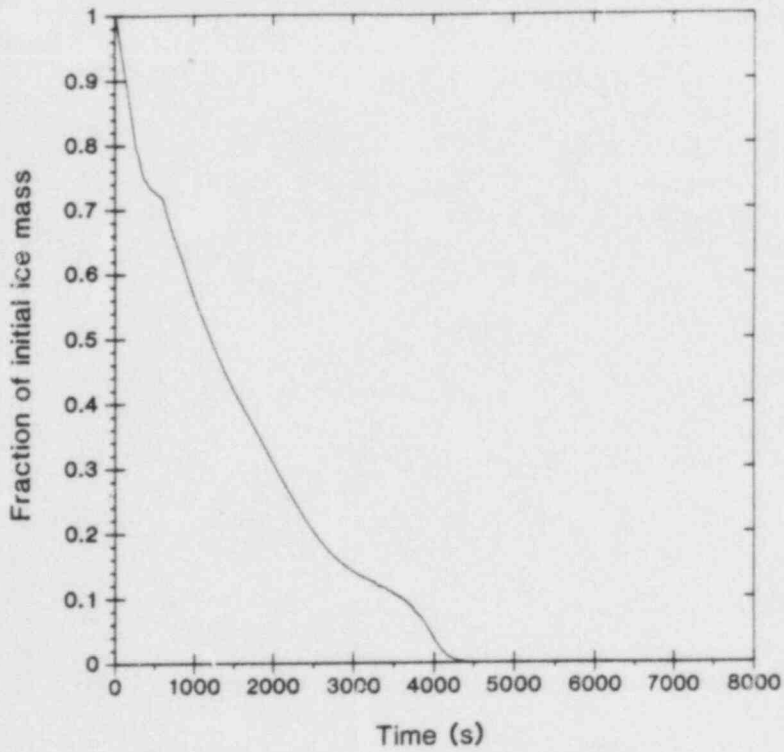


Figure 4-48. Ice Inventory History for Case I.04

Case I.05 was run to examine the effects of increasing the surface heat transfer coefficients by a factor of 5. The dome pressure response for this case is shown in Figure 4-49. Some pressure reduction compared to case I.00 is predicted at late times due to increased steam condensation rates. The only other major difference is that one burn was predicted that propagated into the dome. However, the basic results are unchanged.

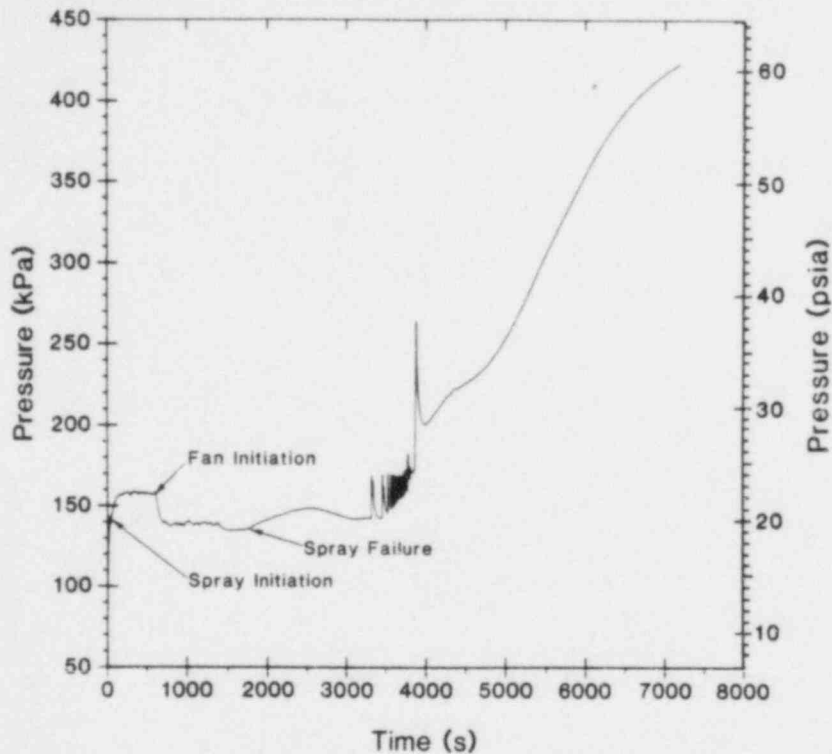


Figure 4-49. Pressure Response in Dome for Case I.05

Case I.06 shows the effects of partial oxygen depletion. The dome pressure response for this case is shown in Figure 4-50. While the final pressures are similar to those for case I.00, there are some differences earlier in the scenario while burns are occurring. As in the "F" and "H" cases, partial oxygen depletion tends to produce inerting in the upper plenum, resulting in a large burn in the dome at around 4000 s.

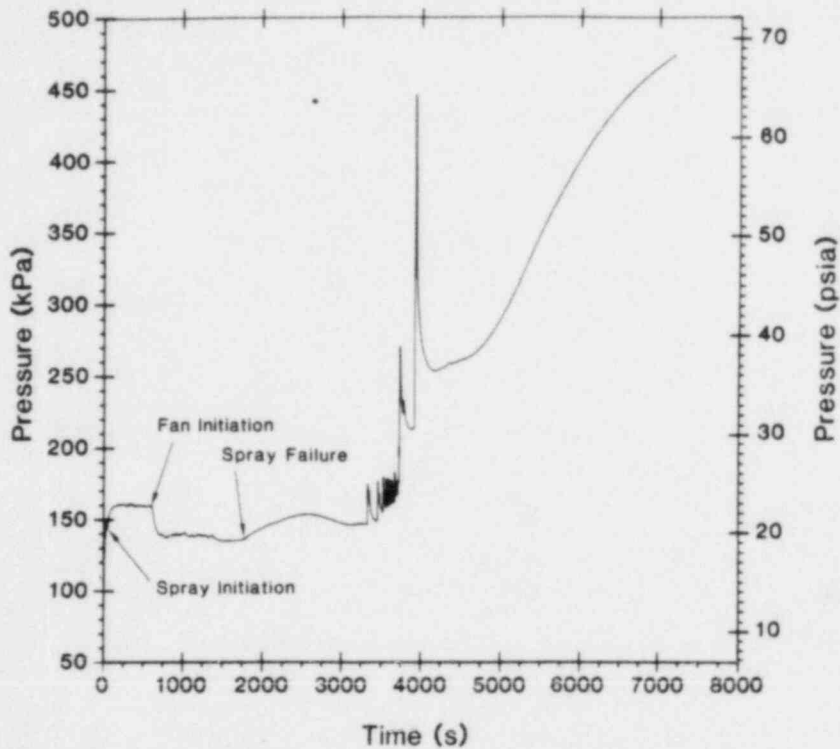


Figure 4-50. Pressure Response in Dome for Case I.06

THIS PAGE INTENTIONALLY BLANK

4.3.13 "L" and "M" Cases - TMLU and TMLB Scenarios

Cases L.00 and M.00 represent TMLU and TMLB scenarios, respectively. In case L.00 the fans and sprays work normally, while in case M.00 the fans and sprays are assumed to come on when power is recovered at about 8440 s into the accident. The dome pressure responses for the two cases are shown in Figures 4-51 and 4-52 and are very similar. As long as the sprays and fans are restored well before the hydrogen is released, there will tend to be little difference in these scenarios. Large numbers of burns occur in the upper plenum with some propagation upward into the dome in both cases, and propagation downward into the ice compartments (6-9) predicted in case M.00. Some burning is predicted in the lower compartments in both cases. Near the end of the accident, both cases also predict a relatively large burn, which begins in the dome. Cases L.01 and M.01 were run to examine the effects of partial oxygen depletion. For these cases there were only minor differences in the results.

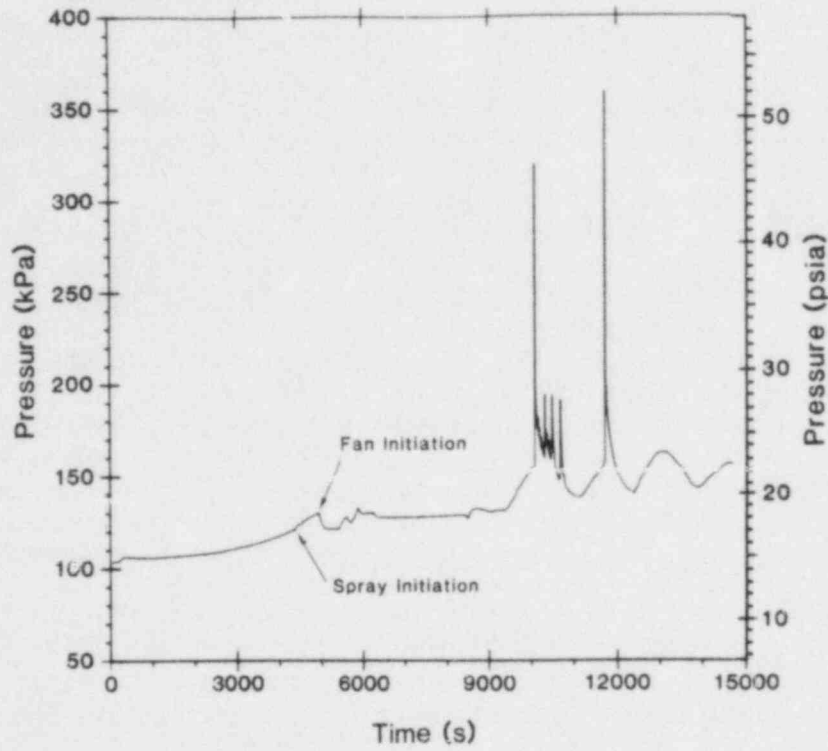


Figure 4-51. Pressure Response in Dome for Case L.00

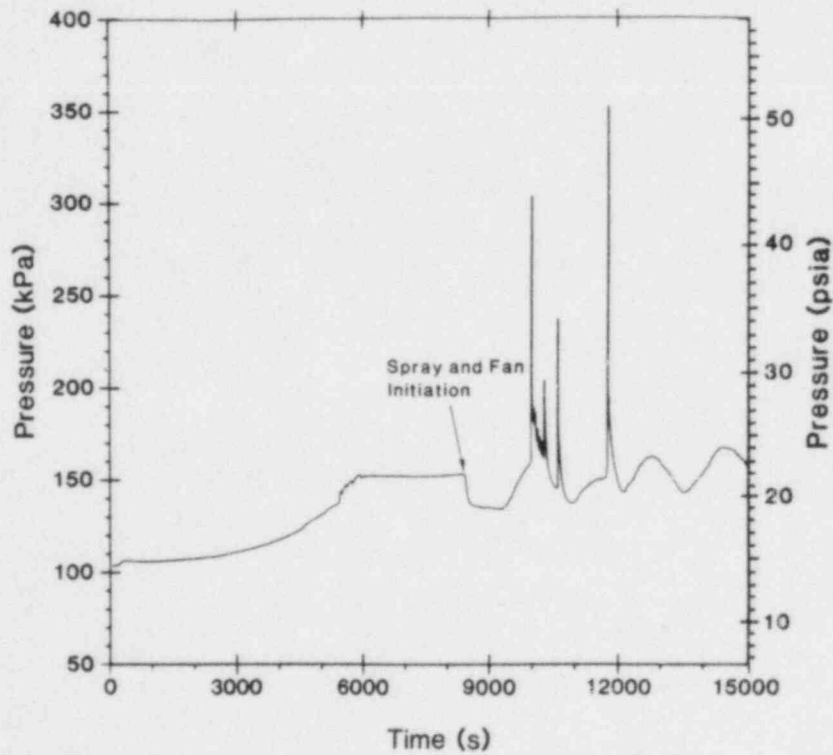


Figure 4-52. Pressure Response in Dome for Case M.00

4.4 Results for Core-Meltdown Accidents

The core-meltdown accident scenarios are designated in Table 2-1 by the letters D, E, J, K, N, O, and P. Results for these cases are summarized in Table 4-1. The source terms for these cases are described in Chapter 3. Each of these cases is discussed in more detail below.

4.4.1 "D" Cases - S₂D Core-Meltdown Scenarios, 100% Zirconium Oxidation

The "D" cases represent S₂D accident scenarios. These cases are different from the "A" cases, in that the accident proceeds through core meltdown and assumes 100% zirconium oxidation. The dome pressure response for case D.00 is shown in Figure 4-53. The sprays and fans are assumed operational, and the default combustion parameters are used. Vessel failure occurs just before the first large pressure spike at about 4100 s. Before vessel breach, relatively small quantities of hydrogen are released, resulting in burns that are initiated in the lower compartment and the upper plenum, with some propagation into lean mixtures in other compartments. These burns produce the small pressure spikes that appear between about 3800 and 4100 s.

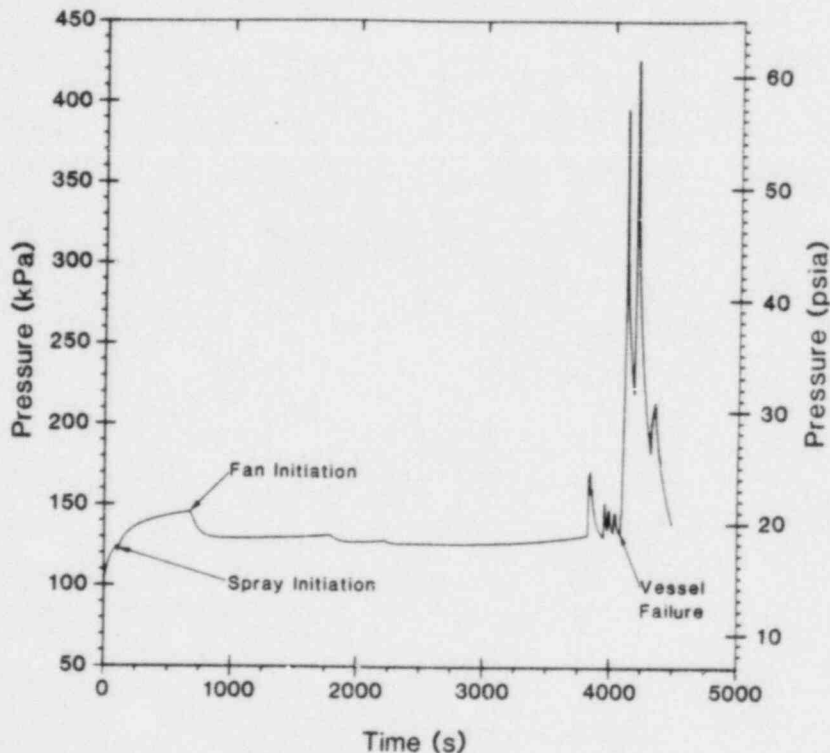


Figure 4-53. Pressure Response in Dome for Case D.00

After vessel breach, the results are quite different. Large quantities of steam and hydrogen are injected rapidly into the containment at the time of vessel breach (see Chapter 3). Coincidentally, a burn starts in the lower compartment just before vessel breach; however, this burn has little effect on the results, as this compartment becomes inert due to oxygen depletion soon afterward (the lower compartment also rapidly becomes steam inerted). The more important phenomena are the rapid injection of steam and hydrogen, raising the baseline pressure significantly, and the transport of the hydrogen into the upper plenum and dome. This hydrogen is ignited in the upper plenum, and the burn propagates into a leaner mixture in the dome. Because the baseline pressure is high and because hydrogen is being rapidly transported into the upper compartments during the early part of the burn, the pressure rise is relatively high. After this burn is completed, more hydrogen is transported upward from the steam and hydrogen rich lower compartments, resulting in a second large pressure spike when combustion occurs. This "multiple spike" behavior is typical of what HECTR predicts for the core-meltdown cases.

Case D.01 was run to examine the effects of containment venting. A 0.75 m^2 (8.1 ft^2) vent was set to open in the dome at a pressure of 273.7 kPa (39.7 psia) and to close when the pressure fell below 239.2 kPa (34.7 psia). All other parameters for case D.01 were the same as for case D.00. The dome pressure plot for case D.01 is shown in Figure 4-54. The vent opens during the two large burns, producing some reduction in pressure, particularly for the second large burn. The change in the second large burn is due to the fact that the vent alters the gas transport, and thus the concentrations are different when the second burn begins. Also, some hydrogen escaped to the atmosphere during the venting process. Vents of this size would have some positive benefits, but they would not completely mitigate the effects of combustion.

Case D.02 shows the effects of partial oxygen depletion. The dome pressure plot is presented in Figure 4-55. As in cases D.00 and D.01, a large double peak is predicted following vessel breach. In case D.02, however, fewer total burns occur and, as shown in Figure 4-56, a significant amount of hydrogen remains unburned due to a lack of oxygen. Thus, the addition of more hydrogen or carbon monoxide due to core-concrete interactions or other sources would not result in additional burning unless a source of oxygen were available.

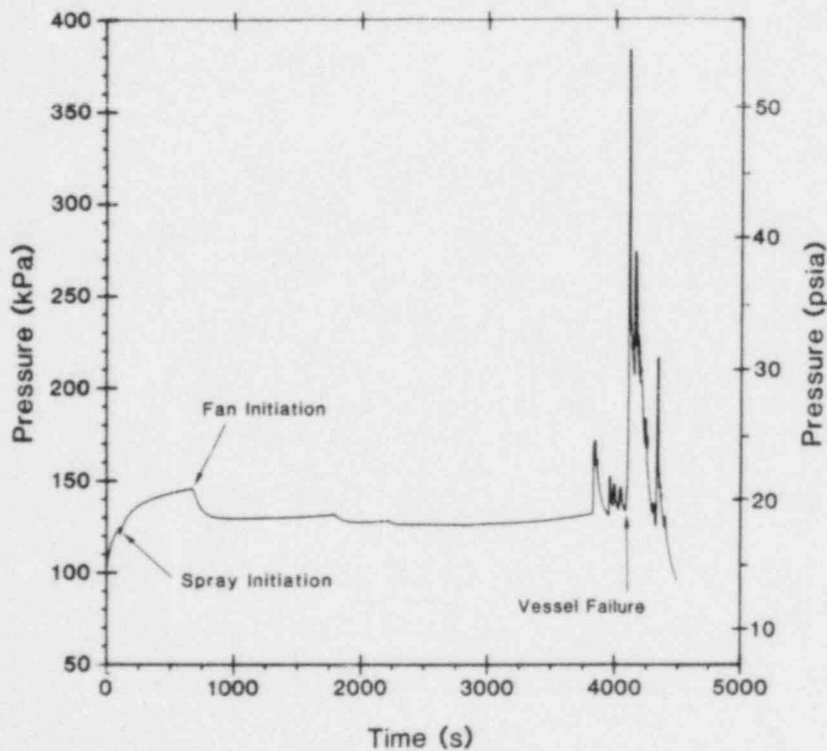


Figure 4-54. Pressure Response in Dome for Case D.01

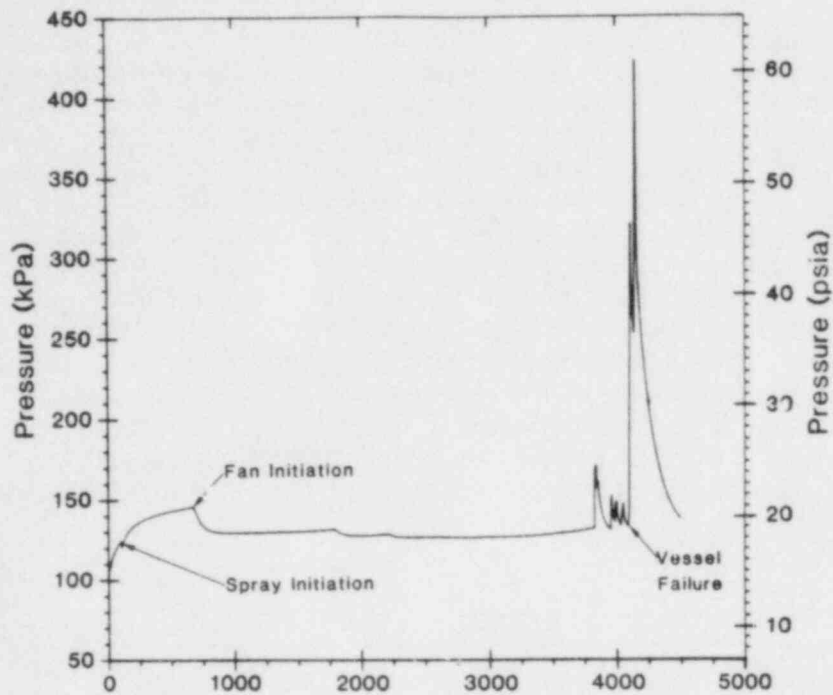


Figure 4-55. Pressure Response in Dome for Case D.02

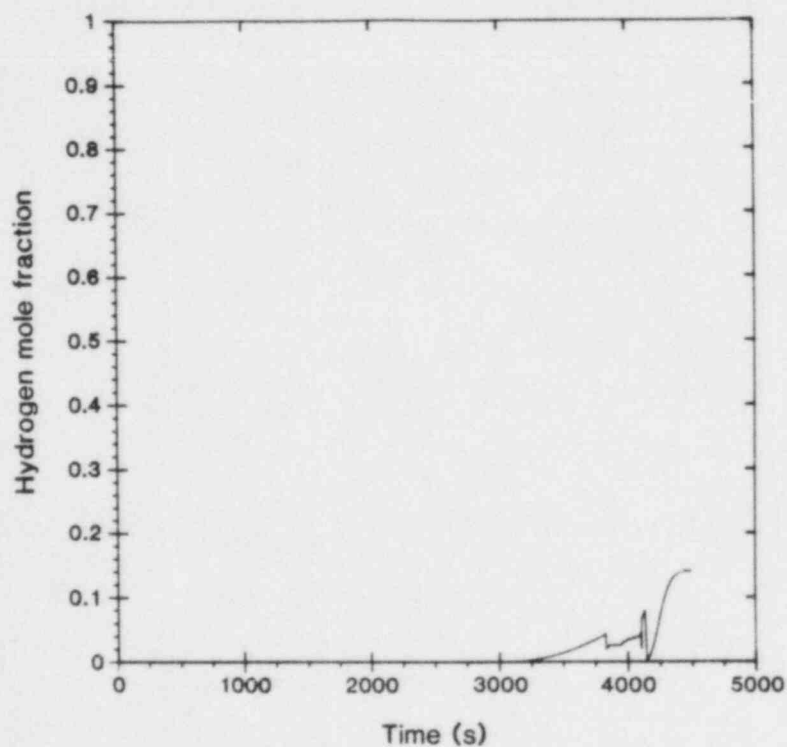


Figure 4-56. Dome Hydrogen Concentration for Case D.02

4.4.2 "E" Cases - S₂D Core-Meltdown Scenarios, 36% Zirconium Oxidation

The "E" cases also represent S₂D accident scenarios, but with minimal in-vessel zirconium oxidation occurring, as discussed in Chapter 3 (36% as opposed to 100% for the "D" cases). The pressure response for case E.00 is shown in Figure 4-57. As with case D.00, multiple peaks are predicted after vessel breach. However, the pressure rises are much smaller, and fewer total burns occur because less hydrogen is released. The pressure rises are smaller because the hydrogen and steam are injected at rates such that less hydrogen is present in the dome when combustion begins in the upper plenum (see Figures 3-37 through 3-40). In Case E.00 the burns propagate into much leaner mixtures in the dome than in case D.00, and the burns are proportionately smaller. Also, less hydrogen is introduced into the dome and upper plenum during the burn than in case D.00.

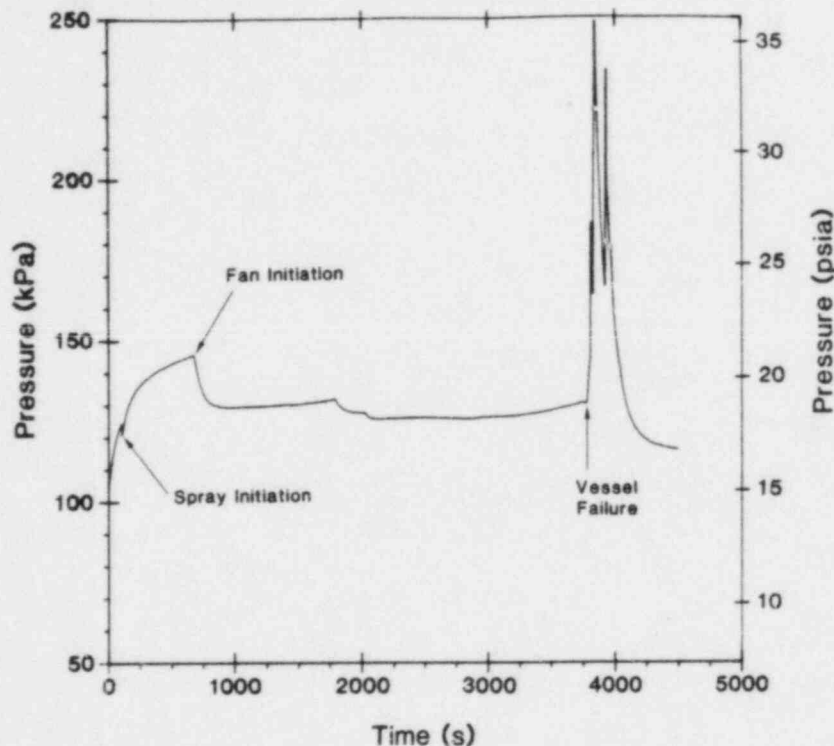


Figure 4-57. Pressure Response in Dome for Case E.00

No vent case was run for the "E" set of scenarios, because the vent opening pressure was not exceeded in case E.00. Case E.01 was run to examine the effects of partial oxygen depletion. As shown in Figure 4-58, multiple-peak behavior is predicted following vessel breach; however, the pressure rise for the final burn is higher than for case E.00. This is because HECTR predicts temporary inerting in the upper plenum due to oxygen depletion before the final burn. This allows much more hydrogen to be transported into the dome before the final burn begins, and thus produces a higher pressure rise.

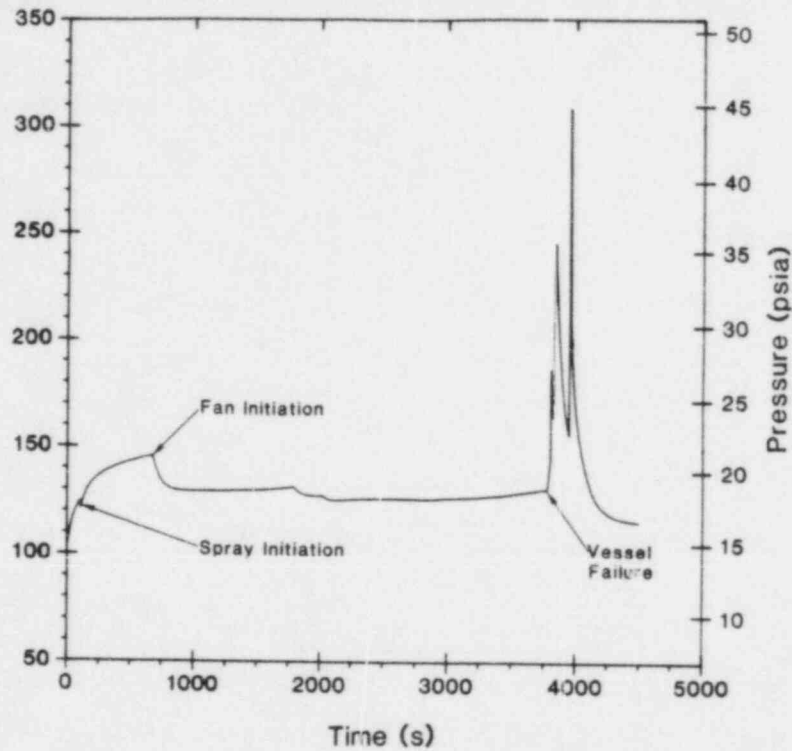


Figure 4-58. Pressure Response in Dome for Case E.01

4.4.3 "J" Cases - S₁HF Core-Meltdown Scenarios, 100% Zirconium Oxidation

The "J" cases are S₁HF cases similar to the "I" cases, except that the accident is assumed to progress through vessel breach, and 100% zirconium oxidation is assumed. The dome pressure response for case J.00 is shown in Figure 4-59. A multiple-peak response is shown after about 4200 s; however, there are some significant differences between this case, an S₁HF scenario, and case D.00, an S₂D scenario. In case D.00, MARCH predicts that vessel breach will occur almost immediately following core slump, because of the pressure rise in the primary system accompanying core slump. However, in case J.00 the primary system pressure is significantly lower, because of the larger break size. Since the primary system pressure is lower, the vessel remains intact following core slump until about 5200 s. Thus, in case J.00 the multiple peaks occur subsequent to core slump but prior to vessel breach.

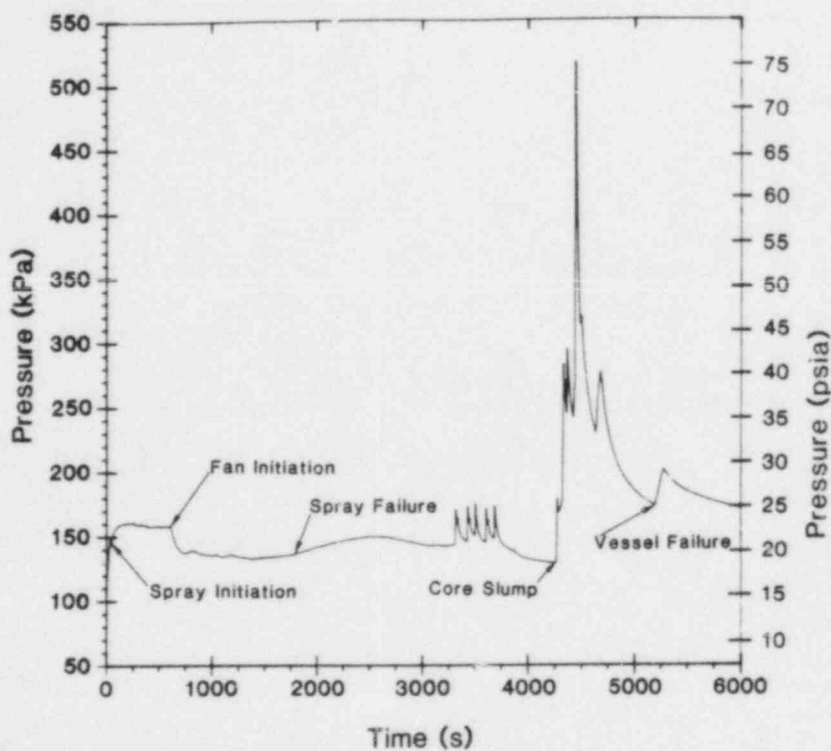


Figure 4-59. Pressure Response in Dome for Case J.00

At the time of core slump, hydrogen and steam are injected rapidly into containment, producing burns primarily in the lower compartment and upper plenum. The lower compartment does not become steam inert prior to vessel breach, although the steam concentrations are significantly increased. The large pressure spike at about 4500 s is due to a burn that begins in the dome, after the upper plenum has become inert due to oxygen depletion. The pressure rise is large because the baseline pressure is high and because oxygen is pushed back into the upper plenum, resulting in a burn at a high hydrogen concentration. When vessel breach finally occurs at about 5200 s, the consequences are small, because all of the zirconium has already been oxidized (steel oxidation is not treated in these calculations), and there is a minimal amount of water remaining in the primary system to be injected into containment.

Case J.01 was run to examine the effects of venting. Figure 4-60 shows the dome pressure response for this case. The results are identical to those for case J.00 until the large burn occurs at about 4500 s. For this burn the vent opens, producing about 120 kPa (17.4 psi) in pressure reduction. After this burn some differences are predicted, due to differences in gas transport and the fact that some of the hydrogen was vented during the previous burn.

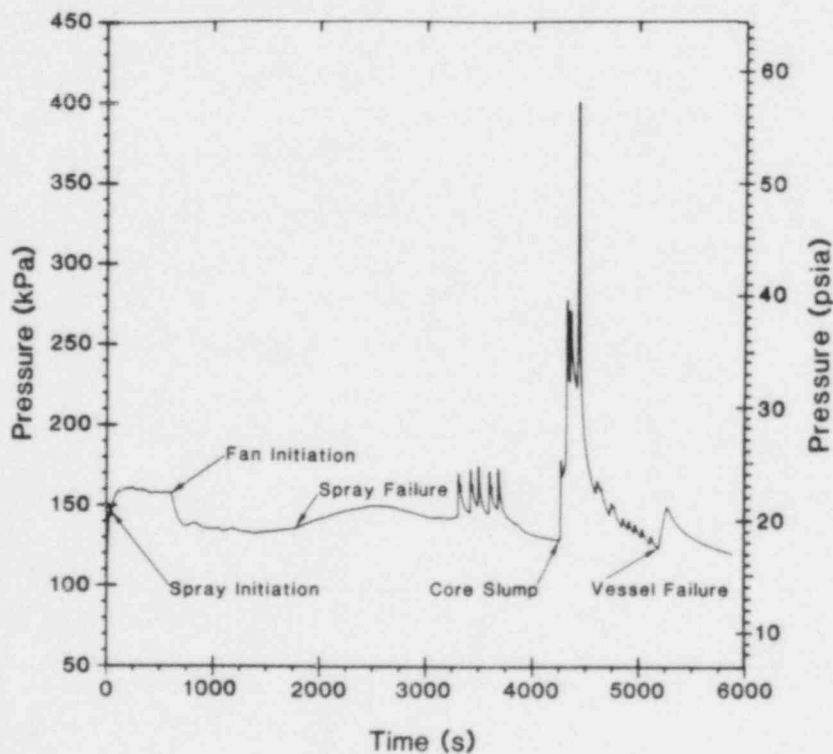


Figure 4-60. Pressure Response in Dome for Case J.01

Case J.02 was run to examine the effects of partial oxygen depletion. As shown in Figure 4-61, the results are initially similar to those for case J.00. However, the upper plenum becomes inert slightly sooner, thus altering the scenario and producing a somewhat lower pressure rise. Also, the containment is inert due to a lack of oxygen following the large burn (the mole fraction of oxygen is less than 0.04 in all compartments), and no further burns can occur. A substantial amount of hydrogen remains unburned, with concentrations ranging between 13 and 14% throughout the containment at the end of the run.

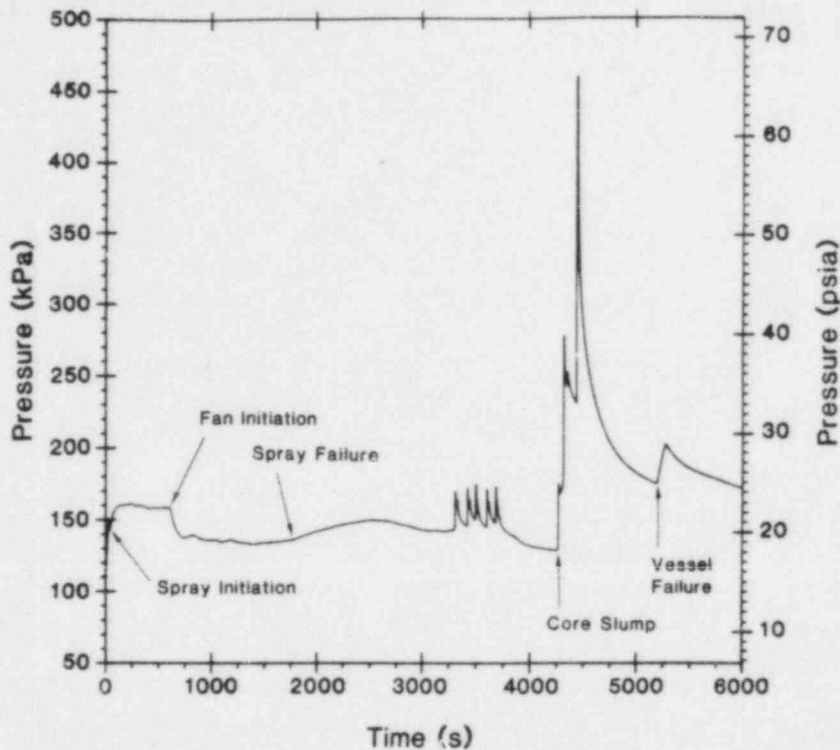


Figure 4-61. Pressure Response in Dome for Case J.02

4.4.4 "K" Cases - S₁HF Core-Meltdown Scenarios, 37% Zirconium Oxidation

The "K" cases are S₁HF accident scenarios with the parameters in MARCH adjusted to minimize oxidation (37% zirconium oxidation, see Chapter 3). The dome pressure response for case K.00 is shown in Figure 4-62. In this case core slump is predicted to occur just before 4000 s, and vessel breach is predicted to occur at about 6500 s. For this case nearly all of the hydrogen is released prior to core slump, resulting in burns in the lower regions of containment and the upper plenum. No burns are predicted to occur in the dome, and thus the pressure rises are small. The fairly slow pressure rise at the time of core slump is due to steam pressure only; nearly all of the hydrogen is released prior to core slump, and no burns are predicted to occur after that time.

Because the vent opening pressure was not exceeded in case K.00, no vent case was run for the "K" scenarios. Case K.01 was run to examine the effects of partial oxygen depletion. In this case, because of the lesser amount of hydrogen involved and the relatively slow rate at which it is released, no inerting is predicted to occur in any compartment, and the results are very close to those for case K.00.

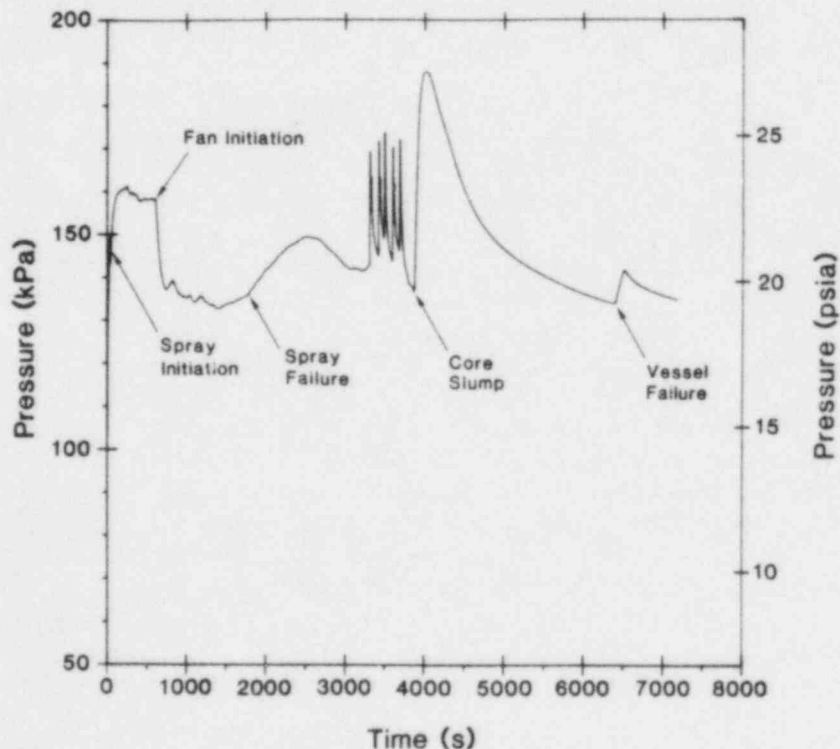


Figure 4-62. Pressure Response in Dome for Case K.00

4.4.5 "N" Cases - TMLB' Core-Meltdown Scenarios, 100% Zirconium Oxidation

The "N" cases represent TMLB' accident scenarios with a total loss of ac power. With a total loss of ac power, neither the sprays nor the fans are assumed to operate. Also, because the igniters will not operate without ac power, the ignition threshold was arbitrarily set to 12% hydrogen. Ignition may be a random event in such a case, depending on electrostatic discharge, an operable piece of electrical equipment, or perhaps the discharge of molten core debris following vessel breach. As discussed in Chapter 3, very little hydrogen is produced prior to core slump, which is predicted to occur just past 9000 s. Much of the hydrogen is released at the time of core slump, with another large release from the primary system predicted to occur a few minutes later at the time of vessel breach. Note that the HECTR model lumps the containment sump and the reactor cavity together. For the TMLB' scenarios, the reactor cavity may be dry prior to vessel breach. The reactor cavity will be treated more correctly and the effect of our current assumptions will be addressed in future analyses.

The dome pressure response for case N.00 is shown in Figure 4-63. The very large pressure spike is due to a burn that begins in the dome with a 12% hydrogen concentration. The burn begins in the dome, because the upper plenum was rendered inert due to oxygen depletion by a previous burn. The pressure rise is very high, because of a high baseline pressure, 12% ignition limits, and the presence of large quantities of hydrogen in the upper plenum which burns once oxygen is pushed back in from the dome. (Ignition limits higher than 12% would lead to even higher predicted peak pressures.) No burns occur in the lower compartment, which is steam inerted during the time of hydrogen injection. Also, as with other cases in which the fans are inoperable, very high hydrogen concentrations are predicted to occur in the upper ice compartments (8, 9).

Case N.01 was run to examine the effects of containment venting. As shown in Figure 4-64, venting produces a reduction in peak pressure of about 190 kPa (27.6 psi) and minor variations in the sequence of events. Case N.02 was run to examine the effects of partial oxygen depletion. The results were essentially the same as those for case N.00, except that there was some oxygen remaining in case N.00, while in case N.02 the containment was inert due to lack of oxygen at the end of the run.

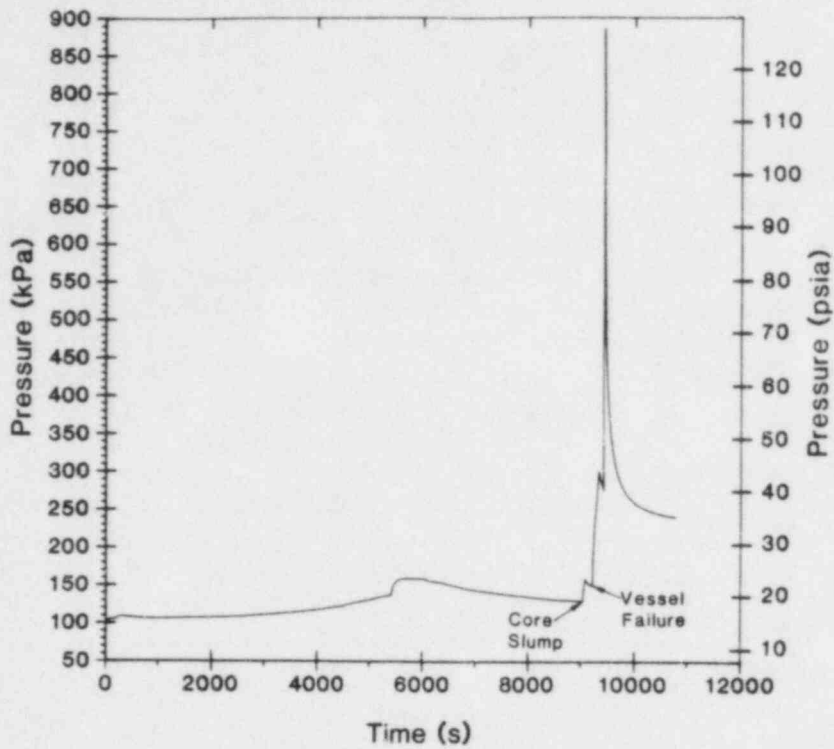


Figure 4-63. Pressure Response in Dome for Case N.00

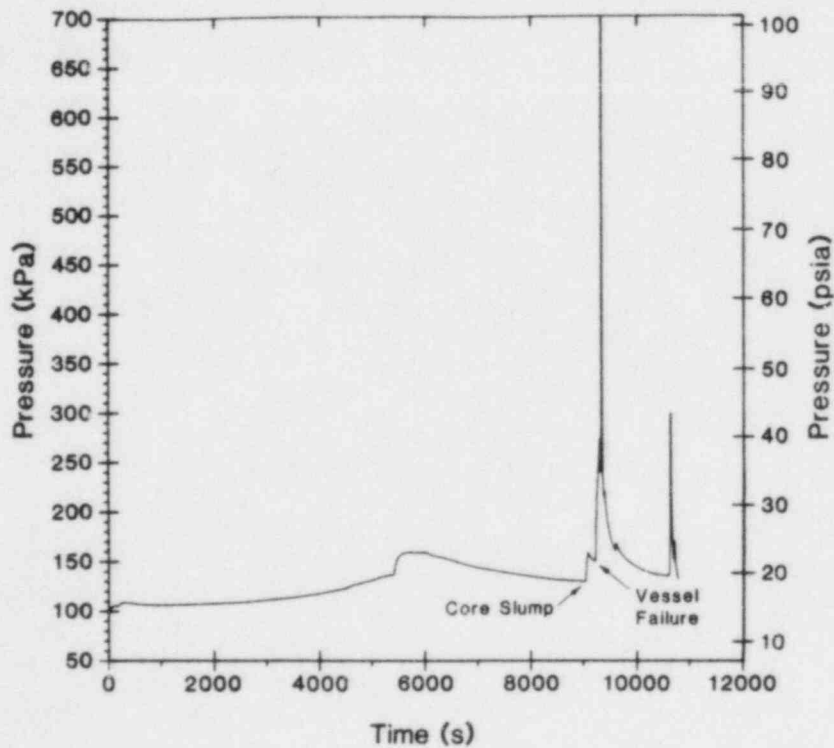


Figure 4-64. Pressure Response in Dome for Case N.01

4.4.6 "O" Cases - TMLB' Core-Meltdown Scenarios, 27% Zirconium Oxidation

The "O" cases are also TMLB' accident scenarios, but with minimal zirconium oxidation (27% zirconium oxidation, see Chapter 3). The case O.00 pressure response for the dome is shown in Figure 4-65. Only small pressure rises are predicted, due to burns that are predicted to occur in the upper plenum and propagate down into the ice compartments (6-9). No burns occur in the lower compartment, because of steam inerting with the fans inoperable. Also, no burns occur in the dome, due to the lesser amount of hydrogen released, which allows the hydrogen to be burned in the upper plenum and the ice compartments. However, even in this case with a minimum amount of zirconium oxidation, near-stoichiometric hydrogen concentrations are predicted for the upper ice compartments (8, 9). Case O.01 with partial oxygen depletion is similar to case O.00, because insufficient hydrogen was generated to make a significant difference.

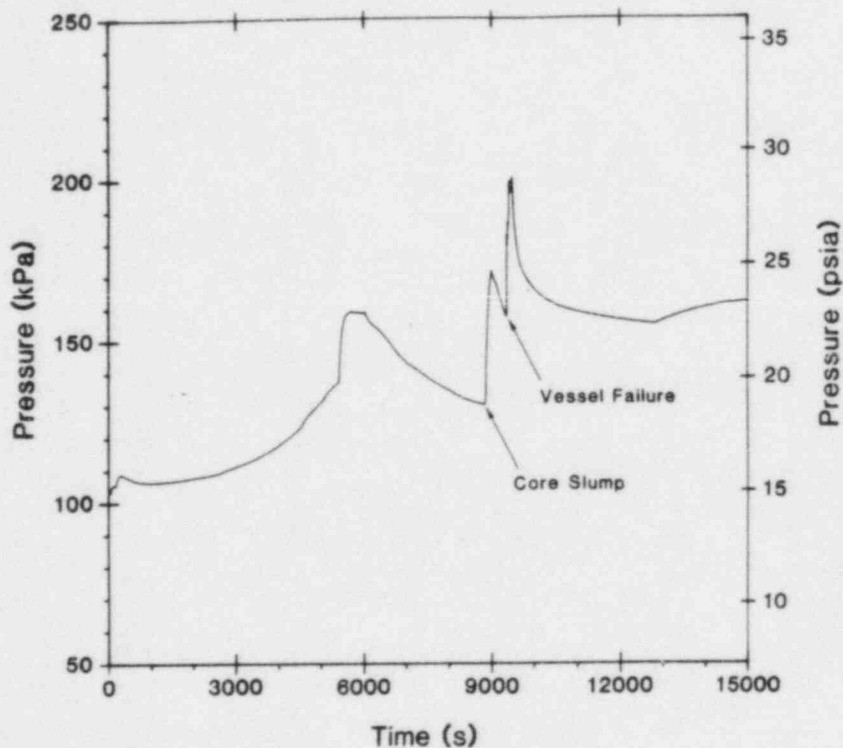


Figure 4-65. Pressure Response in Dome for Case O.00

4.4.7 "P" Cases - TMLB' Core-Meltdown Scenarios, 65% Zirconium Oxidation

The P cases are also TMLB' scenarios, but with an intermediate amount of oxidation (65%, see Chapter 3). The "N", "O", and "P" cases taken together represent a parametric treatment of the amount of zirconium oxidation. The dome pressure response for case P.00 is shown in Figure 4-66. The pressure response for this case is somewhat similar to that for case N.00. Burning initially occurs in the upper plenum and in the ice compartments. The large spike is due to a burn that begins in the upper plenum and propagates upward into the dome. However, the pressure rise is significantly less than for case N.00, because the hydrogen concentration in the dome is significantly less when the burn occurs. This is due to a lesser quantity of hydrogen being injected into containment and a lower injection rate.

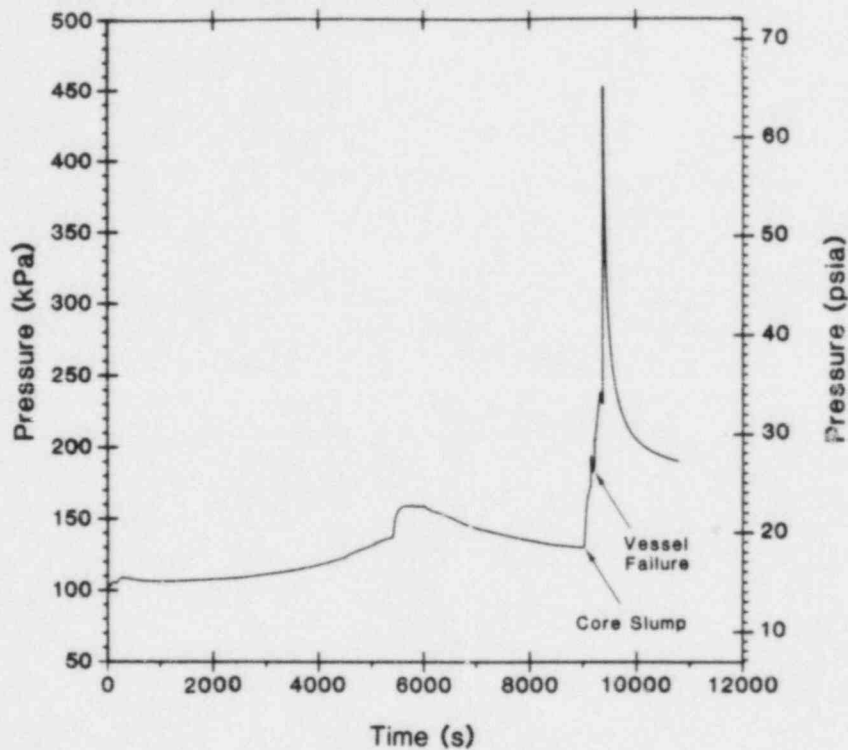


Figure 4-66. Pressure Response in Dome for Case P.00

Case P.01 shows the effects of containment venting. As shown in Figure 4-67, the behavior is very similar to that for case P.00. For this case the vent results in about a 45 kPa (6.5 psi) pressure reduction.

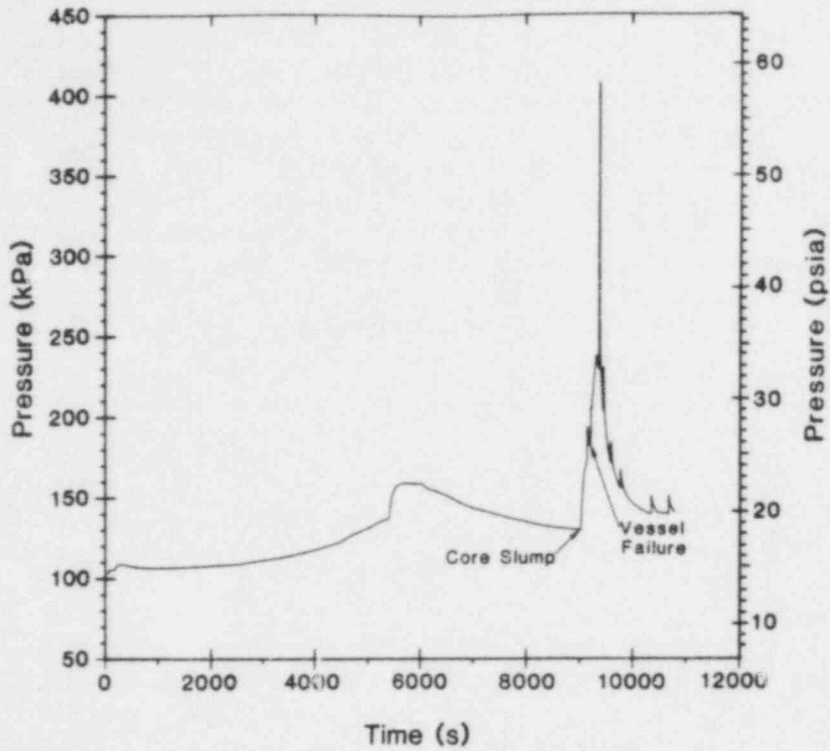


Figure 4-67. Pressure Response in Dome for Case P.01

5. CONCLUSIONS

A large number of widely varying results were presented in Chapter 4, making it difficult for the reader to draw specific conclusions regarding the response of an ice-condenser containment. In the paragraphs that follow, we will attempt to discuss the results in a manner that makes them more readily understood. We will address the differences between the degraded-core and core-meltdown scenarios, the effects of the major parameters important to both scenarios, the effectiveness of the igniter system, and recommendations for future work.

5.1 Degraded-Core versus Core-Meltdown Scenarios

Prior to vessel breach, the degraded-core and core-meltdown cases show similar behavior and sensitivities. Hydrogen is released fairly slowly (a few kilograms per second [a few hundred pounds per minute] or less), and the results are governed by the common parameters discussed later in this section. Prior to vessel breach, many of the core-meltdown cases are actually less severe than the degraded-core cases. In the core-meltdown cases (no restoration of ECC), little hydrogen is released from the primary system until vessel breach occurs. Therefore, hydrogen burns before the time of vessel breach (if they occur) are relatively benign.

Most of the significant differences between degraded-core and core-meltdown accidents occur due to the events during and subsequent to vessel breach. The single most important aspect of vessel breach addressed by this analysis is the rapid injection of steam and hydrogen into containment due to release from the primary system and quenching in the reactor cavity. Peak hydrogen injection rates of several tens of kilograms per second (several thousand pounds per minute) are predicted by MARCH. The hydrogen released to containment following vessel breach is predicted to produce high peak pressures for three major reasons. First, the large steam release rate raises the baseline or preburn pressure. Second, because of the high hydrogen release rates, the burns are fed hydrogen as they progress. Finally, enough hydrogen is usually released to result in two or more successive burns that are close enough together in time for their effects to be somewhat cumulative. Generally, these burns occur in the upper regions of containment (upper plenum and dome), because the steam released just after vessel breach rapidly makes inert the atmosphere in the lower compartment (if it is not already inert prior to vessel breach because of postulated failure of the air return fans).

The possible effects of steam explosions, noncoolable debris beds, ejection of melt from the vessel breach or

reactor cavity, aerosol generation and dispersal, and core/concrete interactions are not considered in this study but will be considered in future SASA analyses. The discussions in Sections 5.2 through 5.9 below examine sensitivities common to both degraded-core and core-meltdown scenarios.

5.2 Steam and Hydrogen Source Terms

Much of the difference in result for different cases can be attributed to different accident scenarios and correspondingly different source terms. The location of the burns and their magnitude are influenced by the source terms, which can be characterized by two parameters: (1) the hydrogen-to-steam ratio and (2) the injection rates. Low hydrogen-to-steam ratios tend to cause burns to occur preferentially in the upper regions of containment (upper plenum and dome), because the high steam content makes the lower compartment less combustible.

Rapid steam and hydrogen source-injection rates tend to raise the baseline pressure and produce correspondingly higher burn pressures. Slow source-injection rates lead to a better-mixed containment prior to burning and may lead to burns of a more global nature. It is clear from the results that it is not sufficient to examine the hydrogen injection rates alone. Steam injection plays a major role in these accident scenarios. The sensitivity to source terms encountered in this analysis is unfortunate, as there is a high degree of uncertainty in the MARCH-generated source terms.

A degraded-core case with only 35% zirconium oxidation yields peak pressures slightly higher than those predicted for a similar case with 75% zirconium oxidation. Intuitively, one would expect the maximum pressure rise due to combustion to increase monotonically with the amount of hydrogen released. However our calculations indicate this is not the case for degraded-core scenarios in an ice-condenser containment. Instead there is a threshold amount of hydrogen above which the peak pressures cease to increase (assuming the ignitors are operating).

This finding raises questions as to the level of conservatism implied by the interim hydrogen rule for ice-condenser plants. Specifically, the rule states that these plants must be able to withstand the effects of degraded-core scenarios in which hydrogen from 75% zirconium oxidation is released to containment. Results from this study indicate that the selection of 75% oxidation provides no margin of safety in the containment loads over that which would be produced by only 35% oxidation (for a degraded-core scenario). More calculations are needed to clearly define the relationship between amount of zirconium oxidized and maximum pressure rise due to combustion.

5.3 Containment Sprays

Containment sprays are essential for long-term accident mitigation, because the ice condenser has a finite lifetime; without sprays, containment will eventually be breached either by leakage or by steam overpressure unless the steam release is terminated. The upper-bound failure pressure for Sequoyah, 515 kPa (75 psia), was not exceeded in any scenario in which the sprays, the recirculation fans, and the igniters were operating. In the short term, sprays keep the baseline pressure down prior to burns and remove heat during hydrogen burns. Also, the heat removed following hydrogen burns will make the pressure (and temperature) rises less cumulative. The effectiveness of sprays during a burn will depend on the flame speed, with longer burns allowing more heat removal. It is likely that the turbulence induced by the sprays will increase the speed and completeness of combustion; however, we feel that the positive benefits of sprays far outweigh this potential negative aspect. For the accident scenarios analyzed, automatic spray actuation on high containment pressure always occurred before the first burn was predicted, so that no changes in spray actuation logic would seem to be warranted.

5.4 Recirculation Fans

Operation of the fans tends to reduce the baseline pressures by increasing the effectiveness of the ice condenser. Also, operation of the fans generally prevents sustained periods of steam inerting in the lower compartment. This is significant because burns originating in the lower compartment generally result in lower peak pressures than burns originating in the dome or burns originating in the upper plenum and propagating into the dome. When the fans are off, very high hydrogen concentrations are predicted in the ice condenser, raising the possibility of accelerated flames or local detonations. These high hydrogen concentrations occur due to less air entering the bottom of the ice condenser with the hydrogen and lower flow rates through the ice condenser. The treatment of accelerated flames and local detonations is beyond the scope of this report. As for the sprays, the existing logic for automatic actuation of the recirculation fans appears satisfactory.

5.5 Combustion Parameters

The results of varying the ignition limits, combustion completeness, and flame speed are fairly straightforward, with increasing values of these parameters producing higher pressures. High values for ignition limits and combustion completeness produce fewer burns with more hydrogen consumed in each burn. The specific pressure rise for a particular case depends strongly on the initial pressure. However, we can say that with the fans and sprays operating, burns that

consume the equivalent of 6 to 7% hydrogen either in a single, confined compartment or on a containment-wide basis will generally not directly threaten containment. Burns ignited at higher concentrations in compartments that can vent into other compartments may also produce relatively low pressure rises, assuming that the amount of venting is significant over the burn time. However, if the recirculation fans are not operating, burns ignited at 6 to 7% hydrogen could propagate into a region where much higher concentrations may be present, leading to burns at higher effective concentrations and possibly accelerated flames or local detonations.

For scenarios such as TMLB', where the ignition system fails, we assumed arbitrary ignition limits (12% hydrogen in most cases). In fact, ignition in these cases may be a stochastic process, depending on available ignition sources, and may occur at hydrogen concentrations greater or less than 12%. A better analysis of these scenarios would consider ignition probability as a function of time during the accident.

Information is not now available that will let us accurately predict flame speeds in the very large scales (and possibly turbulent environments) of reactor containments. We can say that if the burns are a few seconds or less in duration, the pressures will be a significant fraction (> 80%) of the adiabatic values. For longer burns the containment sprays can significantly reduce the pressure rises.

5.6 Ice-Condenser Parameters

Generally, we found the results to be relatively insensitive to the ice-condenser parameters (drain temperature and heat transfer coefficient). Consistent results were observed for a wide range of parameters. However we only examined the effects of these parameters for one set of accident scenarios, the S₁HF scenarios. It is possible that more significant effects would appear for other scenarios.

5.7 Containment Venting

For those cases where high pressures were predicted, containment venting during burning had some positive effects. Compared to cases without venting, pressure reductions in the range of 10 to 20% were typical. These reductions depend on the vent size (0.75 m² [8.1 ft²] assumed here) and the flame speed (burn time).

5.8 Partial Oxygen Depletion

The calculations performed here do not show large benefits from partial oxygen depletion and in some cases show negative effects. However, these results are due to the particular accident scenarios considered and to modeling limitations. Clearly, partial oxygen depletion limits the total amount of hydrogen that can be burned. Generally, the combustion of hydrogen from 100% zirconium oxidation will render the containment inert due to depletion of oxygen below the requisite minimum concentration (nominally 5%). Partial oxygen depletion will render the containment inert well before the hydrogen from 100% zirconium oxidation is consumed. During core-meltdown accidents, significant amounts of carbon monoxide may be produced before the oxygen inerting of the containment atmosphere occurs. Limiting the amount of carbon monoxide burned is important since it has a higher ignition limit and heat of reaction than hydrogen, and thus, could produce higher pressure rises. Also, note that the analysis did not treat possible decreases in flame speed and combustion completeness due to decreased oxygen content, either as a result of an initially oxygen depleted atmosphere or of an atmosphere that became oxygen depleted as a result of repeated burning.

The HECTR analyses presented here indicate that partial oxygen depletion tends to produce inerting in the upper plenum of the ice condenser, thus promoting combustion in the dome. While it is clear that partial oxygen depletion will cause inerting to occur in local regions at an earlier time, the nine-compartment model is probably not adequate to address this question. A more appropriate model would divide the upper plenum into regions with and without igniters and more correctly treat the amount of hydrogen that reaches the dome without burning.

5.9 Effectiveness of Igniter System

Based on our HECTR results, an igniter system is beneficial for many accident scenarios involving the release of hydrogen. Pressure rises due to deflagrations will almost certainly be decreased from what might be obtained from random combustion with no igniters present. The two most important considerations appear to be (1) whether the igniters are operating and (2) whether the fans are operating. A deliberate ignition system of the type installed at Sequoyah is not operable in all accident sequences (in our analyses the system is operable in all of the degraded-core sequences and some of the core-meltdown sequences). For example, the igniters at Sequoyah are ac-powered. To reduce the risk due to accidents involving total loss of ac power, dc power to the igniters would be required.

Also, for Sequoyah, no igniters are located in the ice regions. As a result, in accidents involving recirculation fan failure, high hydrogen concentrations can accumulate in the ice regions. The potential for accelerated flames or local detonations during such accidents could be reduced by installing a limited number of igniters in the ice regions. These igniters would probably not need to be activated if the recirculation fans were operating. Future development of a passive igniter system could alleviate many of the concerns regarding loss-of-power accidents.

Although ice-condenser containments are all similar in configuration, our calculations are for a specific ice-condenser containment design (Sequoyah--Watts Bar), and care should be exercised in extending the results to other plants. The benefits of a deliberate ignition system installed in other ice-condenser containments might be different. Also, our calculations do not address the possibility of continuous burning due to stable diffusion flames or jets, or the possibility of equipment failures as a result of combustion events. Future considerations of these possibilities might alter the perceived benefits of deliberate ignition. For example, diffusion flames would be beneficial in that low pressure rises would be produced; however, high gas temperatures would be produced that might fail adjacent equipment.

5.10 Future Work

5.10.1 Unresolved Issues

It is beyond the scope of this report to attempt to resolve several issues regarding hydrogen combustion in ice-condenser containments. These issues are:

- The potential for accelerated flames or local detonations in or near the ice condenser
- The effects of additional combustible (and noncondensable) gas generation from other metal-water reactions and molten core-concrete interactions
- The likelihood and effects of stable diffusion flames either near the hydrogen release point, in the ice condenser, or near the fan exits
- The response of safety-related equipment to combustion, particularly if diffusion flames are present
- Ignition in accidents in which the igniter systems may fail (either with or without ac power available)
- The relationship between maximum peak pressures and amount of zirconium oxidized for degraded-core scenarios

5.10.2 Plans for Resolution of Issues

Work is in progress which will address most of the above issues. The potential for accelerated flames or detonations in the ice condenser will be addressed experimentally at Sandia (Hydrogen Behavior Program). HECTR is now being modified to address combustion in the presence of the carbon monoxide and carbon dioxide formed during core-concrete interactions (Hydrogen Behavior Program). Experiments are in progress to address diffusion flames, and models are being developed for future incorporation into HECTR (Hydrogen Behavior and Hydrogen Mitigation Programs). Equipment survival will be addressed in a subsequent report, using boundary conditions obtained from the analyses described in this report (Hydrogen Burn Survival Program). The feasibility of passive igniters that would function during an accident involving the total loss of ac power is also being studied at Sandia (Hydrogen Mitigation Program). A follow-on study is planned (Severe Accident Sequence Analysis Program) to more clearly define the relationship between the maximum pressure rise in containment and the amount of zirconium oxidized in degraded-core scenarios.

6. REFERENCES

1. A. M. Kolaczowski et al, Interim Report on Accident Sequence Likelihood Reassessment (Accident Sequence Evaluation Program), Sandia National Laboratories and Science Applications, Inc., Draft February 1983.
2. R. O. Wooton and H. I. Avci, MARCH (Meltdown Accident Response Characteristics) Code Description and User's Manual, NUREG/CR-1711, U. S. Nuclear Regulatory Commission, Washington, DC, 1980.
3. F. E. Haskin and C. J. Shaffer, "Impact of Meltdown Modeling Developments on PWR Analyses," in Proceedings of ANS-ENS International Meeting on Thermal Nuclear Reactor Safety, Chicago, IL, August 29-September 2, 1982.
4. A. L. Camp, M. J. Wester, and S. E. Dingman, "HECTR: A Computer Program for Modeling the Response to Hydrogen Burns in Containments," in Proceedings of the Second International Workshop on the Impact of Hydrogen on Water Reactor Safety, Albuquerque, NM, October, 1982.
5. S. E. Dingman, M. J. Wester, and A. L. Camp, "Applications of HECTR to Reactor Containments," in Proceedings of the Second International Workshop on the Impact of Hydrogen on Water Reactor Safety, Albuquerque, NM, October, 1982.
6. J. C. Cummings et al, Review of the Grand Gulf Hydrogen Igniter System, NUREG/CR-2530, SAND82-0218, Sandia National Laboratories, Albuquerque, NM, March 1983.
7. Safety Evaluation Report Related to the Operation of Sequoyah Nuclear Plant, Units 1 and 2, NUREG-0011 Supplement No. 6, U.S. Nuclear Regulatory Commission, Draft Copy, November 1982.
8. L. Greimann et al, Final Report, Containment Analysis Techniques: A State of the Art Summary, NUREG/CR-3653, Ames Laboratory, Ames, IA, 1984.
9. Letter from L. M. Mills, Tennessee Valley Authority, to E. Adensam, Director of Nuclear Reactor Regulation, USNRC, December 1, 1981.
10. D. D. Carlson et al, Reactor Safety Study Methodology Applications Program: Sequoyah #1 PWR Power Plant, NUREG/CR-1659, SAND80-1897, Sandia National Laboratories and Battelle Columbus Laboratories, February 1981.

11. J. B. Rivard, ed. Interim Technical Assessment of the MARCH Code, NUREG/CR-2285, SAND81-1672, Sandia National Laboratories, Albuquerque, NM, 1981.
12. American Nuclear Society Standards Committee Working Group ANS-5.1, "American National Standard for Decay Heat Power in Light Water Reactors," ANSI/ANS-5.1-1979, August 1979.
13. Sequoyah Nuclear Plant Core Degradation Program, Vol. 2, Report on the Safety Evaluation of the Interim Distributed Ignition System, December 15, 1980.
14. J. T. Larkins and P. Worthington, "The NRC Hydrogen Behavior and Mitigation Research Programs," in Proceedings of the Second International Workshop on the Impact of Hydrogen on Water Reactor Safety, Albuquerque, NM, October, 1982.

APPENDIX A

HECTR MODEL DESCRIPTIONS

The basic structure of HECTR has been described previously.[1-3] Therefore, in this appendix only the new models and those models that are particularly relevant to this report are described. In the paragraphs that follow, discussions are provided for the combustion models, the ice-condenser model, the door model, and the sump model.

Combustion Models

The combustion models consist of correlations for ignition, propagation, combustion completeness, and flame speed. HECTR does not track a flame front, as such, but uses the flame speed to determine a chemical reaction rate within a compartment. The combustion completeness and flame speed correlations were derived from experiments that were performed in the VGES and FITS experimental facilities at Sandia.[4 5] Ignition limits and propagation limits may be user-specified for each compartment separately, or default values may be used, as shown in Table A-1. For most of the cases the default values were used. Ignition was not allowed in compartments 3, 6, 7, 8, and 9 because there are no igniters located in those compartments; however, burns were allowed to propagate into those compartments.

Table A-1

Ignition and Propagation Default Values

Parameter	Mole Fraction			
	H ₂	O ₂	N ₂	H ₂ O
Ignition Limits	≥0.08	≥0.05	--	≤0.55
Upward Propagation	≥0.041	≥0.05	--	≤0.55
Horizontal Propagation	≥0.06	≥0.05	--	≤0.55
Downward Propagation	≥0.09	≥0.05	--	≤0.55

When a burn propagates from a burning compartment i to a nonburning compartment j , the time at which propagation will occur must also be determined. This propagation time, t_p , is specified as a fraction of the burn time in compartment i ($0 \leq t_p \leq 1$). The value may be user-specified, or the default value of 0.5 may be used. The various compartment relationships determining whether propagation would be upward, downward, or sideways are specified in the input.

Combustion completeness may be user-specified, or the default correlation for combustion completeness may be used:

$$X_f = \text{Max} [(1.0 - 12.4375X_i)X_i, 0.005X_i] \quad (\text{A-1})$$

where X_i and X_f are the initial and final mole fractions of hydrogen, respectively. Using the default correlation, combustion is assumed to be complete for hydrogen concentrations at or above 8%.

Either the flame speed or the burn time may be user-specified. Default flame speed correlations are included in HECTR and may be used instead of user-specified values. The correlations are shown below, where X_s is the initial mole fraction of steam, and the velocity is given in m/s.

For $0.0 \leq X_i \leq 0.1$:

$$V = (59.2X_i + 1.792)C$$

$$C = \begin{cases} 1.0 - 4.53X_s + 5.37X_s^2 & \text{for } X_s < 0.4 \\ 0.05 & \text{for } X_s \geq 0.4 \end{cases}$$

For $0.1 < X_i \leq 0.2$:

$$V = (172.88X_i - 9.576)C$$

$$C = \begin{cases} 1.0 - 4.53X_s + 5.37X_s^2 & \text{for } X_s < 0.4 \\ 0.05 & \text{for } X_s \geq 0.4 \end{cases}$$

For $0.2 < X_i \leq 0.3$:

$$V = (50.0X_i + 15.0)C$$

$$C = \begin{cases} (1.0 - 4.53X_s + 5.37X_s^2)(3.0 - 10.0X_i) \\ + (1.0 - 1.129X_s)(10.0X_i - 2.0) & \text{for } X_s \leq 0.4 \\ 0.15 - 5.0X_i + (1.0 - 1.129X_s)(10.0X_i - 2.0) \\ \text{for } X_s > 0.4 \end{cases}$$

For $0.3 < X_i \leq 0.4$:

$$V = (-50.0X_i + 45.0)C$$

$$C = 1.0 - 1.29X_g$$

For $0.4 < X_i < 0.6$:

$$V = (-75.0X_i + 55.0)C$$

$$C = 1.0 - 1.29X_g$$

For $X_i \geq 0.6$:

$$V = \text{Max} [(-64.3X_i + 48.58)C, C]$$

$$C = 1.0 - 1.29X_g$$

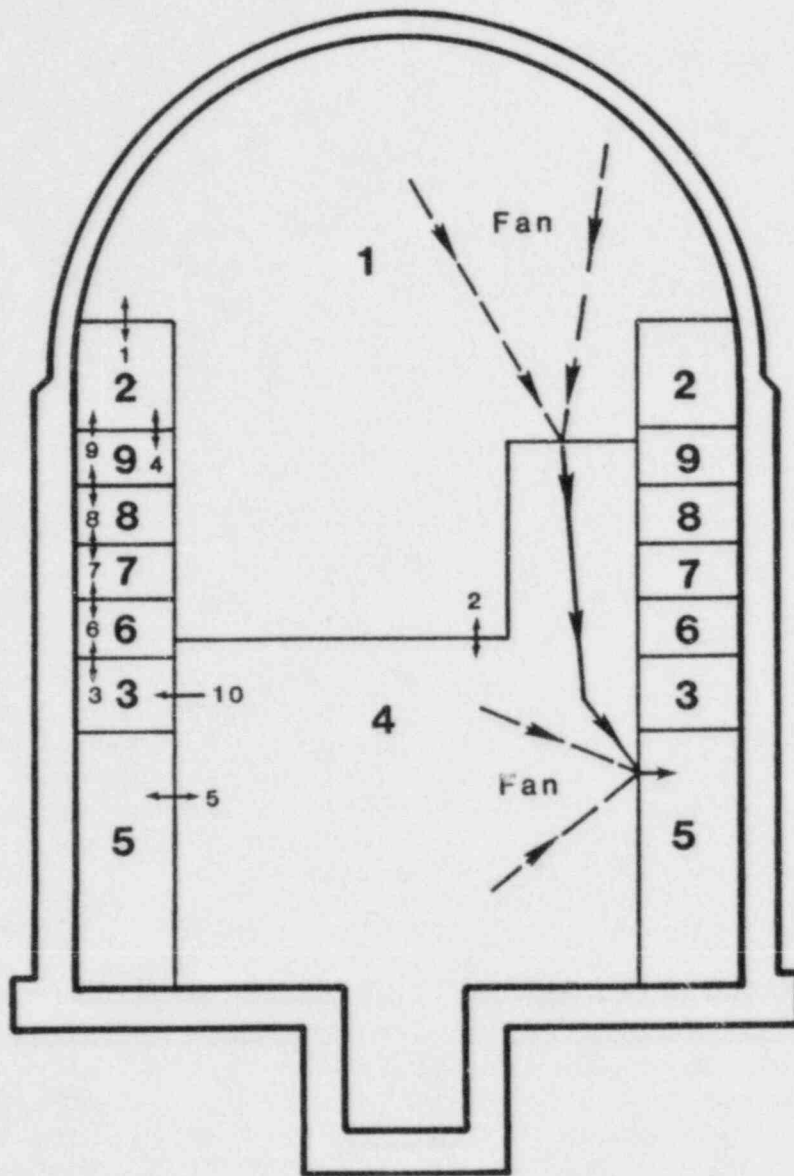
Burn times are calculated by dividing a user-specified, characteristic compartment dimension by the flame speed. Once the burn time has been calculated, it remains fixed during the burn, and the chemical reaction rate is adjusted each time step to account for flows out or injection of sources so that the burn finishes at the predetermined time with the correct final mole fraction of hydrogen.

Ice-Condenser Model

To model an ice condenser in HECTR, we subdivide the ice region into four compartments and use two more compartments for the lower and upper plenums (see Figure A-1). This relatively large number of compartments is necessary because the steam concentration can vary significantly across the ice condenser. There is no limit on the number of surfaces in the lower and upper plenums, but only two surfaces are used for each compartment in the ice region. One of the two surfaces in each ice region compartment models the ice and the other surface models the ice condenser walls and portions of the metal baskets that are free of ice. Each ice surface is maintained at a constant temperature. The metal surfaces are treated as lumped masses. Sensible heat transfer in the ice condenser is determined from

$$\text{Nu} = 0.023 C \text{Re}^{0.8} \text{Pr}^{0.3} \quad (\text{A-2})$$

where Nu, Re, and Pr are the Nusselt, Reynolds, and Prandtl numbers, respectively, and C is a correction factor to account for surface roughness and the presence of a liquid film. C is currently set to 5.0. The above correlation is somewhat arbitrary, as no data are available for small-break LOCA



KEY

- 1** - Compartment Number
- 1 - Flow Junction Number
- - One-way Flow Junction
- ↔ - Two-way Flow Junction

Note: Igniters Present in
Compartments 1, 2, 4, and 5.

Compartment Descriptors

- 1. Dome
- 2. Upper Plenum
- 3. Lower Plenum
- 4. Lower Compartment
- 5. Dead-Ended Region
- 6-9. Ice Compartments

Figure A-1. HECTR Ice-Condenser Containment Model

LOCA situations. However, as shown in Chapter 4, the results for the cases examined are relatively insensitive to this correlation. The condensing mass flux is determined from the following equation:

$$J = \frac{D \ln(X_{aw}/X_a) P (X_{sw} - X_s) \text{Nu} (\text{Pr}/\text{Sc})^{2/3}}{RTL (X_{aw} - X_a)} \quad (\text{A-3})$$

where

- J = mass flux (mol/m²/s)
- Sc = Schmidt number
- D = diffusion coefficient (m²/s)
- X_{aw} = mole fraction of air at wall
- X_a = mole fraction of air in bulk gas
- X_{sw} = mole fraction of steam at wall
- X_s = mole fraction of steam in bulk gas
- P = total pressure (Pa)
- R = gas constant (J/mol/K)
- T = bulk gas temperature (K)
- L = characteristic surface length (m)

The ice melting rate is calculated by the following expression:

$$W_i = qA_i / (h_l - u_i) \quad (\text{A-4})$$

where

- W_i = ice melting rate
- q = sensible heat flux to ice
- A_i = ice heat transfer area
- h_l = enthalpy of water at 273.15 K
- u_i = internal energy of ice at ice temperature

The ice is assumed to melt from the bottom up in each compartment. The mass of unmelted ice is calculated by integrating the ice melting rate during the transient. The corresponding surface area of the ice for heat transfer is calculated using

$$A_i = (M_i/M_{i,0}) A_{i,0} \quad (\text{A-5})$$

where

$A_{i,o}$ = initial ice heat transfer area

M_i = unmelted ice mass

$M_{i,o}$ = initial ice mass

As the ice melts, the metal baskets containing the ice will be exposed and subsequently will be heated by the steam. To account for this heat sink, we increase the mass and surface area of the metal surface in each ice region as the ice melts and adjust the surface temperature using the following equations:

$$M_m = M_{m,p} + M_b(M_i - M_{i,p})/M_{i,o} \quad (A-6)$$

$$A_m = A_{m,p} + A_b(A_i - A_{i,p})/A_{i,o} \quad (A-7)$$

$$T_m = \frac{[(M_{m,p} T_{m,p}) + (M_m - M_{m,p}) T_i]}{M_m} \quad (A-8)$$

where

M_b = mass of baskets

M_m = mass of metal heat transfer surface

$M_{m,p}$ = M_m from previous time step

$M_{i,p}$ = M_i from previous time step

A_b = area of baskets

A_m = area of metal heat transfer surface

$A_{m,p}$ = A_m from previous time step

$A_{i,p}$ = A_i from previous time step

T_m = temperature of metal surface

$T_{m,p}$ = T_m from previous time step

Much of the liquid water formed in the ice regions by melting ice and steam condensation falls down through the ice condenser to a sump on the floor of the lower plenum. Although this process is too poorly characterized at present to allow analytical modeling, the heat and mass transfer to the water is significant. Therefore, we have included a simple model for the process in HECTR that can be varied parametrically to bound the phenomena. For this model we assume that the water does not heat up significantly in the ice region. Thus, all of the heat and mass transfer occurs while the water falls through the lower plenum. The controlling parameter is the ice-condenser drain temperature, and the water is assumed to heat up to this temperature. Making the assumption that the latent heat transfer dominates the sensible

heat transfer, we calculate the condensation rate in the lower plenum from:

$$W_{lp} = \sum_{n=1}^4 \frac{(W_{mi} + W_{ci})(h_d - h_{li}) + W_{cm}(h_d - h_{lm})}{(h_s - h_d)} \quad (A-9)$$

where

- W_{lp} = condensation rate in the lower plenum
- W_{mi} = rate of ice melting in compartment n
- W_{ci} = rate of condensation on ice in compartment n
- W_{cm} = rate of condensation on metal surface in compartment n
- h_d = enthalpy of liquid at drain temperature
- h_{li} = enthalpy of liquid at ice melting temperature
- h_{lm} = enthalpy of liquid at metal surface temperature in compartment n
- h_s = enthalpy of steam in the lower plenum

With the above expressions we can calculate the total amount of water that drains from the ice condenser into the sump.

Door Model

HECTR includes a model for the doors that are found at the entrance to the lower plenum and between the ice region and the upper plenum (junctions 9 and 10 in Figure A-1). This model was taken, with few changes, from Reference 6. A minimum differential pressure is specified that must be exceeded before a door will be allowed to open. Once the doors are open, the flow area is determined from the following expressions:

$$\frac{A}{A_0} = \frac{1.0 - \cos \theta}{1.0 - \cos \theta_0} \quad (A-10)$$

and

$$\frac{\theta}{\theta_0} = \frac{P \cos \theta}{P_0 \cos \theta_0} \quad (A-11)$$

where

- A = flow area
- A_0 = fully open flow area
- P = differential pressure across door minus minimum pressure to open

- P_0 = differential pressure to hold doors fully open
 θ = door opening angle
 θ_0 = fully open door angle

Values for the above parameters can be found in Table D-4 in Appendix D.

The door flow area is very sensitive to small changes in pressure, and thus, the flows through the doors can vary dramatically from one time step to the next and cause some numerical problems for HECTR. To alleviate these problems, some artificial smoothing was employed in the door model. The flow area used in the calculation was determined from

$$A_n = 0.8A_p + 0.2A \quad (A-12)$$

where A_n is the area used in the calculation, A_p is the area used in the previous time step, and A is the value determined from the expressions shown previously.

Sump Model

A sump model was also added to HECTR. The sump collects water from the following sources: the portion of the break flow that does not flash to steam, condensation on the containment surfaces and on the sump, spray droplets that reach the bottom of a compartment, water draining from the ice condenser, and steam removed from a compartment that is supersaturated. Water is drawn from the sump for ECC and containment sprays when the recirculation modes are active, and water can be lost from the sump due to evaporation or boiling. Conservation of mass and energy relations determine the sump temperature and volume as a function of time. The free volume of the lower compartment is appropriately modified to reflect changes in the sump volume. For the cases that assume a molten core eventually falls into the sump, the hydrogen generation rates and heat transfer rates are taken from MARCH, and the hydrogen is injected into the lower compartment at the sump temperature, with the remaining energy (accounting properly for the energy carried away by the hydrogen) being transferred into the sump. If a sufficient amount of energy is transferred into the sump to raise its temperature to the saturation point, then boiling can occur.

References for Appendix A

1. A. L. Camp, M. J. Wester, and S. E. Dingman, "HECTR: A Computer Program for Modeling the Response to Hydrogen Burns in Containments," in Proceedings of the Second International Workshop on the Impact of Hydrogen on Water Reactor Safety, Albuquerque, NM, October, 1982.
2. S. E. Dingman, M. J. Wester, and A. L. Camp, "Applications of HECTR to Reactor Containments," in Proceedings of the Second International Workshop on the Impact of Hydrogen on Water Reactor Safety, Albuquerque, NM, October, 1982.
3. J. C. Cummings et al, Review of the Grand Gulf Hydrogen Igniter System, NUREG/CR-2530, SAND82-0218, Sandia National Laboratories, Albuquerque, NM, March 1983.
4. W. B. Benedick, J. C. Cummings, and P. G. Prassinis, "Experimental Results from Combustion of Hydrogen:Air Mixtures in an Intermediate-Scale Tank," in Proceedings of the Second International Workshop on the Impact of Hydrogen on Water Reactor Safety, Albuquerque, NM, October, 1982.
5. S. F. Roller and S. M. Falacy, "Medium-Scale Tests of H₂:Air:Steam Systems," in Proceedings of the Second International Workshop on the Impact of Hydrogen on Water Reactor Safety, Albuquerque, NM, October, 1982.
6. "Report on the Grand Gulf Nuclear Station Hydrogen Ignition System," Mississippi Power and Light Co., August 31, 1981.

APPENDIX B

MARCH INPUT FOR DEGRADED-CORE CASES

This appendix contains all of the MARCH input information used in the degraded-core cases. A complete MARCH input deck is listed for case A.00. For all other cases, any parameter values that differed from those for case A.00 are listed.

Case A.00

```

111182SQS2H      SQS2H--SEQUOYAH S2D DEGRADED CORE
$CHANGE
ACBRK=-1.0,      CPSTP=180.0,      FDRP=-1.0,      HIMX=-1.0,
HIOX=-1.0,      ID=830214,      IFISH=-1,      IFPM=10,
IFPV=10,        IGASX=10,      IHOTX=10,      IPLOT=0,
IS=4,           JS=0,          LST7=1,        MEL=-1,
NCRST=1,        NCT7=1,        PFAIL=-1.0,    PRST=1000.0,
TFX=-1.0,       TMX=-1.0,      TRST=250.,     WALLX=-1.0,
$END

                      SEQUOYAH--S2D DEGRADED CORE
$NLMAR
DTINIT=0.02,    H2HI=0.08,      H2LO=0.0,      HIOXY=0.05,
HIG=0.55,      H2UP=0.041,    H2HZ=0.06,     H2DN=0.09,
H2VO=352.8,    H2VX=11650.,   H2DIST(1)=90.,110.,
IBLDF=0,       IBLDI=0,       IBLDP=0,       IBRK=1,
IBURNL=1,      IBURNL=2,      ICBRK=1,       ICE=1,
ICKV=0,        IECC=2,        IFPSM=2,       IFPSV=2,
IPDEF=0,       IPDTL=7,      IPLOT=0,       ISPRA=1,
ITRAN=1,       IU=0,         IXPL=0,       NINTER=20,
NPAIR=0,       TAP=1.0512E6, TIME=0.0,      VOLC=1.191E6,
$END

$NLINTL
EW(1)=20*0.0,
T(1)=20*0.0,
W(1)=20*0.0,
$END

STEEL          CONCRETE
UC DOME        UC CONCRETE UC STEEL  UP STEEL  LC STEEL  LC CONCRETE
DE STEEL       DE CONCRETE ICE STEEL

$NLSLAB
DEN(1)=489.0,150.0,
DTD(1)=15*0.0,
HC(1)=0.115,0.192,
HIF(1)=15*0.0,
IPRINT=0,
IVL(1)=4*2,4*1,2,6*0,
IVR(1)=4*2,4*1,2,6*0,
MAT1(1)=1,2,3*1,2,1,2,1,6*0,

```

MAT2(1)=1,2,1,2*1,2,1,2,1,6*0,
 NMAT=2,
 NNO1(1)=3,10,3,2,5,10,4,10,3,6*0,
 NNO2(1)=15*0,
 NOD(1)=1,14,19,24,48,
 NSLAB=9,
 SAREA(1)=18967.,25116.,21511.,4823.,32309.,45777.,
 19740.,35059.,285948.,6*0.0,
 TC(1)=26.0,0.8,3*0.0,
 TEMP(1)=18*85.0,29*100.0,3*20.0,150*0.0,
 X(1)= .0, .0209, .0417,
 .0, .151, .302, .453, .604, .755, .906,
 1.056, 1.207, 1.358,
 .0, .023, .0459,
 .0, .00522,
 .0, .057, .113, .170, .226,
 .0, .172, .344, .516, .688, .860, 1.032,
 1.204, 1.376, 1.549,
 .0, .034, .068, .102,
 .0, .163, .327, .490, .653, .817, .980,
 1.143, 1.307, 1.470,
 .0, .00633, .01268,

\$END

\$NLECC

ACMO=2.480E5, CSPRC=0.143, DTSUB=-100.0, ECCRC=0.343,
 NP=0,
 P(1)=6*0.0,
 PACMO=454.7, PHH=2500.0, PLH=181.0, PSIS=1513.0,
 PUHIO=1064.7, RWSTM=2.9007E6, STP(1)=6*1.0E6,
 STPHH=1.0E6, STPLH=1.0E6, STPSIS=1.0E6,
 TACM=100.0,
 TMMH=39.15, TMLH=39.15, TMSIS=39.15,
 TM(1)=6*0.0,
 TRWST=100.0, TUHI=100.0, UHIO=6.200E4,
 WEC(1)=6*0.0,
 WHH1=-641.0, WLH1=-6850.0, WSIS1=-859.0,
 WTCAV=100.0,

\$END

\$NLECX

EQR=3.74E7, ETP1R=137.0, ETS1R=95.0, EWPR=2.47E4,
 EWSR=4.12E4,

\$END

\$NLCSX

SQR=2.526E8, STP1R=190.0, STS1R=85.0,
 SWPR=6.60E4, SWSR=9.64E4,

\$END

\$NLCOOL

CQR=0.0, CTPR=0.0, CTSR=0.0, VAP=0.0,
 CWPR=0.0, CWSR=0.0,
 JCOOL=0, NCOOL=0, PCOOL=0.0, POFF=0.0,

QRCOOL=0.0, TCOOL=0.0,
 \$END
 \$NLMACE
 AREA(1)=4256.0,7350.0,6*0.0,
 AVBRK=0.0,
 BK(1,1)=0.0, BK(1,2)=30.5, BK(2,1)=10.5, BK(2,2)=0.0,
 CVBRK=0.0,
 C1(1)=17.7,17.7,1.0,7*0.0,
 C2(1)=9500.0,8.0E4,8*0.0,
 C3(1)=100.0,2.00,8*0.0,
 C4(1)=400.0,0.0,8*0.0,
 DCF=100.0, DCFICE=100.0, DTO=0.05,
 DTPNT=10., DTS=5.0E3,
 FALL=0.7, FSPRA=0.0, HMAX=280.0,
 HUM(1)=2*0.30,6*0.0,
 IBETA=0, ICECUB=2, IDRY=1, IVENT=0, IWET=2,
 N=3,
 NC(1)=2,1,2,7*0,
 NCAV=1, NCUB=2, NRPV1=1, NRPV2=1, NRPV3=0,
 NS(1)=2,2,1,7*0,
 NSMP=1, NSMP2=1,
 NT(1)=1,8,9,7*0,
 PO=14.7, PVNT=0.0, STPECC=1.0E6, STPSPR=1.0E6,
 TEMPO(1)=100.0,85.0,6*0.0,
 TICE=32.0, TPOOL=0.0, TSTM=105.0, TVNT1=0.0,
 TVNT2=0.0, TWTR=190.0, TWTR2=98.6,
 VC(1)=3.830E5,8.084E5,6*0.0,
 VCAV=15000.0, VDRY=0.0, VFLR=51000.0, VTORUS=0.0,
 WICE=2.45E6, WPOOL=0.0, WVMAKS=5.221E5,
 WVMAX=0.0,
 \$END
 \$NLBOIL
 AB(1)=16*0.0,
 ABRK=2.182E-2, ACOR=51.1,
 AH(1)=196.0,72.0,2.060E5,160.0,2.036E3,326.0,
 ANSK=0.0,
 AR(1)=51.1,4.13,44.4,0.0,-2.00,-10.0,
 ATOT=101.20,
 CM(1)=669.0,1.044E3,4.180E5,887.0,1.470E4,8.768E3,
 CLAD=1.923E-3, CSRV=151.7,
 D=3.117E-2, DC=11.06,
 DD(1)=0.580,2.29,6.460E-2,5.770E-2,0.123,0.438,
 DF=2.688E-2, DH=3.863E-2, DPART=0.0164,
 DTK=1.0E3, DTPN=5.0, DTPNTB=10.,
 DUO2=2.688E-2,
 F(1)=0.230,0.540,0.770,0.960,1.11,1.22,1.29,1.33,1.32,1.28,
 1.24,1.21,1.18,1.17,1.18,1.22,1.22,1.17,1.09,0.98,
 0.85,0.68,0.49,0.27,
 FCOL=0.95, FDCR=-1.0, FDROP=0.95, FM=0.0,
 FR=0.0, FULSG=3.676E5,

FZMCR=1.0,
 FZOCR=1.0, FZOS1=0.0, F12=0.445,
 H=12.0, HO=104.0, HW=300.0,
 ICON=-1, IFP=2, IGRID1=1, IGRID2=0,
 IHC=0, IHEAD=-1, IHR=1,
 IMWA=3, IMZ=100,
 ISAT=0, ISG=3, ISRV=1, ISTM=0, ISTR=3,
 KRPS=0, MELMOD=-1, MWORNL=0, NDTM=1.0E5,
 NDZ=24, NDZDRP=2, NNT=55777, NR=50952,
 PF(1)=1.18,1.18,1.17,1.15,1.12,1.05,0.99,0.85,0.74,0.57,
 PSET=2500.0, PSG=1185.0, PVSL=2250.0,
 QPUMP1=0.0, QPUMP2=0.0, QZERO=1.16417E10,
 RHOCU=58.6, R1=1, R2=10,
 TAFW=100.0, TALF1=1.0E10, TALF2=1.0E10,
 TB(1)=16*1.0E6, TCAV=1100.0, TDK=0.0,
 TFAIL=1832.0, TFEOO=618.0, TFUS=5320.0,
 TGOO=580.0,
 TMAFW=1.0, TMELT=4130.0,
 TMLEG(1)=3*1.0E6,
 TMSG1=1.0E6, TMSG2=1.0E6, TMUP1=1.0E6, TMUP2=1.0E6,
 TMYBK=1.0E6, TPM=1.0, TPN=20.0, TPUMP1=1.0E6,
 TPUMP2=1.0E6, TRPS=0.0,
 TSB(1)=0.25,0.02,0.25,1.0,
 TSCT(1)=0.0,37.0,42.0,1.0E10,
 TT(1)=613.0,610.0,494.0,580.0,580.0,580.0,
 VF(1)=10*0.10,
 VOLP=12145.0, VOLS=356.0, WAFW=13000., WATBH=4.781E4,
 WCST=3.30E6, WDED=30489.0,
 WFE2=5.52E4, WMUP1=0.0, WMUP2=0.0, WTRSG=3.676E5,
 XOO=3.28E-6, YB=0.0, YBRK=16.2, YBRK2=1.0E3,
 YLEG=16.2, YLEG2=1.0E3, YT=0.0,
 \$END
 \$NLRAD
 ECROS=0.70, ELONG=0.214, ESTRU=0.60, EWAT=0.95,
 IAXC=0, ICONV=0,
 IRAD=0, PITCH=.04133, WBAR=4770.0,
 \$END
 \$NLHEAD
 COND=5.0, DBH=14.4, E1=0.8, E2=0.5,
 FOPEN=0.0,
 THICK=0.436, TMLT=4130.0, TVSL=500.0,
 WFEC=1.080E4, WGRID=1.280E5, WHEAD=7.760E4,
 WUO2=222739.0, WZRC=50913.0,
 \$END
 \$NLHOT
 CON=5.0, DP=0.197, FLRMC=0.0, IHOT=101, MWR=0,
 NSTOP=1000, TPOOLH=125.0, WTR=0.0,
 \$END
 \$NLINTR
 CAYC=1.50E-2, CPC=1.45, DENSC=2.35, DPRIN=7200.0,

DT=0.50,
EPSI(1)=0.50,0.50,8*0.0,
FC1=0.460, FC2=0.140, FC3=0.360, FC4=4.0E-2,
FIOPEN=1.0,
HIM=1.0E-2, HIO=1.0E-2, IGAS=1, IWRC=1,
NEPS=2, R=6.0E3, RBR=0.135, RO=259.0,
TAUL=0.50, TAUS=5.0, TEPS(1)=0.0,3.6E7,8*0.0,
TIC=302.5, TF=3.601E4, TPRIN=0.,
WALL=1.0E6, ZF=1000.0,
\$END

Case B.00

\$NLECC
TMHH=39.15, TMLH=39.15, TMSIS=39.15,

Case F.00

\$NLECC
TMHH=59.7, TMLH=1.0E6, TMSIS=1.0E6,
\$NLBOIL
ABRK=0.1963,
TSCT(1)=0.0,40.0,80.0,1.0E10,

Case G.00

\$CHANGE
TRST=120.,
\$NLECC
TMHH=54.1, TMLH=1.0E6, TMSIS=1.0E6,
\$NLBOIL
ABRK=0.1963,
TSCT(1)=0.0,40.0,80.0,1.0E10,

Case H.00

\$CHANGE
TRST=50.,
\$NLECC
PLH=2500.,
STPHH=22.50, STPSIS=22.50,
TMHH=0.0, TMLH=53.80, TMSIS=0.0E6,
WLH1=-641.0,
\$NLBOIL
ABRK=0.1963,
TSCT(1)=0.0,40.0,80.0,1.0E10,

Case L.00

\$CHANGE
TRST=300.,
\$NLMAR
IBRK=0,
\$NLECC
TMHH=141.6, TMLH=0.0, TMSIS=0.0,
\$NLMACE
N=2,
\$NLBOIL
AB(1)=0.0308,15*0.0,
ABRK=0.0,
TB(1)=141.6,15*1.0E6,
TMAFW=1.0E+6,
TSCT(1)=0.0,135.0,170.0,1.0E10,
YBRK=105,

Case M.00

\$CHANGE
TRST=300.,
\$NLMAR
IBRK=0,
\$NLECC
TMHH=140.7, TMLH=140.7, TMSIS=140.7,
\$NLMACE
C1(1)=140.7,140.7,1.0,7*0.0,
N=2,
NS(1)=1,1,1,7*0,
\$NLBOIL
AB(1)=0.0308,15*0.0,
ABRK=0.0,
TB(1)=140.7,15*1.0E6,
TMAFW=1.0E6,
TSCT(1)=0.0,135.0,170.0,1.0E10,
YBRK=105,

APPENDIX C

MARCH INPUT FOR CORE-MELTDOWN CASES

This appendix contains all of the MARCH input information used to make the runs for the core-meltdown cases. A full MARCH input deck is found here for case D.00. For other cases, any parameter values that differed from those for case D.00 are listed.

Case D.00

```

111182SQS2D      SQS2D--SEQUOYAH S2D, 2 IN., 100% OXIDATION
$CHANGE
ACBRK=-1.0, CPSTP=500.0, FDRP=-1.0,
HIMX=-1.0, HIOX=-1.0, ID=830601, IFISH=-1,
IFPM=10, IFPV=10, IGASX=10, IHOTX=10,
IPLT=0, IS=6, JS=0, LST7=1, MEL=10,
NCRST=1, NCT7=1, PFAIL=-1.0, PRST=1000.0,
TFX=-1.0, TMX=-1.0, TRST=90., WALLX=-1.0,
$END
SEQUOYAH--S2D, 2 IN., 100% OXIDATION
$NLMAR
DTINIT=0.02, H2HI=0.08, H2LO=0.0, HIOXY=0.05,
HIG=0.55, H2UP=0.041, H2HZ=0.06, H2DN=0.09,
H2VO=352.8, H2VX=11650., H2DIST(1)=90.0,110.0,
IBLDF=0, IBLDI=0, IBLDP=0,
IBRK=1, IBURN=1, IBURNL=2,
ICBRK=1, ICE=1, ICKV=0, IECC=2,
IFPSM=2, IFPSV=2,
IPDEF=0, IPDTL=7, IPLT=0,
ISPRA=1, ITRAN=1, IU=0, IXPL=0,
NINTER=20, NPAIR=0, TAP=1.0512E6, TIME=0.0,
VOLC=1.191E6,
$END
$NLINTL
EW(1)=20*0.0,
T(1)=20*0.0,
W(1)=20*0.0,
$END
STEEL      CONCRETE
UC DOME    UC CONCRETE UC STEEL  UP STEEL  LC STEEL  LC CONCRETE
DE STEEL   DE CONCRETE ICE STEEL
$NL SLAB
DEN(1)=489.0,150.0,
DTD(1)=15*0.0,
HC(1)=0.115,0.192,
HIF(1)=15*0.0,

```

```

IPRINT=0,
IVL(1)=4*2,4*1,2,6*0,
IVR(1)=4*2,4*1,2,6*0,
MAT1(1)=1,2,3*1,2,1,2,1,6*0,
MAT2(1)=1,2,1,2*1,2,1,2,1,6*0,
NMAT=2,
NNO1(1)=3,10,3,2,5,10,4,10,3,6*0,
NNO2(1)=15*0,
NOD(1)=1,14,19,24,48,
NSLAB=9,
SAREA(1)=18967.,25116.,21511.,4823.,32309.,45777.,19740.,
35059.,285948.,6*0.0,
TC(1)=26.0,0.8,3*0.0,
TEMP(1)=18*85.0,29*100.0,3*20.0,150*0.0,
X(1)=.0, .0209, .0417,
.0, .151, .302, .453, .604, .755, .906,
.0, 1.056, 1.207, 1.358,
.0, .023, .0459,
.0, .00522,
.0, .057, .113, .170, .226,
.0, .172, .344, .516, .688, .860, 1.032,
.0, 1.204, 1.376, 1.549,
.0, .034, .068, .102,
.0, .163, .327, .490, .653, .817, .980,
.0, 1.143, 1.307, 1.470,
.0, .00633, .01268,

$END
$NLECC
ACMO=2.480E5, CSPRC=0.143, DTSUB=-100.0, ECCRC=0.343,
NP=0,
P(1)=6*0.0, PACMO=454.7,
PHH=2500.0, PLH=131.0, PSIS=1513.0, PUHIO=1064.7,
RWSTM=2.9007E6,
STP(1)=6*1.0E6,
STPHH=1.0E6, STPLH=1.0E6, STPSIS=1.0E6,
TACM=100.0,
TMHH=1.0E6, TMLH=1.0E6, TMSIS=1.0E6,
TM(1)=6*0.0,
TRWST=100.0, TUHI=100.0, UHIO=6.200E4,
WEC(1)=6*0.0,
WHH1=-641.0, WJH1=-6850.0, WSIS1=-859.0,
WTCAV=100.0,
$END
$NLECX
EQR=3.74E7, ETP1R=137.0, ETS1R=95.0, EWPR=2.47E4,
EWSR=4.12E4,
$END
$NLCSX
SQR=2.526E8, STP1R=190.0, STS1R=85.0, SWPR=6.60E4,
SWSR=9.64E4,
$END

```

\$NLCOOL

CQR=0.0, CTPR=0.0, CTSR=0.0,
CVAP=0.0, CWPR=0.0, CWSR=0.0,
JCOOL=0, NCOOL=0,
PCOOL=0.0, POFF=0.0, QRCOOL=0.0, TCOOL=0.0,
\$END

\$NLMACE

AREA(1)=4256.0,7350.0,6*0.0,
AVBRK=0.0,
BK(1,1)=0.0, BK(1,2)=30.5, BK(2,1)=10.5, BK(2,2)=0.0,
CVBRK=0.0,
C1(1)=17.7,17.7,1.0,7*0.0,
C2(1)=9500.0,8.0E4,8*0.0,
C3(1)=100.0,2.00,8*0.0,
C4(1)=400.0,0.0,8*0.0,
DCF=100.0, DCFICE=100.0,
DTO=0.05, DTPNT=10.0, DTS=5.0E3,
FALL=0.7, FSPRA=0.0, HMAX=280.0,
HUM(1)=2*0.30,6*0.0,
IBETA=0, ICECUB=2, IDRY=1,
IVENT=0, IWET=2,
N=3,
NC(1)=2,1,2,7*0, NCAV=1,
NCUB=2, NRPV1=1, NRPV2=1, NRPV3=0,
NS(1)=2,2,1,7*0,
NSMP=1, NSMP2=1,
NT(1)=1,8,9,7*0,
PO=14.7, PVNT=0.0, STPECC=1.0E6, STPSPR=1.0E6,
TEMPO(1)=100.0,85.0,6*0.0,
TICE=32.0, TPOOL=0.0, TSTM=105.0,
TVNT1=0.0, TVNT2=0.0, TWTR=190.0, TWTR2=98.6,
VC(1)=3.830E5,8.084E5,6*0.0,
VCAV=15000.0, VDRY=0.0, VFLR=51000.0, VTORUS=0.0,
WICE=2.45E6, WPOOL=0.0,
WVMAKS=5.221E5, WVMAX=0.0,
\$END

\$NLBOIL

AB(1)=16*0.0,
ABRK=2.182E-2, ACOR=51.1,
AH(1)=196.0,72.0,2.060E5,160.0,2.036E3,326.0,
ANSK=0.0,
AR(1)=51.1,4.13,44.,0.0,-2.00,-10.0,
ATOT=101.20,
CM(1)=669.0,1.044E3,4.180E5,887.0,1.470E4,8.768E3,
CLAD=1.923E-3, CSRV=151.7,
D=3.117E-2, DC=11.06,
DD(1)=0.580,2.29,6.460E-2,5.770E-2,0.123,0.438,
DF=2.688E-2, DH=3.863E-2, DPART=1.640E-2,
DTK=1.0E3, DTPN=5.0, DTPNTB=10.0,
DUO2=2.688E-2,

F(1)=0.230,0.540,0.770,0.960,1.11,1.22,1.29,1.33,1.32,1.28,
1.24,1.21,1.18,1.17,1.18,1.22,1.22,1.17,1.09,0.98,
0.85,0.68,0.49,0.27,

FCOL=0.728,

FDCR=1.0, FDROP=0.728, FM=0.0, FR=0.0,

FULSG=3.676E5,

FZMCR=1.0, FZOCR=1.0, FZOS1=0.0, F12=0.445,

H=12.0, HO=104.0, HW=300.0,

ICON=-1, IFP=2, IGRID1=1, IGRID2=0,

IHC=0, IHEAD=-1, IHR=1,

IMWA=3, IMZ=100,

ISAT=0, ISG=3, ISRV=1, ISTM=0, ISTR=3,

KRPS=0, MELMOD=1, MWORNL=0,

NDTM=1.0E5, NDZ=24, NDZDRP=2,

NNT=55777, NR=50952,

PF(1)=1.18,1.18,1.17,1.15,1.12,1.05,0.99,0.85,0.74,0.57,

PSET=2500.0, PSG=1185.0, PVSL=2250.0,

QPUMP1=0.0, QPUMP2=0.0, QZERO=1.16417E10,

RHOCU=58.6, R1=1, R2=10,

TAFW=100.0, TALF1=1.0E10, TALF2=1.0E10,

TB(1)=16*1.0E6,

TCAV=1100.0, TDK=0.0, TFAIL=1832.0,

TFEOO=618.0, TFUS=5320.0,

TGOO=580.0,

TMAFW=1.0, TMELT=4130.0,

TMLEG(1)=3*1.0E6,

TMSG1=1.0E6, TMSG2=1.0E6, TMUP1=1.0E6, TMUP2=1.0E6,

TMYBK=1.0E6, TPM=1.0,

TPN=20.0, TPUMP1=1.0E6, TPUMP2=1.0E6, TRPS=0.0,

TSB(1)=4*0.25,

TSCT(1)=0.0,3*1.0E10,

TT(1)=613.0,610.0,494.0,580.0,580.0,580.0,

VF(1)=10*0.10,

VOLP=12145.0, VOLS=356.0,

WAFW=13000., WATBH=4.781E4,

WCST=3.30E6, WDED=30489.0,

WFE2=5.52E4, WMUP1=0.0, WMUP2=0.0,

WTRSG=3.676E5, XOO=3.28E-6,

YB=0.0, YBRK=16.2, YBRK2=1.0E3,

YLEG=16.2, YLEG2=1.0E3, YT=0.0,

\$END

\$NLRAD

ECROS=0.70, ELONG=0.214, ESTRU=0.60, EWAT=0.95,

IAXC=0, ICONV=0, IRAD=0, PITCH=.04133,

WBAR=4770.0,

\$END

\$NLHEAD

COND=5.0, DBH=14.4, E1=0.8, E2=0.5,

FOPEN=0.0,

THICK=0.436, TMLT=4130.0, TVSL=500.0,

WFEC=1.080E4, WGRID=1.280E5, WHEAD=7.760E4,

WUO2=222739.0, WZRC=50913.0,

\$END

\$NLHOT
CON=5.0, DP=0.197, FLRMC=0.0, IHOT=101,
MWR=0, NSTOP=200, TPOOLH=125.0, WTR=0.0,
\$END

\$NLINTR
CAYC=1.50E-2, CPC=1.45,
DENSC=2.35, DPRIN=7200.0, DT=0.50,
EPSI(1)=0.50, 0.50, 8*0.0,
FC1=0.460, FC2=0.140, FC3=0.360, FC4=4.0E-2,
FIOOPEN=1.00,
HIM=1.0E-2, HIO=1.0E-2, IGAS=1, IWRC=1,
NEPS=2, R=6.0E3, RBR=0.135, RO=259.0,
TAUL=0.50, TAUS=5.0,
TEPS(1)=0.0, 3.6E7, 8*0.0,
TIC=302.5, TF=3.601E4, TPRIN=0.0,
WALL=1.0E6, ZF=1000.0,
\$END

Case E.00

\$CHANGE
TRST=100.,
\$NLBOIL
DPART=0.15,
FDCR=-0.4,
IMWA=1,

Case J.00

\$CHANGE
MEL=-1,
TRST=250.,
\$NLMAR
IECC=-2,
ISPRA=-1,
\$NLECC
TMHH=0.0, TMLH=0.0, TMSIS=0.0,
\$NLBOIL
ABRK=1.9635E-1,
\$NLHOT
NSTOP=1000,

Case K.00

\$CHANGE
MEL=-1,
TRST=250.,
\$NLMAR
IECC=-2,
ISPRA=-1,

\$NLECC
TMHH=0.0, TMLH=0.0, TMSIS=0.0,
\$NLBOIL
ABRK=1.9635E-1,
DPART=0.15,
FDCR=-0.4,
IMWA=1,
\$NLHOT
NSTOP=1000,

Case N.00

\$CHANGE
CPSTP=599.0,
TRST=180.,
\$NLMAR
H2HI=0.12,
IBRK=0,
ISPRA=0,
\$NLMACE
C1(1)=10*0.0,
C2(1)=10*0.0,
C3(1)=10*0.0,
C4(1)=10*0.0,
N=0,
NC(1)=10*0,
NS(1)=10*0,
NT(1)=10*0,
\$NLBOIL
ABRK=0.0,
TMAFW=1.0E6,
\$NLHOT
NSTOP=1000,

Case O.00

\$CHANGE
TRST=250.,
\$NLMAR
H2HI=0.12,
IBRK=0,
ISPRA=0,
\$NLMACE
C1(1)=10*0.0,
C2(1)=10*0.0,
C3(1)=10*0.0,
C4(1)=10*0.0,
N=0,
NC(1)=10*0,
NS(1)=10*0,
NT(1)=10*0,

```
$NLBOIL  
  ABRK=0.0,  
  DPART=0.15,  
  FDCR=-0.4,  
  IMWA=1,  
  TMAFW=1.0E6,  
$NLHOT  
  NSTOP=1000,
```

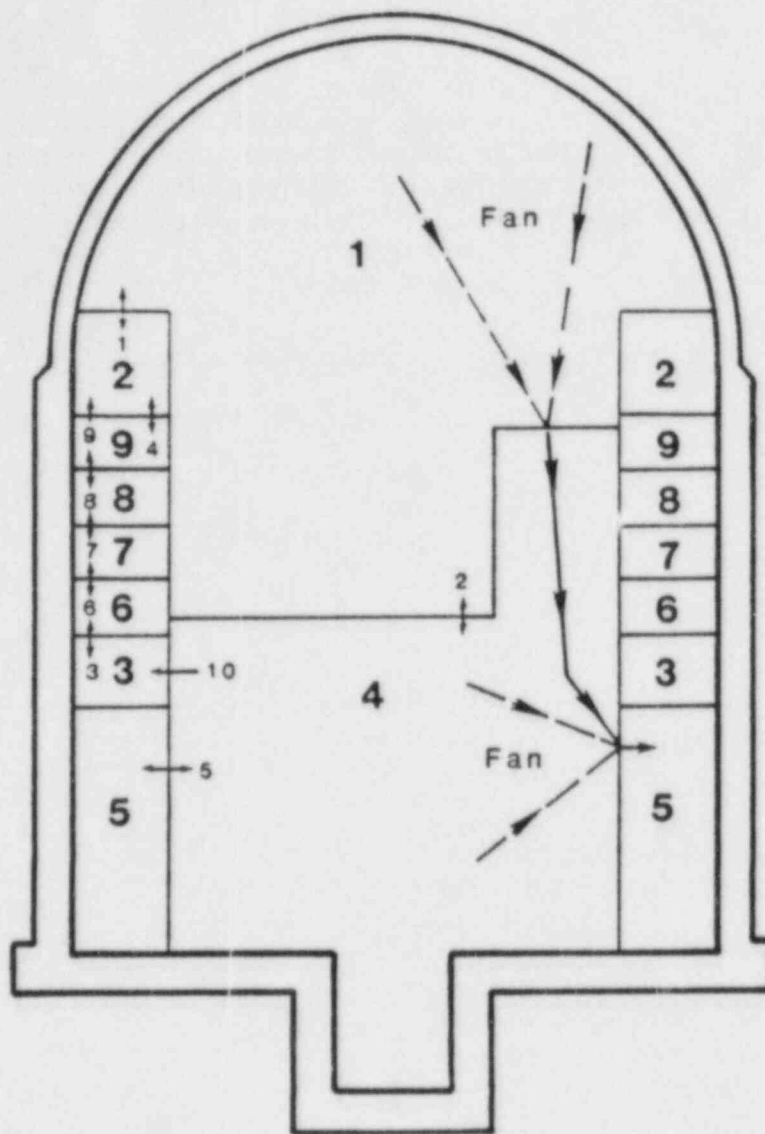
Case P.00

```
$CHANGE  
  CPSTP=599.0,  
  TRST=180.,  
$NLMAR  
  H2HI=0.12,  
  IBRK=0,  
  ISPRA=0,  
$NLMACE  
  C1(1)=10*0.0,  
  C2(1)=10*0.0,  
  C3(1)=10*0.0,  
  C4(1)=10*0.0,  
  N=0,  
  NC(1)=10*0,  
  NS(1)=10*0,  
  NT(1)=10*0,  
$NLBOIL  
  ABRK=0.0,  
  FDCR=0.5,  
  TMAFW=1.0E6,  
$NLHOT  
  NSTOP=1000,
```


APPENDIX D

HECTR INPUT DESCRIPTION

The Sequoyah compartment and flow junction arrangement is shown in Figure D-1. Tables D-1 to D-7 describe the input used for most of the HECTR calculations. The input was formulated based on information in References 1 and 2. This input description applies specifically to case A.00 but is generally valid for the other cases as well. A listing of the input for Base A.00 is included in Table D-8 for those who desire more details.



KEY

- 1** - Compartment Number
- 1** - Flow Junction Number
- - One-way Flow Junction
- ↔** - Two-way Flow Junction

Note: Igniters Present in
Compartments 1, 2, 4, and 5.

Compartment Descriptors

- 1. Dome
- 2. Upper Plenum
- 3. Lower Plenum
- 4. Lower Compartment
- 5. Dead-Ended Region
- 6-9. Ice Compartments

Figure D-1. HECTR Ice-Condenser Containment Model

Table D-1

Compartment Input Data (Excluding Ice Condenser)

Compartment	Volume (m ³)	Relative Elevation (m)	Flame Propa- gation Length (m)	Temp. (K)	Initial Conditions			
					Partial Pressures (kPa)			
					H ₂ O	N ₂	O ₂	H ₂
1 Dome	18 435	29	17.5	303	0.345	81.475	21.5	0.0
2 Upper Plenum	1 330	29	9.0	273.5	0.620	81.2	21.5	0.0
3 Lower Plenum	685	10	3.5	273.5	0.620	81.2	21.5	0.0
4 Lower Compartment	8 184	0	12.0	311	0.620	81.2	21.5	0.0
5 Dead-Ended Region	2 662	0	6.0	311	0.620	81.2	21.5	0.0

Table D-2

Surface Input Data (Excluding Ice Condenser)

Sur- face	Compartment	Description	Area (m ²)	Thick- ness (m)
1	1	Steel Dome	1762	0.0127
2	1	Concrete	2333	0.414
3	1	Steel	2000	0.013
4	1	Thin-Walled Component	0.061935	0.003175
5	1	Thick-Walled Component	0.061935	0.01693
6	1	Transducer	0.0208	0.0064
7	2	Steel	1000	0.013
8	2	Thin-Walled Component	0.061935	0.003175
9	2	Thick-Walled Component	0.061935	0.01693
10	2	Transducer	0.0208	0.0064
11	3	Steel Walls	280	0.013
12	3	Ice Condenser Support Structure	2660	0.0081
13	3	Concrete Floor	310	0.1
14	4	Steel	3000	0.069
15	4	Concrete	3569	0.472
16	4	Sump	353	---
17	4	Thin-Walled Component	0.061935	0.003175
18	4	Thick-Walled Component	0.061935	0.01693
19	4	Transducer	0.0208	0.0064
20	5	Steel	1834	0.031
21	5	Concrete	3257	0.448

Table D-3
Flow Junction Input Data

Junction*	Area (m ²)	Flow Coefficient	L/A Ratio for Inertial Term (m ⁻¹)
1	186	1.43	0.015
2**	0.204	1.5	1.0
3	167	0.2	0.044
4	1.8581	1.5	0.2
5	27.7	4.2	0.007
6	167	0.2	Calculated
7	167	0.2	Calculated
8	167	0.2	Calculated

*See Figure A-1.

**Junction 2 is removed when the sprays are initiated or when the sump volume exceeds 750 m³.

Table D-4
Ice-Condenser Door Input Data

	Junction*	
	9	10
Maximum Area (m ²)	91.3	78.0
Differential Pressure to Open (kPa)	0.2634	0.0
Differential Pressure for Full Open (kPa)	37.91	0.14207
Maximum Open Angle (°)	89	55
Flow Coefficient	0.2	0.089
L/A Ratio for Inertial Term (m ⁻¹)	0.049	0.0055

*See Figure D-1.

Table D-5
Fan Input Data

	Fan 1	Fan 2
Connected Compartments	1 → 5	4 → 5
Setpoint Actuation Pressure (kPa)	121.59	121.59
Delay Time (s)	600	600
Maximum Flow Rate (m ³ /s)	54.7	1.17
Shutoff Head (kPa)	1.327	1.327

Table D-6
Ice-Condenser Input Data

Total Ice Mass*	1.11 x 10 ⁶ kg
Ice Surface Area	2.48 x 10 ⁴ m ²
Ice Volume	2.0 x 10 ³ m ³
Total Height	14.53 m
Wall Area	2058 m ²
Wall Mass	2.0 x 10 ⁵ kg
Basket Area	9920 m ²
Basket Mass	1.47 x 10 ⁵ kg
Drain Temperature	310 K
Initial Gas Volume	2444 m ³
Ice Temperature	273.5 K
Initial Gas and Surface Temperature	273.5 K
Initial Partial Pressures	
H ₂ O	0.620 kPa
N ₂	81.2 kPa
O ₂	21.5 kPa
H ₂	0.0 kPa

*The ice condenser is divided into four identical compartments. Values in the table are for the complete ice condenser.

Table D-7
Spray Input Data

Flow Rate	0.599 m ³ /s
Number of Drop Sizes	2
Frequency of 1st Drop Size	0.95
Frequency of 2nd Drop Size	0.05
Diameter of 1st Drop	309 μm
Diameter of 2nd Drop	810 μm
Pressure Setpoint	121.59 kPa
Delay Time	30 s
Fall Height	16 m
Injection Temperature*	311 K

*Once the sprays are switched to the recirculation mode, the temperature is calculated in HECTR based on the sump temperature and heat exchanger values.

Table D-8

Input Listing for HECTR Case A.00

```
SEQUOYAH CASE A.00$
HECTR VERSION 0.1
8 % IGNITION
TIME STEPS      MAX
FLOW            0.5
HEAT TRANS      0.5
SOURCE TERMS - MARCH - APPROX 75% CLAD REACTION
FANS AUTO
SPRAYS AUTO
35000. ! FAILURE PRESSURE (36 PSIG)
5 4 ! NUMBER OF COMPARTMENTS EXCLUDING ICE REGION, SUMP VOLUME
!
! FOR EACH COMPARTMENT: THE VOLUME, ELEVATION, FLAME PROPAGATION
! LENGTH,
! NUMBER OF SURFACES, AND AN INTEGER SPECIFYING WHETHER OR NOT
! THE SPRAYS GO DIRECTLY TO THE SUMP.
!
UPPER COMPARTMENT$
18435.
29.
17.5
6
1
UPPER PLENUM$
1330.
29.
9.0
4
0
LOWER PLENUM$
685.
10.
3.5
3
0
LOWER COMPARTMENT$
8184.
0.
1.2.0
6
0
DEAD ENDED REGIONS$
2662.
0.
6.0
2
```

Table D-8

Input Listing for HECTR Case A.00
(continued)

```

0
!
! FOR EACH SURFACE: TYPE OF SURFACE (1-SLAB,2-LUMPED MASS,3-POOL),
! MASS OF SURFACE, AREA OF SURFACE, FRACTION OF AREA FOR RADIATION
! CALCULATIONS, THICKNESS, CHARACTERISTIC LENGTH, THERMAL DIFFUSIVITY,
! THERMAL CONDUCTIVITY, SPECIFIC HEAT, EMISSIVITY, INTEGER INDICATING
! WHETHER OR NOT THE CONDENSATE GOES DIRECTLY TO THE SUMP, AND NODE
! INFORMATION (0'S INDICATE THE NODING WILL BE DONE INTERNALLY). NOTE
! THAT SOME OF THE NUMBERS SET TO 1. ARE NOT USED FOR THAT SURFACE TYPE.
!
! UPPER COMPARTMENT SURFACES
!
DOMES$
1 1. 1762. 1. .0127 8.0 1.28E-5 47.25 1. .9 1
0. 0 0
UPPER COMPARTMENT CONCRETES$
1 1. 2333. 1. .414 5. 5.8E-7 1.454 1. .9 1
0. 0 0
UPPER COMPARTMENT STEELS$
1 1. 2000. 1. .013 1. 1.28E-5 47.25 1. .9 1
0. 0 0
U.C. THIN WALLED COMPONENTS$
1 1. .061935 1. .003175 .1016 7.4E-5 182. 1. .89 1
0. 0 0
U.C. THICK WALLED COMPONENTS$
1 1. .061935 1. .01693 .1016 7.4E-5 182. 1. .89 1
0. 0 0
U.C. TRANSDUCERS$
1 1. .0208 1. .0064 .1625 1.42E-5 52. 1. .9 1
0. 0 0
!
! UPPER PLENUM SURFACES
!
UPPER PLENUM STEELS$
1 1. 1000. 1. .013 5. 1.28E-5 47.25 1. .9 1
0. 0 0
U.P. THIN WALLED COMPONENTS$
1 1. .061935 1. .003175 .1016 7.4E-5 182. 1. .89 1
0. 0 0
U.P. THICK WALLED COMPONENTS$
1 1. .061935 1. .01693 .1016 7.4E-5 182. 1. .89 1
0. 0 0
U.P. TRANSDUCERS$
1 1. .0208 1. .0064 .1625 1.42E-5 52. 1. .9 1
0. 0 0
!

```

Table D-8

Input Listing for HECTR Case A.00
(continued)

```

! LOWER PLENUM SURFACES
!
LOWER PLENUM WALLS$
1 1. 280. 1. .013 3. 1.28E-5 47.25 1. .9 1
0. 0 0
ICE-CONDENSER SUPPORT STRUCTURES$
1 1. 2660. 1. .0081 .2 1.28E-5 47.25 1. .9 1
0. 0 0
LOWER PLENUM FLOORS$
1 1. 310. 1. .1 4. 5.8E-7 1.454 1. .9 1
0. 0 0
!
! LOWER COMPARTMENT SURFACES
!
LOWER COMPARTMENT STEELS$
1 1. 3000. 1. .069 2. 1.28E-5 47.25 1. .9 1
0. 0 0
LOWER COMPARTMENT CONCRETES$
1 1. 3569. 1. .472 4. 5.8E-7 1.454 1. .9 1
0. 0 0
SUMP SURFACES$
3 1. 353. 1. 1. 6. 1. 1. .94 1
L.C. THIN WALLED COMPONENTS$
1 1. .061935 1. .003175 .1016 7.4E-5 182. 1. .89 1
0. 0 0
L.C. THICK WALLED COMPONENTS$
1 1. .061935 1. .01693 .1016 7.4E-5 182. 1. .89 1
0. 0 0
L.C. TRANSDUCERS$
1 1. .0208 1. .0064 .1625 1.42E-5 52. 1. .9 1
0. 0 0
!
! DEAD ENDED COMPARTMENT SURFACES
!
DEAD ENDED STEELS$
1 1. 1834. 1. .031 4. 1.28E-5 47.25 1. .9 1
0. 0 0
DEAD ENDED CONCRETES$
1 1. 3257. 1. .448 4. 5.8E-7 1.454 1. .9 1
0. 0 0
!
! FLOW JUNCTION DATA: COMPARTMENT ID'S, FLOW AREA, LOSS COEFFICIENT, L/A
! RATIO, AND TYPE OF CONNECTION (1-WAY OR 2-WAY). COMPARTMENT ID OF 0
! INDICATES THE ICE-CONDENSER. JUNCTIONS WITHIN THE ICE-CONDENSER ARE SET
! UP INTERNALLY.

```

Table D-8

Input Listing for HECTR Case A.00
(continued)

```

!
2 1 186. 1.43 .015 2
4 1 .204 1.5 1.0 2
3 0 167. 0.2 .044 2
0 2 1.8581 1.5 0.2 2
5 4 27.7 4.2 .007 2
0 2 91.3 0.2 .049 1
4 3 78. 0.89 .0055 1
$
!
! COMPARTMENT RELATIONS: 1 FOR I ABOVE J, 0 FOR I BESIDE J, -1 FOR I
! BELOW J, 3 FOR I NOT CONNECTED TO J. UPPER RIGHT HALF OF MATRIX IS
! INPUT.
!
1 3 1 1
3 3 3
1 3
0
!
! ice-condenser INPUT
!
! LOWER AND UPPER PLENUM COMPARTMENTS
3 2
! ICE DESCRIPTION: TOTAL MASS, AREA, TEMPERATURE, LENGTH,
! EMISSIVITY,VOLUME.
1.11E6 2.48E4 273.5 14.53 .94 2.0E3
! WALL AND STRUCTURES IN ice-condenser (EXCLUDING BASKETS): MASS, AREA,
! SPECIFIC HEAT, EMISSIVITY
2.0E5 2058. 485.7 .9
! MASS OF BASKETS, AREA OF BASKETS, DRAIN TEMPERATURE.
1.47E5 9.92E3 310.
! ELEVATION OF BOTTOM FOURTH OF ICE, FLOW AREA, LOSS COEFFICIENT FOR
! EACH ICE JUNCTION, TOTAL FREE GAS VOLUME
13. 167. .2 2444.
!
! FAN DATA
! TEMP. AND PRESS. SETPOINTS, DELAY TIME.
1000. 121590. 600.
! COMPARTMENT ID'S, FLOW RATE, SHUTOFF HEAD (PA), EFFICIENCY.
! (- INDICATES USE OF HEAD CURVE)
1 5 -54.7 1327.3575 1.
4 5 -1.17 1327.3575 1.
$
!

```

Table D-8

Input Listing for HECTR Case A.00
(continued)

```

! RADIATIVE BEAM LENGTHS - UPPER RIGHT HALF OF MATRIX IS INPUT.
! ICE SURFACES ARE NOT INCLUDED HERE. (THEY ARE DONE INTERNALLY)
!
17.5 23. 20. 17.5 17.5 17.5 12. 12. 12. 12. 0. 0. 0. 0. 0. 0. 0. 0.
0. 0. 0.
10. 15. 20. 20. 20. 0. 0. 0. 0. 0. 0. 0. 0. 0. 0. 0. 0. 0.
10. 17.5 17.5 17.5 10. 10. 10. 10. 0. 0. 0. 0. 0. 0. 0. 0. 0. 0.
0. 0. 0. 12. 0. 0. 0. 0. 0. 0. 0. 0. 0. 0. 0. 0. 0. 0.
0. 0. 12. 0. 0. 0. 0. 0. 0. 0. 0. 0. 0. 0. 0. 0. 0. 0.
0. 12. 0. 0. 0. 0. 0. 0. 0. 0. 0. 0. 0. 0. 0. 0. 0. 0.
5. 5. 5. 5. 0. 0. 0. 0. 0. 0. 0. 0. 0. 0. 0. 0. 0. 0.
0. 0. 0. 0. 0. 0. 0. 0. 0. 0. 0. 0. 0. 0. 0. 0. 0. 0.
0. 0. 0. 0. 0. 0. 0. 0. 0. 0. 0. 0. 0. 0. 0. 0. 0. 0.
0. 0. 0. 0. 0. 0. 0. 0. 0. 0. 0. 0. 0. 0. 0. 0. 0. 0.
8. 5. 5. 0. 0. 0. 0. 0. 0. 0. 0. 0. 0. 0. 0. 0. 0. 0.
5. 3. 0. 0. 0. 0. 0. 0. 0. 0. 0. 0. 0. 0. 0. 0. 0. 0.
0. 0. 0. 0. 0. 0. 0. 0. 0. 0. 0. 0. 0. 0. 0. 0. 0. 0.
3. 3. 5. 3. 3. 3. 0. 0.
3. 5. 3. 3. 3. 0. 0.
0. 5. 5. 5. 0. 0.
0. 0. 0. 0. 0.
0. 0. 0. 0.
0. 0. 0.
3. 3.
3.
!

! VIEW FACTORS: UPPER RIGHT HALF OF MATRIX IS INPUT
! ICE SURFACES ARE NOT INCLUDED HERE.
!
.45 .3 .19993847 1.5818E-5 1.5818E-5 5.312E-6 .05 1.0545E-5
1.0545E-5 3.5414E-6 0. 0. 0. 0. 0. 0. 0. 0. 0. 0. 0. 0.
.6 .17341236 5.309E-6 5.309E-6 1.783E-6 0. 0. 0. 0. 0.
0. 0. 0. 0. 0. 0. 0. 0. 0. 0.
.5965434 9.29025E-6 9.29025E-6 3.12E-6 .025 1.5484E-6 1.5484E-6
5.2E-7 0. 0. 0. 0. 0. 0. 0. 0. 0. 0. 0. 0.
0. 0. 0. .0500087 0. 0. 0. 0. 0. 0. 0. 0. 0. 0. 0. 0. 0. 0.
0. 0. .0500087 0. 0. 0. 0. 0. 0. 0. 0. 0. 0. 0. 0. 0. 0.
0. .0500248 0. 0. 0. 0. 0. 0. 0. 0. 0. 0. 0. 0. 0. 0. 0.
.8617993 4.025775E-5 4.025775E-5 1.352E-5 0. 0. 0. 0. 0. 0. 0. 0. 0.
0. 0. 0.
0. 0. 0. 0. 0. 0. 0. 0. 0. 0. 0. 0. 0. 0. 0.
0. 0. 0. 0. 0. 0. 0. 0. 0. 0. 0. 0. 0. 0. 0.
0. 0. 0. 0. 0. 0. 0. 0. 0. 0. 0. 0. 0. 0. 0.
.4 .3 .3 0. 0. 0. 0. 0. 0. 0. 0. 0. 0.
.88345910 .084962 0. 0. 0. 0. 0. 0. 0. 0. 0.
0. 0. 0. 0. 0. 0. 0. 0. 0. 0.

```

Table D-8

Input Listing for HECTR Case A.00
(continued)

```

.4411473 .5 .0588333 8.258E-6 8.258E-6 2.773E-6 0. 0.
.53125134 .048446687 6.9414E-6 6.9414E-6 2.331E-6 0. 0.
0. 3.50907E-5 3.50907E-5 1.1785E-5 0. 0.
0. 0. 0. 0. 0.
0. 0. 0. 0.
0. 0. 0.
.36 .64
.6396193
!
! SPRAY INPUT
! NUMBER OF COMPARTMENTS WITH SPRAYS, AND ID OF THOSE COMPARTMENTS.
1
! SPRAY TEMP DURING INJECTION PHASE, FLOW RATE (M**3/S), NUMBER OF
! DROP SIZES, FREQUENCY AND DIAMETER (MICRONS) FOR EACH DROP SIZE.
3.11.
0.599
2
0.95 309.
0.105 810.
$
! COMPARTMENT ID AND SPRAY FALL HEIGHT FOR THAT COMPARTMENT.
1 15.
$
! TEMPERATURE AND PRESSURE SETPOINTS AND DELAY TIME FOR SPRAYS.
! HIGH TEMPERATURE INDICATES THAT NUMBER WON'T BE USED.
10000. 121590. 30.
! INJECTION TIME, RATED SPRAY FLOW RATE (KG/S), HEAT EXCHANGER RATED
! EFFECTIVENESS (W/K), SECONDARY SIDE INLET TEMP, RATED SECONDARY
! SIDE FLOW RATE (KG/S).
1915. 587. 3.74E6 301.5 7.55E2
! SIMULATION TIME
12000.
!
! COMPARTMENT INITIAL CONDITIONS: TEMP; PARTIAL PRESSURES OF STEAM,
! NITROGEN, OXYGEN, HYDROGEN; CONVECTIVE VELOCITY.
!
! UPPER COMPARTMENT
303.
345. 81475. 21500. 0.
.3
! UPPER PLENUM
273.5
620. 81200. 21500. 0.
.3

```

Table D-8

Input Listing for HECTR Case A.00
(continued)

```

! LOWER PLENUM
273.5
620. 81200. 21500. 0.
.3
! LOWER COMPARTMENT
311.
620. 81200. 21500. 0.
.3
! DEAD ENDED COMPARTMENT
311.
620. 81200. 21500. 0.
.3
! ice-condenser INITIAL CONDITIONS
273.5
620. 81200. 21500. 0.
! CLASIX source terms
!4 0.
!0. 4965.1 -2.63E5
!2172. 4796.4 -2.6367E5
!2478. 1129.23 -2.3893E5
!3180. 1347.78 -2.3655E5
!3804. 876.7 -2.3615E5
!4428. 538.81 -2.3215E5
!4752. 1219.12 -2.397E5
!5700. 488.96 -2.4072E5
!6012. 354.25 -2.4065E5
!6960. 132.26 -2.4002E5
!7062. 118.79 -2.3994E5
!7206. 102.22 -2.3936E5
!$
$
!4 0.
!0. 0. -257.
!3480. 0. -257.
!3804. 9.293 -144.
!4116. 58.5 24784.
!4428. 166.5 11669.
!4752. 240.8 11287.
!5700. 96.75 8671.
!6330. 50.18 7763.
!6648. 36. 7440.
!6960. 26.33 7177.
!8070. 8.258 7177.
!$
$

```

Table D-8

Input Listing for HECTR Case A.00
(continued)

```

! INITIAL SURFACE TEMPERATURES
! UPPER COMPARTMENT
303. 303. 303. 303. 303. 303.
! UPPER PLENUM
273.5 273.5 273.5 273.5
! LOWER PLENUM
273.5 273.5 273.5
! LOWER COMPARTMENT
311. 311. 311. 311. 311. 311.
! DEAD ENDED COMPARTMENT
311. 311.
!
! NAMELIST INPUT
!
XHMNIG=.08
! SET IGNITION LIMITS TO 1. IN LOWER PLENUM AND ice-condenser (NO
! IGNITERS)
XHMNIG( 3)=1.
XHMNIG( 6)=1.
XHMNIG( 7)=1.
XHMNIG( 8)=1.
XHMNIG( 9)=1.
! PROPAGATION TIME IN L.C. EQUAL .1 TIMES THE BURN TIME. KPROP = .5
! ELSEWHERE.
KPROP ( 4)=0.1
! MAX HEAT TRANSFER TIME STEP.
DTMPMX=10.0
DTHTMX=0.5
SPRAYS=AUTO
FANS =AUTO
MRCHSC=4
$

```

References for Appendix D

1. Letter from D. M. Mills, Tennessee Valley Authority, to E. Adensam, Director of Nuclear Reactor Regulation, USNRC, December 1, 1981.
2. Sequoyah Nuclear Plant, Final Safety Analysis Report, Tennessee Valley Authority.

Distribution List

Division of Technical Information
and Document Control
NRC Distribution Contractor
U.S. Nuclear Regulatory Commission
15700 Crabbs Branch Way
Rockville, MD 20850
275 copies for R3

U.S. Department of Energy (2)
Operational Safety Division
Albuquerque Operations Office
P.O. Box 5400
Albuquerque, NM 87185
Attn: J. R. Roeder, Director
Dr. M. Peehs

U.S. Nuclear Regulatory Commission (6)
Office of Nuclear Regulatory Research
Washington, DC 20555
Attn: G. A. Arlotto
R. T. Curtis
J. T. Larkins
L. C. Shao
K. G. Steyer
P. Worthington

Battelle Columbus Laboratory (2)
505 King Avenue
Columbus, OH 43201
Attn: P. Cybulskis
R. Denning

Bechtel Power Corporation
P.O. Box 3965
San Francisco, CA 94119
Attn: R. Tosetti

U.S. Nuclear Regulatory Commission (5)
Office of Nuclear Regulatory Research
Washington, DC 20555
Attn: B. S. Burson
M. Silberberg
J. L. Telford
T. J. Walker
R. W. Wright

Bechtel Power Corporation
15740 Shady Grove Road
Gaithersburg, MD 20877
Attn: D. Ashton

Brookhaven National Laboratory (2)
Upton, NY 11973
Attn: W. T. Pratt
G. Green

U.S. Nuclear Regulatory Commission (6)
Office of Nuclear Reactor Regulation
Washington, DC 20555
Attn: J. K. Long
J. F. Meyer
R. J. Palla
K. I. Parczewski
G. Quittschreiber
D. D. Yue

Duke Power Co. (2)
P.O. Box 33189
Charlotte, NC 28242
Attn: F. G. Hudson
A. L. Sudduth

U.S. Nuclear Regulatory Commission (5)
Office of Nuclear Reactor Regulation
Washington, DC 20555
Attn: V. Benaroya
W. R. Butler
G. W. Knighton
Z. Rosztoczy
C. G. Tinkler

EG&G Idaho (2)
Willow Creek Building, W-3
P.O. Box 1625
Idaho Falls, ID 83415
Attn: R. Gottula
S. Bailing

U.S. Nuclear Regulatory Commission (2)
Office of Nuclear Regulatory Research
Washington, DC 20555
Attn: M. A. Cunningham
B. Agrawal

Electric Power Research
Institute (3)
3412 Hillview Avenue
Palo Alto, CA 94303
Attn: J. J. Haugh
K. A. Nilsson
G. Thomas

Factory Mutual Research Corporation
P.O. Box 688
Norwood, MA 02062
Attn: R. Zalosh

Fauske & Associates
627 Executive Drive
Willowbrook, IL 60521
Attn: F. Henry

General Electric Co.
175 Curtner Avenue
Mail Code N 1C157
San Jose, CA 95125
Attn: K. W. Holtzclaw

Los Alamos National Laboratory (3)
P.O. Box 1663
Los Alamos, NM 87545
Attn: R. Gido
J. Travis
B. E. Boyack

Purdue University
School of Nuclear Engineering
West Lafayette, IN 47907
Attn: T. G. Theofanous

Sandia National Laboratories (20)
Directorate 6400
P.O. Box 5800
Albuquerque, NM 87185
Attn: R. Cochrell

Sandia National Laboratories (20)
Organization 6427
P.O. Box 5800
Albuquerque, NM 87185
Attn: G. Shaw

UCLA
Nuclear Energy Laboratory
405 Hilgard Avenue
Los Angeles, CA 90024
Attn: I. Catton

Westinghouse Corporation (3)
P.O. Box 355
Pittsburgh, PA 15230
Attn: N. Liparulo
J. Olhoeft
V. Srinivas

Westinghouse Hanford Company (3)
P.O. Box 1970
Richland, WA 99352
Attn: G. R. Bloom
L. Muhlstein
R. D. Peak

University of Wisconsin (2)
Nuclear Engineering Department
1500 Johnson Drive
Madison, WI 53706
Attn: M. L. Corradini
G. A. Moses

Maine Yankee Atomic Power Company
83 Edison Drive
Augusta, ME
Attn: John Garrity

New York Power Authority (2)
12th Floor
123 Main Street
White Plains, NY 10601
Attn: R. E. Deem
S. S. Iyer

Oak Ridge National Laboratory (2)
Bldg. 9104-1
Station 59, 9201-3
Y-12 Plant
Bear Creek Road
Oak Ridge, TN 37830
Attn: S. Greene
S. A. Hodge

Risk Management Associates
5353 Wyoming NE, Suite 83
Albuquerque, NM 87109
Attn: C. J. Shaffer

Science Applications International
Corp.
505 Marquette Ave., NW
Albuquerque, NM 87102
Attn: L. N. Smith

Tennessee Valley Authority (8)
400 West Summit Hill Drive
Knoxville, TN 37902

Attn: R. Christie
F. A. Koontz, Jr.
W. Lau
M. Linn
W. Mims, W10D188C-K
L. Proctor
J. A. Raulston, W10C126
W. D. Salyer

American Electric Power (2)
Nuclear Safety & Licensing
1 Riverside Plaza
Columbus, OH 43216-6631
Attn: J. Feinstein
D. Medek

McGill University
315 Querbes
Outremont, Quebec
CANADA H2V 3W1
Attn: John H. S. Lee

Gesellschaft für Reaktorsicherheit
(GmbH)
D-8046 Garching
FEDERAL REPUBLIC OF GERMANY
Attn: H. L. Jahn

Sandia Distribution:

6400 A. W. Snyder
6410 J. W. Hickman
6411 A. S. Benjamin
6411 V. L. Behr (15)
6411 S. E. Dingman
6411 R. D. Gasser
6411 A. C. Peterson
6412 A. L. Camp
6412 F. T. Harper
6415 J. M. Griesmeyer
6415 F. E. Haskin
6420 J. V. Walker
6421 J. B. Rivard
6422 D. A. Powers
6425 W. J. Camp
6427 M. Berman
6427 J. T. Hitchcock
6427 J. Kotas
6427 L. S. Nelson
6427 M. P. Sherman
6427 S. R. Tieszen
6427 M. J. Wester
6427 C. C. Wong
6440 D. A. Dahlgren
6442 W. A. von Rieseemann
6444 S. L. Thompson
6445 J. H. Linebarger
6445 E. H. Richards
6445 V. J. Dandini
6449 K. D. Bergeron
8024 M. A. Pound
8523 K. D. Marx
8523 B. R. Sanders
3141 C. M. Ostrander (5)
3151 W. L. Garner

BIBLIOGRAPHIC DATA SHEET

NUREG/CR-3912
SAND83-0501

SEE INSTRUCTIONS ON THE REVERSE

2 TITLE AND SUBTITLE

MARCH-HECTR Analysis of Selected Accidents in
an Ice-Condenser Containment

3 LEAVE BLANK

4 DATE REPORT COMPLETED

MONTH YEAR

5 AUTHOR(S)

A. L. Camp, V. L. Behr, F. E. Haskin

6 DATE REPORT ISSUED

MONTH YEAR

December 1984

7 PERFORMING ORGANIZATION NAME AND MAILING ADDRESS (Include Zip Code)

Sandia National Laboratories
Albuquerque, NM 87185

8 PROJECT/TASK/WORK UNIT NUMBER

9 FUND GRANT NUMBER

A1246, A1258, A1322

10 SPONSORING ORGANIZATION NAME AND MAILING ADDRESS (Include Zip Code)

Division of Accident Evaluation
Office of Nuclear Regulatory Research
U.S. Nuclear Regulatory Commission
Washington, DC 20555

11a TYPE OF REPORT

Technical

b PERIOD COVERED (Inclusive dates)

12 SUPPLEMENTARY NOTES

13 ABSTRACT (200 words or less)

The MARCH and HECTR computer codes are used in this study to examine hydrogen production, transport, and combustion in an ice-condenser containment for a number of hypothesized severe accidents. Both degraded-core and core-meltdown accidents are treated. The sensitivity of the containment pressure-temperature response is assessed for a number of factors, including the hydrogen and steam source-term assumptions, ignition and propagation limits, combustion completeness, flame speed, spray operation, and recirculation fan operation. The highest containment pressures occur for those cases where the igniters are assumed to fail, the recirculation fans or containment sprays are assumed to fail, or very large steam and hydrogen releases accompanying vessel breach are predicted.

14 DOCUMENT ANALYSIS - a KEYWORDS/DESCRIPTORS

b IDENTIFIERS/OPEN ENDED TERMS

15 AVAILABILITY STATEMENT

Unlimited

16 SECURITY CLASSIFICATION

(This page)

Unclassified

(This report)

Unclassified

17 NUMBER OF PAGES

225

18 PRICE

120555078877 1 1AN1R3
US NRC
ADM-DIV OF TIDC
POLICY & PUB MGT BR-PDR NUREG
W-501 DC 20555
WASHINGTON